UNIVERSIDADE DO PORTO
FACULDADE DE ENGENHARIA

Application of Magnetic Resonance Imaging in the Biomechanical Analysis of the Female Pelvic Floor Muscles

Dissertação apresentada às provas para obtenção do grau de Doutor em Engenharia Biomédica, nos termos do Decreto-Lei nº 115/2013, de 7 de agosto de 2013, orientada pelo Professor Doutor Renato Manuel Natal Jorge, Professor Associado com Agregação da Faculdade de Engenharia da Universidade do Porto, e co-orientada pela Professora Doutora Maria Teresa da Quinta e Costa Mascarenhas Saraiva, Professora Associada da Faculdade de Medicina da Universidade do Porto.

Fernanda Sofia Quintela da Silva Brandão

Outubro de 2017

Faculdade de Engenharia da Universidade do Porto
Rua Dr. Roberto Frias, s/n 4200-465 Porto PORTUGAL

VoIP/SIP: feup@fe.up.pt **ISN:** 3599*654
Telefone: +351 22 508 14 00 **Fax:** +351 22 508 14 40
URL: http://www.fe.up.pt **Correio Electrónico:** feup@fe.up.pt

Brandão, S. (2017). *Application of Magnetic Resonance Imaging in the Biomechanical Analysis of the Female Pelvic Floor Muscles.*

A thesis submitted in conformity with the requirements for the Doctoral Degree in Biomedical Engineering, Faculty of Engineering, University of Porto

Keywords: Pelvic Floor Muscles; Female Pelvic Floor Dysfunction; Magnetic Resonance Imaging; Computational Modeling; Finite Element Method

"O que resta de mim fundir-se-á com o que resta dele, e seremos um ser completo outra vez. Eu tenho o espírito que ele nunca teve. Reanimarei o seu corpo com o meu espírito. (...) Será loucura pensar que tal possa ser possível? Se for loucura, então estou contente por ser louco porque viverei. Estou suficientemente louco, enquanto ainda faço planos, para creditar que há esperança. Essa esperança permite-me prosseguir em frente."

O Prestígio

Christopher Priest

Abstract

Female pelvic floor dysfunction often results from weakening or damage of the pelvic floor muscles or connective tissue. It is studied in the clinical setting, and computational biomechanical analysis has contributed along the years, in a translational research basis. The great anatomical detail and tisue contrast for morfo-functional evaluation make magnetic resonance imaging (MRI) an important tool in this process.

This Thesis aimed to contribute to the current literature regarding the biomechanical analysis of the female pelvic floor muscles and pelvic floor dysfunction. Study I showed that thinner *puboviscerali*s muscle and increased hiatal area may be indicators of decreased resistance to deformation due to increased intra-abdominal pressure. In Study II, former high-impact sports practitioners evidenced lower ability to contract the pelvic floor muscles when compared to the control group ($p=0.004$), using optimized axial dynamic images. In Study III, a MR-based finite element model reproduced active contraction of the pelvic floor muscles, with antero-cranial nodal displacements slightly superior to that of the dynamic MRI of the same women (0.2 mm anterior and 4.1 mm upward). In Study IV, simulation of valsalva maneuver with healthy ligaments resulted in an opening of the α-angle and bladder neck dislocation close to that of the dynamic MRI (105.71º *vs.* 103.31º, and 5.7 mm *vs.* 5 mm, respectively). Furthermore, impairment of the pubourethral ligaments seems to have the greatest impact on the urethral and bladder neck mobility, with values in the range of those reported in incontinent women, and in line of anatomical models of stress urinary incontinence. Study V evidenced that the numerical model built was able to reproduce the presence of a midurethral synthetic sling when the supportive structures are impaired, by reducing the α-angle and the displacement of the bladder and bladder neck to values measured in

asymptomatic women. A mesh with higher stiffness implies higher force (3.4 vs. 2.3 N), which may be relevant when considering post-operative voiding dysfunction or urethral erosion. In Study VI, it was possible to compare the direction of the *puboviscerali*s muscle fibers retrieved from the strain tensor from the modeling process and that from the MRI-based diffusion tensor. The results showed less similarity in the muscle anterior insertions in the *symphysis pubis* and in its most curved pathway in the anorectal junction.

In conclusion, MRI is an important non-invasive imaging technique to be used when modeling the biomechanical behavior of the pelvic floor muscles. It provides geometrical imputs of the pelvic organs and supportive structures to the models, detailed orientation of the muscle fibers, and validation to the results obtained from the numerical simulations.

Keywords: Pelvic Floor Muscles; Female Pelvic Floor Dysfunction; Magnetic Resonance Imaging; Computational Modeling; Finite Element Method

Resumo

As disfunções do pavimento pélvico feminino resultam frequentemente do enfraquecimento ou dano dos músculos do pavimento pélvico. Estas condições são estudadas no contexto clínico, e a análise computacional biomecânica tem contribuído ao longo dos anos, numa base de investigação de translação. O detalhe anatómico e contraste entre os tecidos que a imagiologia por ressonância magnética (IRM) permite na avaliação morfo-funcional fazem dela uma ferramenta importante neste processo.

Esta Tese teve como objetivo contribuir para a literatura atual no contexto da análise biomecânica dos músculos do pavimento pélvico feminino e das disfunções do pavimento pélvico. O Estudo I mostrou que o músculo pubovisceral mais fino e uma área do hiato pélvico maior podem ser indicadores de uma resistência diminuída à deformação pelo aumento da pressão intra-abdominal. No Estudo II, anteriores praticantes de desportos de alto-impacto evidenciaram uma capacidade reduzida de contração dos músculos do pavimento pélvico quando comparadas com o grupo de controlo ($p=0.004$), aplicando imagens dinâmicas otimizadas no plano axial. No Estudo III, um modelo de elementos finitos baseado em imagens de RM reproduziu a contração ativa dos músculos do pavimento pélvico, com deslocamentos nodais antero-craniais ligeiramente superiores aos obtidos em imagens dinâmicas de RM da mesma mulher (0.2 mm de deslocamento anterior e 4.1 mm de deslocamento cranial). No Estudo IV, a simulação da manobra de valsalva e ligamentos saudáveis resultou na abertura do ângulo α e deslocamento do colo vesical próximo ao observado na RM dinâmica (105.71º *vs.* 103.31º, e 5.7 mm *vs.* 5 mm, respetivamente). Para além disso, o dano dos ligamentos pubouretrais parece ter o maior impacto na mobilidade uretral e do cólo vesical, com valores na gama do que foi reportado em mulheres incontinentes, e em linha com os modelos anatómicos de incontinência

urinária de stress. O Estudo V evidenciou que o model numérico construído foi capaz de reproduzir a presença de uma fita sintética uretral quando as estruturas de suporte estão danificadas, ao reduzir o ângulo α e o deslocamento da bexiga e do cólo vesical para valores medidos em mulheres asintomáticas. Uma malha com uma rigidez superior implica um valor de força maior (3.4 vs. 2.3 N), o que pode ser relevante quando se considera a disfunção miccional pós-operatória ou a erosão uretral. No Estudo VI, foi possível comparar a direção das fibras do músculo pubovisceral obtidas através do tensor de deformação no processo de modelação e o obtido através do tensor de difusão por RM. Os resultados mostraram menor semelhança nas regiões de inserção anteriores na sínfise púbica e no seu trajeto com maior curvatura na junção anorectal.

Em conclusão, a IRM é uma técnica de imagem não-invasiva importante na modelação do comportameno biomecânico dos músculos do pavimento pélvico. Esta técnica fornece *inputs* geométricos dos orgãos pélvicos e das estruturas de suporte aos modelos, a orientação detalhada das fibras musculares, e a validação dos resultados obtidos nas simulações numéricas.

Palavras-chave: Músculos do Pavimento Pélvico; Disfunção do Pavimento Pélvico Feminino; Imagiologia por Ressonância Magnética; Modelação Computacional; Método dos Elementos Finitos

Agradecimentos / Acknowledgements

No decurso desta etapa de mais de cinco anos felizmente pude contar com a ajuda de várias pessoas. Agradeço ao Professor Renato Natal Jorge pelo apoio na conceptualização por vezes complexa de várias tarefas em simultâneo. Ainda, pelas discussões criativas, e por tentar perceber a distância que nos separa em termos de *background*. Ainda assim, tentou sempre fazer salientar o que seriam as minhas mais-valias, e a aplicação prática do trabalho num contexto clínico, esse que foi sempre o meu objetivo primordial. À Professora Teresa Mascarenhas, pela disponibilidade e carinho. Ao Professor Marco Lages Parente, pela ajuda na execução prática dos processos de análise biomecânica computacional. Ao Professor Pedro Martins, que percebia muito do que eu lhe perguntava com o pouco que dizia. Ao Professor Jorge Belinha, que me explicou muita coisa "de contexto", mesmo sem saber.

Aos amigos do INEGI, pela simpatia e consideração, pelos sorrisos que me aproximaram do espírito de camaradagem e da amizade que fazem parte dos trajetos demorados e duros na vida. À Julinha, pela delicadeza e dedicação a todos nós. À Thuane, a cúmplice de trabalho e de longas discussões. Obrigada por ainda hoje fazeres parte da minha vida; ensinaste-me o valor do sorriso, e que nada é intransponível. Só queria que estivesses mais perto de nós, fisicamente, já que estás sempre nos nossos corações.

Aos meus pais por terem um orgulho imensurável por mim e por tentarem respeitar a minha vida, mesmo quando isso lhes custa a minha presença. À minha família, por todas as festas em que não estive presente, pelos telefonemas rápidos.

A minha carreira profissional sempre foi simultânea. Quem me conhece bem sabe o valor que eu dou à igualdade de géneros e oportunidades, de mostrar capacidades no trabalho e na discussão. Tenho tido sempre o apoio daqueles que me fazem sentir uma

parceira importante no dia-a-dia. Obrigada Daniela, Duarte, Bruno, Carina, Zé Manel, António. Nunca é demais dizer que vocês fazem parte da minha expressão pessoal. Lembrei-me muitas vezes do que disseste Dani: "O Doutoramento é como uma maratona"; e tinhas razão, a gestão pessoal do esforço é o segredo. Obrigada também à Professora Isabel, por nunca me ter dito "não", por me ter dado oportunidades de valorização, e ter visto sempre mais adiante.

À Marilene, pelo apoio incondicional a todas as horas, dias, meses; por (tentar sempre) compreender os meus objetivos. À Luísa e à Rita (o teu interesse e ajuda foram preciosos), à Raquel, minhas companheiras. Ao "brother" Nuno, inteligente e crítico, que conhece os (meus) limites mas muitas vezes os ignora, e ainda bem.

Ao Rui. Bom, ao Rui há tudo para dizer, e muito ficou já por fazer. Obrigada por fazeres da minha vida um conjunto de histórias, por respeitares os meus silêncios e preocupações, os dias maus e os péssimos, por teres feito tudo o que eu não podia. Tu que me conheces melhor do que eu própria.

Ao Emanuel. Foi um dia feliz aquele em que me cruzei consigo; fez de mim uma pessoa melhor, e é também muito seu o fruto destes anos.

Por fim, são indispensáveis os agradecimentos institucionais aos Centro Hospitalar de Sçao João-EPE e Centro Hospitalar de Lisboa Norte (Hospital de Sta Maria), pela autorização e apoio nas aquisições de Ressonância Magnética pélvica às mulheres incluídas nos artigos que constituem os estudos apresentados na Tese.

Funding Sources

There was no funding for the PhD Programme.

The co-authors acknowledged their funding in the papers included in this Thesis.

Table of Contents

List of Figures

Chapter II

Review Article

Magnetic Resonance Imaging of the pelvic floor: from clinical to biomechanical imaging

Chapter III

Original Articles

Study I

Moment of inertia as a means to evaluate the biomechanical impact of pelvic organ prolapse.

Study II

Do asymptomatic former high-impact sports practitioners maintain the ability to contract the pelvic floor muscles?

Study III

Modeling the contraction of the pelvic floor muscles.

Study IV

Biomechanical study on the bladder neck and urethral positions: simulation of impairment of the pelvic ligaments.

Study V

On the stiffness of the mesh and urethral mobility: a finite element analysis.

Study VI

***Puboviscerali*s muscle fiber architecture determination: comparison between biomechanical modeling and diffusion tensor imaging.**

List of Tables

Chapter III

Original Articles

Study I

Moment of inertia as a means to evaluate the biomechanical impact of pelvic organ prolapse.

Study II

Do asymptomatic former high-impact sports practitioners maintain the ability to contract the pelvic floor muscles?

Study III

Modeling the contraction of the pelvic floor muscles.

Study IV

Biomechanical study on the bladder neck and urethral positions: simulation of impairment of the pelvic ligaments.

Study V

On the stiffness of the mesh and urethral mobility: a finite element analysis.

Study VI

***Puboviscerali*s muscle fiber architecture determination: comparison between biomechanical modeling and diffusion tensor imaging.**

List of Abbreviations & Acronyms

AR anorectal

AP anterior-to-posterior

ATFP *arcus tendineous fasciae pelvis*

CL cardinal ligaments

BMI body mass index

DT diffusion tensor / **DTI** diffusion tensor imaging

DW diffusion weighted

EPI echo planar imaging

FEM finite element method

FI fecal incontinence

FSE fast spin echo

HASTE half-Fourier acquisition single-shot fast spin-echo

HS higher-stiffness

IAP intra-abdominal pressure

ICIQ-SF international consultation on incontinence questionnaire - short form

IPAQ-SF international physical activity questionnaire - short form

L left

LA *levator ani*

LH *levator hiatus*

LLR lateral ligaments of the rectum

LMMSE least minimum mean square error

LS lower-stiffness

MET metabolic equivalent of task

MPL mid-pubic line

MOI moment of inertia

MPSL maximum principal stress lines

MR magnetic resonance / **MRI** magnetic resonance imaging

NSA number of signals averaged

OEM *obturator externus* muscle

OIM *obturator internus* muscle

PCL pubococcygeal line

PCM *pubococcygeous* muscle

PFD pelvic floor dysfunction

PFIQ-7 pelvic floor impact questionnaire - short form 7

PF pelvic floor muscles

PFa pelvic fascia

PFM pelvic floor muscles

POP pelvic organ prolapse

POP-Q pelvic organ prolapse quantification system

PR puborectal

PRM puborectal muscle / *puborectalis* muscle

PS *pubic symphysis*

PUL pubourethral ligaments

PVM pubovisceral muscle / *pubovisceralis* muscle

R right

RL right-to-left

SCIPP sacrococcygeal-inferior pubic point

SENSE sensitivity encoding

SNR signal-to-noise ratio

SP *symphysis pubis*

SPAIR spectrally adiabatic inversion recovery

SSFSE single-shot fast spin-echo

SSFP steady state free precession

SS-SE-EPI single-shot spin-echo echo planar imaging

SUI stress urinary incontinence

T2-w T2-weighted

TE echo time

TOT transobturator tape

TR repetition time

TrueFISP true state imaging with steady state precession

TVT transvaginal tape

UI urinary incontinence

US ultrasound

USL uterosacral ligaments

VM valsalva maneuver

Chapter 1

General Introduction

The female pelvis may be divided in three compartments: the anterior (bladder and urethra), middle (vagina and uterus), and the posterior or anorectal. The pelvic floor muscles are a focus when studying pelvic support and pelvic floor dysfunction (PFD). They expand from a three-layer muscular system from the *symphysis pubis* towards the coccyx, along the sidewalls of the bony pelvis, comprising the pelvic diaphragm, the deep urogenital diaphragm muscles layer, and the superficial perineal layer. The pelvic diaphragm muscles include the *levator ani* - composed by the *puborectalis*, *pubococcygeus* and *iliococcygeus* muscles -, the *coccygeus* (or *ischiococcygeus*) and the *obturator internus* and the associated connective tissue, which support and protect the urogenital area and the organs. The term *pubovisceralis* muscle (PVM) is sometimes applied to include the *puborectalis* and the *pubococcygeus* muscles (DeLancey, Kearney et al. 2003) (Loubeyre, Copercini et al. 2012) (Yang, Yang et al. 2006). This multi-level system provides passive support - through the connective tissue of the pelvic fascia and ligaments - while the pelvic floor muscles provide both passive resting tonus and active support (Ashton-Miller and DeLancey 2007) (Herschorn 2004) (Verelst and Leivseth 2007). Voluntary contraction, mainly that of the *puborectalis* sling, promotes closure of the *levator hiatus* and the active support (Raizada and Mittal 2008) (Verelst and Leivseth 2007).

Female PFD includes different conditions, such as voiding dysfunction, fecal or urinary incontinence (UI), or pelvic organ prolapse (POP), which affect almost one third of adult women (Walker and Gunasekera 2011). These disorders are the subject of study of different medical specialties, such as obstetrics and gynecology, surgery, urology, radiology and physical therapy. Furthermore, female PFD requires a broader approach, for which (bio)mechanical and biomedical engineering have contributed along the years (Constantinou, Hvistendahl et al. 2002) (Noakes, Pullan et al. 2008) (Parente, Natal Jorge

et al. 2009a) (Parente, Jorge et al. 2009b) (Parente, Natal Jorge et al. 2010) (Rivaux, Rubod et al. 2013) (Yip, Kwok et al. 2014).

The global model of female PFD includes: 1) predisposing factors (family history); 2) promoting factors (menopause, high-impact sports practice) (Mannella, Palla et al. 2013) (Simeone, Moroni et al. 2010); and c) aggravating factors (obesity, vaginal delivery with neuromuscular lesion) (Bozkurt, Yumru et al. 2014) (Rodriguez-Mias, Martinez-Franco et al. 2015). History of pelvic surgery and chronic constipation - due to the repetitive increase in intra-abdominal pressure (IAP) - are also related to the increase in prevalence of UI and POP (Lacima and Espuna 2008) (Moalli, Jones Ivy et al. 2003) (Rodriguez-Mias, Martinez-Franco et al. 2015).

Stress UI (SUI) is the most common presentation of UI among several groups: elderly women, pregnant (and postpartum) (Demaagd and Davenport 2012) (Gill, Moore et al. 2010) (Sangsawang and Sangsawang 2013), and some studies also point to a high prevalence in athletes, mostly those practicing high-impact sports (Da Roza, Brandao et al. 2015) (Eliasson, Larsson et al. 2002) (Fozzatti, Riccetto et al. 2012) (Poswiata, Socha et al. 2014). SUI often relates to urethral hypermobility and vaginal vault prolapse, while defecation disorders are often associated to symptoms of anorectal defects and prolapse. Multi-compartment PFD can also be present and, in this circumstance, concomitant UI and POP have to be managed (Maglinte, Kelvin et al. 1999).

Physical examination may be insufficient in diagnosing the various forms of PFD. Added value of imaging evaluation is in areas where clinical evaluation is limited, such as in patients with severe/recurrent prolapse, defecatory dysfunction, multi-compartment symptoms, because although patients may have a predominant presenting symptom, pelvic floor abnormalities often involve multiple sites.

Widening of the *urogenital hiatus* due to *levator ani* defects and connective tissue failure can lead to PFD, and is often related to lower *levator ani* strength during voluntary contraction (Chamochumbi, Nunes et al. 2012) (DeLancey, Morgan et al. 2007) (Weidner, Barber et al. 2000) (Vakili, Zheng et al. 2005) (Verelst and Leivseth 2007). In this context, clinical evidence benefits from both detailed functional evaluation of the pelvic floor muscles confirmation and imaging with static and dynamic ultrasound or magnetic resonance imaging (MRI) of the pelvic floor (Boyadzhyan, Raman et al. 2008) (DeLancey, Morgan et al. 2007) (Dietz 2010).

MRI may be considered an important adjuvant tool in the diagnosis of female PFD in the clinical setting. Although its high costs and low availability cannot be neglected, MRI of the female pelvic floor has the *a priori* advantages of being a non-ionizing technique that allows a morfo-functional multiplanar evaluation of the pelvic cavity with great anatomical detail and soft tissue contrast (Ahmad, Hainsworth et al. 2015) (Boyadzhyan, Raman et al. 2008) (El Sayed, El Mashed et al. 2008). It enables objectively assessing a variety of possible disorders affecting the pelvic floor in one examination, with increased patient comfort, decreased complexity. Also, allows diagnosing unexpected or masked functional abnormalities, which are sometimes discrepant from the dominant symptoms and may influence the choice of the treatment options (El Sayed, Alt et al. 2016) (Law and Fielding 2008).

The pelvic organs, ligaments and fascial attachments can be evaluated in static images (Macura and Genadry 2008) (Tunn, DeLancey et al. 2001). Also, *levator ani* defects can be assessed (Lammers, Prokop et al. 2013) with overall good to high levels of inter-rater agreement (Kearney, Miller et al. 2006) (Morgan, Umek et al. 2007), although Kearney *et al.* reported poor correlation with physical examination (Kearney, Miller et al. 2006).

Hoyte *et al*. described decreased dome shape of the *levator ani*, lower muscle mass and wider *levator hiatus* in symptomatic women with SUI and POP (Hoyte, Jakab et al. 2004) (Hoyte, Schierlitz et al. 2001) when compared to controls. In this sense, it might be pertinent to be able to establish a quantitative property that could at least substantially relate the cross-sectional shape of the *levator ani* and *urogenital hiatus* and the biomechanical reply. From a biomechanical point-of-view, thinner muscles associated to a wider *levator hiatus* may have lesser resistance to deflection and deformation when the force against the pelvic floor is elevated, for instance when coughing, and lesser ability to actively contract.

Complementing of the anatomical evaluation performed from the static images can be achieved with dynamic imaging by acquiring ultrafast MR sequences. These are sequentially performed, imaging along the sagittal plane both at rest and during maximal voluntary contraction, valsalva maneuver, straining and/or defecation so as to enable appraising the (ab)normal positioning of the structures (Hecht, Lee et al. 2008) by applying reference lines (e.g., the pubococcygeal line (PCL) or the H-line) (Boyadzhyan, Raman et al. 2008) (Brandao and Ianez 2013) (Pizzoferrato, Nyangoh Timoh et al. 2014). The sagittal plane demonstrates the relationship and position of the pelvic organs relative to the main axis of the pelvic floor muscles (i.e., approximately coincident with the axial plane). In that sense, it provides an (in)direct assessment of the mobility of the pelvic floor muscles during those maneuvers. The selection of an axial (angulated) plane could also be explored to perform those *cine* sequences, as the evaluation of the antero-posterior and/or lateral diameters of the *levator hiatus* during the dynamic maneuvers would perhaps allow complementary morfo-functional analysis in a similar plane and fashion to that of dynamic ultrasound (Dietz 2010).

Computational modeling of the pelvis brought additional insight into the study and comprehension of the pelvic floor biomechanics along the years. MR images have been used as input information to models that intend to describe the biomechanical behavior of the support structures (Chanda, Unnikrishnan et al. 2015) (Chen, Ashton-Miller et al. 2006) (Chen, Ashton-Miller et al. 2009) (Larson, Hsu et al. 2010) (Ren, Xie et al. 2015).

Some of these studies are based on the finite element method (FEM), which involves discretizing the domain of the pelvic structures´ geometry into a three-dimensional mesh of finite elements, connected at specific points by nodes, to which boundary conditions are applied to mimic for example, ligament or muscle insertions. To model the global problem, several sets of partial differential equations have to be solved. Besides geometry, the FEM takes into account the material properties, the constitutive models and respective equations that describe the mechanical behavior of those specific tissues, and also the simulation conditions, such as the load so as to mimic the valsalva maneuver. One of the main challenges in developing and validating these models is that there is still a lack of standardization of these parameters (Chanda, Unnikrishnan et al. 2015).

Intense work has been developed to explain the biomechanical features of anterior vaginal wall prolapse and cystocele formation during raised IAP, by simulating impairment of muscles and ligaments or fascia (Chen, Ashton-Miller et al. 2006) (Chen, Ashton-Miller et al. 2009) (Lamblin, Delorme et al. 2015) (Larson, Hsu et al. 2010). In the context of SUI and bladder neck support, previous 2D biomechanical model of Yip and colleagues showed that the impairment of the pelvic floor muscles has a major role. In their numerical simulations, the stiffness of apical uterine ligaments has shown to increase, conceivably to compensate for higher muscle impairment, which is concordant with clinical data, and sustains the evidence that pelvic floor muscle tone and strength are relevant factors to maintain vaginal and bladder support and position (Yip, Kwok et al. 2014).

Modeling muscle voluntary contraction is also of interest, since active conscious contraction also helps to maintain support and continence. Until now, few studies modeled muscle contraction (d'Aulignac, Martins et al. 2005) (Parente, Natal Jorge et al. 2010) (Saleme, Parente et al. 2011), which should ideally include the organs, fascial connections and ligaments to reflect the real circumstances inside the pelvic cavity.

In fact, the Integral Theory of Petros *et al.* (Petros and Ulmsten 1990) (Petros and Woodman 2008) emphasizes the idea that damaged structures which provide support to the proximal urethra and bladder neck may dissipate muscle contraction, causing SUI. In that sense, the role of the pubourethral ligaments (PUL) may be more substantially focused. They are important urethral stabilizers acting as a fulcrum to avoid downward motion of the anterior urethral wall (Petros 1998). Indeed, urethral hypermobility and rotational descent are common features in SUI. Modeling ligaments of the three pelvic compartments may add information on their support role to the bladder neck and urethra, especially when their mechanical properties are altered.

Employing midurethral slings is one of the surgical approaches to correct sole SUI (Wood and Anger 2014). Tension-free midurethral polypropylene slings are loosely placed retropubically under the midurethra to create artificial pubourethral neo-ligaments (Atherton and Stanton 2005) (Petros and Woodman 2008). Slings may vary in configuration, material, properties and manufacturing, and there is still no agreement regarding which is the most effective, between the need for having lower complication rates and being easy to adjust (Costantini, Lazzeri et al. 2007). Meshes with different structural (Dietz, Vancaillie et al. 2003) and thermal features (Afonso, Jorge et al. 2009) (Afonso, Martins et al. 2008) exhibit distinct mechanical properties, namely their stiffness, which is an important parameter to account for. In fact, a mesh with excessive stiffness or

tension may be partially responsible for recurrent post-operative voiding dysfunction (Shah and Badlani 2012).

Recent finite element biomechanical analysis of single-incision sling MiniArc^{TM} indicates that the position of the sling in the mid-distal urethra may provide sufficient correction, with reduced sling-urethra interaction force which could be the cause of urinary retention and pain (Peng, Khavari et al. 2015). However, the effect of the stiffness of the midurethral sling has not been studied yet.

Besides the fact that the origin and insertion points define the muscle force's line of action, the function of skeletal muscles is strongly influenced by their geometry and internal organization. Muscle pennation angle is an important structural property as well. Fusiform muscles allow a higher range of motion, while a pennate structure favors greater force production. In that sense, some constitutive models used in finite element analysis assume muscles to be transversely isotropic which means accepting a directional anisotropy (i.e. directional dependence) in their physical and mechanical properties, such as stiffness. (Morrow, Haut Donahue et al. 2010) (Takaza, Moerman et al. 2013).

The pelvic floor is a multi-layered and multi-directional structure, in which muscles have distinct thickness, direction and hence, different origin and attachment points. Despite the high tissue contrast and anatomical detail provided by conventional MR images, they cannot probe muscle architecture. Diffusion tensor (DT) MRI and its 3D representation (fiber tractography) was already applied to skeletal muscles, recently including application to the pelvic floor muscles (Zijta, Froeling et al. 2011) (Zijta, Lakeman et al. 2012) (Rousset, Delmas et al. 2012). Yet, diffusion-tensor imaging (DTI) should be carefully interpreted in this region due to several technical challenges and sources of artifacts, and still lacks validation.

The principle underlying muscle DTI is that water diffusion in striated muscles is higher in the longitudinal direction due to greater barriers to water diffusion in the transverse direction, i.e., it is directionally anisotropic (Damon, Buck et al. 2011). In DTI, the eigenvectors can be derived from the eigen-decomposition of the DT by evaluating the diffusion coefficient along at least 6 directions. Since the largest eigenvalue occurs along the main axis (maximum principal eigenvector), one can state that the diffusion profile is intimately coupled with local tissue structure, despite not being representative of the number of muscle fibers.

A similar assumption is made when performing the numerical simulation. One method for obtaining the course of the muscle fibers of the pelvic floor muscles is by applying a pressure normal to the finite element mesh, assuming that for each finite element, muscle direction corresponds to the direction of the maximum principal stress. Therefore, this is an indirect method for obtaining the direction of muscle fibers, which can depend on the boundary conditions (mainly in those elements closest to the muscle´s origin and insertion points) manually defined by the observer. Despite the aforementioned caveats, their comparison and inclusion in the modeling of the pelvic region can be explored, similarly to what has already been done for studying animal anatomy (Van Donkelaar, Kretzers et al. 1999) and numerical modeling of head injury (Colgan, Gilchrist et al. 2010).

Taking into consideration the need of interplay between the clinical and engineering applications of MRI in the biomechanical analysis of PFD, and the aforementioned gaps in the current literature, the present work aims to contribute to a better understanding of some of these questions. This Thesis is divided into six sections. This General Introduction overviews the clinical usage and interpretation of MR images, and also refers to previous MR-based modeling of PFD. Furthermore, it highlights some topics that require further

investigation, which were the basis for the Original Studies of this PhD Thesis. The Theoretical Background (section 2) refers to a Review Article where some of these aspects are addressed. The third section comprises six Original Studies, each one designed to meet different goals:

In Study I, entitled "Moment of inertia as a means to evaluate the biomechanical impact of pelvic organ prolapse", the aim was to seek for a correlation between the morphology of the PVM and *levator hiatus* and the Moment of Inertia (MOI). Women with POP - who are generally assumed to have thinner muscles, wider *hiatus* and caudally positioned organs - were compared with a control group.

Study II, entitled "Do asymptomatic former high-impact sports practitioners maintain the ability to contract the pelvic floor muscles?" intended to explore the axial plane during dynamic imaging with "rest *vs.* maximal contraction" blocks. A group of former high-impact sports practitioners and a control group were scanned. PVM and *levator hiatus* morphological features, as well as muscle contraction, were evaluated.

In Study III entitled: "Modeling the contraction of the pelvic floor muscles.", the focus was to model muscle voluntary contraction. An MR-based pelvic FE model was developed, and for the used constitutive model, muscle fibers activation was incorporated. The resultant displacement was validated against dynamic MR images.

Study IV, entitled "Biomechanical study on the bladder neck and urethral positions: simulation of impairment of the pelvic ligaments." was designed to evaluate the effect of progressive impairment of the pelvic ligaments in the support of the bladder neck, in the absence of muscle damage.

Still in the context of the previous paper, Study V entitled: "On the stiffness of the mesh and urethral mobility: a finite element analysis." was motivated by the hypothesis

that the stiffness of the midurethral slings may affect the resultant urethral mobility. A midurethral sling modeled with different stiffness of the mesh was applied during simulation of maximal valsalva maneuver.

In the last original article, Study VI entitled: "*Puboviscerali*s muscle fiber architecture determination: comparison between biomechanical modeling and diffusion tensor imaging.", the target was to compare the probable direction of the muscle fibers obtained by the tensor describing the maximum principal stress lines along the modeling process, and that of DT-MRI.

Section four presents the main contributions of the six Original Studies and an Integrated Discussion of the results.

Finally, the fifth and sixth sections gather the main Conclusions of the Thesis and the work to be fulfilled in a near future, respectively.

The bibliographic references that support the main concepts and findings are presented. The appendices are included at the end of the document.

Chapter 2

Theoretical Background

Review Article

Magnetic resonance imaging of the pelvic floor: from clinical to biomechanical imaging.

Brandão S, Da Roza T, Parente M, Ramos I, Mascarenhas T, Natal Jorge RM.

Proc Inst Mech Eng H. 2013 Dec;227(12):1324-1332.

doi: 10.1177/0954411913502952. Epub 2013 Sep 12.

Review Article

Institution of MECHANICAL ENGINEERS
Journal of ENGINEERING IN MEDICINE

Proc IMechE Part H:
J Engineering in Medicine
227(12) 1324–1332

DOI: 10.1177/0954411913502952
pih.sagepub.com
SAGE

Magnetic resonance imaging of the pelvic floor: From clinical to biomechanical imaging

Sofia Brandão[1], Thuane Da Roza[2], Marco Parente[2], Isabel Ramos[1,3], Teresa Mascarenhas[3,4] and Renato M Natal Jorge[2]

Abstract

This article reviews the current role of magnetic resonance imaging in the study of the pelvic floor anatomy and pelvic floor dysfunction. The application of static and dynamic magnetic resonance imaging in the clinical context and for biomechanical simulation modeling is assessed, and the main findings are summarized. Additionally, magnetic resonance–based diffusion tensor imaging is presented as a potential tool to evaluate muscle fiber morphology. In this article, focus is set on pelvic floor muscle damage related to urinary incontinence and pelvic organ prolapse, sometimes as a consequence of vaginal delivery. Modeling applications that evaluate anatomical and physiological properties of pelvic floor are presented to further illustrate their particular characteristics. Finally, finite element method is described as a method for modeling and analyzing pelvic floor structures' biomechanical performance, based on material and behavioral properties of the tissues, and considering pressure loads that mimic real-life conditions such as active contraction or Valsalva maneuver.

Keywords

Pelvic floor morphology, magnetic resonance imaging, magnetic resonance tractography, biomechanics, finite element method

Date received: 28 February 2013; accepted: 2 August 2013

Introduction

Female pelvic floor dysfunction (PFD) includes conditions such as urinary incontinence (UI) (involuntary urine leakage), pelvic organ prolapse (POP) (when pelvic organs descend from their position) or fecal incontinence.[1] Its high prevalence and harmful effects on quality of life make it a focus of different professionals, such as primary care doctors, gynecologists, urologists and bioengineers (as it concerns image processing and biomechanical features). The pathophysiology of PFD is multifactorial, and it includes aging, high-impact sports, chronic straining and hormonal status.[2] In addition, vaginal delivery and high parity are also related to PFD, in consequence of nerve, muscle, ligament or connective tissue damage.[3] In fact, vaginal delivery is the most relevant risk factor,[4] and some women show clinical or imaging proof of disrupted support to the pelvic organs.[5,6]

In this article, an overview of the role of conventional magnetic resonance imaging (MRI) on the diagnosis of PFD and on computational applications is performed. Conventional MRI does not fully allow complete insight into muscle structure. To overcome this problem, diffusion tensor imaging (DTI) may be used as a means to obtain detailed information on tissue organization. Muscle fiber direction provided by DTI adds information on pelvic floor muscle (PFM), fiber orientation and pennation (i.e. the obliquity between muscle fibers and the main axis of the muscle), and for that reason, it may be used as additional input for biomechanical simulation procedures. To be used as inputs in computational procedures, some strategies

[1]Department of Radiology, Centro Hospitalar de São João—EPE, Porto, Portugal
[2]IDMEC, Faculty of Engineering, University of Porto, Porto, Portugal
[3]Faculty of Medicine, University of Porto, Porto, Portugal
[4]Department of Obstetrics and Gynecology, Centro Hospitalar de São João—EPE, Porto, Portugal

Corresponding author:
Sofia Brandão, Department of Radiology, Centro Hospitalar de São João—EPE, Alameda Prof. Hernâni Monteiro, 4200–319 Porto, Portugal.
Email: sofia.brand@gmail.com

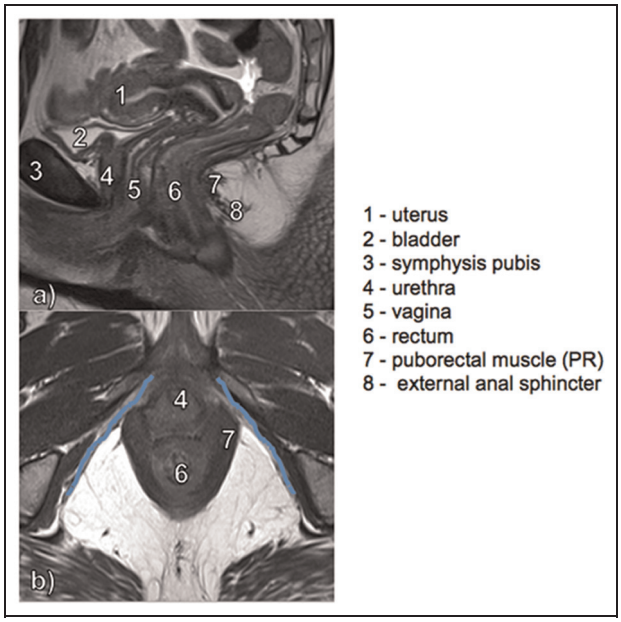

Figure 1. High-resolution MR images on the (a) sagittal and (b) axial planes. The sagittal plane is very important to assess organ positioning at rest. The axial plane is very important to evaluate the pelvic floor muscles, especially the puborectal (PR). The fascial attachment on the bony structures of the pelvis and on the muscles is more difficult to assess (blue line on (b)).

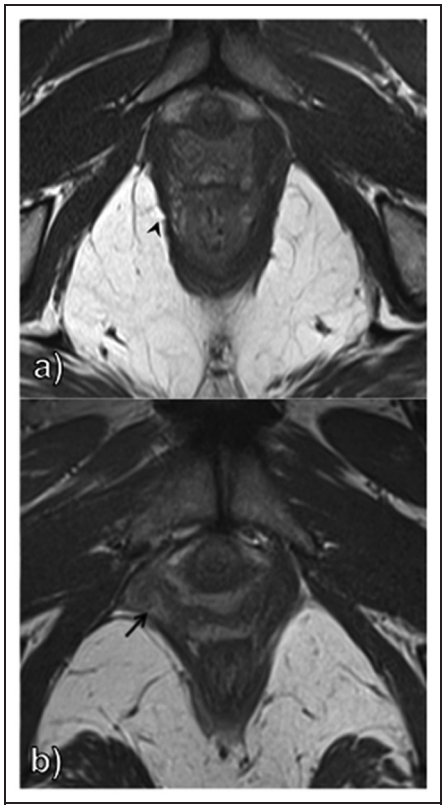

Figure 2. Levator hiatus and pelvic floor muscles. Scoring systems on MR images enable the classification of (a) subtle (arrowhead on (a)) or (b) major (arrow on (b)) muscle defects.

for PFM segmentation on MRI are presented, as well as an introduction to some applications of finite element method (FEM).

Review

Clinical MRI

Anatomical features of PFD were successfully described by ultrasound and MRI.[7,8] MRI plays an important role in understanding some physiopathological aspects of PFD.[9] Its tissue contrast and spatial resolution allow to identify and measure *levator ani* (LA) and its subdivisions, fascia and ligaments.[7] Figure 1 shows pelvic MRI images of a healthy woman in sagittal (Figure 1(a)) and axial (Figure 1(b)) planes. The pelvic floor, fascia and ligaments provide support to the pelvic organs (urethra, bladder, vagina, uterus and rectum). With regard to the pelvic floor, which is a physiologically complex system, it comprises striated and smooth muscles along with fascial insertions, which act together to share pelvic organ load.[10] Striated muscles include the LA, consisting of the puborectal (PR), pubococcygeal and iliococcygeal portions, associated with the coccygeal and internal obturator muscles. As PR and the pubococcygeal muscles are often difficult to distinguish, they are sometimes referred to as pubovisceral muscle. These LA components have distinct thickness, direction and attachment points. The PR muscle (Figure 1(a)) forms a sling around the urethra, vagina and rectum that is anteriorly inserted, while the iliococcygeal is the major support of the posterior pelvic compartment, arising from the anal sphincter and inserting laterally in the inner pelvic surface. Therefore, one may suggest that consequences of LA injury might depend on which or how these portions are damaged, as they might be expected to have a different functional effect. Muscle–bone attachment on the inner pubic surface is a common site inspected for rupture. Disruption of endopelvic fascia (blue line on Figure 1(b)) is more subtle and much more difficult to assess by MRI, despite also having implications on UI and POP.[11,12] The endopelvic fascia provides a surface for muscle insertion, and thus passive support.

Scoring systems were developed to assess LA (ab)normal morphology.[13] According to DeLancey and colleagues,[13,14] left and right sides of the PFM can be evaluated in the axial static MR images and further categorized as having a normal structure, minor/partial injuries and major damage/tear. Incomplete insertion and asymmetry are common imaging features of pelvic floor lesion, along with (subtle) misalignment of structures.[11,13] Axial images in Figure 2 illustrate minor and major LA defects in women with stress UI (leakage during any kind of effort) and POP. Figure 2(a) shows a subtle irregularity in the middle-right segment of the PR muscle (arrowhead) in a woman with stress UI. This is expected to have less impact on pelvic organ support than when the whole muscle insertion is

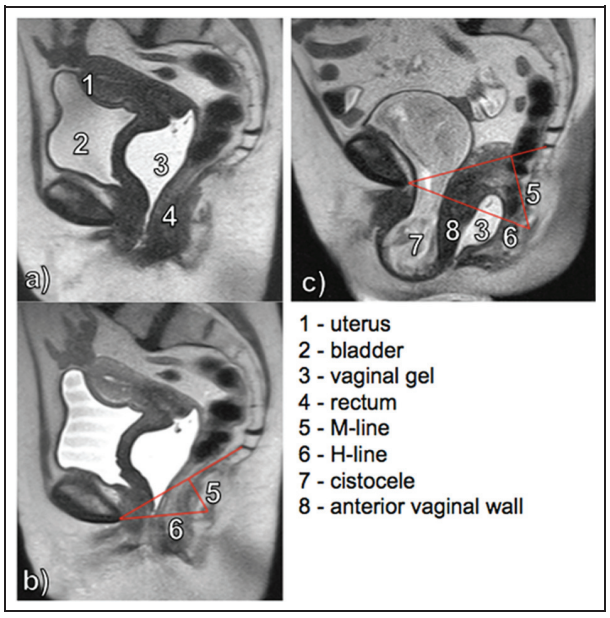

Figure 3. Prolapse assessment on static (a) and dynamic ((b) and (c)) MRI sagittal acquisitions. In (a), the T2-weighted high resolution image displays the pelvic organs: uterus (1), bladder (2), and rectum (4). A hyperintense gel was used to fill the vagina (3). The M- (5) and H-lines (6) were drawn to evaluate organ positioning. A severe prolapse of the bladder (7) and vagina (8) is present (c) during the VM. The most inferior portion of the bladder is 6.48 cm below the H-line.

detached, which is the case of Figure 2(b) (arrow). In this case, the weakened muscle will be pulled downward along with the pelvic organs, as is seen in the case of women with POP.

Dynamic MRI complements this evaluation, by measuring the increase in levator hiatus (LH) diameter. This condition leads to organ downward movement due to weakened hiatal closure force when intra-abdominal pressure increases, for example, during sneezing or coughing. Reference landmarks are drawn on the images acquired during contraction or Valsalva maneuver (VM) to assess the degree of organ prolapse[7] (Figure 3). Using the pubococcygeal line (PCL), which extends from the symphysis pubis anteriorly to the last coccygeal joint, is a reliable measure of pelvic organ descend.[15] Other references are the H-line (e.g. the PR line, a measure of the LH anteroposterior dimension) and the M-line (perpendicular to the PCL and toward the PR muscle). The HMO grading system ("O" for organ prolapse) describes the stages of the visceral prolapse beyond the H-line. Grade 0 (no prolapse) is considered if the organ is above the H-line, Grade 1 (mild prolapse) for $0 < \text{H-line} \leqslant 2$ cm below, Grade 2 (moderate) for $2 < \text{H-line} \leqslant 4$ cm below and Grade 3 (severe) for H-line $\geqslant 4$ cm.[16]

In the case illustrated in Figure 3, endovaginal ultrasound gel helps to define uterus cervix position. Sagittal high-resolution T2-weighted image (Figure 3(a)) shows pelvic organs in their resting position. Images in Figure 3(b) and (c) were acquired at rest and during VM, respectively. The PCL, H- and M-lines were drawn, and a severe prolapse was diagnosed on Figure 3(c). A large cystocele forces anterior vaginal wall to descend, and the endovaginal contrast medium is displaced to the posterior vagina. Bladder and vagina are positioned below the PCL, with elongation of the H- and M-lines, in relation to a weak pelvic floor support.

Sometimes, there is a mismatch between these imaging measures and clinical evidence.[17,18] This may be partially explained by the differences between patient's positioning during physical examination and in the MRI scanner but may also be related to insufficient patient training to perform reproducible VM.[19] Also, readers' training and experience[12] may influence imaging scoring, which would benefit from interdisciplinary teams with gynecologists and radiologists.

Despite the anatomical detail provided by axial MRI, full understanding of the PFM anatomy and physiology has not been achieved. For that reason, thin slices acquired in the three orthogonal planes or volumetric acquisitions are part of the imaging protocol.[20] High-field-strength imaging allows a gain in signal intensity and spatial resolution and may help to partially overcome this problem. Nevertheless, problems related to its higher sensitivity to magnetic and radiofrequency artifacts arising from tissues with very different magnetic susceptibilities and proton content may imply an adjustment in the imaging protocol. When these problems occur in the rectal ampulla or in the bladder-to-fat and muscle-to-fat interface,[21] they may hinder PFM evaluation.

In the past recent years, DTI evidenced its value on the characterization of neuronal pathways[22] and skeletal muscle fibers.[23,24] This MR-based technique enables the detection and measurement of the mobility and directionality of water diffusion at an image voxel scale, thus allowing the assessment of tissue microstructure (Figure 4(a) and (b)).[25] The magnitude of the diffusivities ($\lambda_1 \geqslant \lambda_2 \geqslant \lambda_3$), according to the three orthogonal directions, is represented by the eigenvectors (ε_1, ε_2, ε_3) and can be used to achieve tissue representation. As illustrated in Figure 4(c), the main axis (ε_1) corresponds to the direction where there is evidence of maximum diffusion (λ_1), and the two smaller axes are ε_2 and ε_3, the latter being the axis where the diffusion process is the lowest (λ_3). The major vector of the voxel provides the dominant orientation. As muscle fibers are highly directional (anisotropic) structures, water molecules move preferably along them, and therefore, it is expected that PFM could be depicted.

Tractography is the visualization of the fibers resulting from DTI postprocessing. For this purpose, multiple postprocessing algorithms have been reported to date, and detailed description is available in Mori and van Zijl[26] and Parker.[27]

Three articles focusing on the use of DTI to study the anatomy of the PFM were recently published. The pubovisceral, anal sphincter and internal obturator muscles were satisfactorily represented.[28–30]

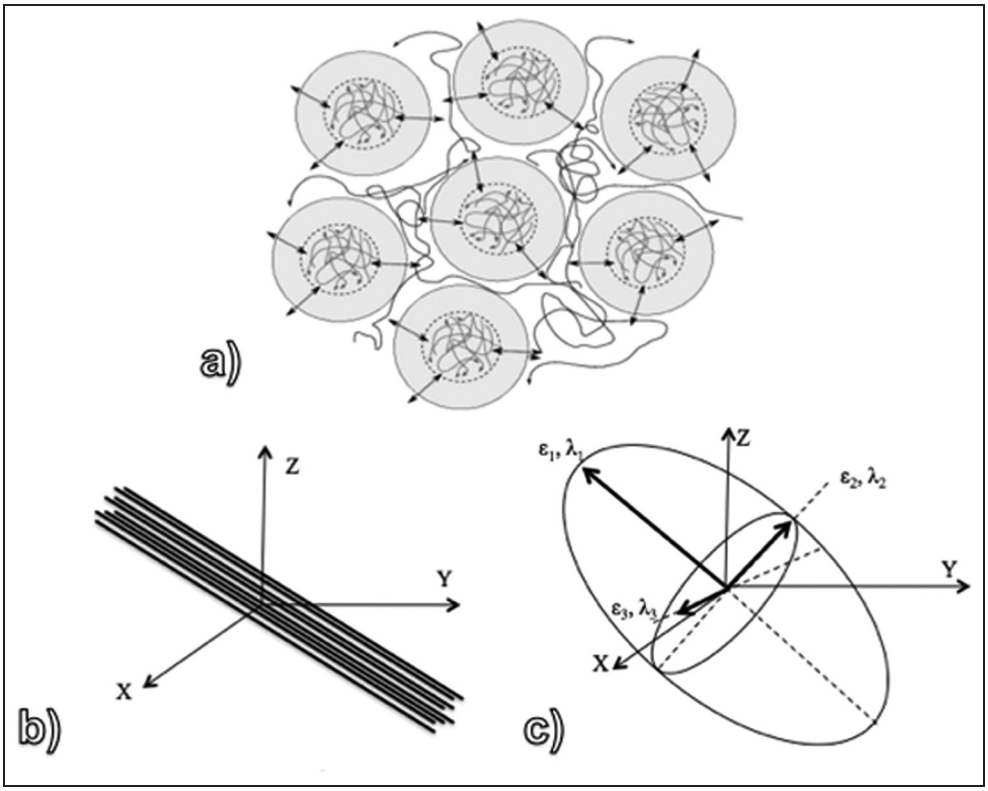

Figure 4. The Diffusion Tensor Imaging (DTI) allows to evaluate water diffusion in the intra and extracellular spaces (a), thus enabling an insight on tissue structure and its orientation in the 3D space (b). Long and fibrous tissue tend to have more prominent water diffusion movements along $\lambda 1$ (c).

As tractography offers a visual approach to muscle pennation, LA defects may be better described. Indeed, DTI may help to improve understanding of the subtle abnormal morphology of the PFM when PFD is present. Although some authors have emphasized that a homogeneous low signal, symmetric shape and attachment of the pubovisceral muscle are imaging features of negative diagnosis for stress UI,[8,31] others have found left- and right-side differences on asymptomatic women,[32] as well as very subtle differences in thickness between incontinent and continent women.[33] Figure 5(b) reveals the overall positioning and orientation of pubovisceral muscle fibers when using fiber tractography postprocessing in an asymptomatic young woman. In this case, despite the symmetric appearance of the pubovisceral muscle on the T2-weighted images (Figure 5(a)), its inner structure is not equal on the right and left portions (arrows).

MRI toward biomedical engineering

Besides its clinical application, MRI is also useful for pelvic modeling. Computational models enable a more precise understanding of physiological aspects of the pelvic floor by performing biomechanical simulations of (individual) image datasets from healthy women or from women with PFD.[34] FEM is one of the most common approaches to model pelvic structure biomechanical behavior, which may be used for surgical planning or to simulate the effects of vaginal childbirth.[35]

Static and dynamic MR images[34,36] have been used as inputs to these models.[37,38] Besides the anatomy and geometry of pelvic structures, modeling applications also require detailed description of the muscle material properties and interaction with bone, fascia and ligaments, taking into account loading conditions that mimic real events.[39] Models include information about muscle positioning, thickness, volume and also mechanical performance whenever recruited for (in)voluntary contraction,[35,40] which is not possible to evaluate by experimental studies in vivo.[41]

Figure 6 presents computational models of the pubovisceral muscle of a healthy woman (Figure 6(a)–(c)) and a woman with POP (Figure 6(d)–(f)), at rest (left column), during contraction (middle column) and during VM (right column). The anterior portion of the muscle attached to the pubis is seen in the upper position, while the rectal portion (with a "V" shape) is seen below. Apart from the larger muscle diameter of the POP woman (transverse lines), its most posterior portion does not open during VM (Figure 6(f)) as happens in the healthy woman (Figure 6(c)), due to a Grade 1 posterior prolapse. In both women, the anterior portion opens from rest to VM in a satisfactory way.

Figure 7 shows a three-dimensional (3D) model of the pelvic floor based on the FEM in a vaginal childbirth simulation. The fetus passage through the LH may cause muscle and nerve disruption.[42,43] Therefore,

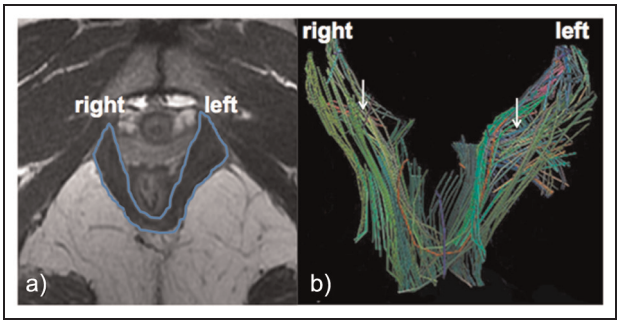

Figure 5. Pubovisceral muscle fiber tract representation. Asymmetric muscle inner structure is seen on tractography (arrows in (b)), despite not being evident on (a) the morphological T2-weighted image.

detailed anatomical knowledge of the different muscles' position, shape, thickness, resistance and insertion points may help to assess the effects of that damage, in both clinical and research contexts.

MR image segmentation of anatomically significant components such as bones, pelvic organs and LA is the usual starting point for modeling. Different strategies may be followed afterward, depending on the purpose and the specific image inputs. Surface rendering of these structures followed by a marching cubes algorithm was used to build a color-coded model of the components of the LA in continent women to estimate their global volume.[44] Using a solid modeling technique, Hoyte et al.[45] found decreased muscle volumes in both stress UI and POP patients when compared to controls (23.3 and 18.4 versus 32.2 cm^3), as well as a negative relationship between the number of vaginal deliveries and muscle volume. Results may also be presented as a color map used to mathematically characterize the LA in different portions according to measures in different points of their inner and outer surfaces.[46] Multiplanar images may also be used to quantify muscle after damage, using a volume-rendering model of cross-sectional area and global orientation of the remaining muscle after rupture. In the work of Chen et al.,[47] a group of POP patients with unilateral defects revealed decreased bilateral area in pubic portion of PR, but not in the iliococcygeal, which is consistent with the findings in women with PFD.[48]

Understanding LA dynamic behavior and displacement[37] during contraction and straining is also imperative to completely assess PFD. Maximum force developed by the skeletal muscle is related to its cross-sectional area perpendicular to fascicle muscle.[47] This plays an important role as a morphological determinant of muscle capacity, and based on muscle 3D representation, some constitutive biomechanical models take into account fiber direction and compressibility.

Delmas et al.[49] used vectorial animation reconstruction based on MRI to analyze LA contraction properties on rest and dynamic coronal images. The modeling started with manual segmentation, and then sets of points were put on the pelvic bone insertion points. The authors found iliococcygeal muscle to be mainly responsible for assuring LH closure and pelvic organ support against abdominal strain, perhaps due to its

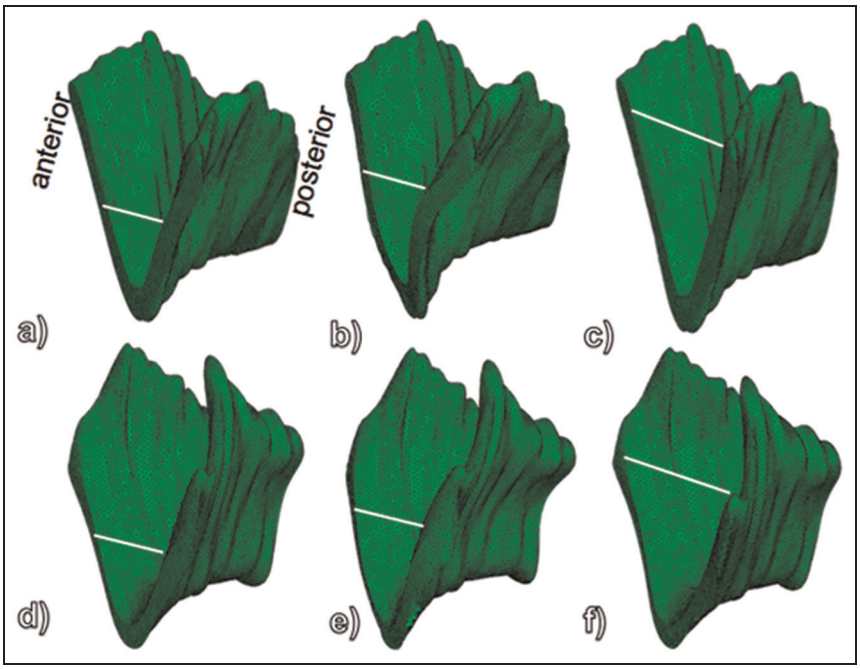

Figure 6. Biomechanical models of (a–c) healthy and (d–f) POP women (20 and 45 years old, respectively). Images display numerical simulation models and muscle position at rest (left column), on contraction (middle column) and during VM (right column). MR images were segmented, and a mesh was created for numerical simulation using ABAQUS™ software. In the case of POP, a weaker response of the posterior portion of the muscle on VM was seen (f).

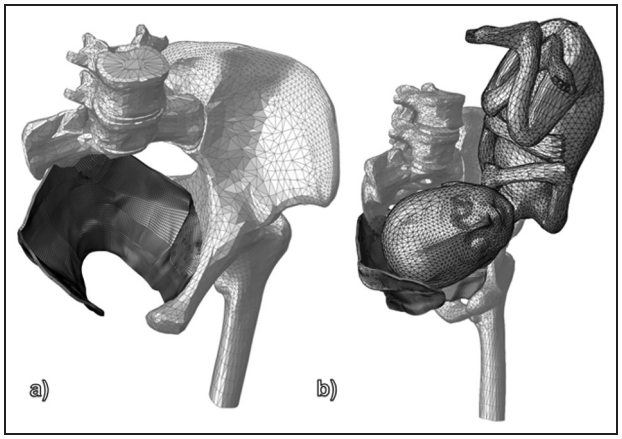

Figure 7. FEM numerical simulation of vaginal childbirth to evaluate the damage on (a) the pelvic floor muscles and (b) during the fetus passage.

more distributed support points on the stiff osseous frame.[49] A relation was found between damage in specific portions of PFM where they attach to fascial tissue and PFD symptoms.[31] Otcenasek et al.[50] built 3D models of normal and avulsed PR muscles after segmentation and surface modeling and reported a relation between the location of muscle avulsion, fascial detachment and destabilization of both anterior and posterior vaginal walls. They also built a 3D multisource model of the fascia by combining MRI, dissection and surgical data. By adding the description of organ geometry to the definition of their fascial insertions, it is easier to understand LA shape and connections.[51]

As stated before, most modeling applications start with manual segmentation of the structures. Besides being time-consuming, this relies on the readers' knowledge of the anatomy of pelvic structures (Figure 8). Furthermore, technical issues such as image noise and low tissue contrast increase the degree of difficulty to define boundaries.[52] (Semi-)automated algorithms may be an alternative to improve segmentation.[52] MRI is well suited for contrast-based segmentation, as it generally enables good tissue discrimination. Nevertheless, in the case of the pelvis, the irregular shape of the organs, the thin margins and the fact that PFM has low intermuscular fat content (which would exhibit high signal against the hypointense muscles) make segmentation procedures a hard task.[53] Also, MR-related artifacts, nonuniform signal and Gaussian noise may hamper segmentation.[54] Image preprocessing strategies like resampling, contrast enhancement, noise removal or mathematical operations are often performed prior to segmentation.[55,56] Different (semi-)automated segmentation techniques and image processing frameworks can be applied to medical images[57–61] and to the pelvis.[59] These methods may also have various classifications. As, for example, they can be classified based on (1) pixel gray level threshold (histogram analysis and edge-based or region-based segmentation); (2) texture/morphological features (Markov random field model, expectation–maximization algorithm or wavelets); (3) clustering techniques (k-nearest neighbor classifier, maximum likelihood algorithm, C-means and Fuzzy C-means algorithms) or (4) deformable models (geodesic active contour, active shape models and active appearance model). Some concerns must be addressed when choosing the most appropriate algorithm, such as the imaging technique, the expected accuracy, its computational complexity, time and interactivity. A priori shape inputs are important to compensate for reduced definition of organ boundaries or poor image contrast.[62] Also, clustering techniques may be efficient where edge points are used to identify the boundaries or to define the energy function. Modified geodesic active contour seems adjusted for bladder segmentation,[63] so it can handle the influence of noise and signal intensity variations. To segment LA, deformable models with topology preservation and a priori knowledge may be complementary.[64] Chan–Vese model (derived from geometric active contour) is sensitive to image or tissue contrast inside and outside the moving contour, and to

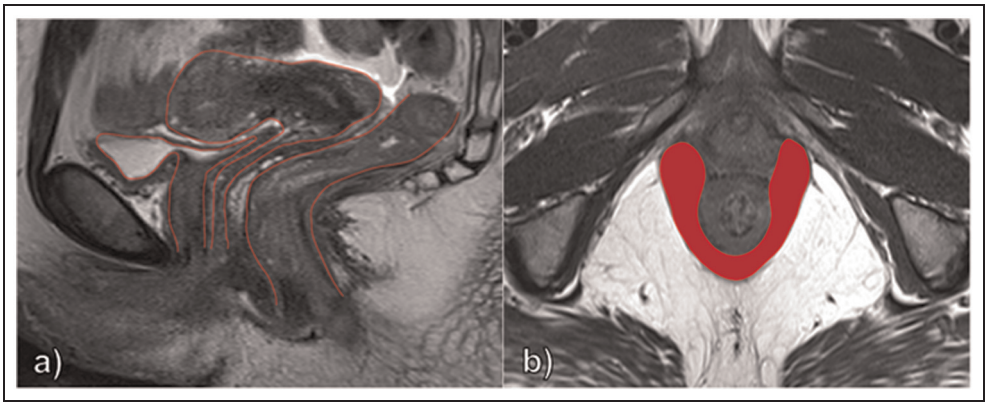

Figure 8. Manual segmentation of pelvic floor structures on high-resolution T2-weighted sagittal and axial MR images: (a) the boundary of the pelvic organs was segmented to build a 3D model of their positioning and (b) pubovisceral portion of the LA was segmented to evaluate area and thickness.

overcome this problem, a shape influence field of the LA may be used to guide the segmentation.[64] A coupled approach for shape and thickness statistical modeling based on harmonic embedding allowed the studying of LA volume at rest, its contraction and straining. Using a set of control points and a statistical shape model, Lee et al. defined the primary features of the muscle surface. The advantage of this approach is that harmonic embedding captures the dynamic information from different levels of stress and subjects by using the statistical modeling of shape and thickness.

From MRI to structure modeling

Computational models have two preliminary requirements: an accurate anatomical representation and information about tissue behavior. The pelvic floor is often evaluated with FEM,[65–67] by using inputs from MRI for structure definition, and also with physical equations based on muscle properties, boundary conditions, and displacement during contraction or VM.

Incomplete knowledge of the constitutive relations and material parameters constrains the accuracy of simulation models. The supporting role of the pelvic fascia and ligaments for the overall pelvic cavity would enrich the simulation with a more realistic display of the different subjects[68] and stress loading conditions regarding the PFM performance. Nevertheless, it is still very difficult to depict all the boundaries and fascial attachments of the PFM to be included in the biomechanical models.[52,69] The definition of the pelvic ligaments and fascial insertions in MRI is a hard task even for experienced readers,[54,70,71] and therefore, fascial and tendinous tissues alongside the pubovisceral muscle attachment are often ignored,[37] and muscles are assumed as connected to the pelvic bone by focal boundary conditions.

Modeling takes into account not only the geometry of the PFM but also their mechanical properties (viscoelasticity and anisotropic mechanical response and (quasi)incompressibility)[34,65–67,72,73] and fiber direction,[73] which is still above conventional MRI spatial resolution. For numerical simulation purposes, muscles are often set to have a near-isotropic behavior, distribution, length and pennation angle.[67] Fiber direction is obtained by applying pressure normal to the surface of the mesh, assuming that for each finite element, the direction of the maximum principal stress coincides with that of the muscle fibers.[66,73] The fact that the direction of the muscle fibers obtained by this method is dependent on the mesh angle and on the boundary conditions, numerical simulations would be improved if more detailed representation of the muscles' inner structure would be possible. Accordingly, DTI may be able to characterize the direction, shape, density, pennation, insertion and eventually internal (dis)arrangement of the PFM, which are beyond the spatial resolution of MR anatomical images. This may improve the numerical simulation methodology because a better definition of the muscle direction and the boundary conditions on the bone and fascia should be easier to achieve.

Conclusion

MRI has proven its value on many clinical conditions. Despite most PFD cases being correctly diagnosed by using clinical assessment, functional tests and ultrasound, detailed imaging enables a better detection of subtle anatomical and functional changes. MR images are not only used in those clinical cases but also used as inputs to modeling applications that serve the purpose of elucidating pelvic organ positioning and PFM response when solicited. Muscle mechanical behavior is conditioned by tissue morphological features that are, so far, very difficult to study in vivo. In fact, there is no in vivo imaging technique to establish both the exact fiber direction and position and the degree of insertion, which are very important issues for biomechanical modeling.

Tractography could help solve that problem since the 3D representation of the muscle and their insertion points should be easier to achieve, including the insertion points that are not attached to the bone but to the rectum, vagina and fascia. Therefore, more precise orientation of the stress forces could be applied to each individual portion of the LA. The added value of this morphological information should influence the processing steps of numerical simulation models.

Acknowledgements

S.B. performed the literature review, the manuscript preparation and writing, and acquired the MR images; T.R. developed some of the FEM models and participated in the discussion of the article's alignment; M.P. developed some of the FEM models; I.R reviewed the MR images; T.M. clinically evaluated the patients whose images are shown in the manuscript and performed its critical revision; and R.N.J. performed critical revision of the manuscript for its intellectual content and participated in the discussion of the article's alignment. All authors read and approved the final manuscript.

Declaration of conflicting interests

None declared.

Funding

This research received no specific grant from any funding agency in the public, commercial or not-for-profit sectors.

References

1. Luber KM. The definition, prevalence, and risk factors for stress urinary incontinence. *Rev Urol* 2004; 6(Suppl. 3): 3–9.

2. Patel PD, Amrute KV and Badlani GH. Pelvic organ prolapse and stress urinary incontinence: a review of etiological factors. *Indian J Urol* 2007; 23(2): 135–141.
3. Chaliha C. Postpartum pelvic floor trauma. *Curr Opin Obstet Gynecol* 2009; 21(6): 474–479.
4. Heilbrun ME, Nygaard IE, Lockhart ME, et al. Correlation between levator ani muscle injuries on magnetic resonance imaging and fecal incontinence, pelvic organ prolapse, and urinary incontinence in primiparous women. *Am J Obstet Gynecol* 2010; 202(5): 488.e1–488.e6.
5. Dietz HP and Wilson PD. Childbirth and pelvic floor trauma. *Best Pract Res Clin Obstet Gynaecol* 2005; 19(6): 913–924.
6. Dietz HP and Simpson JM. Levator trauma is associated with pelvic organ prolapse. *BJOG* 2008; 115(8): 979–984.
7. El Sayed RF, El Mashed S, Farag A, et al. Pelvic floor dysfunction: assessment with combined analysis of static and dynamic MR imaging findings. *Radiology* 2008; 248(2): 518–530.
8. Margulies RU, Hsu Y, Kearney R, et al. Appearance of the *levator ani* muscle subdivisions in magnetic resonance images. *Obstet Gynecol* 2006; 107(5): 1064–1069.
9. Woodfield CA, Krishnamoorthy S, Hampton BS, et al. Imaging pelvic floor disorders: trend toward comprehensive MRI. *AJR Am J Roentgenol* 2010; 194(6): 1640–1649.
10. Abramowitch SD, Feola A, Jallah Z, et al. Tissue mechanics, animal models, and pelvic organ prolapse: a review. *Eur J Obstet Gyncol Reprod Biol* 2009; 144(Suppl. 1): 146–158.
11. DeLancey JO, Kearney R, Chou Q, et al. The appearance of *levator ani* muscle abnormalities in magnetic resonance images after vaginal delivery. *Obstet Gynecol* 2003; 101(1): 46–53.
12. Kearney R, Miller JM and DeLancey JOL. Interrater reliability and physical examination of the pubovisceral portion of the *levator ani* muscle, validity comparisons using MR imaging. *Neurourol Urodyn* 2006; 25(1): 50–54.
13. DeLancey JOL, Morgan DM, Fenner DE, et al. Comparison of *levator ani* muscle defects and function in women with and without pelvic organ prolapse. *Obstet Gynecol* 2007; 109(2 Pt 1): 295–302.
14. Kearney R, Miller JM, Ashton-Miller JA, et al. Obstetric factors associated with levator ani muscle injury after vaginal birth. *Obstet Gynecol* 2006; 107(1): 144–149.
15. Broekhuis SR, Kluivers KB, Hendriks JC, et al. Dynamic magnetic resonance imaging: reliability of anatomical landmarks and reference lines used to assess pelvic organ prolapse. *Int Urogynecol J Pelvic Floor Dysfunct* 2009; 20(2): 141–148.
16. Boyadzhyan L, Raman SS and Raz S. Role of static and dynamic MR imaging in surgical pelvic floor dysfunction. *Radiographics* 2008; 28(4): 949–967.
17. Lakeman MM, Zijta FM, Peringa J, et al. Dynamic magnetic resonance imaging to quantify pelvic organ prolapse: reliability of assessment and correlation with clinical findings and pelvic floor symptoms. *Int Urogynecol J* 2012; 23(11): 1547–1554.
18. Broekhuis SR, Kluivers KB, Hendriks JC, et al. POP-Q, dynamic MR imaging, and perineal ultrasonography: do they agree in the quantification of female pelvic organ prolapse? *Int Urogynecol J Pelvic Floor Dysfunct* 2009; 20(5): 541–549.
19. Tumbarello JA, Hsu Y, Lewicky-Gaupp C, et al. Do repetitive Valsalva maneuvers change maximum prolapse on dynamic MRI? *Int Urogynecol J* 2010; 21(10): 1247–1251.
20. Noakes KF, Bissett IP, Pullann AJ, et al. Anatomically realistic three-dimensional meshes of the pelvic floor and anal canal for finite element analysis. *Ann Biomed Eng* 2008; 36(6): 1060–1071.
21. Schick F. Whole-body MRI at high field: technical limits and clinical potential. *Eur Radiol* 2005; 15: 946–959.
22. Lazar M. Mapping brain anatomical connectivity using white matter tractography. *NMR Biomed* 2010; 23(7): 821–835.
23. Froeling M, Nederveen AJ, Heijtel DF, et al. Diffusion-tensor MRI reveals the complex muscle architecture of the human forearm. *J Magn Reson Imaging* 2012; 36(1): 237–248.
24. Sinha S, Sinha U and Edgerton V-R. In vivo diffusion tensor imaging of the human calf muscle. *J Magn Reson Imaging* 2006; 24(1): 182–190.
25. Ahn S and Lee S. Diffusion tensor imaging: exploring the motor networks and clinical applications. *Korean J Radiol* 2011; 12(6): 651–661.
26. Mori S and van Zijl PC. Fiber tracking: principles and strategies-a technical review. *NMR Biomed* 2002; 15(7–8): 468–480.
27. Parker GJM. Analysis of MR diffusion weighted images. *Br J Radiol* 2004; 77(Suppl. 2): 176–185.
28. Zijta FM, Froeling M, van der Paardt, et al. Feasibility of diffusion tensor imaging (DTI) with fiber tractography of the normal female pelvic floor. *Eur Radiol* 2011; 21(6): 1243–1249.
29. Zijta FM, Lakeman MM, Froeling M, et al. Evaluation of the female pelvic floor in pelvic organ prolapse using 3.0-Tesla diffusion tensor imaging and fiber tractography. *Eur Radiol* 2012; 22(12): 2806–2813.
30. Rousset P, Delmas V, Buy JN, et al. In vivo visualization of the levator ani muscle subdivisions using MR fiber tractography with diffusion tensor imaging. *J Anat* 2012; 221(3): 221–228.
31. Hoyte L, Schierlitz L, Zou K, et al. Two- and 3-dimensional MRI comparison of *levator ani* structure, volume, and integrity in women with stress incontinence and prolapse. *Am J Obstet Gynecol* 2001; 185(1): 11–19.
32. Singh K, Reid WM and Berger LA. Magnetic resonance imaging of normal *levator ani* anatomy and function. *Obstet Gynecol* 2002; 99: 433–438.
33. Kim JK, Kim YJ, Choo MS, et al. The urethra and its supporting structures in women with stress urinary incontinence: MR imaging using an endovaginal coil. *AJR Am J Roentgenol* 2003; 180: 1037–1044.
34. Noakes KF, Pullan AJ, Bissett IP, et al. Subject specific finite elasticity simulations of the pelvic floor. *J Biomech* 2008; 41(14): 3060–3065.
35. Ashton-Miller JA and DeLancey JO. On the biomechanics of vaginal birth and common sequelae. *Annu Rev Biomed Eng* 2009; 11: 163–176.
36. Larson KA, Hsu Y, Chen L, et al. Magnetic resonance imaging-based three-dimensional model of anterior vaginal wall position at rest and maximal strain in women with and without prolapse. *Int Urogynecol J* 2010; 21(9): 1103–1109.
37. Saleme CS, Parente MP, Jorge RM, et al. An approach on determining the displacements of the pelvic floor during voluntary contraction using numerical simulation and MRI. *Comput Methods Biomech Biomed Engin* 2011; 14(4): 365–370.

38. Martins PA, Jorge RM, Ferreira AJ, et al. Vaginal tissue properties versus increased intra-abdominal pressure: a preliminary biomechanical study. *Gynecol Obstet Invest* 2011; 71(3): 145–150.
39. Larson KA, Luo J, Yousuf A, et al. Measurement of the 3D geometry of the fascial arches in women with a unilateral levator defect and "architectural distortion."*Int Urogynecol J* 2012; 23(1): 57–63.
40. Zhang Y, Sweet RM, Metzger GJ, et al. Advanced finite element mesh model of female SUI research during physical and daily activities. *Stud Health Technol Inform* 2009; 142: 447–452.
41. Hoyte L and Damaser MS. Magnetic resonance-based female pelvic anatomy as relevant for maternal childbirth injury simulations. *Ann N Y Acad Sci* 2007; 1101: 361–376.
42. Lavy Y, Sand PK, Kaniel CI, et al. Can pelvic floor injury secondary to delivery be prevented? *Int Urogynecol J* 2012; 23(2): 165–173.
43. Li X, Kruger JA, Nash MP, et al. Anisotropic effects of the levator ani muscle during childbirth. *Biomech Model Mechanobiol* 2011; 10(4): 485–494.
44. Fielding JR, Dumanli H, Schreyer AG, et al. MR-based three-dimensional modeling of the normal pelvic floor in women: quantification of muscle mass. *AJR Am J Roentgenol* 2000; 174(3): 657–660.
45. Hoyte F, Fielding JR, Versi F, et al. Variations in *levator ani* volume and geometry in women: the application of MR based 3D reconstruction in evaluating pelvic floor dysfunction. *Arch Esp Urol* 2001; 54(6): 532–539.
46. Hoyte L, Jakab M, Warfield SK, et al. *Levator ani* thickness variations in symptomatic and asymptomatic women using magnetic resonance-based 3-dimensional color mapping. *Am J Obstet Gynecol* 2004; 191(3): 856–861.
47. Chen L, Hsu Y, Ashton-Miller JA, et al. Measurement of the pubic portion of the *levator ani* muscle in women with unilateral defects in 3D models from MR images. *Int J Gynaecol Obstet* 2006; 92(3): 234–241.
48. Otenásek M, Krofta L, Grill R, et al. Birth injury of the puborectalis muscle–3D ultrasound evaluation. *Ceska Gynekol* 2006; 71(4): 318–322.
49. Delmas V, Ami O and Iba-Zizen MT. Dynamic study of the female *levator ani* muscle using MRI 3D vectorial modeling. *Bull Acad Natl Med* 2010; 194(6): 969–980.
50. Otcenasek M, Krofta L, Baca V, et al. Bilateral avulsion of the puborectal muscle: magnetic resonance imaging-based three-dimensional reconstruction and comparison with a model of a healthy nulliparous woman. *Ultrasound Obstet Gynecol* 2007; 29(6): 692–696.
51. Otcenasek M, Baca V, Krofta L, et al. Endopelvic fascia in women: shape and relation to parietal pelvic structures. *Obstet Gynecol* 2008; 111(3): 622–630.
52. Hoyte L, Brubaker L, Fielding JR, et al.; Pelvic Floor Disorders Network. Segmentation of MRI images of the female pelvic floor: a study of inter- and intra-reader reliability. *J Magn Reson Imaging* 2011; 33(3): 684–691.
53. Blemker SS, Asakawa DS, Gold GE, et al. Image-based musculoskeletal modeling: applications, advances, and future opportunities. *J Magn Reson Imaging* 2007; 25(2): 441–451.
54. Ma Z, Jorge R, Mascarenhas T, et al. Segmentation of female pelvic cavity in axial T2-weighted MR images towards the 3D Reconstruction. *Int J Numer Method Biomed Eng* 2012; 28(6–7): 714–726.
55. Palumbo D, Yee B, Ódea P, et al. Interplay between bias field correction, intensity standardization, and noise filtering for T2-weighted MRI. *Conf Proc IEEE Eng Med Biol Soc* 2011; 2011: 5080–5083.
56. Chen Y, Zhang J and Yang J. An anisotropic images segmentation and bias correction method. *Magn Reson Imaging* 2012; 30(1): 85–95.
57. Heinonen T, Dastidar P, Kauppinen P, et al. Semi-automatic tool for segmentation and volumetric analysis of medical images. *Med Biol Eng Comput* 1998; 36(3): 291–296.
58. Withey DJ and Koles ZJ. Three generations of medical image segmentation: methods and available software. *Int J Bioelectromagn* 2007; 9: 67–68.
59. Ma Z, Tavares JM, Jorge RNM, et al. A review of algorithms for medical image segmentation and their applications to the female pelvic cavity. *Comput Methods Biomech Biomed Engin* 2010; 13(2): 235–246.
60. Sharma N and Aggarwal LM. Automated medical image segmentation techniques. *J Med Phys* 2010; 35(1): 3–14.
61. Yi L and Zhijun G. A review of segmentation method for MR image. In: *Proceedings of the International Conference on Image Analysis and Signal Processing (IASP)*, Zhejiang, China, 9–11 April 2010, New York: IEEE, pp.351–357.
62. Tsai A, Yezzi A Jr, Wells W, et al. A shape-based approach to the segmentation of medical imagery using level sets. *IEEE Trans Med Imaging* 2003; 22(2): 137–154.
63. Ma Z, Jorge R, Mascarenhas T, et al. Novel approach to segment the inner and outer boundaries of the bladder wall in T2-weighted magnetic resonance images. *Ann Biomed Eng* 2011; 39(8): 2287–2297.
64. Ma Z, Jorge RMN and Tavares JM. A shape guided C-V model to segment the *levator ani* muscle in axial magnetic resonance images. *Med Eng Phys* 2010; 32(7): 766–774.
65. Lee SL, Darzi A and Yang GZ. Subject specific finite element modelling of the levator ani. *Med Image Comput Comput Assist Interv* 2005; 8(Pt 1): 360–367.
66. Martins JA, Pato MP, Pires EB, et al. Finite element studies of the deformation of the pelvic floor. *Ann N Y Acad Sci* 2007; 1101: 316–334.
67. Janda S, van der Helm FC and de Blok SB. Measuring morphological parameters of the pelvic floor for finite element modelling purposes. *J Biomech* 2003; 36(6): 749–757.
68. Philips ATM, Pankaj P, Howie CR, et al. Finite element modelling of the pelvis: inclusion of muscular and ligamentous boundary conditions. *Med Eng Phys* 2007; 29: 739–748.
69. Tunn R, DeLancey JO and Quint EE. Visibility of pelvic organ support system structures in magnetic resonance images without an endovaginal coil. *Am J Obstet Gynecol* 2001; 184(6): 1156–1163.
70. Tunn R, Goldammer K, Neymeyer J, et al. MRI morphology of the levator ani muscle, endopelvic fascia, and urethra in women with stress urinary incontinence. *Eur J Obstet Gynecol Reprod Biol* 2006; 126(2): 239–245.
71. Tunn R, DeLancey JO, Howard D, et al. Anatomic variations in the levator ani muscle, endopelvic fascia, and urethra in nulliparas evaluated by magnetic resonance imaging. *Am J Obstet Gynecol* 2003; 188(1): 116–121.
72. Parente MP, Jorge RMN, Mascarenhas T, et al. Deformation of the pelvic floor muscles during vaginal delivery. *Int Urogynecol J Pelvic Floor Dysfunct* 2008; 19(1): 65–71.
73. d'Aulignac D, Martins JA, Pires EB, et al. A shell finite element model of the pelvic floor muscles. *Comput Methods Biomech Biomed Engin* 2005; 8(5): 339–347.

Chapter 3

Original Studies

Original Article

Study I

Moment of inertia as a means to evaluate the biomechanical impact of pelvic organ prolapse.

Brandão S, Da Roza T, Mascarenhas T, Duarte S, Ramos I, Parente M, Jorge RN.

Int J Urol. 2013 Jan;20(1):86-92.

doi: 10.1111/j.1442-2042.2012.03219.x. Epub 2012 Nov 6.

INTERNATIONAL JOURNAL OF UROLOGY

International Journal of Urology (2013) **20**, 86–92 doi: 10.1111/j.1442-2042.2012.03219.x

Original Article: Clinical Investigation

Moment of inertia as a means to evaluate the biomechanical impact of pelvic organ prolapse

Sofia Brandão,[1] Thuane Da Roza,[2] Teresa Mascarenhas,[3] Sonia Duarte,[3] Isabel Ramos,[1] Marco Parente[2] and Renato Natal Jorge[2]

[1]Department of Radiology, Hospital de S. João, [2]Institute of Mechanical Engineering, Faculty of Engineering, University of Porto, and [3]Department of Gynecology and Obstetrics, Hospital de S. João, Faculty of Medicine, University of Porto, Porto, Portugal

Abbreviations & Acronyms
AP = anterior-to-posterior
FI = fecal incontinence
MOI = moment of inertia
MRI = magnetic resonance imaging
PFD = pelvic floor dysfunction
PFM = pelvic floor muscles
POP = pelvic organ prolapse
POP-Q = Pelvic Organ Prolapse Quantification system
PVM = pubovisceral muscle
RL = right-to-left
UI = urinary incontinence
US = ultrasound

Correspondence: Renato Natal Jorge Ph.D., Institute of Mechanical Engineering, Faculty of Engineering, University of Porto, Rua Dr Roberto Frias, Porto 4200-465, Portugal. Email: rnatal@fe.up.pt

Received 31 July 2012; accepted 30 September 2012.
Online publication 6 November 2012

Objectives: To present an alternative measure (moment of inertia) to describe the anatomical features of the pelvic organ prolapse.

Methods: A total of 30 women (21 diagnosed as having pelvic organ prolapse and 9 as controls) were evaluated by clinical scales and magnetic resonance imaging. Imaging biometric measures were carried out. Moment of inertia, pubovisceral muscle thickness and area, and levator hiatus anterior-to-posterior and lateral measures were compared by means of non-parametric tests, as well as their correlation with demographic features of the two sample groups.

Results: Moment of inertia, muscle area and levator hiatus diameters were statistically different between patients and controls. Furthermore, they were also well correlated with prolapse-associated factors, such as the number of vaginal deliveries and age, as well as Pelvic Organ Prolapse Quantification system and imaging staging of levator ani defects.

Conclusions: Moment of inertia can be used as a new parameter to evaluate pelvic floor damage resulting from prolapse.

Key words: biomechanics, moment of inertia, pelvic floor muscles, pelvic organ prolapse, pubovisceral muscle.

Introduction

PFD includes clinical problems affecting a woman's pelvic organs and the structures that support them, such as the pelvic fascia and the PFM. The most common types of female PFD comprise POP, UI and FI. Its high prevalence and impact on quality-of-life makes it a focus of different specialities, such as primary care doctors, gynecologists, urologists and, because of its relationship with biomechanical features, also engineers.

The overall model for PFD in women includes family history, heavy work, high-impact sports activity, chronic straining or hormonal status.[1,2] Pregnancy and vaginal delivery were also proven to relate to nerve and PFM damage, connective tissue or ligament disruption, increasing the risk for both urinary and defecatory symptoms or vaginal bulging. Among the predisposing factors to developing PFD, vaginal delivery is, in fact, the most relevant independent risk factor.[3–7] Evidence of muscle physical damage, denervation and changes in morphology has been reported in women with UI and POP, and progress is being made to assess what specific role levator ani muscle injury plays in the pathogenesis of these common problems.[8–11] The consequences of levator ani damage might depend on which and how its components were damaged. Injury to each component might be expected to have a different functional effect. Pubovisceral muscle includes pubococcygeal and puborectal muscles, which form a sling around the rectum and vagina to promote urogenital hiatus closure.[7,12] Its disruption or thickness abnormalities are associated with UI and POP.[10,12–15]

Anatomical features of PFD were previously described by using US and MRI, with great success.[16,17] Even with a direct association between pubovisceral muscle thinning or defects and the increase of levator hiatus and POP diagnosis,[18] a case–control study showed that

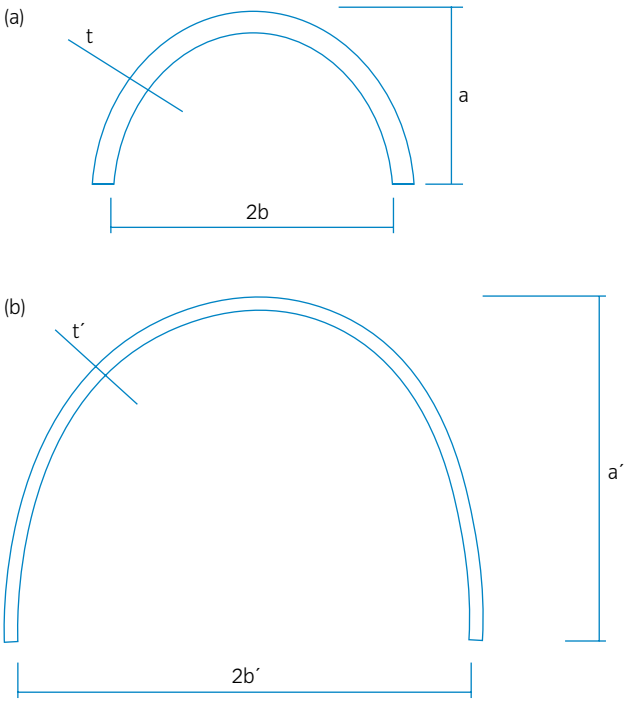

Fig. 1 Morphological features of a structure and its relationship with MOI. This scheme approximates the shape of semi-elliptical donuts, which can be understood as equivalent to a cross-sectional area of the pubovisceral muscle. When the thickness and diameters vary (from [a] to [b]) the value of MOI changes. 2b, Width, which will correspond to RL diameter; a, height, which will correspond to AP diameter; t, thickness.

women with prolapse had an equal likelihood of having minor defects as asymptomatic normal women.[19] Additionally, a recent study showed that defects and loss of muscle bulk in the puborectal muscle were not seen by MRI in women with POP.[20] Despite the advantages of clinical US and MRI, it must be emphasized that most imaging analysis on axial static MRI describes muscle loss, but not its biomechanical impact. So, in a biomechanical perspective, a new predictive measure of prolapse event or severity based on static images would be very useful.

Muscle atrophy, changes in morphology or disruption cause functional weakness and might relate to the reduction of MOI.[21] MOI is a geometrical property of a structure's cross-sectional area that constitutes an important geometrical parameter to define bending or deflection characteristics of that structure. This measure is associated with several morphological properties, such as the area, the thickness and, in a lesser degree, other dimensions of the muscle cross-sectional area, such as the diameters, as described by Young.[22] The greater the MOI, the increased resistance to deformation, which means that less strength is necessary to compensate for positional shifts. The MOI of a cross-sectional area can change according to its morphological features, as shown on Figure 1. For example, when the thickness ($t \rightarrow t'$) and area of the structure decrease, and the diameters increase ($a \rightarrow a'$ and $2b \rightarrow 2b'$), MOI is reduced. In this case, a higher probability of deformation is related to the lower stiffness, and the force necessary to counteract pressure is superior.

POP might be caused by a weaker supportive structure of the PFM that allows viscera to descend through the levator hiatus, a functional gap of the levator ani through which the urethra, vagina and rectum might move down.[23,24] Straining and coughing increase pressure onto the pelvic floor, inducing muscle deformation and reinforcing levator hiatus opening. The thinner the muscle becomes and the wider the levator hiatus becomes, the resistance to deformation in the cross-sectional area, which defines MOI, is lower. The authors explored the idea that perhaps a thinner or disrupted pubovisceral muscle, which is related to levator hiatus widening and POP, and also to a weaker active and passive response to increase pressure, could be related to a lower MOI. However, to date, there is no measure that relates muscle thickness, area and morphology, which would be important in the clinical setting to assess the real biomechanical impact of POP on the PFM. And so, MOI could be an important tool to describe it. Furthermore, it would be very relevant to predict if nulliparous women with pubovisceral muscle with decreased MOI would be at a higher risk of developing POP, and also, what is the association between the decrease in MOI and the number of vaginal deliveries in POP women.

The aim of the present study was to determine if the MOI parameters of the PFM could be correlated to clinical diagnosis and (static MR) imaging measures of POP; additionally, to compare morphological parameters between women with and without POP.

Methods

The present study was approved by the Ethics Committee of the Hospital de São João, Porto. A total sample of 30 women was observed by the same gynecologist. Clinical evaluation and POP–Q were carried out to assess POP. A total of 21 women were diagnosed with POP, whereas nine were used as the control group.

All the women were imaged by means of MRI, using a 3 Tesla scanner. Axial high-resolution T2-weighted images were acquired at rest in the supine position, along the puborectal line.

To carry out image evaluation and measurements, the axial slice closer to the plane of minimal hiatal dimensions was used (Fig. 2). This plane is defined as the minimal AP diameter of the levator hiatus, from the postero-inferior margin of the symphysis pubis to the anterior margin of the pubovisceral muscle, where it defines the anorectal angle.[25–27] In the present study, all the measures were carried out in the pubovisceral muscle, as according to DeLancey

Fig. 2 High-resolution T2-w MR images were acquired along (a) the puborectal line (green line) in order to achieve the orientation of the pubovisceral muscle, and (b) the plan of minimal hiatal dimensions on the axial images.

et al.,[28] the pubococcygeal and puborectal might not be well differentiated on US or MRI.

To calculate pubovisceral muscle MOI and cross-sectional area, it was manually segmented using a contour spline. The software Inventor (Autodesk, San Raphael, CA, USA) was used to draw and calculate those variables (Fig. 3). Additionally, three other measures were carried out in the same slice: thickness of right and left portions of pubovisceral muscle at the level of midvagina and levator hiatus AP and RL dimensions, following the methodology described in Majida *et al*. and Kruger *et al*. (Fig. 4).[29,30] Finally, images were evaluated for levator ani defects as proposed by DeLancey *et al*.,[19] in which women were classified as having "major" (more than half missing), "minor" (less than half of the muscle missing) or no defects.

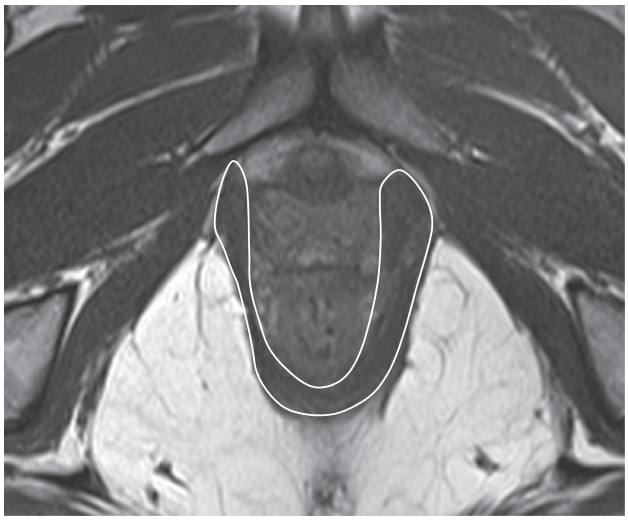

Fig. 3 Manual procedure to draw the pubovisceral muscle contour using Inventor software.

Statistical analysis

All continuous variables were expressed as mean ± SD and range. The numerical data were compared by Student's *t*-test or Mann–Whitney *U*-test. Correlation between variables was determined by Spearman's correlation analysis. Estimation of MOI decrease was calculated by simple linear regression analysis. A *P*-value of 0.05 or less was considered to be significant.

Results

A total of 30 women were evaluated (9 nulliparous and 21 multiparous), with an age range of 21–83 years (mean 48.3 ± 24.6). A total of 40%[12] of the women were in menopause. The range of patients' pregnancies was 0–6 (mean 1.8 ± 2.3) and the number of vaginal deliveries was also 0–6 (mean 1.5 ± 2.0). The POP-Q staging resulted in: 30% (9/30) with stage 0, 23.3% (7/30) with stage 1, 23.3% (7/30) with stage 2 and 23.3% (7/30) with stage 3. According to the DeLancey *et al*. MRI grading system,[19] 10 women were classified as having no defects, nine with "minor" defects and 11 with "major" defects.

The mean values of AP and RL diameters, area, thickness, and MOI of the pubovisceral muscles of the two groups are summarized in Table 1.

Table 2 lists the correlations between MOI and demographic, clinical, and morphological variables. There was a negative correlation, at least moderate, between the MOI with age, pregnancy, vaginal delivery, POP-Q stages and MRI grading system. Pubovisceral muscle area showed very good correlation with MOI ($r = 0.907$, $P = 0.000$) and good correlation with POP-Q stages ($r = –0.695$, $P = 0.001$), pregnancy ($r = -0.677$, $P = 0.001$) and vaginal delivery

Table 1 Measures of levator hiatus diameters, pubovisceral muscle area, thickness and moment of inertia in women with and without prolapse

Variables	Without prolapse ($n = 9$)	With prolapse ($n = 21$)	P-value
Anterior-to-posterior diameter (cm)	4.7 ± 0.56	5.6 ± 0.71	0.007
Lateral diameter (cm)	2.7 ± 0.58	3.7 ± 0.61	0.002
Area of the pubovisceral muscle (mm^2)	748.3 ± 324.8	425.9 ± 111.9	0.006
Thickness, right side (cm)	0.67 ± 0.30	0.43 ± 0.16	0.036
Thickness, left side (cm)	0.97 ± 0.36	0.75 ± 0.30	0.146
Moment of inertia (mm^4)	162 596.7 ± 81 198.8	65 505.3 ± 21 820.3	0.001

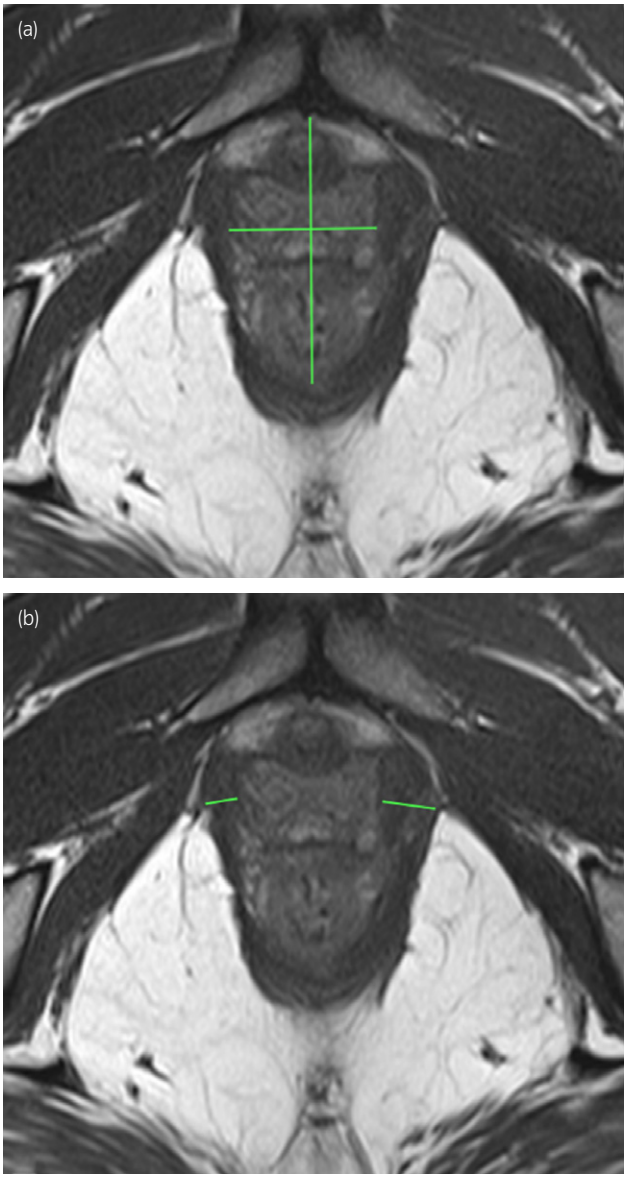

Fig. 4 Levator hiatus diameters and pubovisceral muscle thickness measures. The anterior-to-posterior and lateral dimensions of (a) the levator hiatus were carried out, (b) along with pubovisceral muscle thickness at the level of midvagina.

($r = –0.677$, $P = 0.001$). There were no significant correlations between area and hiatus diameters. Muscle thickness at the level of midvagina, both left and right sides, was positively correlated with MOI ($r = 0.552$ and $r = 0.561$, respectively).

Mean values of muscle thickness on the right and left sides were superior for the control group, but an unexpected finding was the fact that the right side was thinner for both groups. This might be related to an imaging artifact. The thickness on the right side was correlated with pregnancy, vaginal delivery and POP-Q stages ($r = –0.542$, $P = 0.014$; $r = –0.549$, $P = 0.012$ and $r = –0.530$, $P = 0.016$, respectively). However, it was not possible to establish the same correlations for the left side.

As expected, POP-Q staging was correlated with AP and lateral levator hiatus diameters ($r = 0.460$ and $r = 0.760$, respectively).

Discussion

POP has been associated with avulsion of the levator ani from the pubic arch, the size of levator hiatus and PFM weakness.[19,31] However, besides traumatic-related features, muscle morphological characteristics might influence mechanical behavior of the PFM, and might contribute to generate less closure force during a contraction. Thus, in addition to scoring levator ani defects and measuring levator hiatus, it is also important to evaluate the morphology of the PMF. MOI values directly establish an important association with pubovisceral muscle area and morphology, allowing complementary information. Similar to what other authors have described,[10] the present study found significantly increased hiatus AP and RL diameters in POP women. The present results showed a moderate correlation between MOI and AP and RL hiatus diameters and thickness, weaker than the correlation obtained for pubovisceral area.

DeLancey *et al*. found that women with POP could contract the PFM with just 43% of the force generated by women with no POP.[19] By knowing that lower MOI values relate to a weaker muscle biomechanical response as a result of the loss of mechanical elasticity, this means that for the same amplitude of movement, the muscle needs higher force

Table 2 Correlation between MOI and variables

	Age	Pregnancy	Vaginal delivery	Midvagina PVM thickness		Area of PVM	POP-Q	MRI grading-system	AP	RL
				Right	Left					
MOI	$r = -0.534$ $P = 0.015$*	$r = -0.727$ $P = 0.000$*	$r = -0.747$ $P = 0.000$*	$r = 0.561$ $P = 0.010$*	$r = 0.552$ $P = 0.012$*	$r = 0.907$ $P = 0.000$*	$r = -0.790$ $P = 0.000$*	$r = -0.684$ $P = 0.001$*	$r = -0.51$ $P = 0.04$	$r = -0.50$ $P = 0.042$

*Significant correlation.

during its contraction. The present study also showed that POP women had almost one-third of the MOI mean value when compared with the control group (65 505.3 *vs* 162 596.7 mm^4, respectively). Therefore, despite measuring different aspects of the pelvic floor, they might have very similar clinical meaning. Furthermore, as MOI shows a pattern of biomechanical function, it might be seen as complementary information on the ability to resist to abdominal pressure, which can be obtained in static images through anatomical features of the pelvic floor muscles.

The strongest correlations were obtained with the number of vaginal deliveries, which is the most important independent risk factor for developing POP, and also with POP-Q staging system, which is the most widely used clinical measure of POP. This means that MOI might be able not only to identify POP, but also to predict POP-related morphological defects and functional damage. MOI is strongly associated with muscle area, which in turn is dependent on its thickness, and so, it could be used as its indirect measure. As expected, the results showed a significant correlation between MOI and both muscle area and thickness, and a weaker association between MOI and AP and RL hiatus diameters. The levator hiatus diameters were not significantly correlated with these two morphological characteristics of the muscle (area and thickness), even though they were increased, even at rest, when compared with controls. Additionally, POP women showed decreased values of muscle thickness and area. These findings portray the consequences of demographic and clinical characteristics, such as age, pregnancy and the traumatic event of vaginal delivery.

POP is associated with a disrupted levator ani, and also with a wider levator hiatus. Our control group presented 27% lower RL diameter and 16% AP diameter, and also 56% thicker muscle on the right side and 29% on the left side. The passage of the newborn though the birth canal causes injury to the pelvic floor structures, widening the levator hiatus and stretching of the connective tissue.[32] This might cause pelvic organ downward movement and lead to less vaginal closure force during maximal contraction, modifying the biomechanical mechanism. The present results showed a moderate association between pregnancy and vaginal delivery effects on the size of the levator hiatus, but a stronger negative correlation with MOI, which could therefore be regarded as an alternative measure.

The mechanical effect of pregnancy might induce biomechanical, neurological or neuromuscular changes to the pelvic floor and pelvic organ supports,[33] but the effect of pregnancy itself on pelvic organ support is not well studied. However, the impact of the traumatic event of vaginal delivery is well known.[6] To estimate MOI variation, the regression expression was used (137 871 + [−19 116 × number of vaginal deliveries]) as a means to predict how MOI values would decrease with the increasing number of vaginal deliv-

eries. We were able to say that a women having 3.78 vaginal deliveries has a MOI value of 65 612 mm^4, which is, in fact, very close to what we found in our clinically proven POP group (65 505 mm^4).

Although MRI is not the routine imaging technique to evaluate pelvic floor dysfunction, the present article aimed to explore the anatomical features of the muscle on high-resolution MRI to obtain a meaningful biomechanical concept that relates MOI to functional and clinical prediction of muscle performance and damage. Similar procedures are being tested by US, which is more commonly carried out, and offers direct anatomical and functional detail.

The present study has certain limitations. First, the sample size was small. Also, MRI is an expensive technique to be used just for this purpose. Second, although POP-Q was used to establish POP diagnosis and staging, the results of the present study should be confirmed by means of dynamic US measures of levator ani and levator hiatus deformation under load. Finally, a larger group and further research are required to confirm the relevance and significance of the present findings.

Future work will focus on MOI measures in different pelvic compartments to establish typical anterior, middle and posterior values; and also to find threshold values for the different POP stages. Furthermore, biomechanical computer-based simulations of contraction and valsalva maneuver will allow to confirm lateral and downward muscle displacement associated with MOI threshold values.

In conclusion, MOI seems to be a reliable measure of POP-related anatomical changes of the pubovisceral muscle morphology. Furthermore, it presented the strongest correlation with demographic and clinical variables.

Conflict of interest

None declared.

References

1 Bø K. Urinary incontinence, pelvic floor dysfunction, exercise and sport. *Sports Med.* 2004; **34**: 451–64. Epub 2004/07/06.

2 Baert AL, Kanuth M. *Imaging Pelvic Floor Disorders*. Springer-Verlag Berlin Heidelberg, Berlin, 2008.

3 Chiaffarino F, Chatenoud L, Dindelli M *et al*. Reproductive factors, family history, occupation and risk of urogenital prolapse. *Eur. J. Obstet. Gynecol. Reprod. Biol.* 1999; **82**: 63–7. Epub 1999/04/07.

4 Persson J, Wolner-Hanssen P, Rydhstroem H. Obstetric risk factors for stress urinary incontinence: a population-based study. *Obstet. Gynecol.* 2000; **96**: 440–5. Epub 2000/08/29.

5 Minassian VA, Drutz HP, Al-Badr A. Urinary incontinence as a worldwide problem. *Int. J. Gynaecol. Obstet.* 2003; **82**: 327–38. Epub 2003/09/23.

6 Walker GJ, Gunasekera P. Pelvic organ prolapse and incontinence in developing countries: review of prevalence and risk factors. *Int. Urogynecol. J.* 2011; **22**: 127–35. Epub 2010/07/10.

7 Kearney R, Miller JM, Delancey JO. Interrater reliability and physical examination of the pubovisceral portion of the levator ani muscle, validity comparisons using MR imaging. *Neurourol. Urodyn.* 2006; **25**: 50–4. Epub 2005/11/24.

8 Dietz HP, Steensma AB. The prevalence of major abnormalities of the levator ani in urogynaecological patients. *BJOG* 2006; **113**: 225–30. Epub 2006/01/18.

9 Dietz HP, Shek C. Levator avulsion and grading of pelvic floor muscle strength. *Int. Urogynecol. J. Pelvic Floor Dysfunct.* 2008; **19**: 633–6. Epub 2007/11/14.

10 Dietz HP, Simpson JM. Levator trauma is associated with pelvic organ prolapse. *BJOG* 2008; **115**: 979–84. Epub 2008/05/28.

11 Dietz HP, Shek KL. Levator defects can be detected by 2D translabial ultrasound. *Int. Urogynecol. J. Pelvic Floor Dysfunct.* 2009; **20**: 807–11. Epub 2009/06/06.

12 DeLancey JO, Kearney R, Chou Q, Speights S, Binno S. The appearance of levator ani muscle abnormalities in magnetic resonance images after vaginal delivery. *Obstet. Gynecol.* 2003; **101**: 46–53. Epub 2003/01/09.

13 Kearney R, Miller JM, Ashton-Miller JA, DeLancey JO. Obstetric factors associated with levator ani muscle injury after vaginal birth. *Obstet. Gynecol.* 2006; **107**: 144–9. Epub 2006/01/06.

14 Macura KJ, Genadry RR, Bluemke DA. MR imaging of the female urethra and supporting ligaments in assessment of urinary incontinence: spectrum of abnormalities. *Radiographics* 2006; **26**: 1135–49. Epub 2006/07/18.

15 DeLancey JO, Trowbridge ER, Miller JM *et al*. Stress urinary incontinence: relative importance of urethral support and urethral closure pressure. *J. Urol.* 2008; **179**: 2286–90. discussion 2290. Epub 2008/04/22.

16 Margulies RU, Hsu Y, Kearney R, Stein T, Umek WH, DeLancey JO. Appearance of the levator ani muscle subdivisions in magnetic resonance images. *Obstet. Gynecol.* 2006; **107**: 1064–9. Epub 2006/05/02.

17 El Sayed RF, El Mashed S, Farag A, Morsy MM, Abdel Azim MS. Pelvic floor dysfunction: assessment with combined analysis of static and dynamic MR imaging findings. *Radiology* 2008; **248**: 518–30. Epub 2008/06/25.

18 Ansquer Y, Fernandez P, Chapron C *et al*. Static and dynamic MRI features of the levator ani and correlation with severity of genital prolapse. *Acta Obstet. Gynecol. Scand.* 2006; **85**: 1468–75. Epub 2007/01/30.

19 DeLancey JO, Morgan DM, Fenner DE *et al*. Comparison of levator ani muscle defects and function in women with and without pelvic organ prolapse. *Obstet. Gynecol.* 2007; **109** (2 Pt 1): 295–302. Epub 2007/02/03.

20 DeLancey JO, Sorensen HC, Lewicky-Gaupp C, Smith TM. Comparison of the puborectal muscle on MRI in women with POP and levator ani defects with those with normal support and no defect. *Int. Urogynecol. J.* 2012; **23**: 73–7. Epub 2011/08/09.

21 McLester J, Pierre P. *Applied Biomechanics: Concepts and Connections*. Thomson Wardsworth, Belmont, CA, 2008.
22 Young WC. *ROARK'S Formulas for Stress & Strain*, 6th edn. McGraw-Hill International Editions, Singapore, 1989.
23 Hoyte L, Schierlitz L, Zou K, Flesh G, Fielding JR. Two- and 3-dimensional MRI comparison of levator ani structure, volume, and integrity in women with stress incontinence and prolapse. *Am. J. Obstet. Gynecol.* 2001; **185**: 11–19. Epub 2001/08/03.
24 Clark NA, Brincat CA, Yousuf AA, Delancey JO. Levator defects affect perineal position independently of prolapse status. *Am. J. Obstet. Gynecol.* 2010; **203**: 595.e17–22. Epub 2010/09/28.
25 Dietz HP, Shek KL. Tomographic ultrasound imaging of the pelvic floor: which levels matter most? *Ultrasound Obstet. Gynecol.* 2009; **33**: 698–703. Epub 2009/05/13.
26 Kruger JA, Heap SW, Murphy BA, Dietz HP. How best to measure the levator hiatus: evidence for the non-Euclidean nature of the "plane of minimal dimensions". *Ultrasound Obstet. Gynecol.* 2010; **36**: 755–8. Epub 2010/07/21.
27 Gregory WT, Nardos R, Worstell T, Thurmond A. Measuring the levator hiatus with axial MRI sequences: adjusting the angle of acquisition. *Neurourol. Urodyn.* 2011; **30**: 113–16. Epub 2010/11/04.
28 DeLancey JO. The anatomy of the pelvic floor. *Curr. Opin. Obstet. Gynecol.* 1994; **6**: 313–16. Epub 1994/08/01.
29 Majida M, Braekken IH, Bo K, Benth JS, Engh ME. Validation of three-dimensional perineal ultrasound and magnetic resonance imaging measurements of the pubovisceral muscle at rest. *Ultrasound Obstet. Gynecol.* 2010; **35**: 715–22. Epub 2010/02/24.
30 Kruger JA, Heap SW, Murphy BA, Dietz HP. Pelvic floor function in nulliparous women using three-dimensional ultrasound and magnetic resonance imaging. *Obstet. Gynecol.* 2008; **111**: 631–8. Epub 2008/03/04.
31 Braekken IH, Majida M, Ellstrom Engh M, Holme IM, Bo K. Pelvic floor function is independently associated with pelvic organ prolapse. *BJOG* 2009; **116**: 1706–14. Epub 2009/11/13.
32 Shek KL, Dietz HP. The effect of childbirth on hiatal dimensions. *Obstet. Gynecol.* 2009; **113**: 1272–8. Epub 2009/05/23.
33 South MM, Stinnett SS, Sanders DB, Weidner AC. Levator ani denervation and reinnervation 6 months after childbirth. *Am. J. Obstet. Gynecol.* 2009; **200**: 519.e1–7. Epub 2009/03/10.

Editorial Comment

Editorial Comment to Moment of inertia as a means to evaluate the biomechanical impact of pelvic organ prolapse

I was intrigued to read this paper.[1] It exemplifies the benefits to be derived from a collaboration between clinicians, imaging specialists and biomechanical engineers, and it takes us further down the road towards a full understanding of pelvic floor dysfunction. In a nutshell, the moment of inertia (MOI) model claims that a thicker muscle forming a narrower hiatus is stiffer and hence will stretch less. This assumption seems eminently reasonable, and the association observed between MOI and prolapse grading seems to confirm its validity.

Having said that, any model stands and falls with its performance in the real world. It needs to be tested against reality. Hence, it is reasonable to consider whether available literature data allows us to test (confirm or refute) the modeling presented here. In fact, some of this data seems to argue against universal applicability of the concept.

In childbirth, the hiatus is massively overstretched,[2] but in a very substantial minority of vaginally parous women the levator muscle and hiatus return to what they were before, both functionally and anatomically.[3] Surely the MOI concept would argue against a return to normal in such a situation, and yet commonly that is exactly what happens. Second, it has been shown that a thicker levator muscle in athletes is associated with increased rather than decreased distensibility and pelvic organ descent rather than decreased,[4] again suggesting that the MOI concept has limitations.

There are some minor issues with this interesting paper, not the least that it reports a small data set, and that the anatomical information used as input data was obtained in women at rest and in the supine position, without any attempt to control for the high prevalence of pelvic floor trauma. This is a potential problem, as disconnection of the muscle from the sidewall increases distensibility of the hiatus,[5] likely regardless of the MOI of the muscle itself, as a much more distensible tissue; that is, vaginal muscularis and mucosa, now constitute part of the hiatal circumference. In short, the biomechanical properties of the muscle itself might not matter that much if it is disconnected from its insertion, especially if the trauma is bilateral.

The moment of inertia concept would postulate a potentially more passive role for the levator ani muscle in pelvic organ support. Removing distension as a result of prolapse

should lead to shortening and thickening of the muscle, and normalization of functional anatomy. This is not likely to be common, as shown in a recent study demonstrating that prolapse surgery, even if fully effective, does not usually lead to normalization of hiatal dimensions.[6] Having said that, in some women prolapse repair does seem to result in substantial improvement of functional levator anatomy, and the MOI concept might help explain such surprising positive changes. In fact, one wonders whether there might be some therapeutic applicability of this model; for example, by measures that limit the distensibility of the hiatus surgically.[7]

For future work in this field, it might be advantageous to utilize dynamic rather than static imaging. Four-dimensional translabial ultrasound can provide both static measures of levator thickness and hiatal dimensions, as well as document distensibility under load.[8] This would allow testing of MOI modeling in large data sets, both symptomatic and asymptomatic, as well as before and after childbirth, and before and after conservative and surgical interventions, enabling us to apply this intriguing model to real-world situations.

Hans Peter Dietz M.D., Ph.D.
Department of Obstetrics, Gynaecology and Neonatology, Sydney Medical School Nepean, Nepean Hospital, Penrith, New South Wales, Australia
hpdietz@bigpond.com

DOI: 10.1111/iju.12020

Conflict of interest

The author has received an unrestricted educational grant from GE Medical Ultrasound.

References

1 Brandão S, Da Roza T, Mascarenhas T *et al*. Moment of inertia as a means to evaluate the biomechanical impact of pelvic organ prolapse. *Int. J. Urol.* 2013; **20**: 86–92.
2 Svabik K, Shek K, Dietz H. How much does the levator hiatus have to stretch during childbirth? *Br. J. Obstet. Gynaecol.* 2009; **116**: 1657–62.
3 Shek K, Dietz H. Intrapartum risk factors of levator trauma. *Br. J. Obstet. Gynaecol.* 2010; **117**: 1485–92.
4 Kruger J, Dietz H, Murphy B. Pelvic floor function in elite nulliparous athletes and controls. *Ultrasound Obstet. Gynecol.* 2007; **30**: 81–5.
5 Dietz H. Quantification of major morphological abnormalities of the levator ani. *Ultrasound Obstet. Gynecol.* 2007; **29**: 329–34.
6 Andrew B, Shek K, Chantarasorn V, Dietz H. Enlargement of the levator hiatus in female pelvic organ prolapse: cause or effect? *Neurourol. Urodyn.* 2011; **30**: 864–5.
7 Dietz HP, Korda A, Benness C, Wong V, Shek KL, Daly O. Surgical reduction of the levator hiatus. *Neurourol. Urodyn.* 2012; **31**: 872–3.
8 Dietz H, Shek K, Clarke B. Biometry of the pubovisceral muscle and levator hiatus by three-dimensional pelvic floor ultrasound. *Ultrasound Obstet. Gynecol.* 2005; **25**: 580–5.

Original Article

Study II

Do asymptomatic former high-impact sports practitioners maintain the ability to contract the pelvic floor muscles?

Brandão S, Da Roza T, Mascarenhas T, Ramos I, Natal Jorge R.

J Sports Med Phys Fitness. 2015 Nov;55(11):1272-1276. Epub 2014 Oct 30.

J SPORTS MED PHYS FITNESS 2015;55:1272-6

Do asymptomatic former high-impact sports practitioners maintain the ability to contract the pelvic floor muscles?

S. BRANDÃO [1, 2], T. DA ROZA [2], T. MASCARENHAS [3], I. RAMOS [1], R. NATAL JORGE [2]

Aim. **Sports are associated with pelvic floor dysfunction. This work aimed to assess, in nulliparous asymptomatic women, whether previous intense practice of high-impact sports is associated with differences in morphology and contraction of the pelvic floor muscles, when compared to women who practiced low-level physical activity.**

Methods. **In this prospective pilot study, 7 former high-impact sports practitioners and a control group (N.=7) were compared. Clinical evaluation and self-administered questionnaires were used to gather information about pelvic floor dysfunction and physical activity. Static and cine dynamic MR images were acquired. Morphological measures of the pubovisceral muscle area and thickness, and *levator hiatus* (LH) anterior-to-posterior diameter, width and area were taken in the static images. LH anterior-to-posterior diameter was again assessed in the dynamic acquisition (consecutive blocks of rest *vs.* maximal voluntary contraction). The relative variation between these two conditions was used as an indirect measure of contraction.**

Results. **No abnormal clinical or imaging findings were reported. Former high-impact sports practitioners evidenced decreased pubovisceral muscle thickness (right side P=0.005; left side P=0.004) and area (P=0.004), and larger *levator hiatus* width and area (P=0.045; P=0.005). Only its anterior-to-posterior diameter was similar (4.89cm±0.35 and 4.81cm±0.17, respectively). Their ability to perform maximum voluntary contractions seems to have decreased (8.03%±0.81 *vs.* 13.74%±0.95 for controls).**

Conclusion. **The current results suggest that women who previously practiced high-impact sports, even being asymptomatic, may have suffered damage to the pelvic floor muscles due to the biomechanical impact of the sports. They may require pelvic floor muscle training to increase muscle thickness and hiatal closing capacity.**

KEY WORDS: Exercise - Pelvic floor - Urinary incontinence.

Corresponding author: S. Brandão, Centro Hospitalar de São João - EPE Alameda Professor Hernani Marteiro, 4202 - 451 Porto, Portugal. E-mail: sofia.brand@gmail.com

[1]Department of Radiology
Centro Hospitalar de São João-EPE
Faculty of Medicine, University of Porto
Porto, Portugal
[2]LAETA, INEGI, Faculty of Engineering
University of Porto, Porto, Portugal
[3]Department of Obstetrics and Gynecology
Centro Hospitalar de São João-EPE
Faculty of Medicine, University of Porto,
Porto, Portugal

Stress urinary incontinence (SUI) — involuntary urine loss during elevated abdominal pressure [1] — affects approximately 50% of middle-aged women when coughing, straining or during sports.[2] SUI presents high prevalence for high-impact activities such as trampoline, gymnastics and ball games,[3] due to the constant pressure increase upon the pelvic floor muscles (PFM). One hypothesis is that this may lead to a continuous pre-contraction and strengthening during training.[4] However, intense training may overload and stretch the PFM,[3, 5] which explains why athletes develop structural and functional changes that promote SUI.

Defects of the PFM lead to biomechanical weakening.[6] Function and strength can be assessed through vaginal palpation,[7] electromyography, manometry,[8] or dynamic ultrasound and magnetic resonance imaging (MRI).[9] Sagittal cine MRI enables one to evaluate the pelvic organs during active contraction and/or valsalva maneuver, but it does not quantify muscle contraction.

Assuming that women who undertake high-impact sports for a long period overload their PFM,[3] it is expected that these forces cause some degree of

muscle damage or weakening, and widening of the genital *hiatus*, with negative biomechanical outcome in the long-term. Since SUI in exercising women and athletes is not fully understood, we aimed to assess if previous intense sports practice is associated with differences in morphology and contraction of the PFM, when compared to low-level of physical activity. This was done by analyzing the pubovisceral muscle (PVM) and the *levator hiatus* (LH) in nulliparous asymptomatic women through MRI, in order to study on the biomechanical behavior of the PFM in this specific population. To our knowledge, no previous study has either focused on this particular aspect on asymptomatic former practitioners.

Materials and methods

Subjects

The Ethics Committee (CES195/12) approved this prospective pilot study, and all the participants gave their informed consent. We tested the null hypothesis that former high-impact sports practitioners could perform similar degree of contraction of their PFM.

A convenience sample of sixteen asymptomatic nulliparous women, 8 former high-impact sports young practitioners (group 1) and 8 in the control group (group 2) were recruited from regular gynecology consultation. Women underwent clinical evaluation and took pelvic floor dysfunction surveys (ICIQ-SF and PFIQ-7). Additionally, they were instructed on how to perform proper PFM contractions by the same physiotherapist. Subsequently, maximum voluntary contraction was assessed with vaginal digital examination using the Oxford Grading Scale.[10]

Demographic data and the level of physical activity were collected. The International Physical Activity-Short Form Questionnaire (IPAQ-SF) was used to score high, moderate or low levels.[11] Past and current sports, training volume (MET-hours/week) and duration (years) were considered.

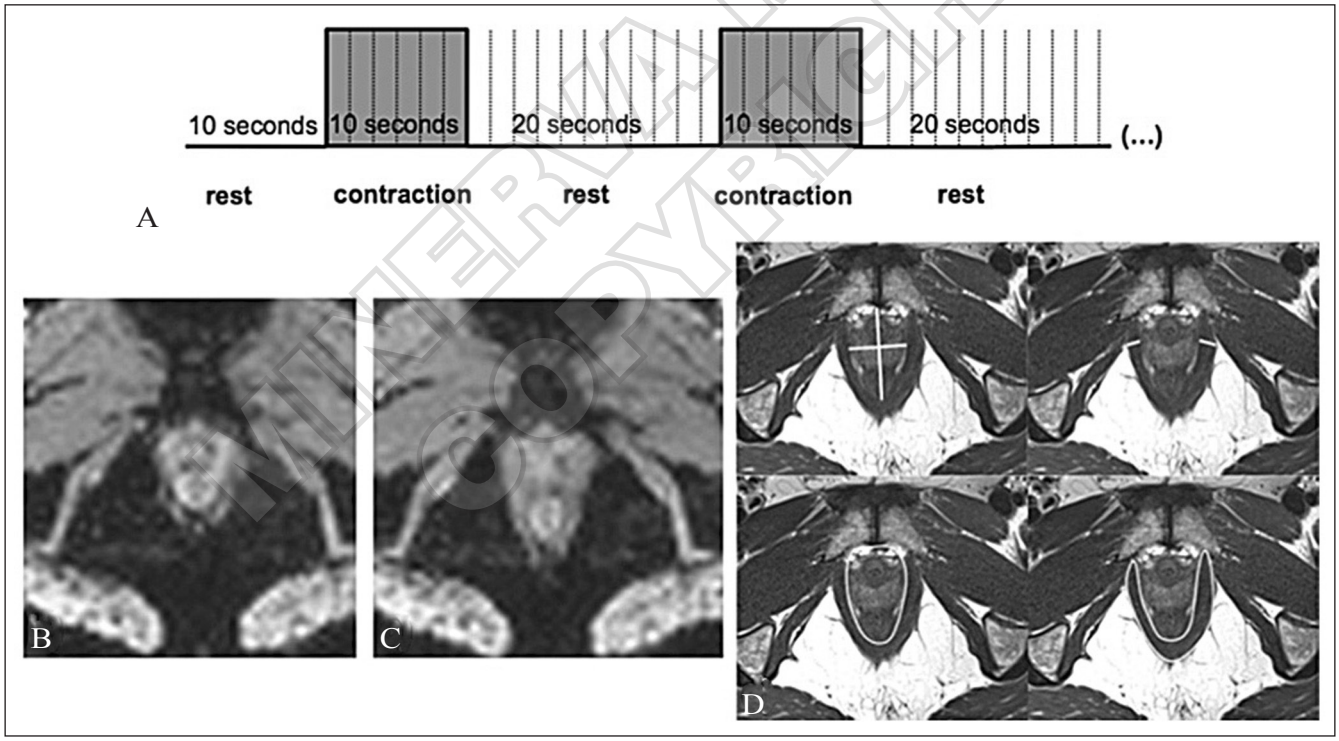

Figure 1.—"Rest-contraction" block design paradigm (A) of the axial dynamic Magnetic Resonance acquisition of the pelvic floor. Seven consecutive blocks of 20-10 seconds were used to evaluate the changes on the *levator hiatus* diameter during 3:44-minutes (B, C). The "rest blocks" were longer to allow some muscle recovery. D) Measures of *levator hiatus* anterior-to-posterior diameter, width and area, as well as pubovisceral muscle thickness (right and left sides) and area.

MRI acquisition and analysis

Women performed pelvic MRI in the supine position, lower limbs flexed to avoid using the gluteus to facilitate PFM contraction. Firstly, axial images were acquired at rest. Then, axial dynamic ("rest-contraction") acquisition was performed for 100 repetitions (Figure 1A), during which women were asked to sustain a maximal voluntary contraction of the PFM for 10 seconds *vs.* 20 seconds of rest (Figure 1B, C). Additional images were acquired to complete pelvic evaluation.

The image analysis was performed *in consensus* by two observers, who were blinded to the clinical data. The static images were scored for *levator ani* defects.[12] Furthermore, pubovisceral muscle (PVM) (thickness and area) and LH (anterior-to-posterior (AP) and lateral diameters and area) were taken (Figure 1D).

The LH AP diameter was measured again in the dynamic acquisition. The difference between rest and contraction was assessed so as to identify the relative variation percentage ([rest-contraction]/rest x 100), which was used as an indirect measure of contraction. The differences between the first and the last contractions were also calculated.

Statistical analysis

The Mann-Whitney *U* test was used to compare the two groups for mean values of age, Body Mass Index, level of physical activity (MET-minutes/week) and measures taken from the MRI datasets. Statistical significance was considered for P≤0.05.

Results

Two out of the 16 women initially enrolled were excluded due to image artifacts. Seven women were included in each group, for whom there was no clinical or imaging evidence of UI or prolapse.

Quantitative data (Table I) shows that previous physical activity was more intense for group 1 than for controls, although it is currently similar. Women from group 1 had high-level physical activity for high-impact sports (mean 6.2 hours/week), for 8±1.7 years in the past (volleyball (N.=4) and football/body pump/body combat (N.=3)). They restarted low-level physical activity (1.5-2 hours/week) 5±1.2 years ago (swimming (N.=3) and gym classes/abdominal/core training/stretching (N.=4)). Women from group 2 maintained low levels of low-impact sports throughout their lives. Two referred previous practice of karate and swimming (1.2 hours/week). Presently, all include some exercise in their daily lives, *e.g.* pilates, yoga, swimming and walking (1-1.5 hours/week).

The morphologic analysis revealed thinner and smaller PVM for women from group 1, as well as increased LH width and area. We reject the null hypothesis, as their Oxford Grading Scale score was lower than that of controls. Also, despite similar

TABLE I.—*Mean values for demographic and clinical data, and morphological features of the pelvic floor for groups 1 and 2.*

Variables	Group 1 (N.=7)	Group 2 (N.=7)	P
Age (years)	32.40±3.20	29.20±4.30	0.247
BMI (kg/m^2)	23.60±3.90	20.80±1.50	0.123
Oxford Grading Scale	3.60	4.83	0.005
IPAQ-SF (previous) (MET-minutes/week)	high (4115.20)	low (250.00)	0.003
IPAQ-SF (current) (MET-minutes/week)	low (204.50)	low (308.16)	0.664
LH AP diameter (cm)	4.89±0.35	4.81±0.17	0.931
LH width (cm)	3.25±0.34	2.62±0.49	0.045
Area of the LH (cm^2)	13.10±1.60	9.30±1.17	0.005
PVM thickness (right side) (cm)	0.40±0.20	0.93±0.20	0.005
PVM thickness (left side) (cm)	0.41±0.10	0.91±0.18	0.004
Area of the PVM (cm^2)	4.92±1.17	8.15±1.54	0.004
Mean percent relative variation in LH AP diameter (%)	8.03±0.81	13.74±0.95	0.004
Difference in mean percent relative variation between the first and last contractions (%)	6.32±0.77	6.95±1.47	0.662

Values are shown in mean value±standard deviation.
BMI: Body Mass Index; IPAQ-SF:International Physical Activity-Short Form Questionnaire; ‡LH AP diameter: *levator hiatus* anterior-to-posterior diameter; PVM: pubovisceral muscle. P≤0.05 statistical significance.

difference between the 1st and the 7th contractions, former high-impact sports practitioners performed worse hiatal closure when compared to women from group 2 (Figure 2). Nevertheless, women from both groups could not perform uniform contractions, thus progressively decreasing the LH closure competence.

Discussion

To our knowledge, this is the first time that a long period of contraction-rest is evaluated through cine MRI in former high-impact exercise practitioners.

Some studies focused on UI in athletes [13-15] or former athletes.[15-18] Although similar symptom rates were found in former high- *vs.* low-impact athletes (41.1% *vs.* 50%) [13], and between former athletes *vs.* non-athletes (36.5% *vs.* 36.9%), high-impact sports, frequent training and years of practice increase the risk for UI.[18] In the present study, former high-impact sports practitioners evidenced wider AP LH diameter during contraction, despite measures at rest were alike. The effect of exercise in PFM thinning due to continuous and subtle muscle stretching seems to be the case in this study, and that would explain the lower Oxford Grading Scale score and worse contraction performance, despite the absence of muscle defects. Maintaining PFM contraction for a long period is stressful.[5] Verelst *et al.* found similar time-to-fatigue between incontinent women and controls (10.5 seconds *vs.* 11.5 seconds) - which was considered when optimizing our imaging protocol — although normalized force was reduced in incontinent.[19] Despite the "rest" periods, LH closure was progressively weaker. Between the 4th and 5th contractions, all women evidenced a reduction in the ability to contract the pelvic floor muscles (3.3% and 1.7%, for groups 1 and 2, respectively) (Figure 2). Overall mean percentage of LH relative variation was almost half for group 1, despite similar differences between the first and the last contractions. When we consider the first contraction, women from group 2 exhibited 17.9% of LH relative variation, which is within range of previous studies using ultrasound.[20, 21] Women from group 1 started with lower contraction (11.05%), probably due to functional weakness from thinner PVM and wider LH than that of the controls.[22]

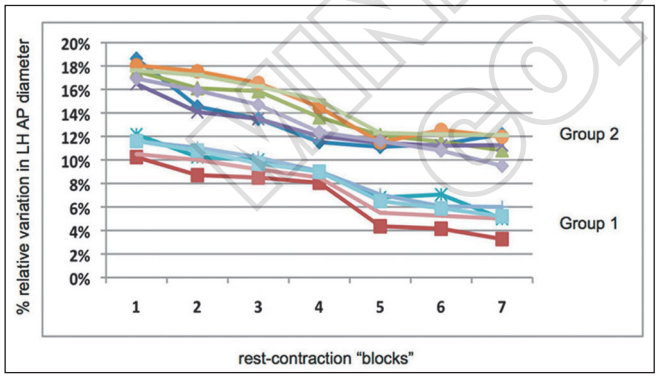

Figure 2.—Percentage of the relative variation of the *levator hiatus* diameter during the dynamic Magnetic Resonance acquisition. The former high-impact sports practitioners (group 1) presented lower values of relative variation of the *levator hiatus* throughout the dynamic acquisition when compared to controls (group 2).

None of the women from group 1 showed complains of pelvic floor dysfunction. Despite thinner PVM, the absence of defects and its "sling shape" around the LH may have contributed to a still effective contraction. Nevertheless, the wider LH may eventually have a negative functional biomechanical should this tendency be maintained. If this is true, muscle contraction will further decrease with time, and symptoms of SUI will probably appear. The differences in voluntary muscle contraction may also be related to damage in connective tissue,[18] but this relation is more difficult to establish.

Despite the small sample size, our results seem to suggest that the weakness of the PFM on the long run may be considered an additional asset to the overall model of pelvic floor dysfunction in female sports practitioners. This is probably a "silent effect" of high-impact exercises over the years, because women do not identify a functional problem despite having a worse contraction performance. If these results are confirmed in the future, they should be taken into account in the clinical context for former elite athletes that do not present any symptoms, but one may also suggest preventive physiotherapeutic protocols to avoid and delay the onset of SUI.

Limitations of our study include the small sample size of this pilot study. Results must be interpreted with caution, and a larger sample or a longitudinal descriptive study would help to uncover more information. Moreover, MRI is an expensive technique, and for this purpose static and dynamic ultrasound could be used instead.

Conclusions

In this pilot study, asymptomatic female high-impact sports practitioners presented larger LH and thinner PVM when compared to controls. They evidenced worse contraction performance, suggesting that this population should perform preventive rehabilitation. Future longitudinal evaluation is necessary to confirm these results.

References

1. Haylen BT, De Ridder D, Freemen RM, Swift SE, Berghmans B, Lee J, *et al.* An International Urogynecological Association (IUGA)/International Continence Society (ICS) joint report on the terminology for female pelvic floor dysfunction. Neurourol Urodynam 2010;29:4-20.
2. Minassian VA, Drutz HP, Al-Badr A. Urinary incontinence as a worldwide problem. Int J Obstet Gynaecol 2003;82:327-38.
3. Bø K. Urinary incontinence, pelvic floor dysfunction, exercise and sport. Sports Medicine 2004;34:451-64.
4. Bø K, Stien R, Kulseng-Hanssen S, Kristofferson M. Clinical and urodynamic assessment of nulliparous young women with and without stress incontinence symptoms: a case-control study. Obst Gynecol 1994;84:1028-32.
5. Ree ML, Nygaard I, Bø K. Muscular fatigue in the pelvic floor muscles after strenuous physical activity. Acta Obstet Gynecol Scand 2007;86:870-6.
6. Dietz HP, Shek C. Levator avulsion and grading of pelvic floor muscle strength. Int Urogynecol J 2008;19:633-6.
7. Talasz H, Himmer-Perschak G, Marth E, Fisher-Colbrie J, Hoefner E, Lecheitner M. Evaluation of pelvic floor muscle function in a random group of adult women in Austria. Int Urogynecol J 2008;19:131-5.
8. Da Roza T, Mascarenhas T, Araújo M, Trindade V, Jorge RN. Oxford Grading Scale *vs.* manometer for assessment of pelvic floor strength in nulliparous sports women. Physiotherapy 2013;99:207-11.
9. Raizada V, Bhargava V, Jung SA, Karstens A, Pretorius D, Mittal PK. Dynamic assessment of the vaginal high-pressure zone using high-definition manometery, 3-dimensional ultrasound, and magnetic resonance imaging of the pelvic floor muscles. Am J Obstet Gynecol 2010;203:172.e1-8.
10. Bø K, Sherburn M. Evaluation of female pelvic-floor muscle function and strength. Phys Ther 2005;85:269-82.
11. Matsudo S, Araújo T, Matsudo V, Andrade D, Andrade E, Oliveira L, *et al.* Questionário Internacional de Atividade física (IPAQ): estudo de validade e reprodutibilidade no Brasil. Atividade Física & Saúde 2001;6:5-18.
12. DeLancey JO, Morgan DM, Fenner DE, Kearney R, Miller JM, Hussain H, *et al.* Comparison of levator ani muscle defects and function in women with and without pelvic organ prolapse. Obstet Gynecol 2007;109(2 Pt 1):295-302.
13. Goldstick O, Constantini N. Urinary incontinence in physically active women and female athletes. Br J Sport Med 2014;48:296-8.
14. Jácome C, Moroni A, Marques A, Sá-Couto P. Prevalence and impact of urinary incontinence among female athletes. Int J Obstet Gynaecol 2011;114:60-3.
15. Simeone C, Moroni A, Pettenò A, Antonelli A, Zani D, Orizio C, *et al.* Occurrence rates and predictors of lower urinary tract symptoms and incontinence in female athletes. Urologia 2010;77:139-46.
16. Bø K, Sundgot-Borgen J. Are former female elite athletes more likely to experience urinary incontinence later in life than non-athletes? Scand J Med Sci Sports 2010;20:100-4.
17. Eliasson K, Edner A, Mattsson E. Urinary incontinence in very young and mostly nulliparous women with a history of regular organised high-impact trampoline training: occurrence and risk factors. Int Urogynecol J 2008;19:687-96.
18. Nygaard IE. Does prolonged high-impact activity contribute to later urinary incontinence? A retrospective cohort study of female Olympians. Obstet Gynecol 1997;90:718-27.
19. Verelst M, Leivseth G. Are fatigue and disturbances in pre-programmed activity of pelvic floor muscles associated with female stress urinary incontinence? Neurourol Urodynam 2004;23:143-7.
20. Braekken IH, Majida M, Engh ME, Bø K. Test-retest reliability of pelvic floor muscle contraction measured by 4D ultrasound. Neurourol Urodynam 2009;28:68-73.
21. Majida M, Braekken IH, Umek W, Bø K, Saltyte Benth J, Ellstrøm Engh M. Interobserver repeatability of three- and four-dimensional transperineal ultrasound assessment of pelvic floor muscle anatomy and function. Ultrasound Obstet Gynecol 2009;33:567-73.
22. Shishido K, Peng Q, Jones R, Omata S, Constantinou CE. Influence of pelvic floor muscle contraction on the profile of vaginal closure pressure in continent and stress urinary incontinent women. J Urol 2008;179:1917-22.

Acknowledgments.—The authors gratefully acknowledge to all the women for their participation in this study.

Funding.—T. Da Roza acknowledges the funding by CNPq from Brazil government and all the authors acknowledge the projects CRUP-Action No. A-10/11 and LAETA - UID/EMS/50022/2013.

Conflicts of interest.—The authors certify that there is no conflict of interest with any financial organization regarding the material discussed in the manuscript.

Received on March 10, 2014.
Accepted for publication on October 23, 2014.
Epub ahead of print on October 30, 2014.

Original Article

Study II

Erratum

During the process of editing the Proofs of the manuscript entitled "*Do asymptomatic former high-impact sports practitioners maintain the ability to contract the pelvic floor muscles?"*, a new version of Figure 2 was sent. However, it was not included in the final version of the manuscript by mistake. The Journal was notified, and an *Erratum* will be published in a nearer future.

Figure 2 is included below, with the corresponding caption.

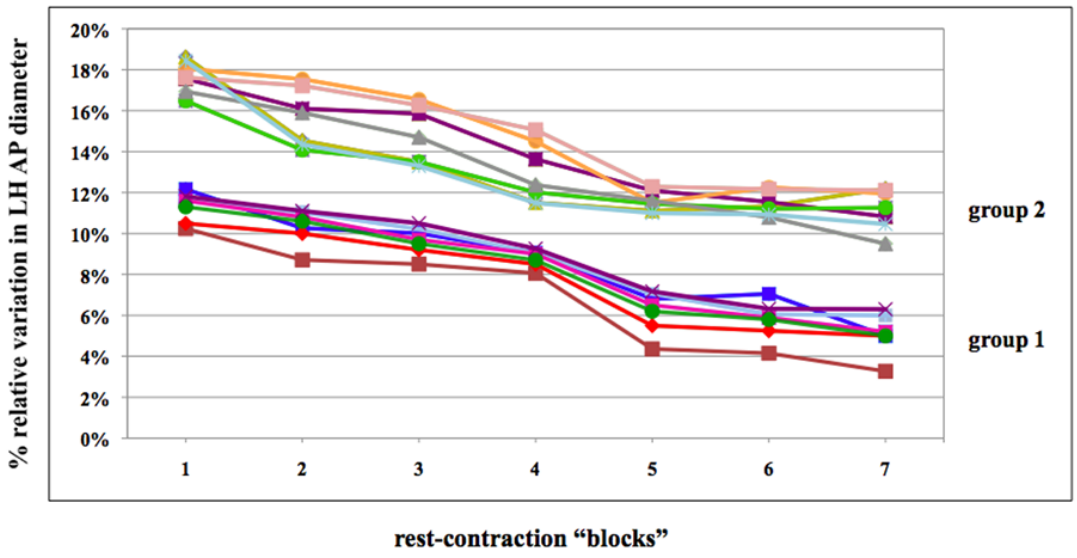

Figure 2. Percentage of the relative variation of the levator hiatus diameter during the dynamic Magnetic Resonance acquisition. The former high-impact sports practitioners (group 1) presented lower values of relative variation of the levator hiatus throughout the dynamic acquisition when compared to controls (group 2).

Original Article

Study III

Modeling the contraction of the pelvic floor muscles.

Brandão FS, Parente MP, Rocha PA, Saraiva MT, Ramos IM, Natal Jorge RM.

Comput Methods Biomech Biomed Engin. 2016;19(4):347-356.

doi: 10.1080/10255842.2015.1028031. Epub 2015 May 8.

Computer Methods in Biomechanics and Biomedical Engineering, 2015
http://dx.doi.org/10.1080/10255842.2015.1028031

Taylor & Francis
Taylor & Francis Group

Modeling the contraction of the pelvic floor muscles[†]

Fernanda Sofia Quintela da Silva Brandão[a]*, Marco Paulo Lages Parente[b1], Paulo Alexandre Gomes Gonçalves Rocha[b2], Maria Teresa da Quinta e Costa de Mascarenhas Saraiva[c3], Isabel Maria Amorim Pereira Ramos[a4] and Renato Manuel Natal Jorge[b5]

[a]*Department of Radiology, CHSJ-EPE/Faculty of Medicine, University of Porto, Alameda Professor Hernâni Monteiro, 4200-319 Porto, Portugal;* [b]*INEGI, Faculty of Engineering, University of Porto, Rua Dr. Roberto Frias s/n, 4200-465 Porto, Portugal;* [c]*Department of Obstetrics and Gynecology, CHSJ-EPE/Faculty of Medicine, University of Porto, Alameda Professor Hernâni Monteiro, 4200-319 Porto, Portugal*

(*Received 7 October 2014; accepted 8 March 2015*)

We performed numerical simulation of voluntary contraction of the pelvic floor muscles to evaluate the resulting displacements of the organs and muscles. Structures were segmented in Magnetic Resonance (MR) images. Different material properties and constitutive models were attributed. The Finite Element Method was applied, and displacements were compared with dynamic MRI findings. Numerical simulation showed muscle magnitude displacement ranging from 0 to 7.9 mm, more evident in the posterior area. Accordingly, the anorectum moved more than the uterus and bladder. Dynamic MRI showed less 0.2 mm and 4.1 mm muscle dislocation in the anterior and cranial directions, respectively. Applications of this model include evaluating muscle impairment, subject-specific mesh implant planning, or effectiveness of rehabilitation.

Keywords: female pelvis; biomechanics; computational modeling; finite element method

1. Introduction

Urinary incontinence and pelvic organ prolapse are related to the weakening or damage of support structures, such as the pelvic floor muscles (PFM) (namely the *levator ani*), the pelvic fascia, and ligaments (Macura & Genadry 2008). Significant risk factors include increased age, hormonal changes, and vaginal delivery, which may be a common ground for damage to these support structures (DeMaagd & Davenport 2012). While the striated skeletal PFM maintain urinary and fecal continence and organ support by means of passive and active forces at rest and during voluntary contraction (Chamochumbi et al. 2012), the pelvic fascia and ligaments provide additional passive stabilization (Brandão & Ianez 2013). The evidence of the inability to maintain organ support and *urogenital hiatus* closure comes from clinical and imaging evaluation of muscle defects, laxity of the pelvic fascia, or damage to the uterine or urethral ligaments (Macura et al. 2006; Tunn et al. 2006). Dynamic ultrasound and Magnetic Resonance Imaging (MRI) during Valsalva maneuver evaluate the effect of increased intra-abdominal pressure (IAP) over the pelvic viscera, and the counteracting (in)voluntary action of the support structures that sustain the organs (Brandão & Ianez 2013). In the same way, while imaging pelvic floor contraction it is possible to quantify the upward and anterior movement of the bladder neck and anorectal junction to close the *urogenital hiatus* (Yang et al. 2009) that result from muscle shortening (Bø et al. 2009) to prevent urine and fecal leakage.

Computational models enable the study of the biomechanics of the pelvis. The Finite Element Method (FEM) is one of the most used approaches to model the biomechanical behavior of the pelvic soft tissue structures (Noakes et al. 2008; Parente et al. 2010a), by including their geometric and material properties (Parente et al. 2009), along with their interactions with the bony pelvis. Previous papers analyzed the behavior of the PFM during vaginal childbirth (Parente et al. 2008, 2010a, 2010b) or straining during defecation (Noakes et al. 2008) by using geometrical nonlinear models (Oomens et al. 2003; Parente et al. 2010a). To our knowledge, so far few studies have simulated muscle contraction (d'Aulignac et al. 2005; Parente et al. 2010b; Saleme et al. 2011). Furthermore, in those works only the muscles were included. Yet, the basal load of the organs, and the presence of the ligament and fascial attachments should be considered to reflect the real circumstances inside the pelvic cavity. This may provide a better understanding of muscle kinematics and therefore their role in preventing pelvic floor dysfunction. Accordingly, the aim of this work was to build a numerical simulation model of the contraction of the PFM using FEM. To accomplish it,

[†]This work was developed in the Institute of Science and Innovation in Mechanical and Industrial Engineering (INEGI) of the Faculty of Engineering of the University of Porto.

*Corresponding author. Email: sofia.brand@gmail.com

the MRI-based model included the pelvic organs and soft tissue support structures, to which material properties and constitutive models were attributed. The displacements of the muscles and pelvic organs were analyzed and compared with dynamic images at maximal voluntary contraction from the same woman.

2. Methods

2.1 Biomechanical model

2.1.1 Anatomical features

The Institutional Review Board approved this work (protocol 195/12), and a young female volunteer gave informed and written consent. She went to a gynecology consultation that showed no clinical evidence of pelvic floor dysfunction. MR images were acquired in the supine position with legs together in a semi-flexed position using a 3T scanner (Magnetom Trio® TIM; Siemens Medical Solutions, Erlangen, Germany). The protocol included multiplanar T2-w high-resolution contiguous 3-mm slices. Additional dynamic images were acquired in the axial and in the mid-sagittal planes at rest, and during a 10-s period of maximal contraction of the PFM. The volunteer was instructed on how to perform proper contractions by a physiotherapist. No pathological findings were described.

To build the 3D model, anatomical landmarks were confirmed in multiplanar images by two readers *in consensus*, and the surfaces of the organs were rendered using the software Inventor® (Autodesk, San Raphael, CA, USA). Figures 1(a) and (b) are sagittal and axial images where the contours of some structures can be seen. Figure 2 (a)–(d) illustrates different views of the 3D model with the pubic bone, the pelvic organs (bladder, uterus, and rectum), and several support structures, e.g., the three main muscles that form the *levator ani* (puborectal, pubococcygeal, and ilioccygeal muscles); the pubourethral, uterosacral, cardinal, and lateral ligaments of the rectum; the pubocervical fascia, and the *arcus tendineus fascia pelvis* (ATFP). A few anatomical details were confirmed in the literature: (1) the anatomical details of the ATFP (Pit et al. 2003; Albright et al. 2005) – its length (9.0 cm) was measured according to attachment points; (2) the length of the urethral and vaginal portions of the pubourethral ligament (2 and 3 cm long, respectively) (Petros 1998), and (3) the width and length of the lateral ligaments of the rectum (1.5 and 2.2 cm, respectively) (Lin et al. 2010).

The Abaqus® software v.6.12 (Dassault Systèmes Simulia Corp., Providence, USA) was used to perform the numerical simulation based on the FEM. It requires discretizing the geometry of the structures in the 3D model into meshes with specific properties. Table 1 shows details about the mesh, such as the type and number of elements, the number of nodes, and the distance between them.

2.1.2 Material properties and constitutive models

For each tissue presented on Table 2, material properties were obtained using experimental data from published studies conducted on a female cadaver without pelvic floor dysfunction (Cosson et al. 2003; Janda 2006; Martins et al. 2011; Rubod et al. 2012; Rivaux et al. 2013). The mechanical properties of the pelvic fascia were assumed as similar to the abdominal fascia, described by Kirilova et al., while the pubic symphysis was fixed and considered as rigid (Dalstra et al. 1993). The organs were described as having hyperelastic mechanical behavior. The volumes inside them were described as fluid cavities, and the fluid was assumed to be incompressible, allowing for isovolumetric transformations. As the soft tissues of the pelvic cavity such as muscles and ligaments are composed of fibers that are aligned with their main anatomical and functional axes, we used simple isotropic models adjusted to take into account the main direction of these structures. Therefore, the Yeoh and Ogden constitutive equations were used to model the behavior of all the soft tissues (Ogden 1972; Yeoh 1993).

The curve-fitting algorithm from Abaqus® was applied to each experimental dataset. Figure 3 shows the

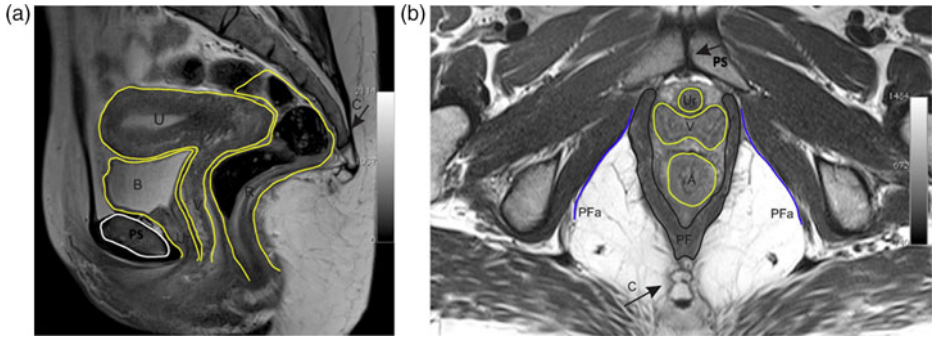

Figure 1. Magnetic resonance images in the sagittal (a) and axial (b) planes, where the surfaces of the some pelvic structures were identified and delineated. (A – anus; B – bladder; C – coccyx; PF – pelvic floor muscles; PFa – pelvic fascia; PS – pubic symphysis; R – rectum; Ur – urethra, V – vagina)

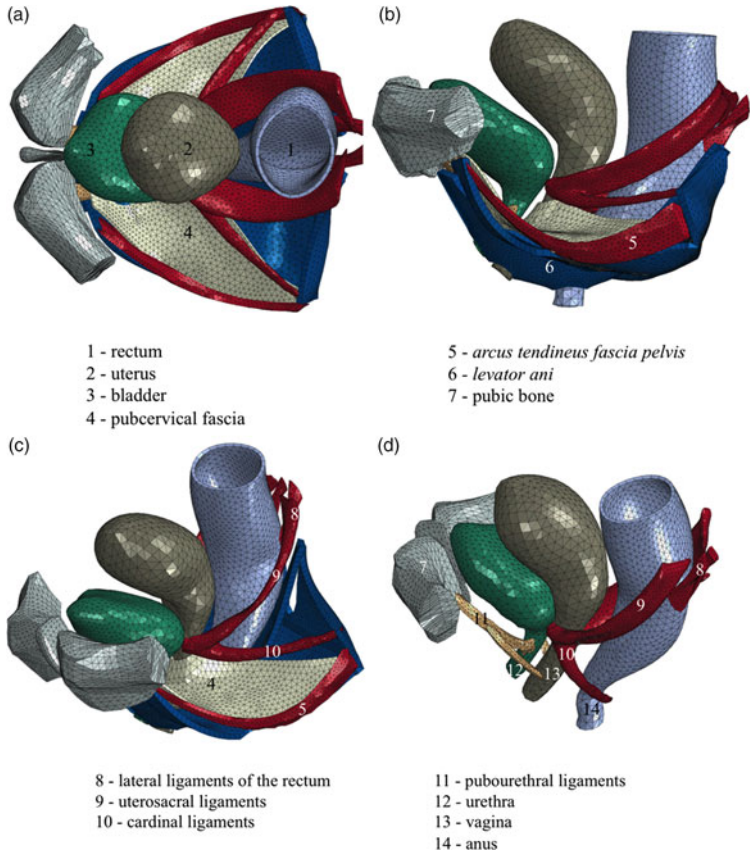

Figure 2. Top and lateral (a,b), and oblique (c,d) views of the 3D model. The pubic bone and several soft tissue support structures were included in the model. In (d), the pelvic floor muscles and the fascia were deleted for a better view of the ligaments.

adjustment obtained in the fitting process for the different soft tissues. The correlation coefficient between the different curves was calculated to determine the hyperelastic constitutive model that better adjusted to each experimental dataset (see Table 2).

In order to simulate the activation of the pelvic floor muscles, it is necessary to apply a user-defined constitutive model through a UMAT interface. The constitutive equation adopted in this work for the 3D passive and active behavior of the muscles is a modified form of the

Table 1. Properties of the finite element mesh.

Mesh	Number of nodes	Number of elements	Distance between nodes (mm)	Type of elements
Pelvic organs				
Bladder and urethra	1941	5796	3–4	C3D4
Vagina and uterus	1426	1411		
Rectum	2780	2739		
Levator ani muscle				
Puborectal	3012	2760	3–4	C3D6
Pubococcygeal	1282	1136		
Iliococcygeal	2982	2737		
Pelvic fascia				
Pubocervical fascia	2372	2142	1–2	C3D6
Arcus tendineus fascia pelvis	1023/1029	3441/3448	1–2	C3D4
Pelvic ligaments				
Pubourethral	492/503	1369/1385	1–2	C3D4
Uterosacral and cardinal	2176/2238	8167/8555		
Lateral ligaments of the rectum	250/248	749/743		

Table 2. Material properties and hyperelastic constitutive models for the structures included in the model.

Structure	α_k[a]	μ_k	–	Model	Experimental data	Fitting error (r)
Bladder and urethra	$\alpha_1 = 0.19$	$\mu_1 = 5.14$	–	Ogden ($N = 1$)	Martins et al. (2011)	$r = 0.9980$
Rectum	$\alpha_1 = 4.25$	$\mu_1 = 13.24$	–	Ogden ($N = 2$)	Rubod et al. (2012)	$r = 0.9956$
	$\alpha_2 = -3.83$	$\mu_2 = 13.24$	–			
Vagina and uterus	$\alpha_1 = -3.41$	$\mu_1 = 92.24$	–	Ogden ($N = 3$)	Rubod et al. (2012)	$r = 0.9929$
	$\alpha_2 = -0.66$	$\mu_2 = 39.29$	–			
	$\alpha_3 = -6.48$	$\mu_3 = 54.68$	–			
Pelvic ligaments and fascia (ATFP, CL, LLR, USL[b])	$\alpha_1 = 10.85$	$\mu_1 = 3.17$	–	Ogden ($N = 1$)	Rivaux et al. (2013)	$r = 0.9983$
Pelvic ligaments (PUL[b])	$\alpha_1 = 10.95$	$\mu_1 = 1.58$	–	Ogden ($N = 1$)	Rivaux et al. (2013)	$r = 0.9994$
	C_{10}	C_{20}	C_{30}			
Pubocervical fascia	0.93	−0.62	0.47	Yeoh	Kirilova et al. (2011)	$r = 0.9962$
Pelvic floor muscles	0.003	0.002	0.001	Yeoh	Janda (2006)	$r = 0.9978$

[a] α_k and μ_k – material constants.
[b] ATFP – *Arcus tendineus fascia pelvis*; CL – cardinal ligaments; PUL – pubourethral ligaments; LLR – lateral ligaments of the rectum; USL – uterosacral ligaments.

incompressible, transversely isotropic, hyperelastic model proposed by Humphrey and Yin for passive cardiac tissues (Humphrey & Yin, 1987), as in the work of Parente et al. (2009).

For the constitutive model used, the strain energy per unit volume of the reference configuration can be written in the following form:

$$U = U_I\left(\bar{I}_1^C\right) + U_f(\bar{\lambda}_f, \alpha) + U_J(J), \tag{1}$$

where U_I is the strain energy stored in the isotropic matrix embedding the muscle fibers, U_f is the strain energy stored in each muscle fiber, and U_J is responsible for ensuring the incompressibility condition. Each term in Equation (1) is defined below.

U_I is described using Equation (2):

$$U_I = c\left[e^{b\left(\bar{I}_1^C - 3\right)} - 1\right], \tag{2}$$

where the constants were $c = 0.0185\,\mathrm{N/mm^2}$ and $b = 1.173$, from Parente et al. (2009).

In Equation (1), $\bar{I}_1^C$ is the first invariant of the right Cauchy-Green strain tensor, **C**, with the volume change

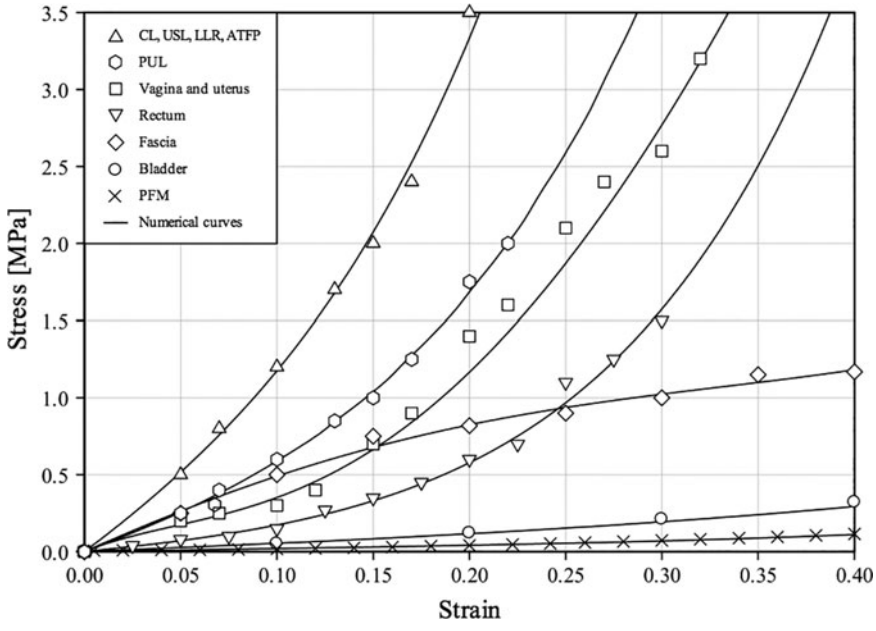

Figure 3. Fitting process to obtain the material properties for the different soft tissues included in the model. The Yeoh and Ogden constitutive equations were chosen to model the behavior of these tissues. (ATFP – *arcus tendineus fasia pelvis*; CL – cardinal ligaments; LLR – lateral ligaments of the rectum; PFM – pelvic floor muscles; PUL – pubourethral ligaments; USL – uterosacral ligaments)

eliminated, i.e.,

$$\bar{I}_1^C = \mathrm{tr}\bar{\mathbf{C}} = \mathrm{tr}(\bar{\mathbf{F}}^T\bar{\mathbf{F}}) = J^{-2/3}\mathrm{tr}\mathbf{C}, \tag{3}$$

where $\bar{\mathbf{F}}$ is the deformation gradient with the volume change eliminated

$$\bar{\mathbf{F}} = J^{-1/3}\mathbf{F}, \tag{4}$$

$\mathbf{F}$ being the deformation gradient, and J refers to the volume change (Equation (5)):

$$J = \det \mathbf{F}. \tag{5}$$

The strain energy stored in each muscle fiber U_f can be divided into a passive elastic part and an active part due to contraction, as follows:

$$U_f(\bar{\lambda}_f, \alpha) = U_{\mathrm{pas}}(\bar{\lambda}_f) + U_{\mathrm{act}}(\bar{\lambda}_f, \alpha), \tag{6}$$

where α is the activation level and $\bar{\lambda}_f$ is the fiber stretch ratio.

The passive elastic part U_{pas} is given by:

$$U_{\mathrm{pas}} = A\{\exp\left[a(\bar{\lambda}_f - 3)^2\right] - 1\}, \tag{7}$$

where $A = 0.028\,\mathrm{N/mm^2}$ and $a = 0.0625$ are constants (Parente et al. 2009). Equation (6) is valid when $\bar{\lambda}_f > 1$, otherwise we consider the strain energy to be zero, assuming that the fibers offer no resistance to compression.

Equation (8) describes the active part U_{act}, as follows (d'Aulignac et al. 2005):

$$U_{\mathrm{act}} = \alpha\ T_0^M \int_1^{\bar{\lambda}_f} 1 - 4(\bar{\lambda} - 1)^2 \mathrm{d}\bar{\lambda}, \tag{8}$$

where α is the activation level, ranging from 0 to 1. When $0.5 < \bar{\lambda}_f < 1.5$, U_{act} is greater than 0; for other values of $\bar{\lambda}_f$ the muscle produces no force, and therefore, the strain energy is zero. The constant T_0^M is the maximum tension produced by the muscle at resting length$\left(\bar{\lambda}_f = 1\right)$. For the active muscle contraction ($\alpha = 1$), the parameter T_0^M was adjusted to a value of $T_0^M = 0.184\,\mathrm{Pa}$ to ensure that the displacements obtained through contraction would be clinically meaningful.

In Equation (1) U_J is responsible for ensuring the incompressibility condition and is defined by Equation (9) as:

$$U_J = \frac{1}{D}(J - 1)^2. \tag{9}$$

In this definition, $D = 0.0001\,\mathrm{mm^2/N}$ (Parente et al. 2009) is a constant associated to the incompressibility condition.

The fiber stretch ratio in Equation (1) in the direction $\mathbf{N}$ of the undeformed fiber is given by:

$$\bar{\lambda}_f = \sqrt{\mathbf{N}^T\bar{\mathbf{C}}\mathbf{N}} = \sqrt{\bar{\mathbf{C}} : (\mathbf{N}\otimes\mathbf{N})}, \tag{10}$$

where $\otimes$ denotes the tensor product.

The strain energy density given in Equation (1) is now used to obtain the 2nd Piola-Kirchhoff stress tensor $\mathbf{S}$

$$\boldsymbol{S} = \frac{\partial U}{\partial \mathbf{E}} = \frac{\partial U_I}{\partial \mathbf{E}} + \frac{\partial U_f}{\partial \mathbf{E}} + \frac{\partial U_J}{\partial \mathbf{E}} \tag{11}$$

where $\mathbf{E}$ is the Green-Lagrange strain tensor.

On the basis of constitutive equations governing the material response at a continuum level the stress tensor, $\boldsymbol{\sigma}$, and the associated material tangent, $\mathbf{H}$, must be provided for numerical calculations. The Cauchy stress tensor $\boldsymbol{\sigma}$ is related to the 2nd Piola-Kirchhoff stress tensor $\mathbf{S}$ by:

$$\boldsymbol{\sigma} = J^{-1}\mathbf{F}\mathbf{S}\mathbf{F}^T. \tag{12}$$

The material version of the tangent operator, which is necessary for the implementation of the constitutive model in Abaqus®, is defined by Equation (13) as follows:

$$\mathbf{H} = \frac{\partial^2 U}{\partial \mathbf{E}\partial \mathbf{E}} = \frac{\partial \mathbf{S}}{\partial \mathbf{E}}. \tag{13}$$

The spatial tangent operator h can now be obtained through the last operation, consistent with the objective Jaumman-Zaremba stress rate (Miehe 1996) (Equation (14)):

$$h^J_{ijkl} = \frac{1}{J}F_{im}F_{jn}F_{kp}F_{lp}H_{mnpq} + \frac{1}{2}\left(\sigma_{ik}\delta_{jl} + \sigma_{il}\delta_{jk} + \sigma_{ik}\delta_{jl} + \sigma_{il}\delta_{jk}\right). \tag{14}$$

To obtain the input of the direction of the muscle fibers, it was initially assumed that the muscles have an isotropic behavior defined by the Yeoh model (see Table 2), and it was also implicit that the directions of the muscle fibers are coincident with the direction of the maximal principal stress lines when the structure is being deformed. For that purpose, a pressure of 1 KPa was applied to the ventral surface of the structures.

The last issue on the modeling process was to establish boundary conditions because they play a central role in the resulting displacements. The nodes corresponding to the pubic bone and the extremities of the soft tissues joining the pubis anteriorly (*levator ani* muscle, pelvic fascia, pubourethral ligaments, and the anterior portion of the ATFP) were considered fixed. The same was applied to the insertion of the lateral ligaments of the rectum in the endopelvic fascia, to the uterosacral ligament attachment in the sacrum-coccyx, to the postero-lateral connection of

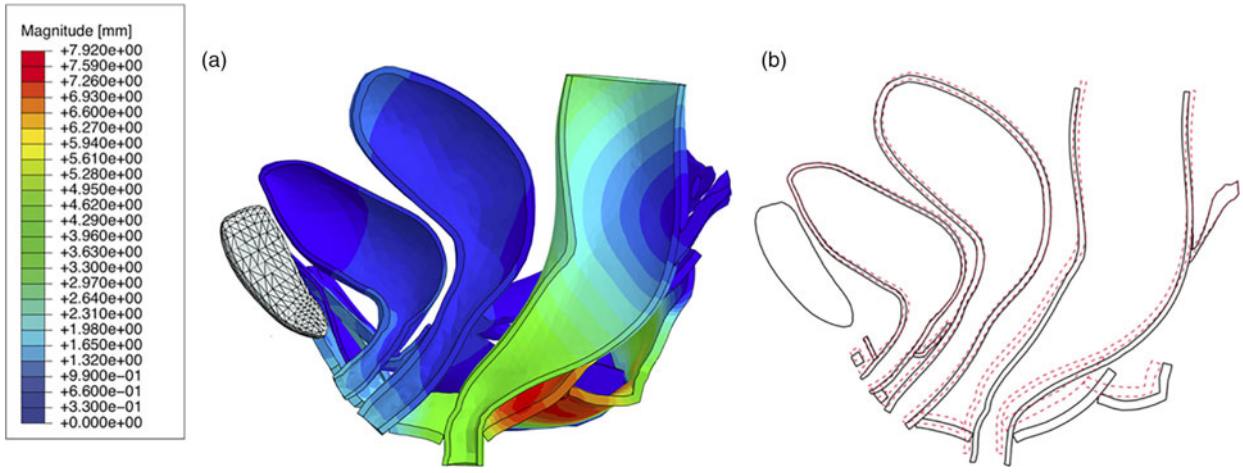

Figure 4. Magnitude values from the nodal displacements of the pelvic organs and pelvic floor muscles (a), and schematic view of the differences in their position from rest (black continuous lines) to contraction (red dashed lines) (b).

the *levator ani* in the *arcus tendineous of the levator ani*, and to the cardinal ligament attachment to the lateral pelvic wall in the obturator fascia of the internal obturator muscle. The interaction between the organs was modeled as frictionless, and established using the default Abaqus® contact pressure-overclosure algorithm.

2.2 *Numerical simulation of contraction*

Numerical simulation of contraction included an initial stage with a baseline pressure of 0.5 KPa applied to the superior surface of the organs – assuming the pressure from organ load in the supine position at rest (Noakes et al. 2008) – and a subsequent stage of simulation of PFM contraction. The rest position was established as the reference for displacement assessment. Nodal displacements of the PFM and pelvic organs in the inferior-to-superior (*y*-) and posterior-to-anterior direction (*x*-axis), as well as the magnitude values of the displacement (*d*) were computed. The results were validated against the displacements obtained through dynamic MRI at maximal voluntary contraction.

3. Results

Numerical simulation of muscle active contraction originated an upward and anterior movement of the PFM and organs. Figure 4(a) illustrates the magnitude of displacement, and (b) the corresponding changes in the position of the pelvic structures from rest (continuous line) to contraction (dashed line). Figures 5(a) and (b) show the displacements in the upward and anterior directions, respectively. The pelvic floor evidenced a magnitude displacement in the range of $d = [0–7.9\,\text{mm}]$. The

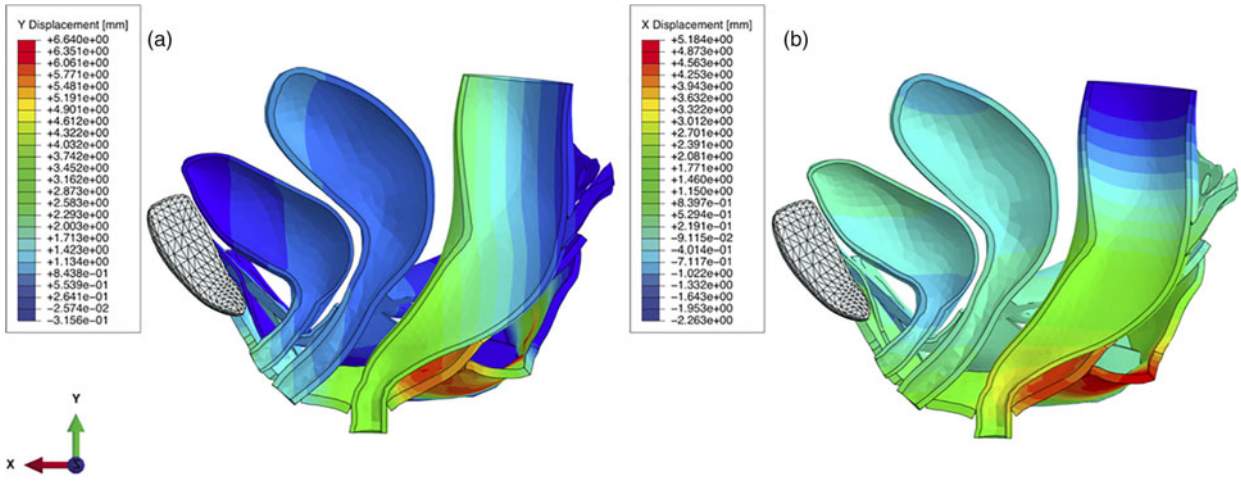

Figure 5. Results from the nodal displacements of the pelvic organs and pelvic floor muscles in the inferior-to-superior and dorsal-to-ventral directions. Simulation of pelvic floor muscle contraction resulted in an upward and anterior movement of the pelvic viscera.

maximum upward and anterior displacements were 6.6 and 5.2 mm, respectively. As shown on Figures 4 and 5, the rectal portion of the pelvic floor showed larger shift when compared to its most anterior part. Accordingly, the anorectum moved in the range of $d = [0.3–5.2\,\text{mm}]$, while the uterus and the bladder evidenced lower magnitude displacements, in the range of $d = [0.6–2.0\,\text{mm}]$ and $d = [0.3–2.0\,\text{mm}]$, respectively. Simulation of muscle contraction led to an upward and anterior motion in the range of: anorectum [1.2–3.8 mm] and [2.1–3.7 mm], vagina [0.6–1.9 mm] and [−0.2–1.1 mm], and urethra [0.7–2 mm] and [−0.9–0.9 mm], respectively.

Figure 6 shows sagittal and axial images at rest (a, b) and at maximal contraction (c, d). Vertical and horizontal reference lines were drawn along the posterior border of the pubic symphysis (thin dashed lines). The contraction of the PFM (c) pulled the posterior rectal wall (contour) and the *levator plate* (asterisk) anterior and superiorly. The same pattern was seen in the axial plane (d), where the anterior-to-posterior diameter of the *levator hiatus* decreased due to the contraction of the puborectal muscle. The pelvic structures exhibited an antero-superior motion: 5 mm anterior (white dashed line) and 2.5 mm superior displacement of the PFM; the anorectum moved 4.4 mm anterior and 2.2 mm superiorly (double asterisk); the vagina went 1.7 mm anterior (white straight line) and 0.7 mm upward, and the urethra moved 1.8 mm anterior (black straight line) and 0.4 mm superiorly (black dashed line).

Figure 7 illustrates the distribution of the von Mises Stress. The highest gradient is located in the uterus near the insertion of the uterosacral–cardinal complex in the cervix, and that of the vaginal portion of the pubourethral ligaments. In those regions, the stress values range from $[8.6 \times 10^{-2}$ to $1.72 \times 10^{-1}]$ MPa, but they increase to a maximum of 2.6×10^{-1} MPa in the attachment points of the ligaments.

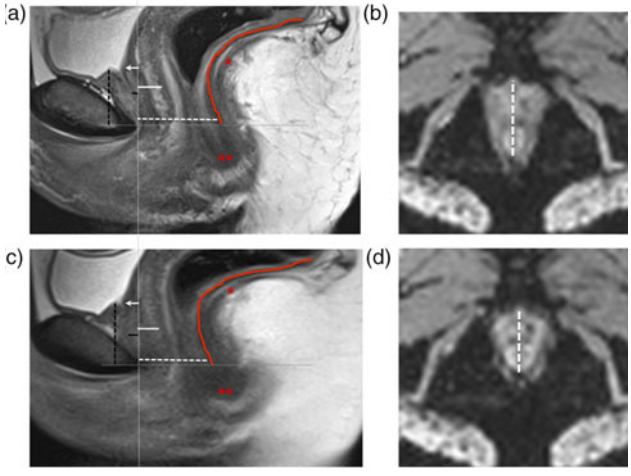

Figure 6. Sagittal (a) and axial (b) MR images acquired at rest and during maximal voluntary contraction of the pelvic floor muscles (c, d). The posterior rectal wall (contour) and the *levator plate* (asterisk) moved superiorly and anteriorly, as well as the anorectum (double asterisk). The anterior-to-posterior diameter of the *levator hiatus* decreased 5 mm (dashed line on the sagittal and axial images), in response to the contraction of the puborectal muscle.

4. Discussion

This work aimed at performing a biomechanical simulation of PFM contraction to evaluate the kinematics of the PFM and organs. Our results showed an antero-cranial movement during voluntary contraction. A proper contraction of the PFM is defined as an inward movement and a squeeze around the urethra, vagina, and rectum (Bø & Sherburn 2005) due to the posterior-to-anterior movement of the puborectal and pubococcygeal muscles around the anorectal angle, actively closing the *urogenital hiatus*. In this study, the pelvic floor moved nearly 8 mm, with maximum of 6.6 mm upward and 5.2 mm anteriorly. The dynamic MRI images showed similar values, with 0.2 mm less anterior and 4.1 mm less upward displacement when compared to numerical simulation. A possible reason for this difference to happen is related to the baseline IAP we have assumed in the modeling process. Nevertheless, the value was the same as Noakes et al. for supine at rest, which is correct according to the woman's position in the MR scanner. Higher pressure would result in a more difficult upward lift of the pelvic floor.

Our results were in the range that previous studies outlined in healthy women. Constantinou et al. (2002) reported mean forward movement of 9.4 ± 1.2 mm for the *levator ani* using MRI – which is in line with the anterior rectal displacement of 5 mm from MRI and 5.2 mm from the numerical simulation – and a relative change of 7.5 ± 1.1 mm of the pubococcygeal muscle in the antero-superior direction, which is 0.4 mm less than the maximum magnitude displacement obtained in our numerical model. During simulation of maximal voluntary contraction, the rectal area showed the highest displacement (see Figure 4 (a)) in the range of what was described by Yang et al. for the anorectal junction using ultrasound, 6.7–25.1 mm. This explains the higher motion of the anorectum when compared to the urethra and vagina for both MRI and numerical simulation. The cranial displacement of the anorectal area was similar for MRI and FEM, and to what was found by Raizada et al. (2010) for the anorectal angle using MRI, although these authors found 7 mm of cranial displacement, which is higher than the maximum 3.8 mm and 2.2 mm obtained in our numerical model and in the dynamic MRI, respectively. The higher displacement of the rectal area is related to the elevation of the *levator plate* (Figure 6, asterisk) – where the *levator ani* inserts in the sacro-coccygeal joint – in addition to the vigorous anterior pulling by the sling shape of the puborectal

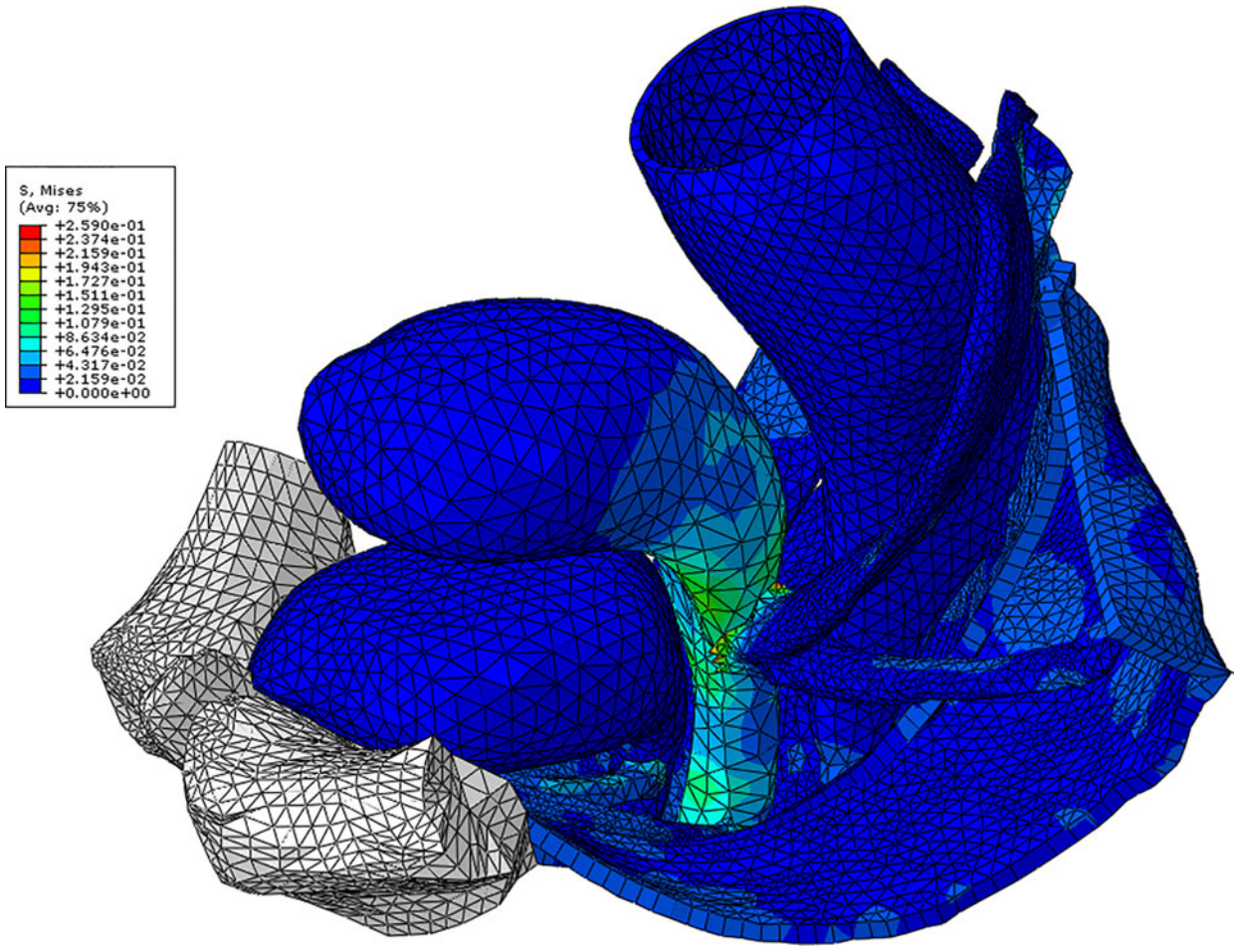

Figure 7. Distribution of the von Mises Stress. The highest gradients are located in the vagina and cervix, in the insertion of the uterine and pubourethral ligaments.

muscle around the anorectal angle. Accordingly, the sagittal MR images acquired during muscle contraction (Figure 6(c)) show that the posterior rectal wall moves anterior and superiorly, which pulls the anus upward (double asterisk). The decrease in anterior-to-posterior diameter of the *urogenital hiatus* in the MR images was similar to the one obtained by Yang et al. (2009) for ultrasound (5 mm vs. 6.2 mm, respectively).

The middle and anterior compartments of the pelvis had lower displacement during contraction, but the results from dynamic and numerical simulation were similar on both *y*- and *x*-axis. The lower dipacement values may be related to the stabilizing effect of the fascia, the uterosacral–cardinal complex, and the pubourethal ligaments on the uterus, vagina, bladder, and bladder neck, preventing their excessive anterior displacement, which is in agreement with the higher gradient in the von Mises Stress in those attachment areas. Previous study from Arab et al. (2009) using ultrasound reported an upward mean bladder base displacement value of 4.9 ± 6.9 mm in young healthy women when at maximal voluntary contraction, which is in line with the values of 2 and 1.8 mm, from the numerical simulation and MRI, respectively, found in our study. The pubocervical fascia attaching the vagina and cervix to the pelvic walls helps to suspend them. In addition to that, the inclusion of the pubourethral ligaments allowed the attachment of the urethra to the pubic bone. In this sense, muscle contraction and its antero-superior movement to promote urethral closure and prevent urine leakage resulted in 0.9 mm posterior displacement of the trigone (arrow on Figure 6).

Previous work from Parente et al. (2010b) evaluated muscle deformation during stress, and therefore, results cannot be compared. d'Aulignac et al. and Saleme et al. performed numerical simulation of active muscle contraction but without including the pelvic organs in their models. Saleme et al. determined the displacements of the pubovisceral muscle during voluntary contraction and found a maximum magnitude displacement of 5.6 mm, which is 1.3 mm lower than the ones we have obtained. However, there are differences between the two models. First, the subject in Saleme's work suffered from stress

urinary incontinence, and the PFM were thinner while the *urogenital hiatus* was wider. Second, the fact that we used the three portions of the *levator ani* instead of the pubovisceral muscle may have increased the muscle mass for active contraction and displacement.

Noakes et al. has published a computational model to simulate defecation, with posterior and downward displacements of the *levator ani* of 18.4 and 27.2 mm, respectively, similar to those obtained from dynamic MRI of the same women (4.7 and 27.9 mm). Pelvic support during Valsalva or defecation is one aspect of the role of the PFM when the pelvic cavity is under stress due to increase in the IAP. However, in our opinion, voluntary contraction of the PFM should also be addressed, as active and conscious contraction is essential to maintain continence and support. This subject-specific FE model was able to replicate the normal kinematics of the PFM and organs, and the results were similar to clinical imaging in healthy women. A validated model that describes the results from active contraction has potential applications for individual MRI-based datasets. It may be used in the future to simulate the effect of damage in muscle, fascia, or ligaments in young women presenting with stress urinary incontinence but showing no imaging evidence of abnormal urethral and muscle anatomy and for whom fascial or ligament damage are not likely. In the same way, in women who have pelvic floor disorders often associated to multi-compartimental prolapse, prediction of the benefits towards improved muscle squeeze and decreased urine leakage with pre-surgical physiotherapy could be helpful to adjust the most appropriate approach for a patient-specific situation and their synergistic potential. Additionally, this information on the kinematics of the PFM will help to improve the design of the mesh for prolapse or urethral hypermobility, since the size and tension applied to the implants may be adjusted to the subject. These applications provide a means to examine the biomechanics of the pelvis for cases where the PFM are thin or slightly disrupted and thus will reduce their active support at contraction. Modeling muscle defects and disrupted ligaments will allow us to understand the biomechanics of modified structural attachments and muscle contraction. Finally, it may be applied to evaluate the effect of physiotherapy by adjusting muscle morphology and material constants that will mimic the changes expected from muscle strengthening. This model may be the first stage of the study of different variations of the female anatomy and their contribution to pelvic floor dysfunction due to a weakening of muscle contraction.

In conclusion, we believe this model corresponds to an adequate approach to simulate PFM contraction on a healthy woman. However, the modeling process assumed simplifications. First, not all the pelvic ligaments were considered because their identification was somehow difficult to achieve even with high-resolution MRI. Second, the literature averaging of some anatomical features was done. Finally, material properties and constitutive models were the same for the pelvic ligaments except for the pobourethral ligaments, although their histological properties may not be exactly the same. Future work is needed to confirm these results, and to better understand the action of the pelvic ligaments during contraction.

Conflict of interest disclosure statement

The authors have no personal or institutional conflicts to disclosure.

Funding

The authors acknowledge the funding of the (Fundação da Ciência e Tecnologia, Portugal under the Grant (grant number PEst-OE/EME/LA0022/2013), and the (Fundo Europeu de Desenvolvimento Regional (FEDER) to the support for the project "Biomechanics: contributions to the healthcare" under the Grant (grant number NORTE-07-0124-FEDER-000035).

Notes

1. Email: mparente@fe.up.pt
2. Email: pauloggrocha@gmail.com
3. Email: tqc@sapo.pt
4. Email: iramos@med.up.pt
5. Email: rnatal@fe.up.pt

References

Albright TS, Gehrich AP, Davis GD, Sabi FL, Buller JL. 2005. Arcus tendineus fascia pelvis: a further understanding. Am J Obstet Gynecol. 193(3):677–681. doi:10.1016/j.ajog.2005.02.129.

Arab AM, Behbahani RB, Lorestani L, Azari A. 2009. Correlation of digital palpation and transabdominal ultrasound for assessment of pelvic floor muscle contraction. J Man Manip Ther. 17(3):75E–79E. doi:10.1179/jmt.2009.17.3.75E.

Bø K, Braekken IH, Majida M, Engh ME. 2009. Constriction of the levator hiatus during instruction of pelvic floor or transversus abdominis contraction: a 4D ultrasound study. Int Urogynecol J Pelvic Floor Dysfunct. 20(1):27–32.

Bø K, Sherburn M. 2005. Evaluation of female pelvic-floor muscle function and strength. Phys Ther. 85(3):269–282.

Brandão AC, Ianez P. 2013. MR Imaging of the pelvic floor: defecography. Magn Reson Imaging Clin N Am. 21(2):427–445.

Chamochumbi CC, Nunes FR, Guirro RR, Guirro EC. 2012. Comparison of active and passive forces of the pelvic floor muscles in women with and without stress urinary incontinence. Rev Bras Fisioter. 16(4):314–319. doi:10.1590/S1413-35552012005000020.

Constantinou CE, Hvistendahl G, Ryhammer A, Nagel LL, Djurhuus JC. 2002. Determining the displacement of the pelvic floor and pelvic organs during voluntary contractions using magnetic resonance imaging in younger and older women. BJU Int. 90(4):408–414. doi:10.1046/j.1464-410X.2002.02907.x.

Cosson M, Boukerrou M, Lacaze S, Lambaudie E, Fasel J, Mesdagh H, Lobry P, Ego A. 2003. A study of pelvic ligament strength. Eur J Obstet Gynecol Reprod Biol. 109(1):80–87. doi:10.1016/S0301-2115(02)00487-6.

Dalstra M, Huiskes R, Odgaard A, van Erning L. 1993. Mechanical and textural properties of pelvic trabecular bone. J Biomech. 26(4-5):523–535. doi:10.1016/0021-9290(93)90014-6.

d'Aulignac D, Martins JA, Pires EB, Mascarenhas T, Jorge RM. 2005. A shell finite element model of the pelvic floor muscles. Comput Methods Biomech Biomed Eng. 8(5):339–347. doi:10.1080/10255840500405378.

DeMaagd GA, Davenport TC. 2012. Management of urinary incontinence. P&T. 37(6):345–361.

Humphrey JD, Yin FC. 1987. On constitutive relations and finite deformations of passive cardiac tissue: I. A pseudostrain-energy function. ASME J Biomech Eng. 109(4):298–304. doi:10.1115/1.3138684.

Janda S. 2006. Biomechanics of the pelvic floor musculature. Ph. D. Thesis, Faculty of Mechanical Maritime and Materials Engineering, Delft University of Technology, Delft, Netherlands, ISBN 90-9020334-6.

Kirilova M, Stoytchev S, Pashkouleva D, Kavardzhikov V. 2011. Experimental study of the mechanical properties of human abdominal fascia. Med Eng Phys. 33(1):1–6. doi:10.1016/j.medengphy.2010.07.017.

Lin M, Chen W, Huang L, Ni J, Yin L. 2010. The anatomy of lateral ligament of the rectum and its role in total mesorectal excision. World J Surg. 34(3):594–598. doi:10.1007/s00268-009-0371-1.

Macura KJ, Genadry RR. 2008. Female urinary incontinence: pathophysiology, methods of evaluation and role of MR imaging. Abdom Imaging. 33(3):371–380. doi:10.1007/s00261-007-9257-6.

Macura KJ, Genadry RR, Bluemke DA. 2006. MR imaging of the female urethra and supporting ligaments in assessment of urinary incontinence: spectrum of abnormalities. Radiographics. 26(4):1135–1149. doi:10.1148/rg.264055133.

Martins PA, Filho AL, Fonseca AM, Santos A, Santos L, Mascarenhas T, Jorge RM, Ferreira AJ. 2011. Uniaxial mechanical behavior of the human female bladder. Int Urogynecol J. 22(8):991–995. doi:10.1007/s00192-011-1409-0.

Miehe C. 1996. Numerical computation of algorithmic (consistent) tangent moduli in large-strain computational inelasticity. Comput Methods Appl Mech Eng. 134(3-4):223–240. doi:10.1016/0045-7825(96)01019-5.

Noakes KF, Pullan AJ, Bissett IP, Cheng LK. 2008. Subject specific finite elasticity simulations of the pelvic floor. J Biomech. 41(14):3060–3065. doi:10.1016/j.jbiomech.2008.06.037.

Ogden RW. 1972. Large Deformation Isotropic Elasticity - On the Correlation of Theory and Experiment for Incompressible Rubberlike Solids. Proc R Soc Lond A. 326(1567):565–584. doi:10.1098/rspa.1972.0026.

Oomens CW, Maenhout M, van Oijen CH, Drost MR, Baaijens FP. 2003. Finite element modelling of contracting skeletal muscle. Philos Trans R Soc Lond B Biol Sci. 358(1437):1453–1460. doi:10.1098/rstb.2003.1345.

Petros PE. 1998. The pubourethral ligaments — an anatomical and histological study in the live patient. Int Urogynecol J Pelvic Floor Dysfunct. 9(3):154–157. doi:10.1007/BF02001085.

Parente MP, Jorge RM, Mascarenhas T, Fernandes AA, Martins JA. 2008. Deformation of the pelvic floor muscles during a vaginal delivery. Int Urogynecol J Pelvic Floor Dysfunct. 19(1):65–71. doi:10.1007/s00192-007-0388-7.

Parente MP, Natal Jorge RM, Mascarenhas T, Fernandes AA, Martins JA. 2009. The influence of the material properties on the biomechanical behavior of the pelvic floor muscles during vaginal delivery. J Biomech. 42(9):1301–1306. doi:10.1016/j.jbiomech.2009.03.011.

Parente MP, Natal Jorge RM, Mascarenhas T, Fernandes AA, Silva-Filho AL. 2010a. Computational modeling approach to study the effects of fetal head flexion during vaginal delivery. Am J Obstet Gynecol. 203(3):217 e1–6.

Parente MP, Natal Jorge RM, Mascarenhas T, Silva-Filho AL. 2010b. The influence of pelvic muscle activation during vaginal delivery. Obstet Gynecol. 115(4):804–808. doi:10.1097/AOG.0b013e3181d534cd.

Pit MJ, De Ruiter MC, Lycklama Á Nijeholt A, Marani AA, Zwartendijk E, Zwartendijk J. 2003. Anatomy of the arcus tendineus fasciae pelvis in females. Clin Anat. 16(2):131–137. doi:10.1002/ca.10102.

Raizada V, Bhargava V, Jung SA, Karstens A, Pretorius D, Krysl P, Mittal RK. 2010. Dynamic assessment of the vaginal high-pressure zone using high-definition manometery, 3-dimensional ultrasound, and magnetic resonance imaging of the pelvic floor muscles. Am J Obstet Gynecol. 203(2):172 e1–8.

Rivaux G, Rubod C, Dedet B, Brieu M, Gabriel B, Cosson M. 2013. Comparative analysis of pelvic ligaments: a biomechanics study. Int Urogynecol J. 24(1):135–139. doi:10.1007/s00192-012-1861-5.

Rubod C, Brieu M, Cosson M, Rivaux G, Clay JC, de Landsheere L, Babriel B. 2012. Biomechanical properties of human pelvic organs. Urology. 79(4):968 e17–22.

Saleme CS, Parente MP, Jorge RM, Pinotti M, Silva-Filho AL, Roza T, Mascarenhas T, Tavares JM. 2011. An approach on determining the displacements of the pelvic floor during voluntary contraction using numerical simulation and MRI. Comput Methods Biomech Biomed Eng. 14(4):365–370. doi:10.1080/10255842.2010.482045.

Tunn R, Goldammer K, Neymeyer J, Gauruder-Burmester A, Hamm B, Beyersdorff D. 2006. MRI morphology of the levator ani muscle, endopelvic fascia, and urethra in women with stress urinary incontinence. Eur J Obstet Gynecol Reprod Biol. 126(2):239–245. doi:10.1016/j.ejogrb.2005.10.018.

Yang SH, Huang WC, Yang SY, Yang E, Yang JM. 2009. Validation of new ultrasound parameters for quantifying pelvic floor muscle contraction. Ultrasound Obstet Gynecol. 33(4):465–471. doi:10.1002/uog.6338.

Yeoh OH. 1993. Some forms of the strain energy function for rubber. Rubber Chem Technol. 66(5):754–771. doi:10.5254/1.3538343.

Original Article

Study III

Erratum

In the *Materials and Methods* section of the paper,

* where you read (**Table 1**): C10=0.003; C20=0.002; C30=0.001 MPa,

it should be: C10=0.03; C20=0.02; C30=0.01 MPa

* in **Eq (7)**, where you read a=0.0625, it should be: a=0.6215

* in **Eq (8)**, the units for the maximum tension produced at resting length are MPa.

Original Article

Study IV

Biomechanical study on the bladder neck and urethral positions: simulation of impairment of the pelvic ligaments.

Brandão S, Parente M, Mascarenhas T, da Silva AR, Ramos I, Jorge RN.

J Biomech. 2015 Jan 21;48(2):217-223.

doi: 10.1016/j.jbiomech.2014.11.045. Epub 2014 Dec 9.

Journal of Biomechanics 48 (2015) 217–223

Contents lists available at ScienceDirect

Journal of Biomechanics

journal homepage: www.elsevier.com/locate/jbiomech
www.JBiomech.com

Biomechanical study on the bladder neck and urethral positions: Simulation of impairment of the pelvic ligaments

Sofia Brandão [a,*], Marco Parente [b], Teresa Mascarenhas [c], Ana Rita Gomes da Silva [c], Isabel Ramos [a], Renato Natal Jorge [c]

[a] Department of Radiology, Centro Hospitalar de São João—EPE, Faculty of Medicine, University of Porto, Alameda Prof. Hernâni Monteiro, 4200-319 Porto, Portugal
[b] IDMEC, Faculty of Engineering, University of Porto, Rua Dr Roberto Frias, s/n, 4200-465 Porto, Portugal
[c] Department of Gynecology and Obstetrics, Hospital de S. João, Faculty of Medicine, University of Porto, Alameda Prof. Hernâni Monteiro, 4200-319 Porto, Portugal

ARTICLE INFO

Article history:
Accepted 28 November 2014

Keywords:
Pelvic floor dysfunction
Biomechanical simulation
Finite element method
Soft tissue analysis
Ligament impairment

ABSTRACT

Excessive mobility of the bladder neck and urethra are common features in stress urinary incontinence. We aimed at assessing, through computational modelling, the bladder neck position taking into account progressive impairment of the pelvic ligaments.

Magnetic resonance images of a young healthy female were used to build a computational model of the pelvic cavity. Appropriate material properties and constitutive models were defined. The impairment of the ligaments was simulated by mimicking a reduction in their stiffness.

For healthy ligaments, valsalva maneuver led to an increase in the α angle (between the bladder neck-symphysis pubis and the main of the symphysis) from 91.8° (at rest) to 105.7°, and 5.7 mm of bladder neck dislocation, which was similar to dynamic imaging of the same woman (α angle from 80° to 103.3°, and 5 mm of bladder neck movement). For 95% impairment, they enlarged to 124.28° and 12 mm. Impairment to the pubourethral ligaments had higher effect than that of vaginal support (115° vs. 108°, and 9.1 vs. 7.3 mm).

Numerical simulation could predict urethral motion during valsalva maneuver, for both healthy and impaired ligaments. Results were similar to those of continent women and women with stress urinary incontinence published in the literature. Biomechanical analysis of the pubourethral ligaments complements the biomechanical study of the pelvic cavity in urinary incontinence. It may be useful in young women presenting stress urinary incontinence without imaging evidence of urethral and muscle lesions or organ descend during valsalva, and for whom fascial damage are not expected.

1. Introduction

Stress urinary incontinence (SUI) and organ prolapse (Patel et al., 2007) have a significant negative impact on quality-of-life. The pathophysiology is multifactorial, including aging, hormonal changes from menopause, vaginal delivery and high parity, often in consequence of nerve, muscle or ligament direct injury, pelvic fascia or ligament collagen degradation (Patel et al., 2007).

As experimental work in vivo is very hard to implement, imaging evidence and biomechanical modelling (Dietz, 2004; Yip et al., 2014) have illustrated the role of striated pelvic floor muscles defects in urinary (in)continence and organ support. While they act by means of passive and active forces (Chamochumbi et al., 2012), the pelvic fascia and ligaments provide additional passive stabilization (Brandão and Ianez, 2013). Evaluating ligament biomechanics according to tissue *status* is relevant to understand SUI features.

Previous computer modelling focused on the normal pelvic mobility (Cosson et al., 2013). Also, in the context of pelvic organ prolapse, the vaginal and vesical position was evaluated considering muscle and apical support weakening and impairment (Chen et al., 2006, 2009; Yip et al., 2014). Results suggest that the extent of anterior vaginal prolapse is related to the degree of both muscle and uterosacral–cardinal support impairment. Simulating 90% and 60% of ligament and pubovisceral muscle impairment, respectively, led to a threefold increase in vaginal prolapse, which explains the vesico-urethral descent.

The role of (ab)normal apical support on vesical position is in this way modelled. However, to our knowledge, the role of pubourethral ligaments (PUL) was never included in such analysis.

Abbreviations: ATFP, arcus tendineous fasciae pelvis; IAP, intra-abdominal pressure; PUL, pubourethral ligaments; SUI, stress urinary incontinence

* Corresponding author. Tel.: +351 96 4089922.
E-mail addresses: Sofia.brand@gmail.com (S. Brandão), mparente@fe.up.pt (M. Parente), rita.mgs89@gmail.com (A.R.G. da Silva), iramos@med.up.pt (I. Ramos), rnatal@fe.up.pt (R.N. Jorge).

http://dx.doi.org/10.1016/j.jbiomech.2014.11.045
0021-9290/

The PUL are important urethral stabilizers that insert on the posterior surface of the pubic bone (El-Sayed et al., 2007; Kim et al., 2003; Petros, 1998), as shown on Fig. 1(a and b). When they suffer from injury or laxity (c–e), an increase in the retropubic space, bladder neck funneling and urethral hypermobility may occur (Pregazzi et al., 2002). As a result, "complaint of any involuntary loss of urine on effort (…)", as defined by the International Continence Society, may occur during events that result in increased intra-abdominal pressure (see Fig. 1f)—as for example, sneezing, coughing, defecating or during physical exercise. This is a common finding in patients suffering from SUI (Kim et al., 2003; Pregazzi et al., 2002).

In what concerns UI, and from a functional aspect, the PUL are critical structures, along with the paraurethral and vaginal tissue and the *levator ani* muscle. The structural degradation of the support structures such as the ligaments and fascia can be another ingredient to develop SUI, as stated by the Integral Theory (Petros and Woodman, 2008). If the mechanical properties of the ligaments induce their laxity, the backward force against the PUL and the downward force against the uterosacral and cardinal ligaments during valsalva may prevent muscles from effectively pushing the urethra against the pubic bone. On the other hand, injury models in rats such as urethrolysis or PUL transection have reproduced trauma, and results showed urethral hypermobility and long-term SUI (Kefer et al., 2008). For these reasons, by modelling the joint action of the PUL along with the apical support may add information on its contribution to (ab)normal bladder neck and urethral mobility, which are findings in young women presenting SUI, but with no evidence of organ prolapse or muscle damage.

Accordingly, the purpose of this work was to model, under a mechanical perspective, the effect of distinct levels of ligament impairment. For this purpose, we measured the bladder neck mobility and the changes in the α angle for valsalva maneuver using live subject MRI and a computational model based on the Finite element method.

2. Materials and methods

2.1. Subject and imaging

The Institutional Review Board approved this work (protocol: CES195/12).

A nulliparous 24-year female with no complains of pelvic dysfunction was the volunteer for the scanning session. A gynecologist observed her and no morphologic or functional abnormalities were found.

The volunteer was instructed on how to perform correct valsalva maneuver at two different time-points. First, a trained nurse and the gynecologist gave full instructions during clinic observation. Second, the nurse and an experienced physiotherapist on pelvic floor rehabilitation gave additional support during the scanning session. Several attempts were performed with the volunteer lying in the scanner table before the beginning of the acquisitions.

Magnetic resonance images were acquired in the supine position at rest using a 3.0 T system (Magnetom® Tim Trio, Siemens Medical Solutions, Erlangen, Germany) equipped with two (anterior and posterior) 6ch-phased-array RF coils. The woman lied in supine position with legs together in a semiflexed position.

Multiplanar pelvic high-resolution T2w fast spin-echo (FSE) images were obtained (TE/TR 96/3860 ms; 2 mm slices (no interslice gap); field-of-view 26 cm; matrix 384 × 384 and 3 NSA (number of signals averaged).

Additional dynamic images were obtained in the mid-sagittal plane, approximately every 1.6 s for 30 s using a half-Fourier acquisition single-shot turbo spin-echo (HASTE) pulse sequence (TE/TR 96/1600 ms; 6 mm slices; field-of-view 28 cm, matrix: 155 × 256 and 1 NSA).

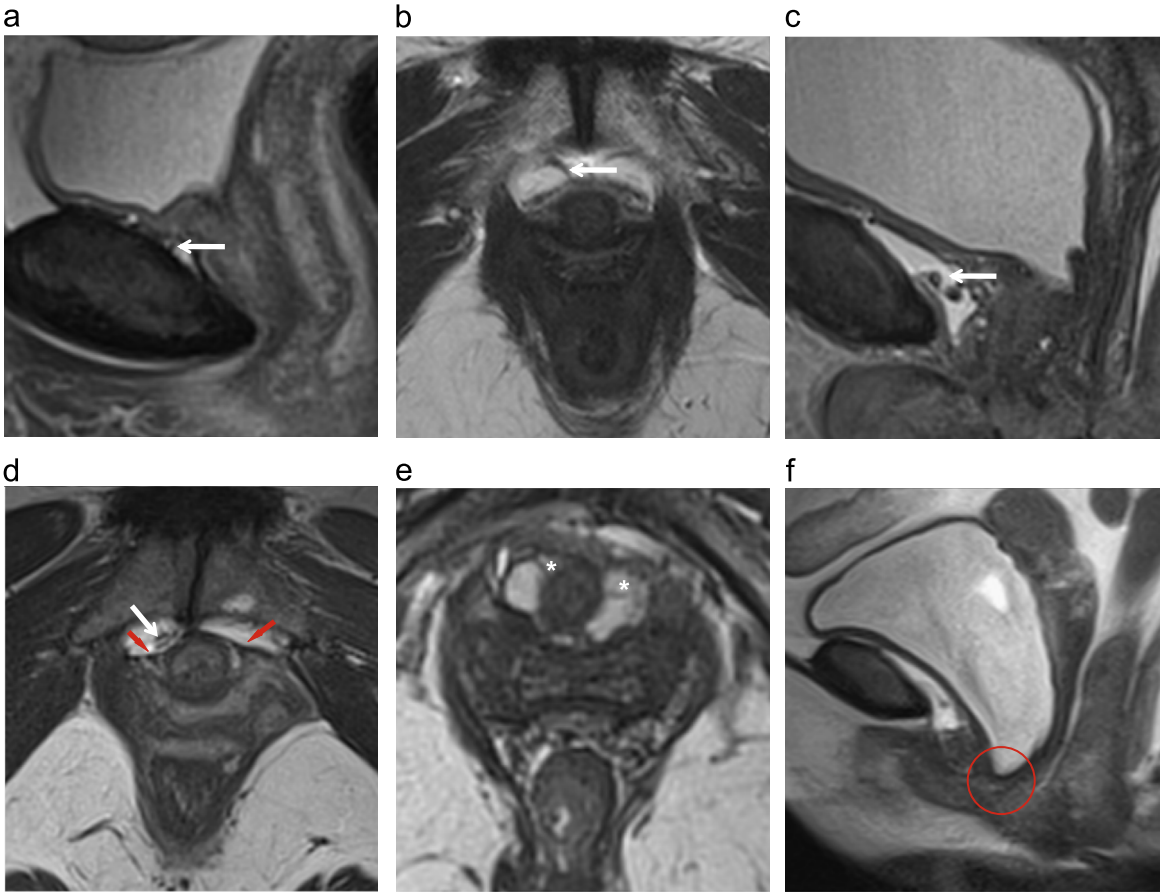

Fig. 1. Magnetic resonance imaging (MRI) of the support to the urethra and bladder. The pubourethral ligaments are thin hypointense bands that attach the bladder neck to the symphysis pubis. They can be seen in sagittal (a) and axial high-resolution images (b) (white arrow). Some women with stress urinary incontinence (SUI) show ligament distortion (c) and (d), and increased retropubic space. The position of urethra may not be maintained, as the peri- and paraurethral ligaments (red arrows on (d)) and (asterisks on (e), respectively) are not stretched tight, and urethral rotation may occur. Urethral hypermobility and bladder neck funneling (red circle on (f)) are shown during valsalva maneuver. (For interpretation of the references to color in this figure legend, the reader is referred to the web version of this article.)

During the dynamic scanning, 2 images were acquired at rest during suspended inspiration (approximately 3 s), 5 during minimal, 5 during moderate and 5 during maximal valsalva (total of 24 s), and the last 2 during normal breathing (approximately 3 s). Three sets of these 19 successive images were acquired 3 times with 2 min interval. The best maximal valsalva image was selected for analysis. It was chosen by measuring the most evident vertical descent of the bladder neck along a horizontal axis drawn at the outer side of the *periosteum* in the inferior edge of the pubic bone, and simultaneously having the wider hiatal sagittal diameter.

The radiologist observed all the images, and no suspicious findings were reported.

2.2. Finite element model

The high-resolution T2w images were used to identify and segment several anatomical structures. Two readers (20 and 15 years experience) *in consensus* confirmed anatomical landmarks. To create the 3D solid model (see Fig. 2) the axial images were imported to the Inventor® software (Autodesk, San Raphael, CA, USA), and the structures were outlined with contour splines. This solid geometry was then discretized into a finite element mesh with tetrahedral elements using the Abaqus® software v.6.12 (Dassault Systèmes Simulia Corp., Providence, RI, USA).

The finite element model included the bony pelvis, the pelvic organs, and some of the main supporting structures (the *levator ani* muscle, the pubourethral, uterosacral, cardinal and the lateral ligaments of the rectum, the pubocervical fascia and the *arcus tendineous fasciae pelvis* (ATFP)). Although we did not expect a direct influence of the lateral ligaments of the rectum on the bladder neck and urethral position, they were included as posterior compartment supporters. The width and length of the lateral ligaments of the rectum (1.5 cm and 2.2 cm, respectively) were confirmed in the literature (Lin et al., 2010). The ATFP length (9.0 cm) was measured by its attachment points and compared with cadaver dissection data (Albright et al., 2005; Occelli et al., 2001); further geometric details were retrieved from the literature (Albright et al., 2005; Pit et al., 2003). Fig. 2 illustrates the 3D model with all the structures considered for the modelling and simulation.

For the modelling, the organs were described as having hyperelastic mechanical behaviour while the bones were fixed and considered as rigid (Dalstra et al., 1993).

As pelvic cavity soft tissues such as muscles and ligaments are composed by fibers that are aligned with their main anatomical and functional axis, we used simple isotropic models adjusted to the main direction of these structures. For that purpose, the Yeoh (1993) and Ogden (1972) constitutive equations were used to model the behaviour of all the soft tissues. The pelvic fascia was assumed as having similar mechanical properties to those of the abdominal fascia (Kirilova et al., 2011). Table 1 presents the constitutive parameters. The material properties were obtained from previous publications using experimental data from female cadaver without pelvic floor dysfunction (Cosson et al., 2003; Janda, 2006; Martins et al., 2011; Rivaux et al., 2013; Rubod et al., 2012). The curve-fitting algorithm from Abaqus® was applied to each experimental dataset. During the fitting process, the model that better adjusted the experimental data was chosen by determining the correlation coefficient (r) between the different curves. Fig. 3 shows the experimental and numerical curves, as well as the correlation coefficient, that were obtained for each tissue.

The supporting structures were attached to the organs and bone by using multi-point constrains (Abaqus® tie). The nodes corresponding to the pubic bone and the extremities of the *levator ani* muscle, pelvic fascia, PUL and anterior portion of the ATFP that attach to the pubic bone were fixed. The same boundary conditions were applied to the insertion of the lateral ligaments of the rectum in the endopelvic fascia, to the sacral attachment of the uterosacral ligaments, to the postero–lateral connection of the *levator ani* in the *arcus tendineous of the levator ani*, and to the cardinal ligament insertion in the obturator fascia. The interaction between the organs was modelled as frictionless, and established using the default Abaqus® contact pressure-overclosure algorithm.

The model was tested using Abaqus® Standard for pressure values that correspond to the IAP for supine rest and supine valsalva maneuver, following the methodology described by Noakes et al. (2008). Despite the fact that the supine position does not mimic the normal physiologic state, the model was built from MR images acquired in the supine position, and therefore the same conditions should be established. Since the muscles already incorporate resting tone in the supine position, the mean pressure at rest (0.5 kPa) was subtracted from the average supine valsalva pressure (4.5 kPa) to obtain the value of 4 kPa.

For those values of pressure, mean values of displacement of the pelvic organs and pelvic floor muscles were evaluated considering all the ligaments as healthy so as to validate the numerical model. Furthermore, in order to have a starting point to evaluate the effect of simulating changes in stiffness of the ligaments, two common measures of vesico-urethral mobility were tested at rest and for valsalva maneuver. The bladder neck mobility was assessed according to the standardized x–y coordinate system described by Schaer et al. (1995) by setting the same reference axis on Abaqus®. A line passing the axis of the symphysis pubis (x-axis) intercepted a second line perpendicular to this to cross at the infero-posterior margin of the symphysis pubis (y-axis). The position of the bladder neck at rest and valsalva maneuver was then defined. The α angle was also evaluated as described by Pregazzi et al. (2002), by measuring the angle between the bladder neck and the symphysis pubis, and the x-axis.

In a second stage, we simulated the valsalva meneuver while considering impairment to all the ligaments, and also considering the anterior, middle and posterior support ligaments. Structural impairment was simulated by reducing material stiffness. Fig. 4 shows the behavior assumed for the impaired ligaments, which were achieved by multiplying the stress/strain curve of a healthy ligament obtained from a uniaxial tension tests (Rivaux et al., 2013) by a given coefficient (0.75, 0.50, 0.25 and 0.05). The new datasets were imputed in the curve-fitting algorithm from Abaqus® software, and new parameters were obtained (numerical curves in Fig. 4). Since we focused exclusively on changing stiffness of the ligaments, we decided to keep the other structures (including organs) intact. The primary outcomes of this second stage were again the α angle and the bladder neck dislocation to compare with the ones of the first simulation.

3. Results

We found that the value of IAP affects the position of the pelvic structures.

Fig. 5 shows the displacement maps that evidence the movement of the pelvic organs and pelvic floor muscles at rest (a) and when simulating valsalva maneuver (b), considering all ligaments as healthy. To better illustrate the displacement, their contour was outlined (c). Dynamic MRI (d) at valsalva is also seen. Results from numerical simulation showed that the uterus, bladder and the rectal portion of the pelvic floor evidenced the highest displacement. The pelvic floor muscles showed an inferior and posterior displacement of 6.1 and 1.6 mm, respectively. Accordingly, the rectum descended 3.7 mm. The uterus went down 10.7 mm further compressing the body of the bladder (9.1 mm) against the pubic bone. This led to a slight posterior movement of the urethra and vagina (0.5 and 0.8 mm, respectively).

In the numerical simulation, the α angle and the bladder neck dislocation varied according to the two conditions. When considering

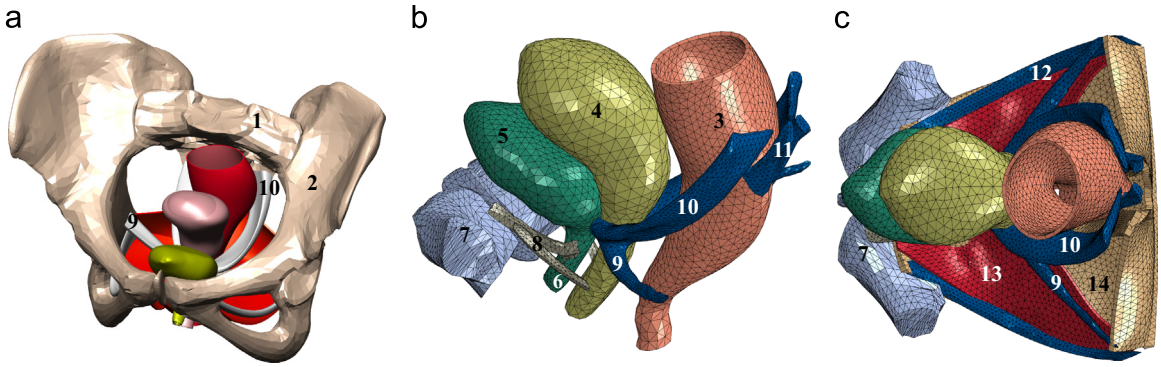

Fig. 2. Anatomical perspective of the 3D model. The pelvic bones, organs and several soft tissue support structures were included (a). In (b) and (c), some of the osseous structures were hidden for a better visualization of the soft tissues. ((1) sacrum; (2) bony pelvis; (3) rectum; (4) uterus; (5) bladder; (6) urethra; (7) symphysis pubis; (8) pubourethral ligaments; (9) cardinal ligaments (10) uterosacral ligaments; (11) lateral ligaments of the rectum; (12) *arcus tendineous fasciae pelvis*; (13) pelvic fascia; (14) pelvic floor muscles).

Table 1
Material properties and hyperelastic constitutive models for the structures included in the model.

Structure	α_k	μ_k	–	Model	Experimental data
Bladder and urethra	$\alpha_1 = 0.19$	$\mu_1 = 5.14$	–	Ogden ($N=1$)	Martins et al. (2011)
Rectum	$\alpha_1 = 4.25$	$\mu_1 = 13.24$	–	Ogden ($N=2$)	Rubod et al. (2012)
	$\alpha_2 = -3.83$	$\mu_2 = 13.24$	–		
Vagina and uterus	$\alpha_1 = -3.41$	$\mu_1 = 92.24$	–	Ogden ($N=3$)	Rubod et al. (2012)
	$\alpha_2 = -0.66$	$\mu_2 = 39.29$	–		
	$\alpha_3 = -6.48$	$\mu_3 = 54.68$	–		
Pelvic fascia and ligaments (ATFP, CL, LLR, USL)	$\alpha_1 = 10.85$	$\mu_1 = 3.17$	–	Ogden ($N=1$)	Rivaux et al. (2013)
Pelvic ligaments (PUL)	$\alpha_1 = 10.95$	$\mu_1 = 1.58$	–	Ogden ($N=1$)	Rivaux et al. (2013)
	C_{10}	C_{20}	C_{30}	**Model**	
Pubocervical fascia	0.93	−0.62	0.47	Yeoh	Kirilova et al. (2011)
Pelvic floor muscles	0.003	0.002	0.001	Yeoh	Janda, (2006)

α_k and μ_k—material constants.
ATFP—*arcus tendineus fascia pelvis*; CL—cardinal ligaments; PUL—pubourethral ligaments; LLR—lateral ligaments of the rectum; USL—uterosacral ligaments.

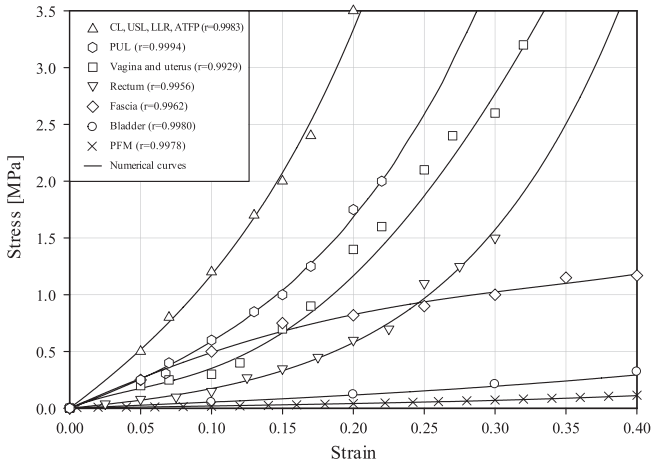

Fig. 3. Fitting process to obtain the material properties for the different tissues included in the model. The experimental and numerical curves are shown. For each tissue, the model that better fitted the experimental data was chosen. (CL—cardinal ligaments; USL—uterosacral ligaments; LLR—lateral ligaments of the rectum; ATFP—*arcus tendineous fasciae pelvis*; PUL—pubouretral ligaments; PFM—pelvic floor muscles).

the ligaments as healthy, valsalva maneuver opened the α angle from 91.8° to 105.7° and the bladder neck moved 5.7 mm posteriorly. Measures taken in the MR images revealed similar values: the α angle changed from 88° to 103.3° and the bladder neck dislocation was 5 mm.

Fig. 6 shows that at valsalva maneuver progressive ligament impairment increases these values, except for the lateral ligaments of the rectum. Between 75% and 95% impairment, a pronounced effect was produced when the impairment was applied to all the ligaments simultaneously, and also for the PUL. Isolated impairment to the PUL resulted in a more evident increase of the bladder neck angle and urethral mobility than damage on the apical vaginal supporters (115° vs. 108°, and 9.1 mm vs. 7.3 mm).

Fig. 7 displays the bladder and urethra contours. A dot was drawn in the region of the bladder neck to illustrate its position. The grey continuous line represents the bladder neck at rest. It changes from 91.8° to 108.7° and moves 6.9 mm for valsalva maneuver considering there has been 50% of impairment to all the ligaments (grey dashed line), and 124.3° and moves 12 mm for a 95% impairment (black continuous line).

4. Discussion

This paper presents a live MRI-based model used to investigate the effect of simulating impairment of the pelvic ligaments in the α angle and the bladder neck mobility during valsalva maneuver, which is often evaluated through diagnostic imaging for women suffering from SUI. Results of numerical simulation were in agreement with dynamic MRI of the same woman, and also with what was reported by Pregazzi et al. (2002) for asymptomatic women (91.8° and 88° vs. 92 ± 6° at rest, 105.7° and 103.3° vs. 100 ± 8° at valsalva). Simulation of impairment on all ligaments revealed an α angle similar to what was described by the same author for incontinent women (124.3° vs. 120 ± 8° at valsalva). Results for bladder neck dislocation are also similar to what was previously described by Peschers et al. (2001) and Howard et al. (2000) (14 ± 9 mm (ranging from 2 mm to 31 mm) and 12.4 ± 4.7 mm, respectively) for continent, and by Viereck et al. (2006) for incontinent women (13.7 mm, ranging from 2 mm to 30 mm). The minor differences between our results from numerical simulation and MRI may be related to the pressure applied. We cannot assure that they were exactly the same, despite the volunteer was instructed on how to perform correct valsalva maneuver. Nevertheless, the value of IAP was correct according to the woman's position in the MR scanner. Still, a different pressure would result in more or less dislocation of the bladder neck and urethra. This can also explain the differences between our results and the literature, as previous studies report a wide range of values that may result from patient cooperation and awareness on performing valsalva maneuver.

Fig. 6 shows that when all the ligaments were considered as impaired, an evident increase in the α angle and bladder neck mobility were seen for valsalva maneuver. The pelvic organs are distensible structures with attachments that allow for normal mobility, which would not be possible with fixed rigid ligaments. Because changes in mechanical strength are dependent on morphology and mechanical properties of the tissue, our results suggest similar results published for the apical ligaments, that is the interrelationship between the impairment of these support structures and their biomechanical behavior. Decreasing ligaments stiffness induces excessive mobility, and therefore when impaired ligaments are tensioned, they will suffer higher deformations that lead to increased urethral mobility.

In our model, the PUL seem to have the greatest effect on the position of the bladder neck. As shown on Fig. 6, if we impose an impairment of 95% of the PUL – that is considering them as almost absent – while maintaining the material properties of the uterine and rectal support ligaments constant, we can recognize that the dynamics of the pelvic cavity measured at the anterior compartment is highly changed. This may be related to their attachment on the midurethra, which explains that injury causes further descent than the one obtained for the apical ligaments.

Deficiency on the PUL is directly associated with the mechanism of urethral hypermobility (Kefer et al., 2008), as severe lesions decrease the leak point pressure, which is likely to lead to loss of urine during cough or exercise. Besides urethral hypermobility,

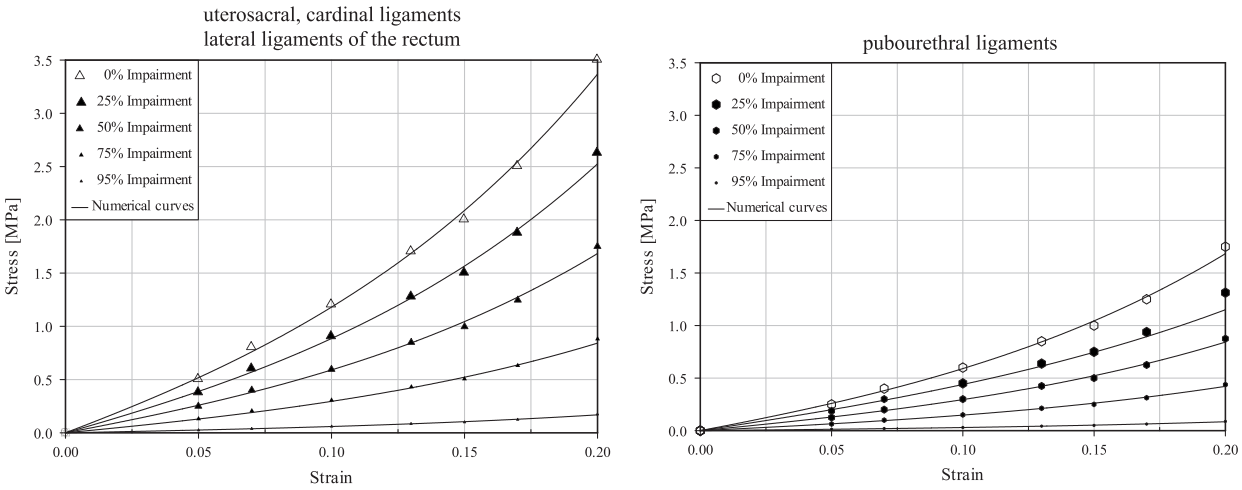

Fig. 4. Numerical curves obtained from Abaqus® software.

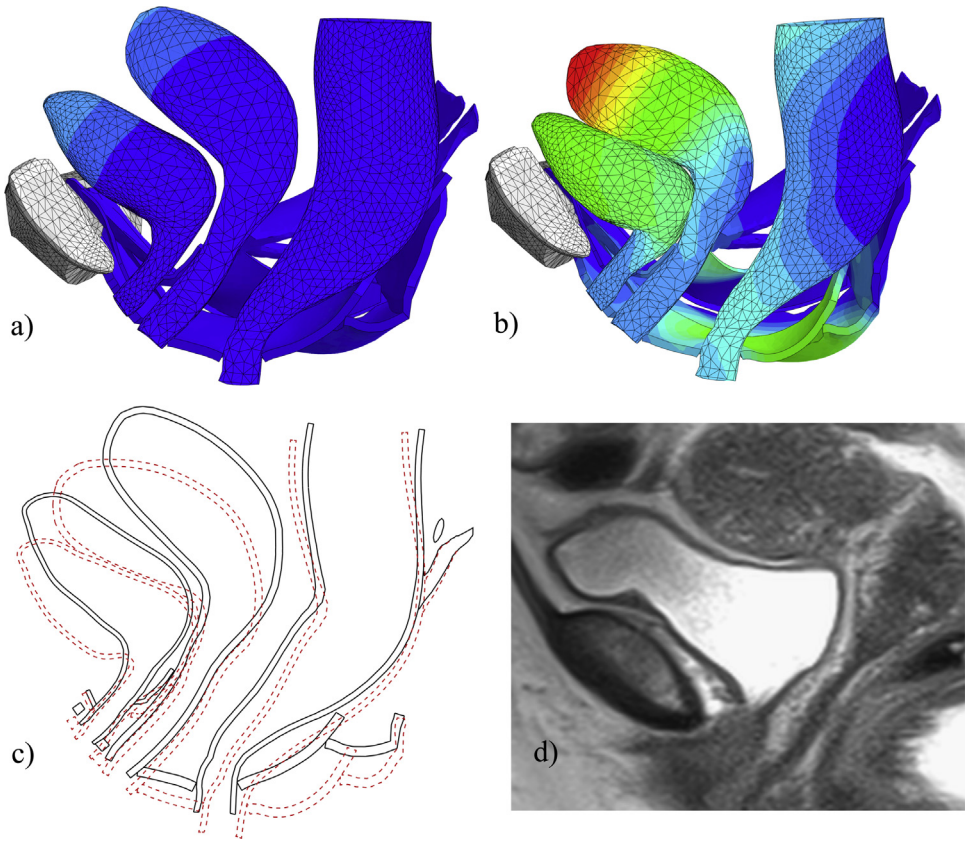

Fig. 5. Pelvic organs and muscles displacement at rest (a) and for valsalva maneuver (b) considering the ligaments as healthy. The body of the uterus, the bladder and the rectal portion of the pelvic floor muscles evidenced the highest displacement. In (c), their contours at rest (black continuous lines) and valsalva maneuver (red dashed lines) were drawn. (For interpretation of the references to color in this figure legend, the reader is referred to the web version of this article.)

other passive mechanisms such as intrinsic sphincter deficiency or abnormal urethral compliance, and also insufficient voluntary contraction of the pelvic muscles may contribute to SUI.

Despite the fact that this model was build based in only one women, this subject-specific Finite Element modelling approach has the potential for application to patient- or patient group-based MRI datasets. It would be helpful in young women presenting SUI but with imaging evidence of normal urethral and muscle anatomy, and pelvic organ positioning during dynamic ultrasound or MRI, for whom fascial damage are not expected. Likewise, prediction of surgical trauma during bladder neck suspension procedures or urethral diverticulectomy could be helpful to adjust the surgical approach for a patient-specific situation. This provides a means to examine the biomechanics of the pelvis for cases where the woman's morphology is a key issue, such as patients with previous hysterectomy due to changes in normal dynamics between anterior and middle compartment, or when the pelvic floor muscles are very thin or are slightly disrupted and thus start reducing their active support. We believe that it could also be applied to future modelling of excessive fetal head compression to the bladder and urethra against the pubis during labor, which would elucidate on the causes for post-partum SUI.

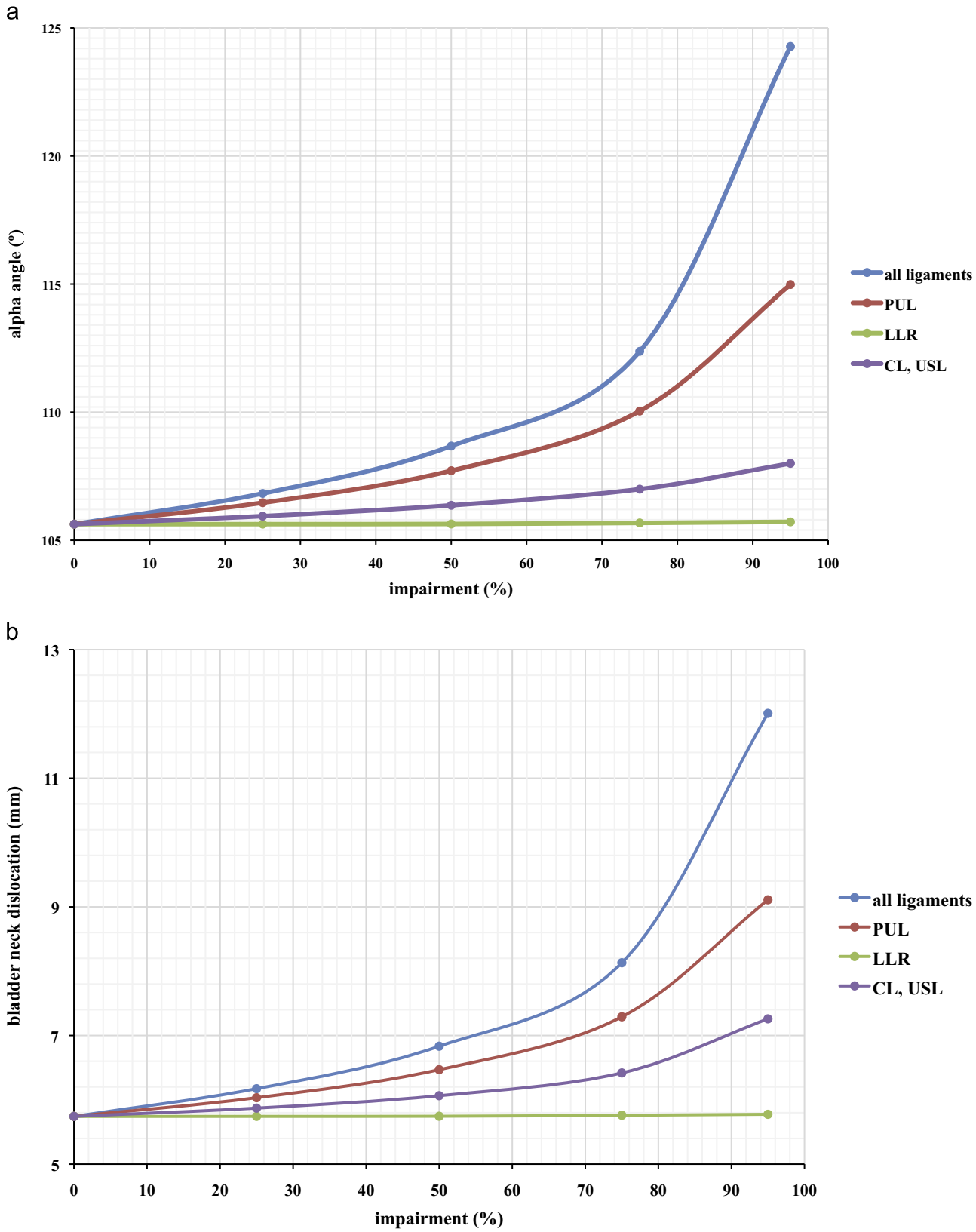

Fig. 6. Values of the α angle (a) and bladder neck dislocation (b) according to the increased impairment of the pelvic ligaments. When considered alone, the impairment of the pubourethral ligaments led to the highest increase on the α angle and bladder neck dislocation. (CL—cardinal ligaments; LLR—Lateral ligaments of the rectum; PUL—pubouretral ligaments; USL—uterosacral ligaments).

There are certain limitations in this study. First, not all the pelvic ligaments were considered in this model. The urethral support does rely not only on the PUL but also on the pubovesical, the periurethral and the paraurethral ligaments. We have chosen to include only the PUL for several reasons: to simplify the model, due to their relevance to the urethral and vaginal anchoring, and

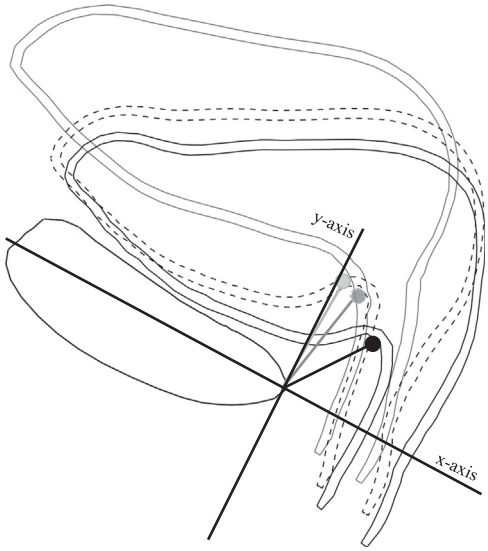

Fig. 7. Variation of the position of the bladder neck.

also the existing evidence of their disruption in SUI patients. Second, the pelvic floor muscles were modelled as a single structure having the same thickness, which is not entirely correct, as the puborectal portion of the *levator ani* is usually thicker. Third, both the MRI acquisitions and modelling were performed considering the supine position, which does not mimic the normal physiologic state, as coughing, exercising, or defecating are performed in the upright or sitting positions. For that purpose simulation of standing valsalva comparing with standing MRI would be interesting. Nevertheless, one may assume that standing up implies higher IAP values.

In spite of the limitations noted, we feel that this model is a step forward in the biomechanical analysis of SUI. These simulations showed the central contribution of the PUL to maintain the bladder neck position.

In conclusion, we presented a biomechanical model that predicted the effect of the position of pelvic organs in real-life circumstances.

Financial disclamer/conflict of interest statement

The authors disclose financial and personal relationships that could inappropriately influence this work.

Funding

The authors acknowledge the funding of the project PEst-OE/EME/LA0022/2013, from Fundação da Ciência e Tecnologia, Portugal and to the project "Biomechanics: contributions to the healthcare", reference NORTE-07-0124-FEDER-000035 co-financed by Programa Operacional Regional do Norte (ON.2—O Novo Norte), through the Fundo Europeu de Desenvolvimento Regional (FEDER).

References

Albright, T.S., Gehrich, A.P., Davis, G.D., Sabi, F.L., Buller, J.L., 2005. *Arcus tendineus fascia pelvis*: a further understanding. Am. J. Obstet. Gynecol. 193 (3 Pt 1), 677–681. http://dx.doi.org/10.1016/j.ajog.2005.02.129.

Brandão, AC, Ianez, P., 2013. MR imaging of the pelvic floor: defecography. Magn. Reson. Imaging Clin. N. Am 21 (2), 427–445. http://dx.doi.org/10.1016/j.mric.2013.01.007.

Chamochumbi, CC., Nunes, FR., Guirro, RR., Guirro, EC., 2012. Comparison of active and passive forces of the pelvic floor muscles in women with and without stress urinary incontinence. Rev. Bras. Fisioter. 16 (4), 314–319. http://dx.doi.org/10.1590/S1413-35552012005000020.

Chen, L., Ashton-Miller, J.A., DeLancey, J.O., 2009. A 3D finite element model of anterior vaginal wall support to evaluate mechanisms underlying cystocele formation. J. Biomech. 42 (10), 1371–1377. http://dx.doi.org/10.1016/j.jbiomech.2009.04.043.

Chen, L., Ashton-Miller, J.A., DeLancey, J.O., Hsu, Y., 2006. Interaction between apical supports and *levator ani* in anterior vaginal support: theoretical analysis. Obstet. Gynecol. 108 (2), 324–332. http://dx.doi.org/10.1097/01.AOG.0000227786.69257.a8.

Cosson, M., Boukerrou, M., Lacaze, S., Lambaudie, E., Fasel, J., Mesdagh, H., Lobry, P., Ego, A., 2003. A study of pelvic ligament strength. Eur. J. Obstet. Gynecol. Reprod. Biol 109 (1), 80–87. http://dx.doi.org/10.1016/S0301-2115(02)00487-6.

Cosson, M., Rubod, C., Vallet, A., Witz, J.F., Dubois, P., Brieu, M., 2013. Simulation of normal pelvic mobilities in building an MRI-validated biomechanical model. Int. Urogynecol. J. 24 (1), 105–112. http://dx.doi.org/10.1007/s00192-012-1842-8.

Dalstra, M., Huiskes, R., Odgaard, A., van Erning, L., 1993. Mechanical and textural properties of pelvic trabecular bone. J. Biomech. 26 (4–5), 523–535.

Dietz, H.P., 2004. Ultrasound imaging of the pelvic floor. Part II: Three-dimensional or volume imaging. Ultrasound Obstet. Gynecol. 23, 615–625. http://dx.doi.org/10.1002/uog.1072.

El-Sayed, R.F., Morsy, M.M., El-Mashed, S.M., 2007. Anatomy of the urethral supporting ligaments defined by dissection, histology, and MRI of female cadavers and MRI of healthy nulliparous women. AJR Am. J. Roentgenol 189 (5), 1145–1157.

Howard, D., Miller, J.M., Delancey, J.O., Ashton-Miller, J.A., 2000. Differential effects of cough, valsalva, and continence status on vesical neck movement. Obstet. Gynecol. 95 (4), 535–540.

Janda, S., 2006. Biomechanics of the Pelvic Floor Musculature (Ph.D. Thesis Dissertation). Delft University of Technology (ISBN:90.9020334).

Kefer, J.C., Liu, G., Daneshgari, F., 2008. Pubo-urethral ligament transection causes stress urinary incontinence in the female rat: a novel animal model of stress urinary incontinence. J. Urol. 179 (2), 775–778.

Kim, J.K., Kim, Y.J., Choo, M.S., Cho, K.S., 2003. The urethra and its supporting structures in women with stress urinary incontinence: MR imaging using an endovaginal coil. AJR Am. J. Roentgenol 180 (4), 1037–1044. http://dx.doi.org/10.2214/ajr.180.4.1801037.

Kirilova, M., Stoytchev, S., Pashkouleva, D., Kavardzhikov, V., 2011. Experimental study of the mechanical properties of human abdominal fascia. Med. Eng. Phys. 33 (1), 1–6. http://dx.doi.org/10.1016/j.medengphy.2010.07.017.

Lin, M., Chen, W., Huang, L., Ni, J., Yin, L., 2010. The anatomy of lateral ligament of the rectum and its role in total mesorectal excision. World J. Surg. 34 (3), 594–598. http://dx.doi.org/10.1007/s00268-009-0371-1.

Martins, P.A., Filho, A.L., Fonseca, A.M., Santos, A., Santos, L., Mascarenhas, T., Jorge, RM., Ferreira, A.J., 2011. Uniaxial mechanical behavior of the human female bladder. Int. Urogynecol. J. 22 (8), 991–995. http://dx.doi.org/10.1007/s00192-011-1409-0.

Noakes, K.F., Pullan, A.J., Bissett, I.P., Cheng, L.K., 2008. Subject specific finite elasticity simulations of the pelvic floor. J. Biomech. 41 (14), 3060–3065. http://dx.doi.org/10.1016/j.jbiomech.2008.06.037.

Ogden, R.W., 1972. Large deformation isotropic elasticity—on the correlation of theory and experiment for incompressible rubberlike solids. Proc. R. Soc. London, Ser. A 326 (1567), 565–584.

Occelli, B., Narducci, F., Hautefeuille, J.P., Querleu, D., Crépin, G., Cosson, M., 2001. Anatomic study of arcus tendineus fasciae pelvis. Eur. J. Obstet. Gynecol. Reprod. Biol 97 (2), 213–219.

Patel, P.D., Amrute, K.V., Badlani, G.H., 2007. Pelvic organ prolapse and stress urinary incontinence: a review of etiological factors. Indian J. Urol 23 (2), 135–141. http://dx.doi.org/10.4103/0970-1591.32064.

Peschers, U.M., Fanger, G., Schaer, G.N., Vodusek, D.B., DeLancey, J.O., Schuessler, B., 2001. Bladder neck mobility in continent nulliparous women. BJOG 108 (3), 320–324. http://dx.doi.org/10.1111/j.1471-0528.2001.00066.x.

Petros, P.E., 1998. The pubourethral ligaments-an anatomical and histological study in the live patient. Int. Urogynecol. J. Pelvic Floor Dysfunct. 9 (3), 154–157.

Petros, P.E., Woodman, P.J., 2008. The integral theory of continence. Int. Urogynecol. J. 19, 35–40. http://dx.doi.org/10.1007/s00192-007-0475-9.

Pit, M.J., De Ruiter, M.C., Lycklama A Nijeholt, A.A., Marani, E., Zwartendijk, J., 2003. Anatomy of the arcus tendineus fasciae pelvis in females. Clin. Anat 16 (2), 131–137. http://dx.doi.org/10.1002/ca.10102.

Pregazzi, R., Sartore, A., Bortoli, P., Grimaldi, E., Troiano, L., Guaschino, S., 2002. Perineal ultrasound evaluation of urethral angle and bladder neck mobility in women with stress urinary incontinence. BJOG 109 (7), 821–827. http://dx.doi.org/10.1111/j.1471-0528.2002.01163.x.

Rivaux, G., Rubod, C., Dedet, B., Brieu, M., Gabriel, B., Cosson, M., 2013. Comparative analysis of pelvic ligaments: a biomechanics study. Int. Urogynecol. J. 24 (1), 135–139. http://dx.doi.org/10.1007/s00192-012-1861-5.

Rubod, C., Brieu, M., Cosson, M., Rivaux, G., Clay, J.C., de Landsheere, L., Babriel, B., 2012. Biomechanical properties of human pelvic organs. Urology 79 (4), 968e17–22. http://dx.doi.org/10.1016/j.urology.2011.11.010.

Schaer, G.N., Koechli, O.R., Schuessler, B., Haller, U., 1995. Perineal ultrasound for evaluating the bladder neck in urinary stress incontinence. Obstet. Gynecol. 85 (2), 224–229.

Viereck, V., Nebel, M., Bader, W., Harms, L., Lange, R., Hilger, R., Emons, G., 2006. Role of bladder neck mobility and urethral closure pressure in predicting outcome of tension-free vaginal tape (TVT) procedure. Ultrasound Obstet. Gynecol. 28, 214–220. http://dx.doi.org/10.1002/uog.2834.

Yeoh, O.H., 1993. Some forms of the strain energy functin for rubber. Rubber Chem. Technol. 66, 754–771.

Yip, C., Kwok, E., Sassani, F., Jackson, R., Cundiff, G., 2014. A biomechanical model to assess the contribution of pelvic musculature weakness to the development of stress urinary incontinence. Comput. Methods Biomech. Biomed. Eng. 17 (2), 163–176. http://dx.doi.org/10.1080/10255842.2012.672564.

Original Article

Study V

On the stiffness of the mesh and the urethral mobility: a finite element analysis.

Brandão S, Parente M, Da Roza T, Silva E, Ramos I, Mascarenhas T, Natal Jorge RM.

J Biomeh Eng. 2017 Aug 1;139(8)

doi: 10.1115/1.4036606.

Sofia Brandão[1]
Department of Radiology,
Centro Hospitalar de São João—EPE
(CHSJ-EPE)/Faculty of Medicine,
University of Porto,
Alameda Professor Hernâni Monteiro,
Porto 4200-319, Portugal;
Associated Laboratory for Energy, Transports and
Aeronautics (LAETA),
Institute of Science and Innovation in Mechanical
and Industrial Engineering (INEGI),
Faculty of Engineering,
University of Porto,
Rua Dr. Roberto Frias s/n,
Porto 4200-465, Portugal
e-mail: sofia.brand@gmail.com

Marco Parente
Associated Laboratory for Energy, Transports
and Aeronautics (LAETA),
Institute of Science and Innovation in Mechanical
and Industrial Engineering (INEGI),
Faculty of Engineering,
University of Porto,
Rua Dr. Roberto Frias s/n,
Porto 4200-465, Portugal
e-mail: mparente@fe.up.pt

Thuane Huyer Da Roza
Biomechanics Laboratory,
Center of Health and Sport Sciences, Santa
Catarina State University (CEFID/UDESC),
Rua Paschoal Simone,
358, Bairro dos Coqueiros,
Florianópolis 88080-350, Santa Catarina, Brazil;
Associated Laboratory for Energy, Transports
and Aeronautics (LAETA),
Institute of Science and Innovation in Mechanical
and Industrial Engineering (INEGI),
Faculty of Engineering,
University of Porto,
Rua Dr. Roberto Frias s/n,
Porto 4200-465, Portugal
e-mail: thuaneroza@yahoo.com.br

Elisabete Silva
Associated Laboratory for Energy, Transports
and Aeronautics (LAETA),
Institute of Science and Innovation in Mechanical
and Industrial Engineering (INEGI),
Faculty of Engineering,
University of Porto,
Rua Dr. Roberto Frias s/n,
Porto 4200-465, Portugal
e-mail: silva.elisabete3@gmail.com

Isabel Maria Ramos
Department of Radiology,
CHSJ-EPE/Faculty of Medicine,
University of Porto,
Alameda Professor Hernâni Monteiro,
Porto 4200-319, Portugal
e-mail: radiologia.hsj@gmail.com

On the Stiffness of the Mesh and Urethral Mobility: A Finite Element Analysis

Midurethral slings are used to correct urethral hypermobility in female stress urinary incontinence (SUI), defined as the complaint of involuntary urine leakage when the intra-abdominal pressure (IAP) is increased. Structural and thermal features influence their mechanical properties, which may explain postoperative complications, e.g., erosion and urethral obstruction. We studied the effect of the mesh stiffness on urethral mobility at Valsalva maneuver, under impairment of the supporting structures (levator ani and/or ligaments), by using a numerical model. For that purpose, we modeled a sling with "lower" versus "higher" stiffness and evaluated the mobility of the bladder and urethra, that of the urethrovesical junction (the α-angle), and the force exerted at the fixation of the sling. The effect of impaired levator ani or pubourethral ligaments (PUL) alone on the organs displacement and α-angle opening was similar, showing their important role together on urethral stabilization. When the levator ani and all the ligaments were simulated as impaired, the descent of the bladder and urethra went up to 25.02 mm, that of the bladder neck was 14.57 mm, and the α-angle was 129.7 deg, in the range of what was found in women with SUI. Both meshes allowed returning to normal positioning, although at the cost of higher force exerted by the mesh with higher stiffness (3.4 N against 2.3 N), which can relate to tissue erosion. This finite element analysis allowed mimicking the biomechanical response of the pelvic structures in response to changing a material property of the midurethral synthetic mesh. [DOI: 10.1115/1.4036606]

[1]Corresponding author.
Manuscript received October 28, 2016; final manuscript received April 17, 2017; published online June 7, 2017. Assoc. Editor: Steven D. Abramowitch.

Teresa Mascarenhas
Department of Obstetrics and Gynecology,
CHSJ-EPE/Faculty of Medicine,
University of Porto,
Alameda Professor Hernâni Monteiro,
Porto 4200-319, Portugal
e-mail: tqc@sapo.pt

Renato Manuel Natal Jorge
Associated Laboratory for Energy, Transports
and Aeronautics (LAETA),
Institute of Science and Innovation in Mechanical
and Industrial Engineering (INEGI),
Faculty of Engineering,
University of Porto,
Rua Dr. Roberto Frias s/n,
Porto 4200-465, Portugal
e-mail: rnatal@fe.up.pt

Introduction

Female stress urinary incontinence (SUI) is defined as the involuntary leakage of urine whenever there is an increase in the intra-abdominal pressure (IAP) (e.g., on effort, sneezing or coughing) [1]. Depending on age, the prevalence of female SUI may range from 9% to 72% [2]. About 50% of women with UI report symptoms of SUI [3,4].

SUI may be associated with intrinsic sphincter insufficiency or with bladder neck and urethral hypermobility. Several soft tissue structures provide support to the main structures of the anterior compartment of the female pelvis (bladder and urethra) (Fig. 1(*a*)). Along with the pelvic floor muscles—namely, the *levator ani* (LA) and the paraurethral and vaginal tissues—the pubourethral ligaments (PUL) are important to stabilize the urethra. When the predominant abnormality is urethral hypermobility, it is important to evaluate the position of the vesical neck both at rest and during stress conditions (often cough, abdominal straining, or Valsalva maneuver) [4]. The rise in abdominal pressure implies increase in the pressure over the bladder, and in the case of inefficient bladder suspension, a descent of the bladder neck and urethra may occur. Often SUI is associated with weakness of the pelvic floor muscles, but laxity or defects of both muscles and ligaments supporting the urethra also cause hypermobility and urine leakage [5,6].

Neuromuscular injury due to obstetric trauma and structural degradation of the connective tissue (fascia and ligaments) due to aging or hormonal alterations are known risk factors for SUI [7]. Long-term excessive load to muscles and ligaments, presumably not only during pregnancy [8] but also during vaginal delivery, leads to decrease in muscle force and fibrosis with aging [9]. Difficult or prolonged labor may exceed the stretch limits of these soft tissues. After delivery, substantial remodeling of the connective tissue components occurs. This remodeling is accomplished by an increase in the synthesis of collagen type I (providing tensile strength) and elastin (providing the ability to stretch), and may explain why postpartum SUI symptoms tend to disappear [10]. Aging and hormonal *status* should be considered together. In menopause, the lack of estrogen reduces the collagen type I, increasing tissue laxity [11].

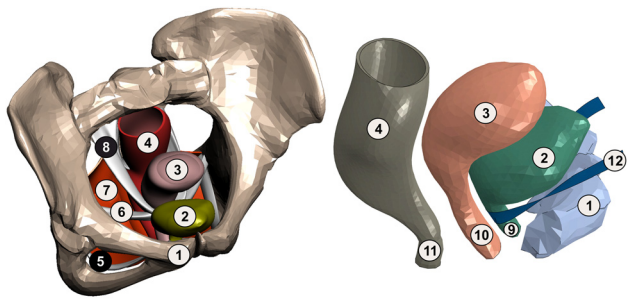

Fig. 1 Anatomical perspective of the pelvis, where (*a*) the pelvic bones, organs, and some of the soft tissue support structures were included in this subject-specific 3D geometrical model, and (*b*) the positioning of the synthetic midurethral sling is seen illustrating a tension-free vaginal tape (TVT) procedure. (1) pubic bone, (2) bladder, (3) uterus, (4) rectum, (5) *arcus tendineous fasciae pelvis*, (6) cardinal ligaments, (7) *levator ani*, (8) uterosacral ligaments, (9) urethra, (10) vagina, (11) anus, and (12) midurethral sling.

Studies have reported that SUI can be successfully managed with lifestyle interventions and pelvic floor muscles training. In those women that do not respond to conservative treatment, incontinence pessaries can be used, and for whom desires or is clinically advised, surgical options are available [12].

Currently, midurethral slings are the most commonly performed surgeries for female SUI [13]. Usually, a small vaginal incision is performed and the sling is placed to provide a ribbon of support under the urethra, in a tension-free manner. The tension-free surgeries may vary by placing the sling arms superior- and anteriorly toward the retropubic space going to the superior rim of the pubic bone, 2 cm either side of the *symphysis pubis* as in the classic tension-free vaginal tape (TVT) procedure (Fig. 1(*b*)) or laterally where it anchors through the obturator *foramina* for a transobturator tape (TOT) approach [14,15]. For the TVT procedure, the sling is placed by using small suprapubic and vaginal incisions [16]. These are considered the gold standard approach [17], with short-term cure rates of 80–90% [4] and long-term cure rates of 81% [18] and 90% [19], for 5- and 10-yr periods, respectively. However, these surgeries carry complications such as voiding dysfunction, urinary retention, infection, and erosion that should not be underestimated [4].

The efficacy of a midurethral sling in restoring continence depends on its biomechanical properties pre- and postimplantation. The synthetic meshes may vary in configuration, material, and manufacturing, and understanding the influence of such properties should ideally be an aspect to account for when choosing the most appropriate mesh and surgical approach. In fact, there is still no agreement in the scientific community regarding which is the most appropriate mesh stiffness [20]. Regarding the sling material, to maximize host tissue acceptance, the mesh must be porous, flexible, and durable. The filament type and structure are important as well. While polypropylene macroporous monofilament meshes have lower complication rates than multifilament meshes, microporous multifilament ones are flexible and less extensive, which makes them easier to adjust [17].

Besides clinical examination, transperineal or translabial ultrasound is quite useful to evaluate the dynamic mobility of the urethra. It can be used to complement clinical diagnosis and also to assess postoperative morphology and functional outcome. For that purpose, the (ab)normal position of the midurethral slings and its movement during stressful maneuvers [21,22]—when they are best seen to rotate around the fulcrum of the pubic bone at the anterior vaginal wall—is assessed. Performing static and dynamic ultrasound is cheap, safe, and easy to perform with patient compliance. The dynamic mobility of the urethra and the bladder neck from rest to Valsalva maneuver must be quantified, and one of the metrics to evaluate it is the α-angle (see Figs. 2(*a*) and 2(*b*)) [23–27]. The α-angle is defined as the angle between the bladder neck and the *symphysis pubis*, and the midline axis of the *symphysis pubis,* as described elsewhere [23,24].

Computational analysis may be an additional tool for understanding the success or failure of the surgery. Recent biomechanical modeling of a single-incision mini-sling showed that the sling placed in the mid-distal urethra may provide sufficient correction with reduced sling-urethra interaction force that may induce urinary retention and pain [28]. Besides its position, experimental mechanical tests evidenced that meshes with different structural and thermal features can exhibit distinct mechanical properties [29–31], namely, their stiffness. In fact, a mesh with excessive stiffness or excessive sling tension and stretching may be partially responsible for the occurrence of postoperative voiding dysfunction [20,32,33].

In this sense, it would be interesting to relate the impairment of supportive structure(s)—the LA and/or pelvic ligaments representative of the three compartments—with urethral mobility, and their repositioning and force exerted according to the stiffness of the mesh. For that purpose, we used a numerical model and simulation of Valsalva maneuver. The displacement magnitude of the bladder and urethra and bladder neck, and also the α-angle were compared between different conditions of muscle and/or ligament impairment, with a "higher stiffness" mesh (Mesh_{HS}) versus "lower stiffness" mesh (Mesh_{LS}). Our first hypothesis is that, during stress, the displacement magnitude and the α-angle will be higher when the LA muscle and PUL are both considered impaired than when their impairment is considered separately. We also expect that applying a sling with a Mesh_{HS} will decrease the displacement and the α-angle, more than a sling with Mesh_{LS} (second hypothesis). Finally, the force exerted in the extremities of the sling was compared to test if using a more flexible sling (Mesh_{LS}) will exert less force (third hypothesis).

Materials and Methods

Computational Model. The institutional review board approved this work (protocol: CES195/12). The magnetic resonance (MR)-based computational model of a nulliparous 24-yr-old young healthy female was the same as in previous publication from Brandão et al. [34]. Figures 3(*a*) and 3(*b*) show the finite element model, which included the pubic bone, the pelvic organs, the LA muscle, and other supporting structures. Further details are available in Ref. [34].

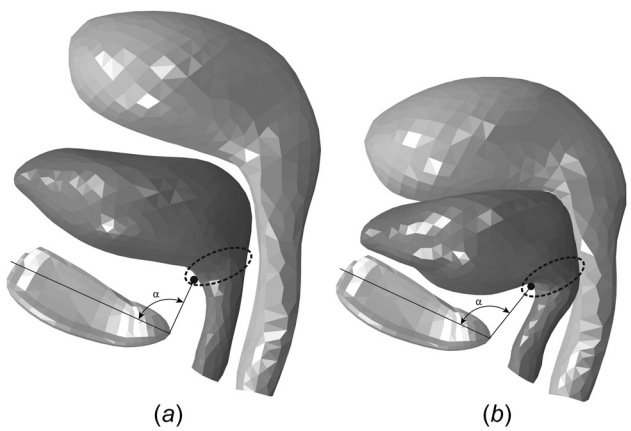

Fig. 2 Evaluation of the α-angle performed (*a*) at rest and (*b*) for Valsalva maneuver

The geometric dimensions of the synthetic implant were based on existing specifications [35–38]. The sling was modeled as a 150 mm × 10 mm polypropylene monofilament strip. Its geometry was then discretized into a finite element mesh with 1600 four nodes membrane M3D4 elements. The mesh refinement used for the synthetic implant was tested [39], and no differences were found in the force–displacement curves.

Figures 3(*c*) and 3(*d*) illustrate the finite element model of the sling placed the same way as in the surgery, that is, transvaginally from the midurethra to the pubic bone. The sling was defined as a tape lying flat against the posterior surface of the midurethra, below the bladder neck, going to the superior rim of the pubic bone, 2 cm either side of the *symphysis pubis*. The nodes corresponding to the fixation between the sling ends and the pubic bone at each side were fixed (see Fig. 3(*c*)). A tied interaction between the mesh and the urethra anteriorly was established. The interaction between the mesh and the vagina, posteriorly, was modeled as frictionless and established using the default Abaqus® contact pressure-overclosure algorithm.

The mechanical behavior of the midurethral sling was modeled assuming an hyperelastic behavior, described by the Veronda constitutive model [40]. This model assumes an isotropic behavior, and therefore the corresponding strain energy function can be expressed as a function of the left Cauchy–Green strain tensor invariants.

The meshes applied in the surgery for SUI are predominantly subjected to traction loads. Furthermore, for this kind of synthetic implants, it is possible to obtain a mesh with a constant orientation of its high stiffness direction along its length. That is the way they are applied, with the high stiffness direction aligned with its length. Using the present Veronda isotropic constitutive model allows characterizing the mechanical behavior of the mesh along its main loading axis, and therefore in our option this model is acceptable for representing the forces to which the current implant is subjected to.

When the material is fully incompressible, the strain energy is a function of the first two invariants. The strain potential proposed by Veronda and Westman [40] is of the following form:

$$U = c_1\{\exp[\beta(I_1 - 3)] - 1\} + c_2(I_2 - 3) + g(J) \tag{1}$$

where c_1, c_2, and β are constants that define the mechanical behavior of the material, and I_1 and I_2 are the first and second invariants of the left Cauchy–Green strain tensor $\mathbf{B}$, defined as follows:

$$\mathbf{B} = \mathbf{F}\mathbf{F}^{\mathrm{T}} \tag{2}$$

where

$$I_1 = \text{trace}\,\mathbf{B} \tag{3}$$

and

$$I_2 = \frac{1}{2}\left(I_1^2 - \text{trace}\,\mathbf{B}^2\right) \tag{4}$$

$\mathbf{F}$ is the deformation gradient tensor, and Eq. (5) describes the volume change

$$J = \det \mathbf{F} \tag{5}$$

If the material is incompressible, then the function g in Eq. (1) becomes zero, i.e., $g(1) = 0$.

The Veronda hyperelastic material was used in the Abaqus® software v.2016 (Dassault Systemes Simulia Corp., Providence, RI) using a UHYPER user subroutine. In this subroutine, the deformation gradient with the volume change eliminated $\bar{\mathbf{F}}$ must be used, and it is thus defined by

$$\bar{\mathbf{F}} = J^{-\frac{1}{3}}\mathbf{F} \tag{6}$$

The modified left Cauchy–Green strain tensor $\bar{\mathbf{B}}$ can then be modified in Eq. (2) and described by the following equation:

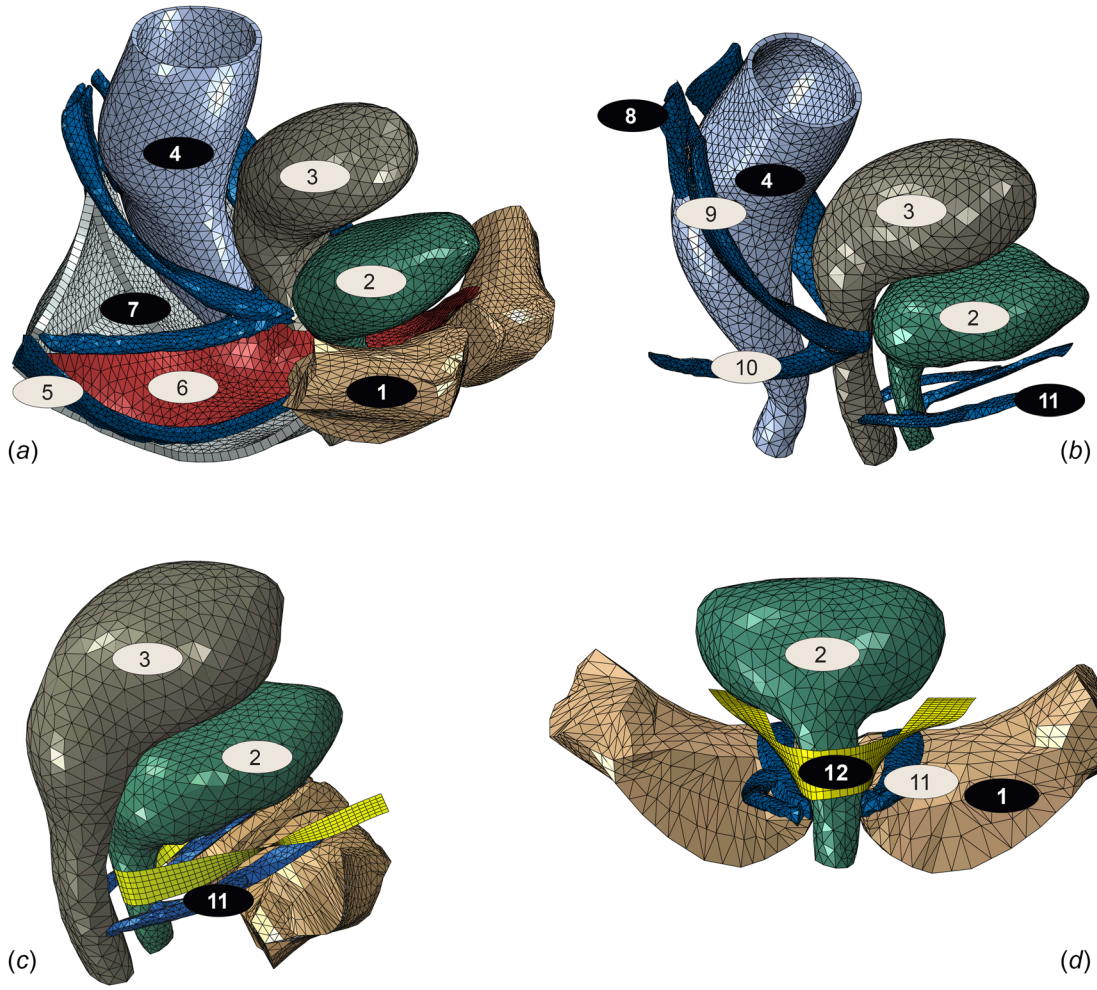

Fig. 3 Finite element model of the pelvis. The pubic bone, the pelvic organs, and the supporting structures (muscles, ligaments, and fascia) were included to achieve a realistic model of the pelvic cavity. In (*c*) and (*d*), the position of the sling just above the native pubourethral ligaments is shown. (1) pubic bone, (2) bladder, (3) uterus, (4) rectum, (5) *arcus tendineous fasciae pelvis*, (6) pelvic fascia, (7) *levator ani*, (8) lateral ligaments of the rectum, (9) uterosacral ligaments, (10) cardinal ligaments, (11) pubourethral ligaments (vaginal and urethral portions), and (12) midurethral sling.

$$\bar{\mathbf{B}} = \bar{\mathbf{F}}\bar{\mathbf{F}}^{\mathrm{T}} \tag{7}$$

In the Abaqus® UHYPER subroutine, the first and second derivatives of the strain energy function U with respect to $\bar{I}_1$ and $\bar{I}_2$ and J must be defined. The first and second invariants of the modified left Cauchy–Green strain tensor $\bar{\mathbf{B}}$, $\bar{I}_1$ and $\bar{I}_2$ are thus defined as

$$\bar{I}_1 = \mathrm{trace}\,\bar{\mathbf{B}} \tag{8}$$

and

$$\bar{I}_2 = \frac{1}{2}\left(\bar{I}_1^2 - \mathrm{trace}\,\bar{\mathbf{B}}^2\right) \tag{9}$$

Assuming the incompressibility condition $J = 1$ and $\mathbf{B} = \bar{\mathbf{B}}$, the following derivatives were implemented on the user subroutine:

$$\frac{\partial U}{\partial \bar{I}_1} = c_1\beta\,\exp\left[\beta(\bar{I}_1 - 3)\right] \tag{10}$$

$$\frac{\partial U}{\partial \bar{I}_2} = c_2 \tag{11}$$

$$\frac{\partial^2 U}{\partial \bar{I}_1^2} = c_1\beta^2\exp\left[\beta(\bar{I}_1 - 3)\right] \tag{12}$$

and all the other partial derivatives of U that are needed were set equal to zero, as referred in the Abaqus® user's manual.

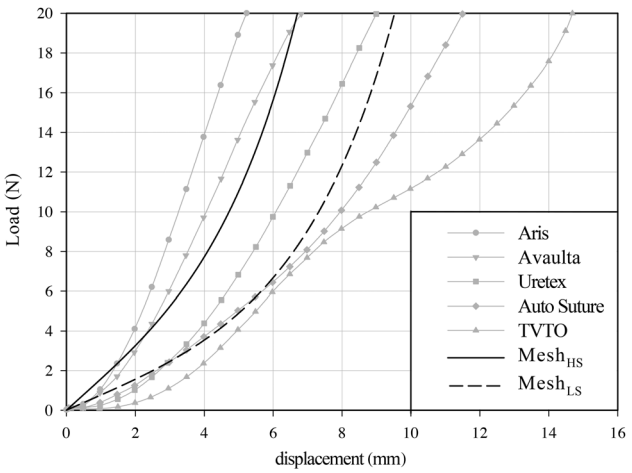

Fig. 4 Experimental curves of the five meshes obtained through load–displacement uniaxial tests (data from the work of Afonso et al. [30]), compared with the numerical ones of the two midurethral slings: Mesh$_{HS}$ (black straight curve) and Mesh$_{LS}$ (black dashed curve)

Table 1 Values of the range of displacement magnitude of the bladder and urethra, the maximum displacement magnitude of the bladder neck, α-angle, and force, for Valsalva maneuver (4.0 kPa)

Simulation of VM		[Min–max] bladder and urethra displacement magnitude (mm)	Max. bladder neck displacement magnitude (mm)	α-angle (deg)	Force (N)
Heathy	rest	—		91.8	—
	VM	[0.85–19.61]	6.93	105.7	—
Impairment, no sling	LA	[0.81–19.64]	7.82	112.5	—
	PUL	[0.78–20.25]	8.02	115.0	—
	LA + PUL	[0.93–23.30]	12.07	124.1	—
	all	[2.06–25.02]	14.57	129.7	—
Impairment, $Mesh_{HS}$	LA	[1.10–17.71]	5.95	103.8	2.5
	PUL	[1.01–17.70]	5.98	104.0	2.8
	LA + PUL	[0.94–17.60]	6.86	104.6	3.0
	All	[2.66–18.63]	7.61	105.7	3.4
Impairment, $Mesh_{LS}$	LA	[1.00–18.20]	6.69	105.1	1.6
	PUL	[0.94–18.20]	6.99	107.5	1.9
	LA + PUL	[0.81–18.16]	7.67	108.2	2.1
	all	[2.47–19.19]	8.94	109.9	2.3

Note: LA = *levator ani*; $Mesh_{HS}$ = mesh with higher stiffness; $Mesh_{LS}$ = mesh with lower stiffness; PUL = pubourethral ligaments; VM = Valsalva maneuver; and "all" includes the LA, the PUL, the uterosacral and the cardinal ligaments, and the lateral ligaments of the rectum.

Figure 4 shows a set of experimental curves of uniaxial load–displacement data from the work of Afonso et al. [30] (gray lines). In order to obtain the material constants for the two slings ($Mesh_{HS}$ and $Mesh_{LS}$), the tensile test was numerically modeled using the finite element method, according to the experimental setup. A manual optimization procedure was used to set the material parameters to achieve two distinct mesh mechanical behaviors (higher and lower stiffness). The numerical curves for those $Mesh_{HS}$ and $Mesh_{LS}$ (straight and dashed black lines, respectively) are compared with the experimental curves of the five meshes tested by Afonso et al. [30]. The material constants used were: $c_1 = 0.10$ MPa, $c_2 = 0.0137$ MPa, $\beta = 10.0$ and $c_1 = 0.06$ MPa, $c_2 = 0.0137$ MPa, $\beta = 8.0$ for $Mesh_{HS}$ and $Mesh_{LS}$, respectively. A thickness of 1 mm was assumed for the membrane M3D4 finite elements.

Simulation of Structural Impairment of the LA and Pelvic Ligaments. Reducing material stiffness was performed to simulate the structural impairment of the LA and pelvic ligaments due to changes in their elasticity. In this work, this was attained by multiplying the stress values from the stress–strain curves of healthy LA and ligaments obtained from experimental tension tests [41,42] by a 0.05 coefficient, following the same methodology as in Ref. [34].

Simulation of Valsalva Maneuver. Numerical simulation of Valsalva maneuver was performed for progressive increase in IAP up to 4 kPa, which was estimated as corresponding to the average value of IAP for Valsalva maneuver in supine position by Noakes et al. [43].

Analysis of the Mobility of the Urethra. To evaluate the effect of the mesh stiffness on the dynamic mobility of the urethra in maximal Valsalva maneuver, several evaluations were performed, starting from healthy *status* of the support structures. The analysis was carried out for different conditions in the numerical simulations, describing the experimental variables: impairment of muscles and/or ligaments (in distinct combinations), and the absence/presence of each midurethral sling with distinct material constants ($Mesh_{HS}$ and $Mesh_{LS}$), as described before. Due to their role on providing support to the proximal urethra and bladder neck [44,45], the PUL and the LA were evaluated here in detail. We simulated the impairment of the LA, PUL, LA + PUL, and finally the LA along with all the pelvic ligaments (PUL, uterosacral and cardinal ligaments, and the lateral ligaments of the rectum) (summarized in Table 1). The measurements (dependent variables) were the following: first, the α-angle (see Figs. 2(*a*) and 2(*b*)); second, the displacement magnitude values [min–max] from the nodal displacements of the bladder and urethra; and

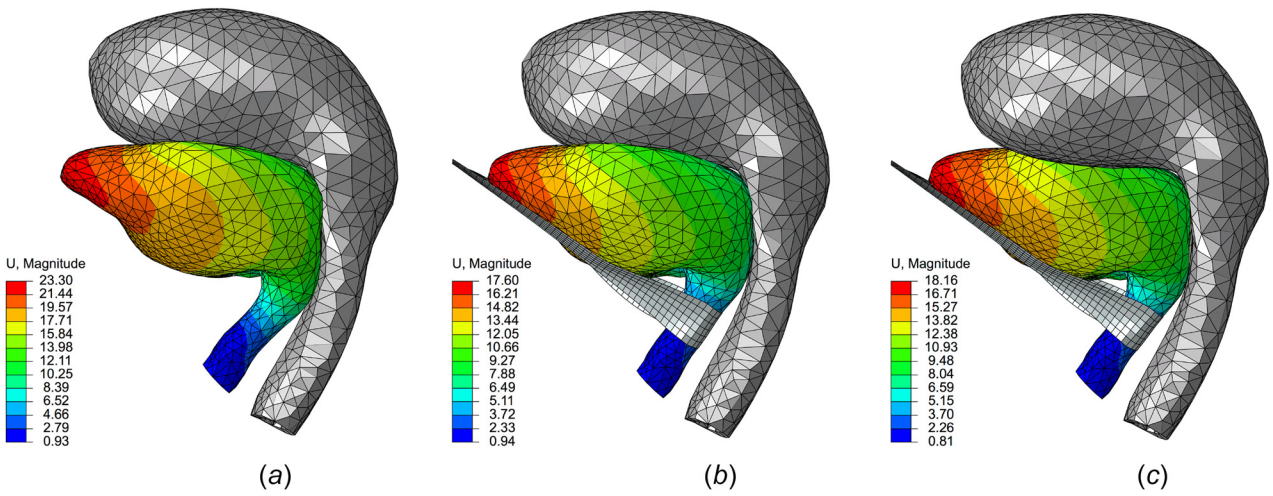

Fig. 5 Displacement magnitude after simulation of Valsalva maneuver and in the presence of combined impairment of the *levator ani* and the pubourethral ligaments, (*a*) without including the sling, (*b*) with the $Mesh_{HS}$, and (*c*) with $Mesh_{LS}$

third, the maximum values of the displacement magnitude of the bladder neck. For the latter, seven nodes distributed around the bladder neck (dashed lines in Figs. 2(*a*) and 2(*b*)) were selected, and the mean value was computed. Finally, the force exerted in the extremities of the sling on the pubic bone, from rest until maximal Valsalva maneuver. These dependent scalar variables were measured for all the simulations performed, and descriptive statistics analysis was performed (Table 1).

Results

Results of the computational analysis showed that the increase in IAP during the Valsalva maneuver affects the mobility of the bladder and the position of the urethra (see Table 1).

Figure 5 shows the displacement magnitude after simulation of Valsalva maneuver and in the presence of combined impairment of the LA and the PUL, (*a*) without including the sling, (*b*) with the $Mesh_{HS}$, and (*c*) with $Mesh_{LS}$.

Figure 6 illustrates the force exerted in the extremities of the slings from rest until maximal Valsalva maneuver. The graphs show similar behavior along the increase in IAP for both $Mesh_{HS}$ (*b*) and $Mesh_{LS}$, with slightly lower values for the latter. The force measured when the LA ("muscles") is impaired is the lowest, followed by that from impairment of the PUL. The highest values are found when all the supporting structures are simulated as impaired, with superior values for the $Mesh_{HS}$ when compared to the $Mesh_{LS}$ (3.4 N versus 2.3 N, respectively), confirming our third hypothesis.

Discussion

Increases in IAP, e.g., during coughing, sneezing or sports practice exert downward forces acting on the pelvic organs, and the pubourethral ligaments and the pubovisceral portion of the LA have an important role on resisting those forces [46]. In case of muscle weakness and decrease in the elasticity of the connective tissue of the ligaments, distortion and abnormal elongation contribute for abnormal urethral positioning [44,46], we may be faced with the pathogenesis of SUI. The results of the present study showed similar influence of isolated impairment of the PUL or the LA on the displacement magnitude of the bladder and urethra, of the bladder neck, and on the α-angle, with slightly higher values for the impairment of the PUL. When their impairment is combined, the α-angle increased almost 20 deg at Valsalva maneuver (from 105.7 deg to 124.1 deg) when compared to simulation of healthy supporters, which is more than when the two structures are considered separately, confirming our first hypothesis. This reflects their role together on avoiding excessive descent and malpositioning, which the present model was able to reproduce.

When representative ligaments of the three pelvic compartments and the LA are considered as impaired, the α-angle goes up to 129.7 deg. Yet, this 5 deg increase in the α-angle, 1.2 mm in the maximum value of the displacement magnitude of the bladder and urethra, and 2.5 mm in the maximum displacement magnitude of the bladder neck seem to reflect a minor effect on those measurements, which is in line with the results of a previous paper of our group where the impairment of the PUL had the most evident effect on opening the α-angle and on the bladder neck dislocation [34]. Nevertheless, the point to retain here is that wider α-angles in ultrasound have shown to illustrate the severity of poor external anatomical support, allowing abnormal mobility of the urethra and bladder neck [25,26].

We applied the same coordinate system in the numerical model as in the ultrasound examinations [23,24], as described previously in the text. The values obtained in the present work were in the range of what was found by Pregazzi et al. [23] and Yang and Huang [27] using the same method, for asymptomatic women at rest and at Valsalva maneuver (92 ± 6 deg and 100 ± 8 deg; 81 ± 15 deg and 113 ± 27 deg), as well as for women with SUI at Valsalva maneuver (120 ± 8 deg and 152 ± 34 deg, respectively). These results along with higher displacement magnitude of the bladder, urethra, and bladder neck seem to point to an adequate reproduction by the present numerical model of the increased mobility of these structures due to lack of support.

TVT midurethral slings are used to reconstitute the defective urethral support by the pubourethral ligaments [47,48], yet without inducing mechanical stress or shrinkage due to its "tension-free" nature [49]. However, some of the rare complications associated to this procedure (retropubic hematoma or vesical or urethral erosion or perforation) [50,51]—while there seems to be a higher risk of vaginal erosion and groin abscesses with the TOT [52]—may in fact be associated with a gain in stiffness with time due to the ingrowth of fibrous tissue [51] when compared to that at the time of implantation, and this could be the scope for future computational analysis. As recently modeled by Peng et al., correct position is a key issue, and the mid-distal region seems to provide lower sling-urethra interaction force with sufficient correction [28].

By surgically replacing the action of the ligaments, the supportive function can be at least partially restored, even when muscles themselves are damaged and weakened [6]. This was shown by the present model, since placing a sling, whether the $Mesh_{HS}$ or $Mesh_{LS}$, brought the α-angle back to a value accepted for asymptomatic women, even when the LA was simulated as impaired

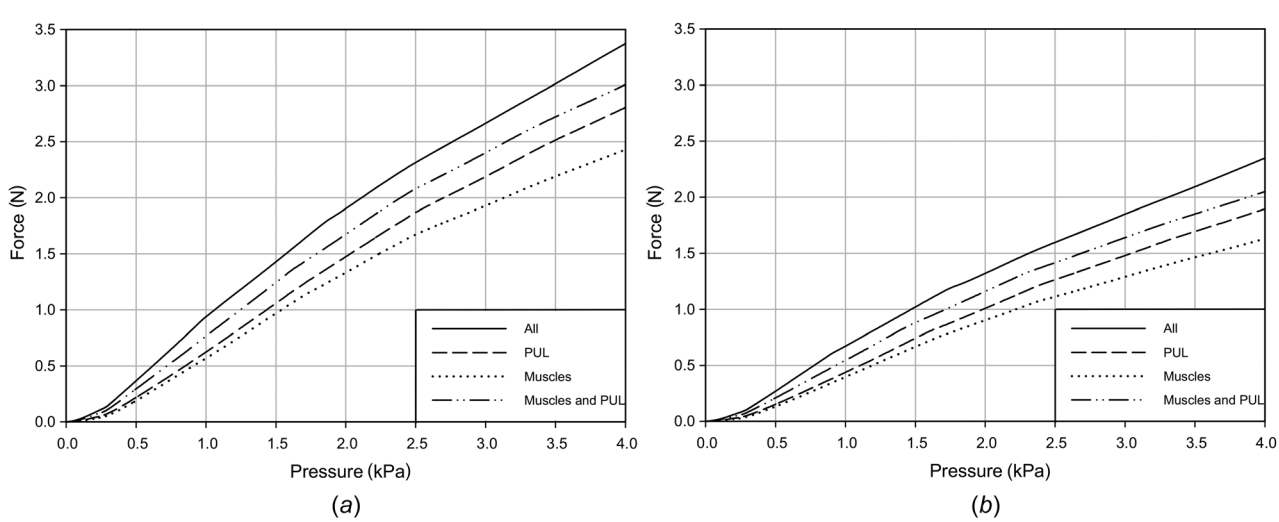

Fig. 6 Graphs of force exerted in the extremities of the sling for the (*a*) $Mesh_{HS}$ and (*b*) $Mesh_{LS}$, for progressive increase in intra-abdominal pressure from rest to Valsalva maneuver

[23,27]. The angles obtained for the $Mesh_{HS}$ were lower, confirming our second hypothesis. The same was seen for the measurements of the range of displacement magnitude of the bladder and urethra, and the maximum displacement magnitude of the bladder neck.

The type of mesh used for the midurethral slings may impact treatment outcomes and complications [32,53,54]. Stiffness may be changed by altering mesh geometry, thickness of the weave, manufacturing, or by using different materials. In the present study, both $Mesh_{HS}$ versus $Mesh_{LS}$ reduced the displacement magnitude of the bladder, urethra, and bladder neck to values that mirror a rebalancing in bladder neck and urethral mobility. Brandt et al. [55] found the horizontal and vertical displacement of the urethrovesical junction to decrease after surgery. Despite not having the same reference axis, still, these measurements (before surgery: horizontal 6.9 ± 4.5 mm and vertical 17.2 ± 5 mm; after surgery: horizontal 0.3 ± 3.4 mm and vertical 5.2 ± 2.4 mm) are in the range of the maximum displacement magnitude obtained for the bladder neck in the numerical simulations.

The impairment of the PUL also seems to imply somewhat higher impact than the one of the LA alone, since it reduces urethral mobility yet at the cost of higher force (1.9 N versus 1.6 N for $Mesh_{HS}$ and 2.8 N versus 2.5 N for the $Mesh_{LS}$, respectively). This can be related to the local loss of urethral support of the PUL, which is compensated by the sling working as an artificial neoligament that carries full load at Valsalva maneuver. The values presented for impairment of the LA are slightly higher than the ones presented by Peng et al. [28] for the same condition, but they may be related to different methodological options on the simulation approach, the fact that they are using a different (mini)-sling, with a distinct fixation procedure, and also on the way to apply the IAP.

Excessive force exerted by the sling on the urethra during cough or straining, especially in overtightened or very stiff slings may be the cause of tissue erosion. Although the stresses will vary along the mesh, since they will be higher in the extremities of the sling on the pubic bone where the boundary conditions mimic the sling fixation (as pointed out in Ref. [56]), the values of force will be similar to the one exerted in the urethra by the sling. Force was around 1 N greater for the $Mesh_{HS}$ for all the simulations performed, as its resistance to deformation at Valsalva maneuver is greater. Despite this small difference, one should not forget that this greater force will be exerted in the native tissue of the urethra in the long-term and at cyclical loading, during sudden increases in IAP in the daily-life, which may even exceed the value of IAP used to simulate Valsalva maneuver. For instance, when women practice some physical activities, the vaginal pressure can reach more than 6.8 kPa when running and around 9.8 kPa when jumping [57].

Our results also show that, when the other ligamentous structures start to fail, e.g., due to aging, the urethra will be then subjected to values of force up to 3.4 N as shown in one of the simulations.

More flexible slings adapt to the urethral surrounding soft tissues better than stiffer slings and reduce the rate of erosions or obstruction due to lower force against the urethra and bladder, which seems to favor their use [20]. Nevertheless, they are not free from drawbacks, such as mesh elongation and thinning when tensioned, and these are some of the pros and cons of having different mechanical properties that change the biomechanical behavior of the slings [20,30,31] and, ultimately, patient outcome. Indeed, to date, experimental research has been performed to compare the biomechanical properties and behavior of different slings, with results showing variation for both stiffness and peak load [20,29–31]. Studies comparing long-term complication rates between higher stiffness versus lower stiffness polypropylene meshes are of outmost importance.

The mechanical properties of the synthetic implants influence biomechanical biocompatibility [58]. The question remains whether something stronger than the native tissue is desired. Ideally, they should have similar biomechanical properties as the native surrounding tissues, and this biomechanical similarity should be optimized. Despite being made from the same material, commercially available synthetic meshes demonstrate variations in their textile properties or structural properties (e.g., pore geometry or stiffness), with impact on the biomechanical behavior and acceptance of the native adjacent soft tissues that support it [59]. The midurethral sling should be stiff enough to restore normal anatomy and positioning of the urethra, but when it is too stiff can lead to a phenomenon referred to as stress shielding. Due to this discrepancy in stiffness between adjacent materials, an inefficient remodeling response may occur. Animal studies showed that a stiffer prolapse mesh had the worst impact in the structural properties of the surrounding tissues [59–61].

The study presents some limitations that have to be addressed. First, this is a subject-specific model of a 24-yr-old and nulliparous female, which may not be fully representative of the anatomical features of many women with SUI. Most of them are related with age and parity. The prevalence of SUI in nulliparous women is lower than parous ones; parity is an important risk factor for SUI in young women [62]. Due to long-term excessive load during pregnancy [8] and vaginal childbirth, the female pelvic floor may suffer relaxation or mechanical injury. Denervation and defective remodeling can cause the base of the bladder and the bladder neck to progressively fall, and increase urethral mobility [63]. Furthermore, the connective tissue remodeled after childbirth is not often as strong as the original tissue that it replaces and is associated with fibrosis with aging [9]. In this sense, some differences can be expected from the morphology of the present model and a model of women suffering from SUI, in line with findings of ultrasound studies, such as: shorter urethra, increased pubovaginal distance, and lower positioning of the bladder neck even at rest [64]; wider *urogenital hiatus* (related with loss of muscular support) [65]; and higher *symphysis pubis*-to-urethra distance but decreased *symphysis pubis*-to-bladder neck distance, due to malpositioning of the bladder neck [66].

Second, anatomical simplifications were assumed. Only the PUL were considered in this model as representing urethral support due to the level of evidence of its association with SUI and urethral mobility [44]. Also, the LA was modeled as a single-thickness structure, which does not reflect the thicker puborectal portion that is a main contributor for the closure of the *levator hiatus* and elevation of the urethrovesical neck. However, care was taken to include the fascial tissue that helps to stabilize urethra and the bladder neck. Second, the value of IAP used to simulate Valsalva maneuver [43] corresponds to supine position to match the MR acquisition conditions, which does not entirely reflect normal daily-life situations, such as coughing, exercising, or defecating.

Despite these limitations, this finite element analysis approach has the potential for application to patient-specific conditions, when the length of the urethra or the anatomy of the vesical neck may be issues, requiring comparative analysis of different slings. Adjusting the mechanical properties of the mesh material in the numerical models is certainly challenging, as the mechanical properties and constitutive models to apply to these pelvic soft tissues and surgical synthetic materials are not fully studied or validated yet. In the present work, our option was to apply the Veronda isotropic constitutive model to characterize the mechanical behavior of the mesh, which is predominantly subjected to traction loads in its main loading axis, and we believe that this is adequate. If we were to simulate a synthetic mesh for correction of organ prolapse, were the loads are biaxial, an anisotropic model would perhaps be more adequate to represent its mechanical behavior, since the material presents preferred stiffness orientations.

Future work in this field, along with clinical studies, will sustain the manufacturer's options and surgeon's choices in the clinical setting.

Acknowledgment

The authors acknowledge the funding of the Research Project No. UID/EMS/50022/2013, from Fundação da Ciência e

Tecnologia, Portugal, and Project No. NORTE-01-0145-FEDER-000022—SciTech—Science and Technology for Competitive and Sustainable Industries, co-financed by Programa Operacional Regional do Norte (NORTE2020), through Fundo Europeu de Desenvolvimento Regional (FEDER).

Nomenclature

HS = higher stiffness
IAP = intra-abdominal pressure
kPa = kilopascal
LS = lower stiffness
mm = millimeter
MR = magnetic resonance
PUL = pubourethral ligaments
SUI = stress urinary incontinence
TOT = transobturator tape
TVT = transvaginal tape
VM = Valsalva maneuver

References

[1] Hayden, B. T., de Ridder, D., Freeman, R. M., Swift, S. E., Berghmans, B., Lee, J., Monga, A., Petri, E., Rizk, D. E., Sand, P. K., and Schaer, G. N., 2010, "An International Urogynecological Association (IUGA)/International Continence Society (ICS) Joint Report on the Terminology for Female Pelvic Floor Dysfunction," Int. Urogynecol. J., **21**(1), pp. 5–26.

[2] Hunskaar, S., Burgio, K., Diokno, A., Herzog, A. R., Hjälmås, K., and Lapitan, M. C., 2003, "Epidemiology and Natural History of Urinary Incontinence in Women," Urology, **62**(4 Suppl. 1), pp. 16–23.

[3] Reynolds, W. S., Dmochowski, R. R., and Penson, D. F., 2011, "Epidemiology of Stress Urinary Incontinence in Women," Curr. Urol. Rep., **12**(5), pp. 370–376.

[4] Harding, C. K., and Thorpe, A. C., 2010, "The Surgical Treatment of Female Stress Urinary Incontinence," Indian J. Urol., **26**(2), pp. 257–262.

[5] Macura, K. J., Genadry, R. R., and Bluemke, D. A., 2006, "MR Imaging of the Female Urethra and Supporting Ligaments in Assessment of Urinary Incontinence: Spectrum of Abnormalities," RadioGraphics, **26**(4), pp. 1135–1149.

[6] Tasali, N., Cubuk, R., Sinanoğlu, O., Sahin, K., and Saydam, B., 2012, "MRI in Stress Urinary Incontinence. Endovaginal MRI With an Intracavitary Coil and Dynamic Pelvic MRI," Urol. J., **9**(**1**), pp. 397–404.

[7] Luber, K. M., 2004, "The Definition, Prevalence, and Risk Factors for Stress Urinary Incontinence," Rev. Urol., **6**(Suppl. 3), pp. S3–S9.

[8] MacLennan, A. H., Taylor, A. W., Wilson, D. H., and Wilson, D., 2000, "The Prevalence of Pelvic Floor Disorders and Their Relationship to Gender, Age, Parity and Mode of Delivery," BJOG, **107**(12), pp. 1460–1470.

[9] Alperin, M., Cook, M., Tuttle, L. J., Esparza, M. C., and Lieber, R. L., 2016, "Impact of Vaginal Parity and Aging on the Architectural Design of Pelvic Floor Muscles," Am. J. Obstet. Gynecol., **215**(3), pp. 312.e1–312.e9.

[10] Thom, D. H., and Rortveit, G., 2010, "Prevalence of Postpartum Urinary Incontinence: A Systematic Review," Acta Obstet. Gynecol., **89**(12), pp. 1511–1522.

[11] Trabucco, E., Soderberg, M., Cobellis, L., Torella, M., Bystrom, B., Ekman-Ordeberg, G., Petraglia, F., and Colacurci, N., 2007, "Role of Proteoglycans in the Organization of Periurethral Connective Tissue in Women With Stress Urinary Incontinence," Maturitas, **58**(4), pp. 395–405.

[12] Wood, L. N., and Anger, J. T., 2014, "Urinary Incontinence in Women," BMJ, **349**, p. g4531.

[13] Kirby, A. C., Tan-Kim, J., and Nager, C. W., 2015, "Midurethral Slings: Which Should I Choose and What is the Evidence for Use?," Curr. Opin. Obstet. Gynecol., **27**(5), pp. 359–365.

[14] Zyczkowski, M., Nowakowski, K., Kuczmik, W., Urbanek, T., Kaletka, Z., Bryniarski, P., Muskala, B., and Paradysz, A., 2014, "Tension-Free Vaginal Tape, Transobturator Tape, and Own Modification of Transobturator Tape in the Treatment of Female Stress Urinary Incontinence: Comparative Analysis," BioMed Res. Int., **2014**, p. 347856.

[15] Moldovan, C. P., Marinone, M. E., and Staack, A., 2015, "Transvaginal Retropubic Sling Systems: Efficacy and Patient Acceptability," Int. J. Womens Health., **7**, pp. 227–237.

[16] Harding, C. K., and Thorpe, A. C., 2008, "Surgical Treatment for Stress Urinary Incontinence," Int. J. Urol., **15**(1), pp. 27–34.

[17] Costantini, E., Lazzeri, M., and Porena, M., 2007, "Managing Complications After Midurethral Sling for Stress Urinary Incontinence," EAU-EBU Update Ser., **5**(6), pp. 232–240.

[18] Ward, K. L., Hilton, P., UK, and Ireland TVT Trial Group, 2008, "Tension-Free Vaginal Tape Versus Colposuspension for Primary Urodynamic Stress Incontinence: 5-Year Follow-Up," Br. J. Obstet. Gynecol., **115**(2), pp. 226–233.

[19] Nilsson, C. G., Palva, K., Rezapour, M., and Falconer, C., 2008, "Eleven Years Prospective Follow-up of the Tension-Free Vaginal Tape Procedure for Treatment of Stress Urinary Incontinence," Int. Urogynecol. J. Pelvic Floor Dysfunct., **19**(8), pp. 1043–1047.

[20] Moalli, P. A., Papas, N., Menefee, S., Albo, M., Meyn, L., and Abramowitch, S. D., 2008, "Tensile Properties of Five Commonly Used Midurethral Slings Relative to the TVT," Int. Urogynecol. J. Pelvic Floor Dysfunct., **19**(5), pp. 655–663.

[21] Dietz, H. P., Barry, C., Lim, Y. N., and Rane, A., 2005, "Two-Dimensional and Three-Dimensional Ultrasound Imaging of Suburethral Slings," Ultrasound Obstet. Gynecol., **26**(2), pp. 175–179.

[22] Sarlos, D., Kuronen, M., and Schaer, G. N., 2003, "How Does Tension-Free Vaginal Tape Correct Stress Incontinence? Investigation by Perineal Ultrasound," Int. Urogynecol. J. Pelvic Floor Dysfunct., **14**(6), pp. 395–398.

[23] Pregazzi, R., Sartore, A., Bortoli, P., Grimaldi, E., Troiano, L., and Guaschino, S., 2002, "Perineal Ultrasound Evaluation of Urethral Angle and Bladder Neck Mobility in Women With Stress Urinary Incontinence," BJOG, **109**(7), pp. 821–827.

[24] Schaer, G. N., Koechli, O. R., Schuessler, B., and Haller, U., 1995, "Perineal Ultrasound for Evaluating the Bladder Neck in Urinary Stress Incontinence," Obstet. Gynecol., **85**(2), pp. 220–224.

[25] Huang, W. C., and Yang, J. M., 2003, "Bladder Neck Funneling on Ultrasound Cystourethrography in Primary Stress Urinary Incontinence: A Sign Associated With Urethral Hypermobility and Intrinsic Sphincter Deficiency," Urology, **61**(5), pp. 936–941.

[26] Akram, W., 2010, "Correlation Between Genuine Stress Incontinence in Women and Bladder Neck Mobility as Assessed by Inter Labial Ultrasound Scan," Iraqi J. Comm. Med., **23**(3), pp. 169–172.

[27] Yang, J. M., and Huang, W. C., 2002, "Discrimination of Bladder Disorders in Female Lower Urinary Tract Symptoms on Ultrasonographic Cystourethrography," J. Ultrasound Med., **21**(11), pp. 1249–1255.

[28] Peng, Y., Khavari, R., Nakib, N. A., Stewart, J. N., Boone, T. B., and Zhang, Y., 2015, "The Single-Incision Sling to Treat Female Stress Urinary Incontinence: A Dynamic Computational Study of Outcomes and Risk Factors," ASME J. Biomech. Eng., **137**(9), p. 091007.

[29] Dietz, H. P., Vancaillie, P., Svehla, M., Walsh, W., Steensma, A. B., and Vancaillie, T. G., 2003, "Mechanical Properties of Urogynecologic Implant Materials," Int. Urogynecol. J. Pelvic Floor Dysfunct., **14**(4), pp. 239–243.

[30] Afonso, J. S., Martins, P. A., Girao, M. J., Natal Jorge, R. M., Ferreira, A. J., Mascarenhas, T., Fernandes, A. A., Bernardes, J., Baracat, E. C., Rodrigues de Lima, G., and Patricio, B., 2008, "Mechanical Properties of Polypropylene Mesh Used in Pelvic Floor Repair," Int. Urogynecol. J. Pelvic Floor Dysfunct., **19**(3), pp. 375–380.

[31] Afonso, J. S., Jorge, R. M., Martins, P. S., Soldi Mda, S., Alves, O. L., Patricio, B., Mascarenhas, T., Sartori, M. G., and Girao, M. J., 2009, "Structural and Thermal Properties of Polypropylene Mesh Used in Treatment of Stress Urinary Incontinence," Acta Bioeng. Biomech., **11**(3), pp. 27–33.

[32] Shah, H. N., and Badlani, G. H., 2012, "Mesh Complications in Female Pelvic Floor Reconstructive Surgery and Their Management: A Systematic Review," Indian J. Urol., **28**(2), pp. 129–153.

[33] Reddy, S. K., Williams, B. J., and Gomelsky, A., 2009, "Is Sling Stiffness Associated With Postoperative Voiding Dysfunction? A Comparison of Two Polypropylene Midurethral Slings," 39th Annual Meeting of the International Continence Society (ICS), San Francisco, CA, Sept. 29–Oct. 3, Paper No. 810.

[34] Brandão, S., Parente, M., Mascarenhas, T., da Silva, A. R., Ramos, I., and Jorge, R. N., 2015, "Biomechanical Study on the Bladder Neck and Urethral Positions: Simulation of Impairment of the Pelvic Ligaments," J. Biomech., **48**(2), pp. 217–223.

[35] Farrell, S. A., 2003, "Tension-Free Vaginal Tape (TVT) Procedure," J. Obstet. Gynaecol. Can., **25**(8), pp. 692–694.

[36] Lentz, G. M., Lobo, R. A., Gershenson, D. M., and Katz, V. L., 2012, *Comprehensive Gynecology*, 6th ed., Mosby, Elsevier, Philadelphia, PA.

[37] Baggish, M. S., and Kana, M. M., 2016, *Atlas of Pelvic Anatomy and Gycecology Surgery*, 4th ed., Elsevier, Philadelphia, PA.

[38] Schuettoff, S., Beyersdorff, D., Gauruder-Burmester, A., and Tunn, R., 2006, "Visibility of the Polypropylene Tape After Tension-Free Vaginal Tape (TVT) Procedure in Women With Stress Urinary Incontinence: Comparison of Introital Ultrasound and Magnetic Resonance Imaging In Vitro and In Vivo," Ultrasound Obstet. Gynecol., **27**(6), pp. 687–692.

[39] Erdemir, A., Guess, T. M., Halloran, J., Srinivas, C., Tadepalli, S. C., and Morrison, T. M., 2012, "Considerations for Reporting Finite Element Analysis Studies in Biomechanics," J. Biomech., **45**(4), pp. 625–633.

[40] Veronda, D. R., and Westman, R. A., 1970, "Mechanical Characterization of Skin—Finite Deformations," J. Biomech., **3**(1), pp. 111–122.

[41] Janda, S., 2006, "Biomechanics of the Pelvic Floor Musculature," Ph.D. thesis, Delft University of Technology, Delft, The Netherlands.

[42] Rivaux, G., Rubod, C., Dedet, B., Brieu, M., Gabriel, B., and Cosson, M., 2013, "Comparative Analysis of Pelvic Ligaments: A Biomechanics Study," Int. Urogynecol. J., **24**(1), pp. 135–139.

[43] Noakes, K. F., Pullan, A. J., Bissett, I. P., and Cheng, L. K., 2008, "Subject Specific Finite Elasticity Simulations of the Pelvic Floor," J. Biomech., **41**(14), pp. 3060–3065.

[44] Petros, P., 2011, "The Integral System," Cent. Eur. J. Urol., **64**(3), pp. 110–119.

[45] Magowan, B. A., Owen, P., and Thomson, A., 2014, *Clinical Obstetrics and Gynecology*, 3rd ed., Saunders, Elsevier, Philadelphia, PA.

[46] Herschorn, S., 2004, "Female Pelvic Floor Anatomy: The Pelvic Floor, Supporting Structures, and Pelvic Organs," Rev. Urol., **6**(S5), pp. 2–10.

[47] Atherton, M. J., and Stanton, S. L., 2005, "The Tension-Free Vaginal Tape Reviewed: An Evidence-Based Review From Inception to Current Status," BJOG, **112**(5), pp. 534–546.

[48] Novara, G., Galfano, A., Boscolo-Berto, R., Secco, S., Cavalleri, S., Ficarra, V., and Artibani, W., 2008, "Complication Rates of Tension-Free Midurethral

Slings in the Treatment of Female Stress Urinary Incontinence: A Systematic Review and Meta-Analysis of Randomized Controlled Trials Comparing Tension-Free Midurethral Tapes to Other Surgical Procedures and Different Devices," Eur. Urol., **53**(2), pp. 288–308.
[49] Natal Jorge, R., Brandão, S., Da Roza, T., Parente, M., and Mascarenhas, T., 2016, "Biomechanical Childbirth Simulations," *Biomechanics of the Female Pelvic Floor*, 1st ed., L. Hoyte, and M. Damaser, eds., Elsevier, Amsterdam, The Netherlands, pp. 415–431.
[50] Serati, M., Ghezzi, F., Cattoni, E., Braga, A., Siesto, G., Torella, M., Cromi, A., Vitobello, D., and Salvatore, S., 2012, "Tension-Free Vaginal Tape for the Treatment of Urodynamic Stress Incontinence: Efficacy and Adverse Effects at 10-Year Follow-Up," Eur. Urol., **61**(5), pp. 939–946.
[51] Dora, C. D., Dimarco, D. S., Zobitz, M. E., and Elliott, D. S., 2004, "Time Dependent Variations in Biomechanical Properties of Cadaveric Fascia, Porcine Dermis, Porcine Small Intestine Submucosa, Polypropylene Mesh and Autologous Fascia in the Rabbit Model: Implications for Sling Surgery," J. Urol., **171**(5), pp. 1970–1973.
[52] Schulz, J. A., Chan, M. C., and Farrell, S. A., 2008, "Midurethral Minimally Invasive Sling Procedures for Stress Urinary Incontinence," J. Obstet. Gynecol. Can., **30**(8), pp. 728–733.
[53] Surkont, G., Wlaźlak, E., and Suzin, J., 2015, "Long-Term Risk of Complications After Mid-Urethral Sling IVS Implantation," Ann. Agric. Environ. Med., **22**(1), pp. 163–166.
[54] Barski, D., and Deng, D. Y., 2015, "Management of Mesh Complications After SUI and POP Repair: Review and Analysis of the Current Literature," BioMed Res. Int., **2015**, p. 831285.
[55] Brandt, F. T., Almeida, R. B., de Alencar, A. V., Albuquerque, C. D. C., and Machado Junior, A. S., 2009, "Urethrovesical Ultrasonography as an Effective Method for Evaluating Prognostic Parameters in the Surgical Management of Stress Urinary Incontinence," Radiol. Bras., **42**(3), pp. 165–169.
[56] Barone, W. R., Amini, R., Maiti, S., Moalli, P. A., and Abramowitch, S. D., 2015, "The Impact of Boundary Conditions on Surface Curvature of Polypropylene Mesh in Response to Uniaxial Loading," J. Biomech., **48**(9), pp. 1566–1574.
[57] Egger, M. J., Hamad, N. M., Hitchcock, R. W., Coleman, T. J., Shaw, J. M., Hsu, Y., and Nygaard, I. E., 2015, "Reproducibility of Intra-Abdominal Pressure Measured During Physical Activities Via a Wireless Vaginal Transducer," Female Pelvic Med. Reconstr. Surg., **21**(3), pp. 164–169.
[58] Knight, K., and Moalli, P. A., 2016, "Mechanics of Pelvic Floor Prosthetic Devices," *Biomechanics of the Female Pelvic Floor*, 1st ed., L. Hoyte, and M. Damaser, eds., Elsevier, Amsterdam, The Netherlands, pp. 149–178.
[59] Feola, A., Abramowitch, S., Jallah, Z., Stein, S., Barone, W., Palcsey, S., and Moalli, P., 2013, "Deterioration in Bio-Mechanical Properties of the Vagina Following Implantation of a High-Stiffness Prolapse Mesh," BJOG, **120**(2), pp. 224–232.
[60] Jallah, Z., Liang, R., Feola, A., Barone, W., Palcsey, S., Abramowitch, S. D., Yoshimura, N., and Moalli, P., 2016, "The Impact of Prolapse Mesh on Vaginal Smooth Muscle Structure and Function," BJOG, **123**(7), pp. 1076–1085.
[61] Liang, R., Abramowitch, S., Knight, K., Palcsey, S., Nolfi, A., Feola, A., Stein, S., and Moalli, P. A., 2013, "Vaginal Degeneration Following Implantation of Synthetic Mesh With Increased Stiffness," BJOG, **120**(2), pp. 233–243.
[62] Rortveit, G., Hannnestad, Y. S., Daltveit, A. K., and Hunskaar, S., 2001, "Age and Type Dependent Effects of Parity on Urinary Incontinence: The Norwegian EPINCONT Study," Obstet. Gynecol., **98**(6), pp. 1004–1010.
[63] Memon, H. U., and Handa, V. L., 2013, "Vaginal Childbirth and Pelvic Floor Disorders," Womens Health (London), **9**(3), pp. 265–277.
[64] Macura, K. J., Thompson, R. E., Bluemke, D. A., and Genadry, R., 2015, "Magnetic Resonance Imaging in Assessment of Stress Urinary Incontinence in Women: Parameters Differentiating Urethral Hypermobility and Intrinsic Sphincter Deficiency," World J. Radiol., **7**(11), pp. 394–404.
[65] Huang, W. C., Yang, S. H., and Yang, J. M., 2006, "Anatomical and Functional Significance of Urogenital Hiatus in Primary Urodynamic Stress Incontinence," Ultrasound Obstet. Gynecol., **27**(1), pp. 71–77.
[66] Cassadó, J., Pessarrodona, A., Tulleuda, R., Cabero, L., Valls, M., Quintana, S., and Rodríguez-Carballeira, M., 2006, "Introital Ultrasonography: A Comparison of Women With Stress Incontinence Due to Urethral Hypermobility and Continent Women," BJU Int., **98**(4), pp. 822–828.

Original Article

Study VI

_Puboviscerali_s muscle fiber architecture determination: comparison between biomechanical modeling and diffusion tensor imaging.

Brandão, S; Parente, M; Silva, E; Da Roza, T; Mascarenhas, T; Leitão, J; Cunha, J; Natal Jorge, R; Nunes, RG.

Ann Biomed Eng. 2017 May;45(5):1255-1265.

doi: 10.1007/s10439-016-1788-y. Epub 2017 Jan 17.

Annals of Biomedical Engineering (© 2017)
DOI: 10.1007/s10439-016-1788-y

*Puboviscerali*s Muscle Fiber Architecture Determination: Comparison Between Biomechanical Modeling and Diffusion Tensor Imaging

Sofia Brandão,[1,2] Marco Parente,[2] Elisabete Silva,[2] Thuane Da Roza,[2,3] Teresa Mascarenhas,[4] João Leitão,[5] João Cunha,[5] Renato Natal Jorge,[2] and Rita Gouveia Nunes[6,7]

[1]Department of Radiology, Centro Hospitalar de São João - EPE, Faculty of Medicine, University of Porto, Alameda Prof. Hernâni Monteiro, 4200-319 Porto, Portugal; [2]Associated Laboratory for Energy, Transports and Aeronautics (LAETA), Institute of Science and Innovation in Mechanical and Industrial Engineering (INEGI), Faculty of Engineering, University of Porto, Rua Dr Roberto Frias, 400, 4200-465 Porto, Portugal; [3]Biomechanics Laboratory, Center of Health and Sport Sciences, University of the State of Santa Catarina (CEFID/UDESC), Rua Pascoal Simone, 358, 88080-350 Florianópolis, Brazil; [4]Department of Obstetrics and Gynecology, Centro Hospitalar de São João - EPE, Faculty of Medicine, University of Porto, Alameda Prof. Hernâni Monteiro, 4200-319 Porto, Portugal; [5]Department of Radiology, Centro Hospitalar de Lisboa Norte-EPE - Hospital de Sta Maria, Faculty of Medicine, University of Lisbon, Avenida Prof. Egas Moniz, 1649-035 Lisbon, Portugal; [6]Instituto de Biofísica e Engenharia Biomédica (IBEB), Faculdade de Ciências, Universidade de Lisboa, Campo Grande, 1749-016 Lisbon, Portugal; and [7]Department of Bioengineering and Institute for Systems and Robotics (ISR/IST), LARSyS, Instituto Superior Técnico, Universidade de Lisboa, Av. Rovisco Pais 1, 1049-001 Lisbon, Portugal

(*Received 7 October 2016; accepted 31 December 2016*)

Associate Editor Estefania Pena oversaw the review of this article.

Abstract—Biomechanical analysis of pelvic floor dysfunction requires knowledge of certain biomechanical parameters, such as muscle fiber direction, in order to adequately model function. Magnetic resonance (MR) diffusion tensor imaging (DTI) provides an estimate of overall muscle fiber directionality based on the mathematical description of water diffusivity. This work aimed at evaluating the concurrence between *puboviscerali*s muscle fiber representations obtained from DTI, and the maximum principal stress lines obtained through the finite element method. Seven datasets from axial T2-weighted images were used to build numerical models, and muscle fiber orientation estimated from the DT images. The in-plane projections of the first eigenvector of both vector fields describing muscle fiber orientation were extracted and compared. The directional consistency was evaluated by calculating the angle between the normalized vectors for the entire muscle and also for the right and left insertions, middle portions, and anorectal area. The values varied between 28° ± 6 (right middle portion) and 34° ± 9 (anorectal area), and were higher than the angular precision of the DT estimates, evaluated using wild bootstrapping analysis. Angular dispersion ranged from 17° ± 4 (left middle portion) to 23° ± 5 (anorectal area). Further studies are needed to examine acceptability of these differences when integrating the vectors estimated from DTI in the numerical analysis.

Keywords—Pelvic floor muscles, Magnetic resonance diffusion tensor imaging, Computational biomechanics, Finite element method.

ABBREVIATIONS

BMI	Body mass index
DTI	Diffusion tensor imaging
FEM	Finite element method
FSE	Fast spin-echo
ICIQ-SF	International Consultation of Incontinence Questionnaire-Short Form
LA	*Levator ani*
LMMSE	Linear minimum mean square error
MPSL	Maximum principal stress lines
MRI	Magnetic resonance imaging
NSA	Number of signals averaged
PFM	Pelvic floor muscles
PVM	*Puboviscerali*s muscle
SENSE	Sensitivity encoding
SNR	Signal-to-noise ratio
SPAIR	SPectral Attenuated Inversion Recovery
SS-SE-EPI	Single-shot spin-echo echo planar imaging

Address correspondence to Sofia Brandão, Department of Radiology, Centro Hospitalar de São João - EPE, Faculty of Medicine, University of Porto, Alameda Prof. Hernâni Monteiro, 4200-319 Porto, Portugal. Electronic mail: sofia.brand@gmail.com

Published online: 17 January 2017

TE Echo time
TR Repetition time

INTRODUCTION

Female pelvic floor dysfunction is associated with muscle, nerve, or connective tissue injury.[37] As a result, urinary incontinence and organ prolapse may occur.

Different factors have to be considered, such as quality of pelvic floor muscles (PFM), presence of nerve lesions, modifications of the mechanical properties of the fascia and ligaments due to aging, obesity, or changes in hormonal levels, and also how physiotherapy or surgical procedures should compensate for these injuries.[1] The need for understanding the overall biomechanics of the pelvic cavity has led to the development of computational models, some of which are based on the finite element method (FEM).[24,26,30] Previous simulations of the Valsalva maneuver or defecation (where there is no conscious voluntary muscle activation)[7,24] vaginal delivery[26] or during contraction[8,30] demonstrated the utility of computational models for this research area.

Due the anatomical detail it provides, magnetic resonance imaging (MRI) is widely used in the modeling process.[7,8,24,30] Figure 1 shows axial MR images of the pelvis, where it is possible to identify (and segment) the pelvic organs and some divisions of the *levator ani* (LA) muscle. The *levator ani* muscle is composed of the *iliococcygeus*, *pubococcygeus* and *puborectalis* muscles. The term *pubovisceralis* muscle (PVM) is sometimes applied to include the *puborectalis* and the *pubococcygeus* muscles.[10] It forms a sling around the rectum, vagina and urethra that promotes the closure of the pelvic floor *hiatus*. Urinary incontinence and pelvic organ prolapse are associated with damage to the PVM, many times due to complicated vaginal delivery.[16] Accordingly, in the present work, we modeled the PVM, the boundaries of which can be easily identified and segmented.

Computational models based on the FEM include inputs from both geometric and viscoelastic tissue properties, governed by appropriate constitutive equations to reproduce a biomechanical response. It is known that muscles, tendons and ligaments share a non-linear stress–strain typical response, and they are modeled as nearly-incompressible hyperelastic structures.[4,22] Due to their highly oriented structure, quasi-incompressible transversely-isotropic constitutive models are often applied,[4,17,22,25] and frequently accommodate both passive and active muscle responses. These constitutive models account for the inclusion of the direction of the muscle fibers in each finite element. Since defining the direction of each fiber through conventional MR images is far beyond their spatial resolution, one approach for modeling muscle

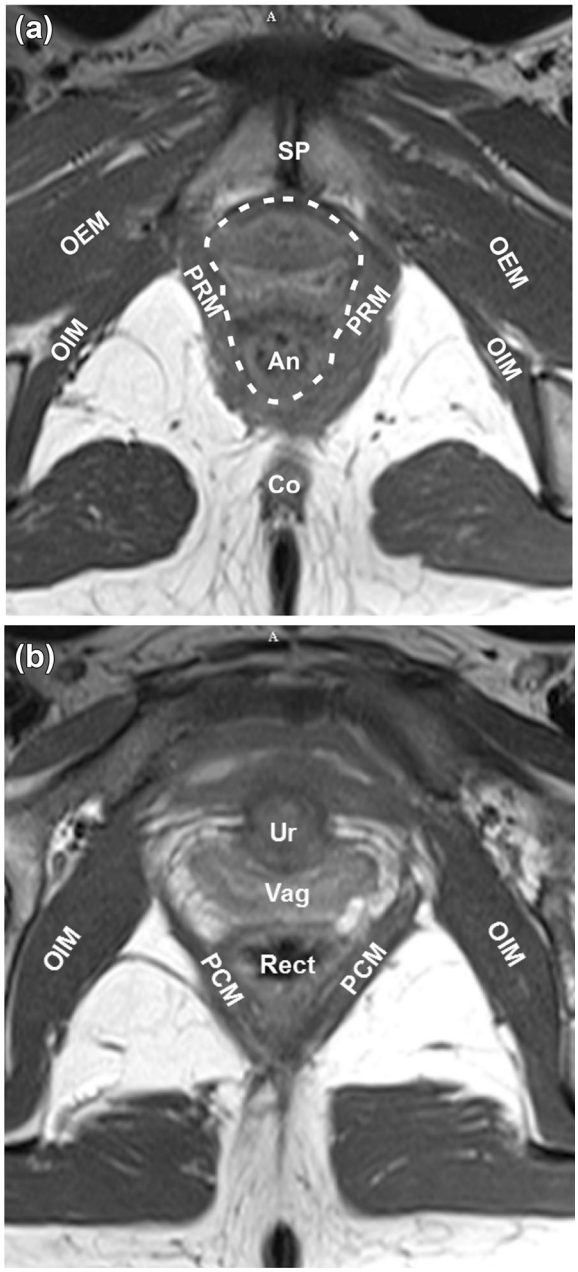

FIGURE 1. Axial MR images of the pelvis in a healthy 37 year-old female, at the level of the lower border of the *symphysis pubis* (a), and 13 mm proximal (b). The anatomical details of the pelvic structures can be identified, such as the urethra (Ur), vagina (Vag) and rectum (Rect) in (b). The *puborectalis* (PRM) and *pubococcygeus* (PCM) muscles are shown. Their thicknesses, along with the shape of the *levator hiatus* (dashed line in (a)), are important anatomical markers in the diagnostic imaging of pelvic floor dysfunction. An, anus; Co, coccyx; OEM, *obturator externus* muscle; OIM, *obturator internus* muscle; PCM, *pubococcygeus muscle*; PRM, *puborectalis* muscle; Rect, rectum; SP, *symphysis pubis*; Ur, urethra; Vag, vagina.

fibers is to assume that the fibers are aligned with the direction of the maximum principal stress lines (MPSL)[6,15] that can be obtained when the model is subjected to a distributed load.[26,30] For that purpose, an initial assumption of isotropic behavior can be taken.

Recent studies have applied MR diffusion tensor imaging (DTI) with fiber tractography to the pelvic floor while maintaining a satisfactory 3D anatomical representation of pelvic floor muscles, such as the *puboviscerali*s and *puborectalis*.[29,43,44] DTI is used to compute principle directions of water diffusion, providing indirect information about tissue architecture.[38] Consequently, orientation of anisotropic tissue can be estimated from the spatial orientation of diffusion tensors, which correspond to directions of diffusion in 3D space. Since muscle fibers are highly anisotropic structures, water molecules are more likely to diffuse along, rather than transverse to, the muscle fiber direction. The major diffusion eigenvector (representing the direction of greatest diffusivity) is assumed to be closer to the muscle's along-fiber direction than to the cross-fiber directions and can be derived from the mathematical calculation of the diffusion tensor in each voxel.[27] From this, overall muscle fiber direction can be determined using fiber tractography algorithms. Tensors may be reconstructed and used to track 3D fiber orientation in a voxel-by-voxel basis.

In the context of muscle finite element modeling, a possible application for this data would be to incorporate muscle anisotropy by means of directly including the local fiber direction for each finite element. In that sense, the purpose of this work was to evaluate the concurrence between the direction of the PVM fibers when comparing DTI and the MPSL obtained from the FEM outputs.

MATERIALS AND METHODS

Subjects and Imaging

This work was approved by the Ethics Committee of Centro Hospitalar de Lisboa Norte-EPE (Hospital de Sta. Maria/Faculty of Medicine, University of Lisbon, IRB675/14). Exclusion criteria included previous pelvic surgery, pregnancy, delivery or complaint of pelvic floor dysfunction. A convenience sample of ten nulliparous women who gave informed consent was recruited. A gynecologist performed clinical observation and assessment for pelvic organ prolapse, and no pathological findings were reported. Demographic characteristics (age, body mass index (BMI)), medical and obstetric histories were collected. Furthermore, all the participants were asked to complete the International Consultation of Incontinence Questionnaire-Short Form (ICIQ-SF)—which is validated for the Portuguese language[36]—to assess the presence and symptoms of urinary incontinence. None of the ten women presented symptoms of pelvic floor dysfunction, and were then invited to undergo a pelvic MRI examination.

Prior to the scanning session the participants were asked to evacuate their bladder and bowel. T2-weighted and DT axial images of the pelvis were obtained at rest, in an Achieva 3.0T system, using a 32-ch phased-array coil. The volunteers lay in supine position with legs joined in a semi-flexed position. The images were planned by evaluating scout T2-weighted sagittal images (not described in the scanning protocol). They were set along the main orientation of the PVM bulk, defined by the plane of minimal hiatal dimensions, from the postero-inferior margin of the *symphysis pubis* to the anterior margin of the PVM, where it defines the anorectal angle.[14] Axial T2-weighted fast spin-echo (FSE) images were acquired (echo time/repetition time TE/TR 90/2400 ms; echo train length 20; voxel size $1.5 \times 1.5 \times 3$ mm^3; 2NSA (number of signals averaged). DTI was performed with a single-shot spin-echo echo planar imaging (SS-SE-EPI) sequence with diffusion probing gradients applied in 32 different gradient encoding directions, at a maximum *b*-value of 400 s/mm^2 (according to previous literature on skeletal muscle DTI)[13] (TE/TR 40/2578 ms; EPI factor 43; voxel size $3 \times 3 \times 3$ mm^3; 2NSA). Parallel imaging was applied in the image domain using sensitivity encoding (SENSE factor 2) to reduce imaging artifacts. High gradient performance was also applied to shorten the EPI-readout for better minimization of susceptibility-induced artifacts. SPectral Attenuated Inversion Recovery (SPAIR) was used for fat suppression, with an inversion delay of 80 ms for the adiabatic pulses. Mean scanning time was less than 20 min.

After carefully reviewing all the MRI datasets, three women were excluded due to excessive image distortion and blurring artifacts on the DT images, mostly due to air in the rectum and to bowel movements. The final sample comprised seven women.

Numerical Models

The T2-weighted axial images were used to create 3D geometrical models through semi-automatic segmentation of consecutive slices where the contours of the PVM, *obturator internus* muscle, coccyx, and *symphysis pubis* were defined, *via* the Mimics® Innovation Suite v.17. An initial pixel intensity threshold was set to obtain the contours of their shape. Additional refinements were hand-made using the original images as reference. The resulting 3D triangulated

surface model was generated from the voxel volume, and then the Mimics 3D default-smoothing algorithm (based on the Laplacian first-order function) was applied.

The triangulated 3D surface model of the PVM was imported to the Abaqus® software v.2016 to create the finite element mesh for each subject, by using hybrid linear tetrahedral elements (Abaqus C3D4H). The number of nodes and elements in the numerical models varied among the subjects according to the morphology of the muscles (ranging between 56,977 and 76,869 elements, and 86,454 and 114,086 nodes). For each model, the element size was set to be approximately constant throughout the geometry, resulting in a mesh with a characteristic element length of 1 mm. The 3D geometric models of the surrounding structures were included in the model for visualization purposes and to correctly define the boundary conditions. Four of the seven numerical models are presented in Fig. 2, where we can appraise the different anatomical muscle and *levator hiatus* shapes.

To obtain the direction of the muscle fibers in the numerical models, the muscle was assumed as an isotropic, homogeneous solid material. The non-linear hyperelastic Yeoh constitutive model was applied, with the mechanical parameters $C_{10} = 3.0 \times 10^{-2}$ MPa; $C_{20} = 2.0 \times 10^{-2}$ MPa; $C_{30} = 1.0 \times 10^{-2}$ MPa, according to previous work.[7] Boundary conditions were imposed to the model to define the insertion points of the muscle in the *symphysis pubis*, *obturator internus* fascia and coccyx (see Fig. 3). They were simulated by using multi-point constraints (Abaqus® tie). To be as realistic as possible to the insertion locations, the anatomical images were reviewed in detail. Fixed boundary conditions were applied to the nodes along the anterior borders of the muscle to mimic the insertion of the *puborectalis* portion of the PVM in the internal surface of the pubic bone, and also on the most superior portion of the PVM (the *pubococcygeus* muscle), corresponding to the attachment to the fascia of the *obturator internus* muscle, which constrains lateral movement. The boundary conditions defined between muscle and coccyx were kept unconstrained in the *z*- (supero-inferior) and *y*- (antero-posterior) directions to allow reproducing the known physiologic angular coccygeal movements.[5]

To obtain information regarding the direction of the muscle fibers, it was implicitly assumed that they are coincident with the direction of the MPSL (Fig. 4) when the structure is being deformed. For that purpose, we reproduced a similar effect to that of the organ load in live subjects by applying a uniform

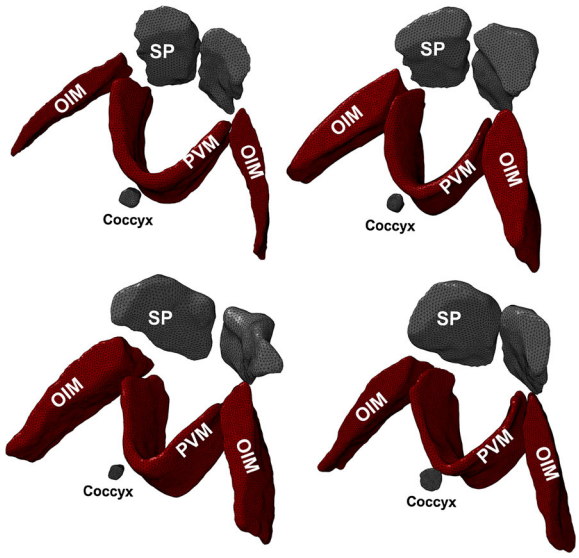

FIGURE 2. Four of the seven numerical models of the *puboviscerali*s muscle. OIM, *obturator internus* muscle; PVM, *puboviscerali*s *muscle*; SP, *symphysis pubis*.

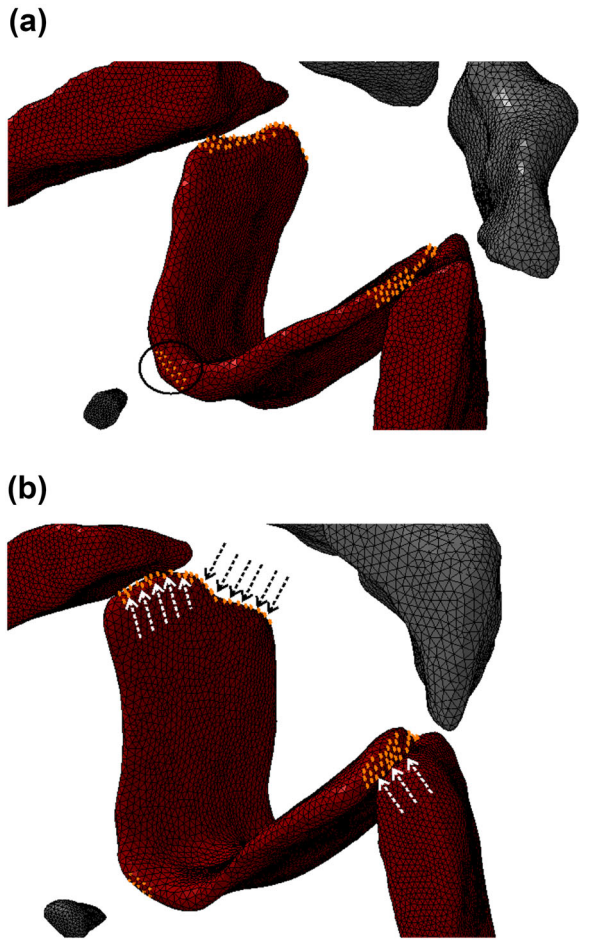

FIGURE 3. Definition of the boundary conditions (orange dots) that mimic muscle attachments to the surrounding structures in the coccyx (black circle in (a)), and in the *symphysis pubis* and *obturator internus* (black and white dashed arrows in (b), respectively).

pressure of 1.0×10^{-3} MPa to the inner surface of the PVM. This step resulted in the expected pattern and adequate deformation of the finite element model, mimicking the default anatomical behavior. The 3 components of the first eigenvector (x-, y-, z-directions) of the tensor that describes fiber orientation were extracted for further comparison with the directions of the first eigenvector obtained from the DTI.

DW Image Processing and DT Estimation

To improve the signal-to-noise ratio (SNR) of the DT images, all the datasets were denoised by using a linear minimum mean square error (LMMSE) filter for Rician MRI noise.[19] The DT images were also co-registered to the T2-weighted images using an affine transformation. The Diffusion Toolkit® v.0.6.2.1 was used to estimate the tensor and to further process the images for muscle fiber tracking. Figure 5 shows DT b400 s/mm^2 (a) and T2-weighted images (b), as well as the representation of the first eigenvector overlaid on the corresponding b400 s/mm^2 image (c). The tensor representation for the PVM, *obturator internus* and *externus* muscles was consistent with expected muscle alignment, contours, and thicknesses.

The images of the PVM used for outlining its contours on the Mimics® software were used as a mask (Fig. 6a) to obtain the three components of the first eigenvector of the DT[3] in each ($3 \times 3 \times 3$ mm^3) voxel within this region.

To obtain a visual representation of the muscle, the tensor-line algorithm and a 90°-threshold angle, which is the maximum angle between the main eigenvectors of two adjacent voxels allowed to continue the fiber tracking propagation, were used. The 90°-threshold angle was chosen for the fiber tracking propagation due to the very pronounced angulation of the muscle expected at the anorectal (posterior) area. The mask was considered as a seed region-of-interest from which tracking was launched in both the retrograde and anterograde directions according to the main eigenvector at each voxel. Only the diffusion pathways that

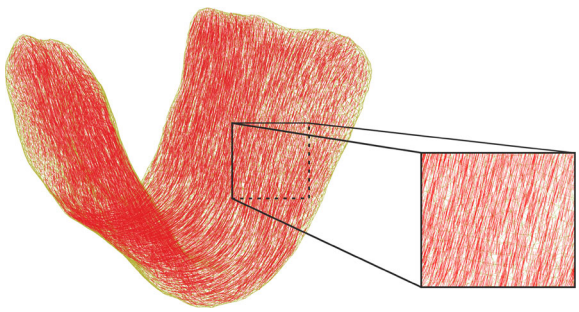

FIGURE 4. Maximum principal stress lines (MPSL) distributed along the finite element mesh. These lines are assumed to be representative of muscle fiber directions.

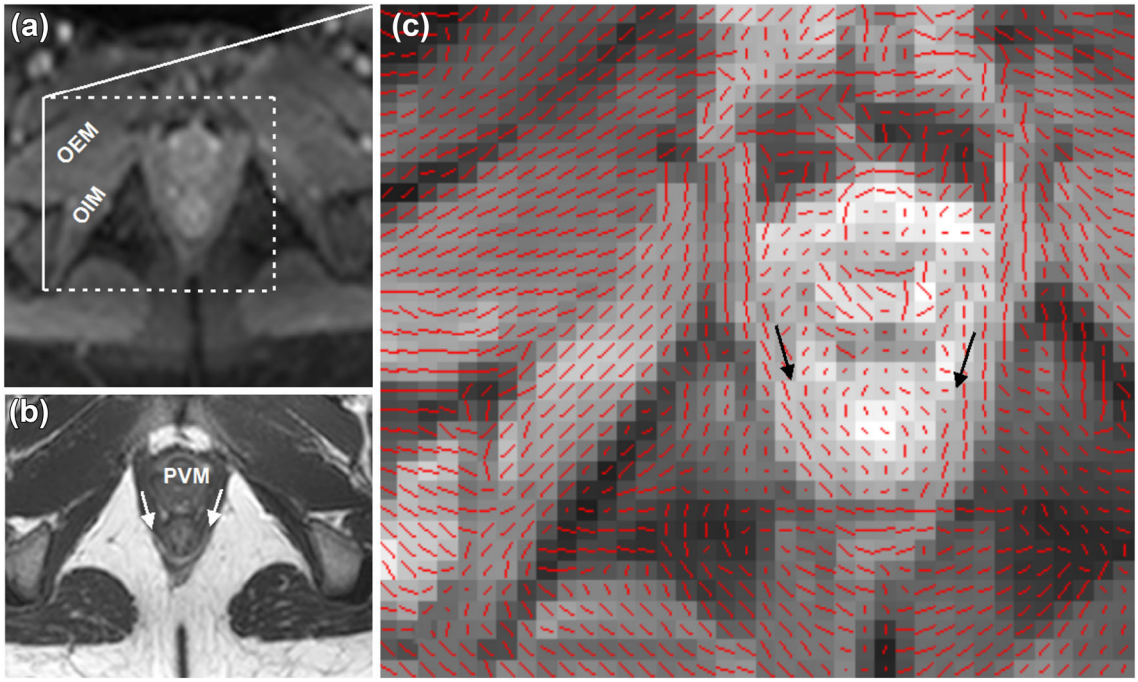

FIGURE 5. Axial DT b400 s/mm^2 (a) and T2-weighted images (b), and representation of the first eigenvector overlaid on the corresponding b400 s/mm^2 image (c). OEM, *obturator externus* muscle; OIM, *obturator internus* muscle; PVM, *puboviscerali*s muscle.

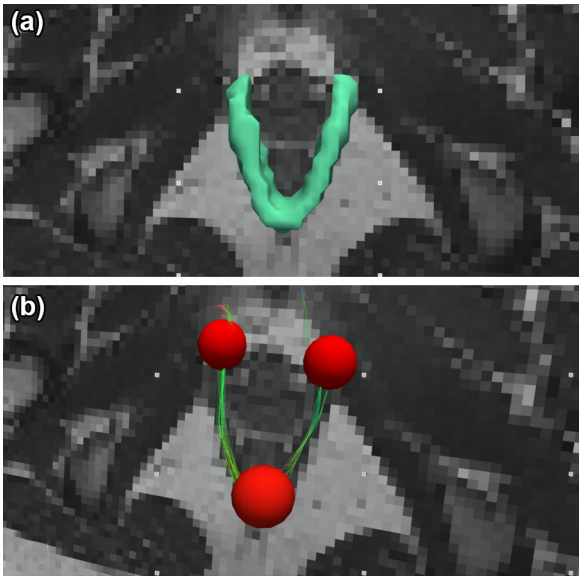

FIGURE 6. Axial images showing the volume that served as mask (a) to launch the fiber tracking overlaid to the co-registered T2-weighted and DT images. Using inclusion and exclusion seed masks (red spheres) the likely representation of the muscle fibers is achieved (b).

were represented inside the defined boundaries were accepted, as seen in Fig. 6.

Directional Consistency Analysis

The data of the tensor field retrieved from both procedures were imported to MATLAB® R2016a. A sub-routine was created to execute four consecutive tasks. Firstly, to co-register the PVM masks drawn on the Mimics® software with the T2-weighted images and the DT images by performing scaling and translation operations (the required transformations were previously confirmed using the Image Registration Toolkit).[35] Secondly, to transform the spatial coordinates of the centroids of the finite element into the coordinate frame used to define the DTI voxels. After that, it searched for the elements contained within each voxel included in the mask. Finally, for each DT image plane, to compare the angle between the in-plane projections of the first eigenvector of both vector fields (DTI vs. MPSL). We should state at this point that only the in-plane projections of the first eigenvector of the DTI were used assuming that the axial imaging plane was correctly established by an experienced observer to be coincident to the direction of the muscle bulk.

The directional consistency was evaluated by considering the mean of all the MPSL vectors within all the elements included in each DW image voxel ($3 \times 3 \times 3$ mm^3) belonging to the PVM mask and then calculating the absolute value of the angle between the two vectors within each voxel by taking the dot product of the normalized vectors.

Figure 7a displays the voxel-by-voxel results for one subject, and Fig. 7b exemplifies, for the same woman, the five different regions that we considered along the muscle's "U shape": the bilateral most anterior portions (that include the insertion areas to the *symphysis pubis*), the middle portions, and the most posterior area (corresponding to the anorectal angle). Color-coded maps were also obtained according to the amplitude of the angles for all the slices representing the PVM muscle mask for each subject.

To test the precision of the estimated DTI principal direction we used the wild bootstrapping statistical analysis[42] with 1000 repetitions and estimated the aperture of the cone of uncertainty, within which 95% of the estimates of the DT principal direction are included.

Statistical Analysis

All analyses were computed using IBM SPSS® v.23.0. Descriptive statistics (mean ± SD) for the continuous variables age, BMI and angle were calculated. The one-way ANOVA was applied to compare the mean values of the angle between the two methods (DTI vs. MPSL) for the five regions considered. Significance level was established as $p < 0.05$.

RESULTS

Seven healthy females were considered appropriate for detailed analysis in this study (mean age 28.1 ± 1.5 years; mean BMI 18.8 ± 2.1 kg/m^2). There was no clinical evidence of pelvic dysfunction, and all the women scored zero in the ICIQ-SF survey. They were scanned for pelvic MRI, and no suspicious or pathological findings were reported.

Table 1 shows the mean values of the angles when comparing DTI vs. MPSL for the seven datasets in the sample, as well as the angular uncertainty (95th percentile) associated to the DT vector estimates evaluated through wild bootstrapping analysis. There were no significant differences between regions for the angles DTI vs. MPSL ($p = 0.51$), nor for the cone of uncertainty determined through wild bootstrapping analysis ($p = 0.29$).

Figure 8 shows 2D color maps displaying the angles (between 0° and 90°) between the vectors from DTI vs. MPSL for two women, for which the geometry of the PVM was included in 9 and 10 slices, respectively. From Table 1, it is possible to see that the amplitude of the angles varies along muscle anatomy. The middle portions of the PVM show lower angle, i.e., higher

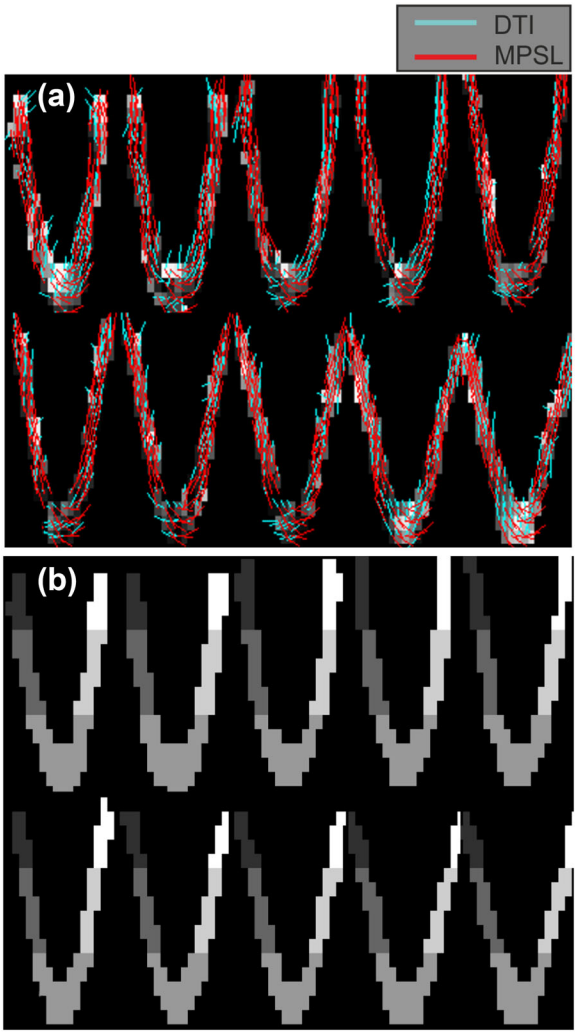

FIGURE 7. Illustration of the vectors retrieved from each voxel included in the PVM mask (DTI vs. MPSL) (a). For a regional comparison, five areas were also considered (b) (from dark grey to white, starting from the anterior right side to the anterior left side).

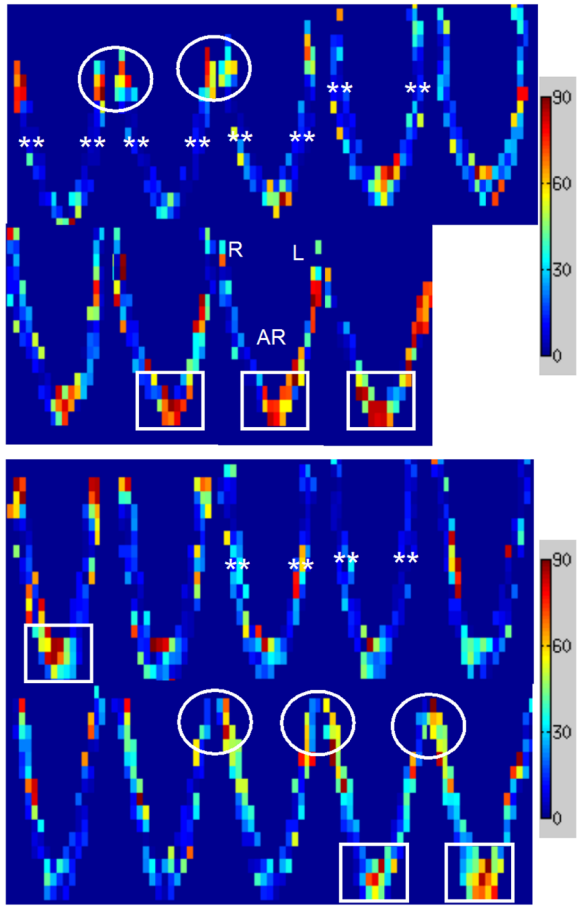

FIGURE 8. Color maps displaying the angles between the vectors from DTI vs. MPSL for two women. The right (R) and left (L) anterior insertion areas (white circles) and the posterior anorectal angle (AR, white rectangles) display higher amplitude, whereas the middle portions of the muscle bulk seem to have greater similarity (white asterisks).

similarity when comparing the vectors from DTI vs. MPSL than the insertion and anorectal areas.

DISCUSSION

Assessing the functional performance of the pelvic floor muscles *in vivo* and non-invasively has been both a need and a challenge in the clinical and research environments. For that purpose, dynamic imaging techniques and computational modeling have been intensively developed. In this regard, morphology, microscopic anatomic features and also muscle's physiologic behavior during passive and active replies should ideally be included during the modeling process.

Despite the fact that there is still no imaging method accurate enough to evaluate all the anatomical details

TABLE 1. Mean values of the angles (°) between the vectors from DTI vs. MPSL, and results from the wild bootstrapping (angular uncertainty) analysis.

Regions	All	ins. L	ins. R	mid. L	mid. R	AR
Voxel-by-voxel (°)	32 ± 5	32 ± 6	33 ± 9	28 ± 6	29 ± 8	34 ± 9
Uncertainty (°)	–	17 ± 6	23 ± 3	17 ± 4	22 ± 4	23 ± 5

AR, anorectal region; ins., insertion area; L, left; mid., middle; R, right.

of such a multilayered and multidirectional muscular structure, several authors applied the MR images as input for 3D computational modeling.[12,28]

Also, efforts have been made in an attempt to define the orientation of the subdivisions of the LA with conventional multi-planar MRI,[12,20] and to approximate the direction of the muscles fibers and their line of action.[21] For that purpose, DTI combined with fiber tractography has given an initial contribution for visualizing fiber orientation, and therefore to appreciate details that may contribute for better understanding of the role of each of the LA subdivisions both for elevating the pelvic floor and for reducing the *levator hiatus*.[29] Despite that, the representation of fiber pathways as seen in Fig. 6 cannot be considered as a direct representation of the underlying muscle fibers; the reconstructed pathways vary depending on the trade-off between the number of diffusion encoding directions, image resolution, SNR, acquisition time and the post-processing methodology applied.

In the present work, we considered only the in-plane projections of the first eigenvector of the DTI to simplify the computation of the MATLAB® sub-routine, assuming that the axial slices follow the anatomical muscle path. In that sense, a perpendicular component would most probably result from random noise, partial volume effect from the surrounding tissue (mainly fat) or involuntary motion that would introduce erroneous data in the tensor estimate. Nevertheless, since we do not have histological information regarding the muscle path to validate the angulation of the axial slices, and given that the analysis of muscle direction was observer-dependent, it should be acknowledged that this methodological option is also not error-free.

The results of the present work showed a fair consistency between the representations of muscle fibers on both methods. Despite the lower angles on the middle portions of the PVM, 28° ± 6 and 29° ± 8 for the right and left sides, respectively, the values were close to the ones of the insertion regions (32° ± 6 and 33° ± 8 for the right and left sides, respectively), with no significant difference between the five regions defined. The wild bootstrapping method estimated mean uncertainties for the DT eigenvector direction ranging from 17° to 23°. Although these results do not fully explain the differences between DT and MPSL directions, supporting additional sources for the observed disparity as discussed below, they do suggest that noise in the DTI data could partly explain these inconsistencies.

The boundary conditions manually placed are very likely to have contributed to the difference between the middle and insertion portions, although they were set according to visual analysis of the anatomical images and *in consensus* between two observers. The anorectal area showed the lowest similarity, which may be due to its anatomical "U" shape, as highly-curved pathways are more challenging to reconstruct using DTI post-processing (Figs. 5c and 7a), while in the finite element model the boundary conditions simulating the coccygeal insertion may have led to a "V" arrangement of the MPSL (see Fig. 7a for comparison).

Since the direction of the muscle fibers in the numerical models requires assuming an isotropic and homogeneous material with no internal orientation, these boundary conditions set in the most anterior and superior borders of the PVM, and also in its posterior region to the coccyx seem to play an important role, by affecting to some extent the resultant inner arrangement of the muscle fibers, represented by the MPSL.

Notwithstanding that, care was taken not to include women with clinical or imaging evidence of muscle asymmetry or avulsion, for whom muscle geometry and architecture would certainly be modified. In any case, muscular internal structure cannot be reliably ascertained using this approach, and therefore, an overall regular alignment of the muscle fibers was assumed.

We considered the same PVM mask to limit the discrepancy between the geometry of the PVM in the computational model and DTI, although we cannot neglect a residual geometric distortion. Also, we believe that the higher number of elements compared to the number of voxels, which required the use of the mean value of the MPSL vectors within the elements included in each DW image voxel, may have also had a strong contribution to the global differences between the two methods. In this regard, it should be pointed out that the size of the elements in the mesh was established so as to allow a good approximation to the global geometry of the PVM, as well as the representation of its curvatures, and also to ensure having more than two elements representing the thickness of the muscle. Future studies should aim to improve the spatial resolution in the DTI acquisition, although the inevitable substantial reduction in SNR, increased geometric distortions in the images make this very challenging to achieve. One option would be to use multi-shot acquisitions, but these require longer acquisition times and in consequence are much more vulnerable to involuntary motion artifacts.

This study has some limitations that have to be pointed out, starting by the small sample size. In addition, three of the ten DTI datasets evidenced major image distortion and blurring artifacts, mostly due to the air in the rectum and bowel movements, which prevented their use. Moreover, the need for a reasonable SNR in an acceptable scanning time for the DT images made it necessary to use larger voxels than

those of the anatomical T2-weighted image, but we consider that this had no negative effect on the definition of muscle contours.

As the study was performed on a set of healthy volunteers, it was not considered appropriate to take additional measures, other than asking them to empty their bladder and bowels prior to the study, which could have helped to minimize the sources of these artifacts further. In the clinical practice, it is highly recommended to consider the intramuscular or intravenous administration of a spasmolytic agent for all pelvic MR examinations to reduce peristalsis-related motion artifacts and the use of cleansing enemas or filling the rectum with ultrasound gel to reduce susceptibility-related artifacts due to the intraluminal air.

Another aspect to be noted is the manual seeding post-processing, which includes some degree of subjectivity that cannot be neglected. To minimize this effect, the masks created using the T2-weighted anatomical images in the Mimics® software that were the basis for the computational models of the PVM were also considered as seed regions-of-interest. By selecting the seed regions using anatomical MR images we also aimed to reduce errors in fiber tracking.

Despite all the abovementioned procedures to reduce bias, we still have to consider that applying pelvic floor muscle DTI to the clinical or research fields should be carefully weighted because its application for estimating fiber orientation has not yet been validated. Although DTI has brought additional information *on in vivo* structural analysis on muscle fibers of human subjects, e.g., fiber orientation,[34] fiber type characterization[31] or mean fiber length during passive lengthening and stretching,[23] it is important to remember that DTI does not provide the ground truth, since it is an indirect method of observation. It is still very dependent on technical aspects[13] of the acquisition technique and the post-processing methods. Furthermore, DTI is especially difficult in areas where there are multidirectional muscles as is the case of the pelvic floor, where fat is also an issue to deal with. Animal DTI studies can be performed with very high resolution and can therefore be validated against direct anatomical inspection and histology,[9,39,40] or even with computational modeling.[32,39] But that is not the case in the pelvis. The very complex anatomical architecture and the impossibility of acquiring DT images with a sufficient spatial resolution to match voxel vs. finite element length, make it very challenging to perform direct comparisons. Furthermore, in *ex vivo* evaluation the LA loses its tone and shape[33] and thus cannot be used to directly characterize these muscles in living women.

We consider this as the first attempt to establish a methodological pathway to retrieve and compare these two indirect methods to obtain the direction of the muscle fibers. To address this difficulty, future work may include comparing fiber orientation from MPSL and DTI with detailed 3D models built by manual digitization of cadaveric tissue,[2,32,41] including *in vivo* information. This information could be obtained from MR imaging, and improved with (semi)-automated methods of ultrasound image analysis.[18]

The numerical methodology applied in this work could be replicated in other muscles, that is, obtaining the MPSL (and comparing the components of the first eigenvector to those obtained from the DTI). For this to be achievable, it would be necessary to reproduce an anatomically reliable muscle function load for the specific muscle, which could be a traction load in the case of a biceps muscle, as opposed to the distributed load/pressure applied in the present work.

Future work will attempt to validate muscle fiber direction retrieved from DTI by including information on the first eigenvector of the diffusion tensor in the finite element numerical simulation of valsalva maneuver and muscle active contraction. The resultant muscle nodal displacement will be compared with the ones performed with the original MPSL to assess the agreement between the two methods, and validated against mid-sagittal dynamic images acquired at the same conditions of valsalva and voluntary contraction.

In this context, while it would be very interesting to perform DTI during active pelvic floor muscles contraction, there are several anticipated challenges. The first is the unfeasibility to sustain a voluntary contraction during the whole DTI acquisition time (3 min). Second, since contracting the pelvic floor muscles produces their cranial and anterior displacement, unless the same contraction level would be maintained, it would be virtually impossible to correctly register the images corresponding to different diffusion directions as required to obtain accurate tensor estimates and perform fiber reconstruction. Finally, the purpose of our study was not to study muscle fibers during active contraction, but rather to reach an (indirect) anatomical representation of the PVM at rest. Although DTI studies on lower limb muscles under contraction showed slight changes in the tensor eigenvectors,[11] and although it would be interesting to perform direct comparison with future FEM simulations of active muscle behavior, it should be noted that the same study conditions could not be replicated in our study.

In conclusion, we compared the vectors that indirectly defined the direction of the PVM, and our results point to a less similar pathway between DTI and MPSL in the anterior regions inserting the *symphysis pubis* and around the anorectal junction where the *puborectalis* muscle forms a sling.

ACKNOWLEDGEMENT

TR acknowledges the funding by CNPq (Grant No. 314649/2014-0) from Brazil government. The authors also acknowledge the funding of the Research Project UID/EMS/50022/2013, from Fundação da Ciência e Tecnologia (FCT), Portugal, and Project NORTE-01-0145-FEDER-000022-SciTech-Science and Technology for Competitive and Sustainable Industries, co-financed by Programa Operacional Regional do Norte (NORTE2020), through Fundo Europeu de Desenvolvimento Regional (FEDER). RGN acknowledges funding by the FCT Investigator Program (IF/00364/2013).

CONFLICT OF INTEREST

The authors declare that there is no conflict of interest.

REFERENCES

[1]Abramowitch, S. D., A. Feola, Z. Jallah, and P. A. Moalli. Tissue mechanics, animal models, and pelvic organ prolapse: a review. *Eur. J. Obstet. Gynecol. Reprod. Biol.* 144(Suppl 1):S146–S158, 2009.

[2]Agur, A. M., V. Ng-Thow-Hing, K. A. Ball, E. Fiume, and N. H. McKee. Documentation and three-dimensional modelling of human *soleus* muscle architecture. *Clin. Anat.* 16(4):285–293, 2003.

[3]Basser, P. J., S. Pajevic, C. Pierpaoli, J. Duda, and A. Aldroubi. *In vivo* fiber tractography using DT-MRI data. *Magn. Reson. Med.* 44(4):625–632, 2000.

[4]Blemker, S. S., and S. L. Delp. Three-dimensional representation of complex muscle architectures and geometries. *Ann. Biomed. Eng.* 33(5):661–673, 2005.

[5]Bø, K., F. Lilleas, T. Talseth, and H. Hedland. Dynamic MRI of the pelvic floor muscles in an upright sitting position. *Neurourol. Urodyn.* 20(2):167–174, 2001.

[6]Boriek, A. M., W. Hwang, L. Trinh, and J. R. Rodarte. Shape and tension distribution of the active canine diaphragm. *Am. J. Physiol. Regul. Integr. Comp. Physiol.* 288(4):R1021–R1027, 2005.

[7]Brandao, S., M. Parente, T. Mascarenhas, A. R. da Silva, I. Ramoss, and R. N. Jorge. Biomechanical study on the bladder neck and urethral positions: simulation of impairment of the pelvic ligaments. *J. Biomech.* 48(2):217–223, 2015.

[8]Brandao, F. S., M. P. Parente, P. A. Rocha, M. T. Saraiva, I. M. Ramos, and R. M. Natal. Jorge. Modeling the contraction of the pelvic floor muscles. *Comput. Methods Biomech. Biomed. Eng.* 19(4):347–356, 2016.

[9]Damon, B. M., Z. Ding, A. W. Anderson, A. S. Freyer, and J. C. Gore. Validation of diffusion tensor MRI-based muscle fiber tracking. *Magn. Reson. Med.* 48(1):97–104, 2002.

[10]DeLancey, J. O., R. Kearney, Q. Chou, S. Speights, and S. Binno. The appearance of *levator ani* muscle abnormalities in magnetic resonance images after vaginal delivery. *Obstet. Gynecol.* 101(1):46–53, 2003.

[11]Deux, J. F., P. Malzy, N. Paragios, G. Bassez, A. Luciani, P. Zerbib, F. Roudot-Thoraval, A. Vignaud, H. Kobeiter, and A. Rahmouni. Assessment of calf muscle contraction by diffusion tensor imaging. *Eur. Radiol.* 18:2303–2310, 2008.

[12]Fielding, J. R., H. Dumanli, A. G. Schreyer, S. Okuda, D. T. Gering, K. H. Zou, R. Kikinis, and F. A. Jolesz. MR-based three-dimensional modeling of the normal pelvic floor in women: quantification of muscle mass. *AJR Am. J. Roentgenol.* 174(3):657–660, 2000.

[13]Froeling, M., A. J. Nederveen, K. Nicolay, and G. J. Strijkers. DTI of human skeletal muscle: the effects of diffusion encoding parameters, signal-to-noise ratio and T2 on tensor indices and fiber tracts. *NMR Biomed.* 26(11):1339–1352, 2013.

[14]Gregory, W. T., R. Nardos, T. Worstell, and A. Thurmond. Measuring the *levator hiatus* with axial MRI sequences: adjusting the angle of acquisition. *Neurourol. Urodyn.* 30:113–116, 2011.

[15]Huiskes, H. W., D. Van Campen, and J. R. de Wijn (Ed.). Biomechanics: Principles and Applications. Selected Proceedings of the 3rd General Meeting of the European Society of Biomechanics Nijmegen, The Netherlands, 21–23 January, 1982.

[16]Kearney, R., J. M. Miller, J. A. Ashton-Miller, and J. O. DeLancey. Obstetric factors associated with *levator ani* muscle injury after vaginal birth. *Obstet. Gynecol.* 107(1):144–149, 2006.

[17]Khodaei, H., S. Mostofizadeh, K. Brolin, H. Johansson, and J. Osth. Simulation of active skeletal muscle tissue with a transversely isotropic viscohyperelastic continuum material model. *Proc. Inst. Mech. Eng. H.* 227(5):571–580, 2013.

[18]Ling, S., B. Chen, Y. Zhou, W. Z. Yang, Y. Q. Zhao, L. Wang, and Y. P. Zheng. An efficient framework for estimation of muscle fiber orientation using ultrasonography. *Biomed. Eng. Online.* 2:98, 2013.

[19]Manjon, J. V., P. Coupe, L. Concha, A. Buades, D. L. Collins, and M. Robles. Diffusion weighted image denoising using overcomplete local PCA. *PLoS ONE* 8(9):e73021, 2013.

[20]Margulies, R. U., Y. Hsu, R. Kearney, T. Stein, W. H. Umek, and J. O. DeLancey. Appearance of the *levator ani* muscle subdivisions in magnetic resonance images. *Obstet. Gynecol.* 107(5):1064–1069, 2006.

[21]Margulies, R. U., M. Huebner, and J. O. DeLancey. Origin and insertion points involved in *levator ani* muscle defects. *Am. J. Obstet. Gynecol.* 196(3):251e1–251e5, 2007.

[22]Martins, J. A., M. P. Pato, E. B. Pires, R. M. Jorge, M. Parente, and T. Mascarenhas. Finite element studies of the deformation of the pelvic floor. *Ann. N. Y. Acad. Sci.* 1101:316–334, 2007.

[23]Mazzoli, V., J. Oudeman, K. Nicolay, M. Maas, N. Verdonschot, A. M. Sprengers, A. J. Nederveen, M. Froeling, and G. J. Strijkers. Assessment of passive muscle elongation using diffusion tensor MRI: correlation between fiber length and diffusion coefficients. *NMR Biomed.* 2016. doi: 10.1002/nbm.3661.

[24]Noakes, K. F., A. J. Pullan, I. P. Bissett, and L. K. Cheng. Subject specific finite elasticity simulations of the pelvic floor. *J. Biomech.* 41(14):3060–3065, 2008.

[25]Odegard, G. M., T. L. Donahue, D. A. Morrow, and K. R. Kaufman. Constitutive modeling of skeletal muscle tissue with an explicit strain-energy function. *J. Biomech. Eng.* 130(6):061017, 2008.

[26]Parente, M. P., R. M. Jorge, T. Mascarenhas, A. A. Fernandes, and J. A. Martins. Deformation of the pelvic floor

muscles during a vaginal delivery. *Int. Urogynecol. J. Pelvic Floor Dysfunct.* 19(1):65–71, 2008.
[27]Parker, G. J. Analysis of MR diffusion weighted images. *Br. J. Radiol.* 77(Spec No 2):S176–S185, 2004.
[28]Peng, Y., R. Khavari, N. A. Nakib, T. B. Boone, and Y. Zhang. Assessment of urethral support using MRI-derived computational modeling of the female pelvis. *Int. Urogynecol. J.* 27(2):205–212, 2016.
[29]Rousset, P., V. Delmas, J. N. Buy, A. Rahmouni, D. Vadrot, and J. F. Deux. *In vivo* visualization of the *levator ani* muscle subdivisions using MR fiber tractography with diffusion tensor imaging. *J. Anat.* 221(3):221–228, 2012.
[30]Saleme, C. S., M. P. Parente, R. M. Natal Jorge, M. Pinotti, A. L. Silva-Filho, T. Roza, T. Mascarenhas, and J. M. Tavares. An approach on determining the displacements of the pelvic floor during voluntary contraction using numerical simulation and MRI. *Comput. Methods Biomech. Biomed. Eng.* 14(4):365–370, 2011.
[31]Scheel, M., P. von Roth, T. Winkler, A. Arampatzis, T. Prokscha, B. Hamm, and G. Diederichs. Fiber type characterization in skeletal muscle by diffusion tensor imaging. *NMR Biomed.* 26(10):1220–1224, 2013.
[32]Schenk, P., T. Siebert, P. Hiepe, D. Güllmar, J. R. Reichenbach, C. Wick, R. Blickhan, and M. Böl. Determination of three-dimensional muscle architectures: validation of the DTI-based fiber tractography method by manual digitization. *J. Anat.* 223(1):61–68, 2013.
[33]Shobeiri, S. A., R. R. Chesson, and R. F. Gasser. The internal innervation and morphology of the human female *levator ani* muscle. *Am. J. Obstet. Gynecol.* 199:681–686, 2008.
[34]Sinha, S., U. Sinha, and V. R. Edgerton. *In vivo* diffusion tensor imaging of the human calf muscle. *J. Magn. Reson. Imaging* 24(1):182–190, 2006.
[35]Studholme, C., D. L. G. Hill, and D. J. Hawkes. An overlap invariant entropy measure of 3D medical image alignment. *Pattern Recogn.* 32(1):71–86, 1999.
[36]Tamanini, J. T., M. Dambros, C. A. D'Ancona, P. C. Palma, and N. Rodrigues Netto, Jr. Validation of the "International Consultation on Incontinence Questionnaire—Short Form" (ICIQ-SF) for Portuguese. *Rev. Saude Publica* 38(3):438–444, 2004.
[37]Tans, T., P. Apinuntrum, T. Phetudom, and P. Phanchart. New insights into the pelvic organ support framework. *Eur. J. Obstet. Gynecol. Reprod. Biol.* 166(2):221–225, 2013.
[38]Trivedi, R., R. K. S. Rathore, and R. K. Gupta. Review: clinical application of diffusion tensor imaging. *Indian J. Radiol. Imaging.* 18(1):45–52, 2006.
[39]Van Donkelaar, C. C., L. J. Kretzers, P. H. Bovendeerd, L. M. Lataster, K. Nicolay, J. D. Janssen, and M. R. Drost. Diffusion tensor imaging in biomechanical studies of skeletal muscle function. *J. Anat.* 194(Pt 1):79–88, 1999.
[40]Van Doorn, A., P. H. Bovendeerd, K. Nicolay, M. R. Drost, and J. D. Janssen. Determination of muscle fibre orientation using diffusion-weighted MRI. *Eur. J. Morphol.* 34(1):5–10, 1996.
[41]Walton, C., Z. Li, A. Pennings, A. Agur, and A. Elmaraghy. A 3-Dimensional anatomic study of the distal biceps tendon. *Orthop. J. Sports Med.* 3(6):2325967115585113, 2015.
[42]Whitcher, B., D. S. Tuch, J. J. Wisco, A. G. Sorensen, and L. Wang. Using the wild bootstrap to quantify uncertainty in diffusion tensor imaging. *Hum. Brain Mapp.* 29(3):346–362, 2008.
[43]Zijta, F. M., M. Froeling, M. P. van der Paardt, M. M. Lakeman, S. Bipat, A. D. van Swijndregt, G. J. Strijkers, A. J. Nederveen, and J. Stoker. Feasibility of diffusion tensor imaging (DTI) with fibre tractography of the normal female pelvic floor. *Eur. Radiol.* 21(6):1243–1249, 2011.
[44]Zijta, F. M., M. M. Lakeman, M. Froeling, M. P. van der Paardt, C. S. Borstlap, S. Bipat, A. D. M. van Swijndregt, G. J. Strijkers, J. P. Roovers, A. J. Nederveen, and J. Stoker. Evaluation of the female pelvic floor in pelvic organ prolapse using 3.0-Tesla diffusion tensor imaging and fibre tractography. *Eur. Radiol.* 22(12):2806–2813, 2012.

Chapter 4

Integrated Discussion

The Original Studies presented in this Thesis corroborate the contribution of MRI in the morfo-functional evaluation of the female pelvic floor muscles for biomechanical analysis and modeling. Firstly, the static images can be used to appraise detailed anatomy and are valuable inputs for subject-specific models. Moreover, dynamic images can be used for real-time observation of the morphologic changes of the pelvic floor muscles and organs, and can furthermore supply validation for the results when modeling contraction, valsalva maneuver, etc. Finally, although the majority of the biomechanical simulation processess rely on the geometry provided by "conventional" images, DTI can further detail on local muscle structure by providing an *in vivo* indirect representation of oriented muscle fibers, which may be required during finite element modeling of muscle active response.

Pelvic floor MR examination protocols usually start with multiplanar images, the axial plane being the firstly used to score pelvic floor muscles defects. Thinner *levator ani* and wider and warped *levator hiatus* shape are frequent findings in symptomatic women with SUI and POP (Hoyte, Jakab et al. 2004) (Hoyte, Schierlitz et al. 2001). Although not being a subjective analysis, evaluating the morphology of both muscles and *hiatus* in the axial images acquired at rest lacks the translation to a biomechanical reply. However, conceptually, muscle architecture and morphology relate with strength (Jones, Bishop et al. 2008), and thus perhaps some conclusions can be drawn. In Study I, we found thinner (and decreased area) *puboviscerali*s muscle, larger *levator hiatus* in women with POP (comparable to previous studies (Hoyte, Schierlitz et al. 2001) (Ying, Li et al. 2012)), and almost one-third of the mean value of the MOI compared to that of the controls. Knowing that the lower the MOI, the lower resistance to deformation, we tried to establish a relation between the values obtained for women with POP and the inferior resistance that their pelvic floor muscles can impose against deformation occuring from increased IAP. A

weaker muscle biomechanical response as a result of the loss of mechanical elasticity may be related to a need for an increased force during contraction (Vakili, Zheng et al. 2005). In fact, the concomitant increased hiatal dimensions - and therefore the diameter for its axis of rotation and bending - may be relevant. Furthermore, it appears that even after surgery, abnormal hiatal distensibility persists in most cases despite its purpose of reducing hiatal area (Andrew, Shek et al. 2013) (Vakili, Zheng et al. 2005), which suggests it as the cause rather than the effect of organ prolapse. This Study I was a pilot study, and should be applied to a larger sample in the future. Moreover, the measures performed in the static images sould be validated against the dynamic images and correlated with hiatal measures taken there.

Performing dynamic imaging is not an easy task, and this has been experienced during the present work. Teaching the subjects on how to perform correct progressive and/or maximal pelvic floor muscles contraction or valsalva maneuver is imperative, as for Studies II, III and IV. Also, repeated acquisitions are advised. Furthermore, optimizing the imaging protocol for these ultrafast MR sequences (T2-weighted single-shot fast spin-echo (SS-FSE) or steady state precession (SSFP, gradient echo-based) needs a balance between tissue contrast, motion artifacts, and spatial *vs.* temporal resolution (El Sayed, Alt et al. 2016) (Reiner and Weishaupt 2013). Six-mm thick half-Fourier acquisition SS-FSE (called HASTE sequences) images were used in the Original Studies. Although they may require slightly longer acquisition time (Hecht, Lee et al. 2008) (Pizzoferrato, Nyangoh Timoh et al. 2014), imaging artifacts related to the presence of air in the rectum (because endorectal ultrasound gel was not used in our studies) are less probable to appear than in the SSFP, and this is important when evaluating the contours of anatomical structures, e.g. the rectum, anterior vaginal wall and urethra, as in Study III. Furthermore, all pelvic examinations were performed in a 3.0T magnetic field intensity scanner, and field in-

homogeneity and susceptibility-related artifacts were expected to be more pronounced in gradient echo-based sequences.

As previously mentioned, the sagital plane is by far the most used. Nevertheless, we were interested in exploring the axial plane, which was in fact recently advised by the European Societies of Gastrointestinal and Abdominal Radiology, and Urogenital Radiology (El Sayed, Alt et al. 2016). In Study II, the plane of minimal hiatal dimensions (Dietz, Shek et al. 2005) (Gregory, Nardos et al. 2011) was used to assess the diameter of the *levator hiatus* as a result of muscle contraction. The pulse sequence that showed better results was a SE-based echo planar imaging (EPI) sequence with fat suppression. With this sequence, we succeeded in optimizing an acquisition protocol of 20 sec "rest" *vs.* 10 sec "maximal contraction" blocks with good quality 3-mm contiguous axial *cine* images, although 2 out of the 16 women were notwithstandingly excluded due to artifacts. In Study II, former high-impact sports practitioners evidenced lower ability to contract the pelvic floor muscles than controls ($p=0.004$), which was corroborated by a lower score on the Oxford Grading Scale ($p=0.005$).

Young athletes and women with high-levels of physical activity are an interesting group to study the long-term effect of high-impact exercising on the pelvic floor muscles. Despite the fact that the women included in our sample do not demonstrate symptoms of SUI at present, they had left the sports practice due to urine loss, and having UI early in life and during elite sport practice seems to be a strong predictor of UI later at some point, according to Bø *et al.* (Bo and Sundgot-Borgen 2010), and Nygaard *et al.* (Nygaard and Shaw 2016). Early diagnosis and preventive pelvic floor muscle training could help decreasing the impact of UI or other PFD later in life (Almeida, Barra et al. 2016).

Although all the women scanned for the purpose of the Original Studies were taught and trained on how to perform correct maneuvers, all the datasets were reviewed and the most suitable images were selected for analysis. The important finding is not that there were changes in the anterior abdominal wall, but the observation of cranial or caudal movement of the organs with simultaneous hiatal shortening or widening (Tumbarello, Hsu et al. 2010) in contraction and valsalva maneuver or defection, respectively.

Acknowledging that the precautions taken can increase the reliability of comparing the results of muscle and organ displacement on dynamic MRI against those from numerical simulation, it would be of interest to have real-time and subject-specific measurements of the IAP in the MR scanner with a vaginal or rectal MR-compatible probe with pressure sensors (van Raalte and Egorov 2015). In that context, the values of IAP used in Studies III, IV and V during the modeling process were the ones published by Noakes *et al.* (0.5 kPa for resting tone and 4.0 kPa for valsalva maneuver), assuming those as average values for the supine position of women during the MR pelvic examination.

However, it must be noted that the supine position does not mimic the normal physiologic state in daily-life activities. Open scanners where the pelvic examinations can be performed in the sitting position seem to increase the sensitivity to pelvic floor descent (Bertschinger, Hetzer et al. 2002) (Iacobellis, Brillantino et al. 2016), and could perhaps be the most suited for this type of studies.

SUI affects between 4% and 35% of adult women (Luber 2004). Aging, neurologic diseases, diabetes, obesity, pregnancy and vaginal childbirth are well-known associated risk factors (Luber 2004) (Stothers and Friedman 2011). Ultrasound is usually the first imaging technique performed to appraise muscle defects and functional anatomy. Bladder neck dislocation and urethral hypermobility can be evaluated by means of the posterior

urethrovesical angle (between proximal urethra and the trigone) and the α-angle (between the bladder neck and the *symphysis pubis*) at maximal valsalva maneuver (Dietz 2010).

Thin-slice high resolution MR images, as in Figure 1 of Study IV, provide excellent anatomical detail of the peri-, para- and pubourethral ligaments, the retropubic space, the thickness and signal intensity of the urethra, the shape of the vagina, etc. Besides that, dynamic mid-sagittal images can be used to apply the abovementioned (or similar) metrics, e.g., the angle of urethral inclination, the posterior urethro-vesical angle and the position of the bladder base, which can be done by using the PCL as reference (Perk, Oral et al. 2002). A positive correlation has been shown between the severity of SUI symptoms and the performed measures (Tarhan, Bilali Gumus et al. 2010), which makes dynamic MRI an alternative to ultrasound. The point to retain is that an optimized set of ultrafast sequences still displays adequate soft tissue contrast and spatial resolution to provide this anatomo-functional information, as shown in Studies III and IV.

In Study IV, we adopted the same coordinate system for the MR images and the numerical model as the ones described in ultrasound to measure the α-angle and the bladder neck dislocation (Pregazzi, Sartore et al. 2002) (Schaer, Koechli et al. 1995). Numerical simulation of valsalva maneuver (before modeling the ligaments as impaired) resulted in values close to the ones from the MR images (α-angle was 105.71º *vs.* 103.31º, and the bladder neck moved postero-inferiorly 5.7 mm *vs.* 5 mm, respectively). When simulating the isolated impairment of the ligaments, that of the PUL seems to have the greatest impact, which is in line with the important role assigned to the PUL in urethral and bladder support (Petros and Woodman 2008).

In this study, the pelvic floor muscles were considered as healthy in the simulation of valsalva maneuver, while evaluating the effect of impairment of the ligaments that provide pelvic organ support. Disruption of the PUL, among the direct urethral supporters, means

the loss of the pivot that keeps the position of the urethra, and is a frequent finding in women with SUI (Macura, Genadry et al. 2006) (Macura, Thompson et al. 2015) (Tasali, Cubuk et al. 2012). Furthermore, muscle defects, loss of symmetry, lateral deviation and thinning have been described, which means loosing the additional force to close the urethra during an increase in IAP (Macura, Genadry et al. 2006).

The magnitude displacement of the pelvic floor muscles increased when the ligaments were simulated as impaired. These results are presented here (not shown in the paper). The maximum magnitude displacement of the pelvic floor muscles when considering all the ligaments as healthy was 8.0 mm. For 95% impairment of all the pelvic ligaments, this value increased to 18.4 mm, and when only the PUL or the cardinal and uterosacral ligaments were considered the values were 17.1 and 16.2 mm. These results seem to reflect the loss of support to the pelvic organs that the ligaments no longer provide during valsalva maneuver. Therefore, the pelvic floor muscles cannot fully sustain by themselves the increased IAP, with consequent downward motion of the organs, which may further increase the pressure over the bladder and the bladder neck.

SUI with urethral hypermobility may be corrected with synthetic midurethral slings. MRI is not a first line imaging technique when it comes to evaluating midurethral slings, mostly due to accessibility and cost, but may be advised when local infection is suspected. The slings are usually depicted in MRI as low intensity structures on the retropubic space, at the level of the mid- or lower urethra, but the close relation to the urethra may be more difficult to evaluate (Denson and Shobeiri 2014) (Giri, Drumm et al. 2011) (Schuettoff, Beyersdorff et al. 2006). Dynamic MRI can also be applied to evaluate its position and effectiveness at restricting the downward movement of the urethra during coughing and voiding (Rinne, Kainulainen et al. 2011).

The meshes vary in configuration, material and manufacturing, and in fact, the choice may be a balance between flexibility and adjustability, and the known post-operative complication rates (Costantini, M. et al. 2007) (Moalli, Papas et al. 2008) (Reddy, Williams et al. 2009) (Shah and Badlani 2012). The sling is initially held in place solely by frictional forces between the mesh and the urethra. Tissue in-growth that occurs afterwards helps to maintain the sling´s position under the effect of increased IAP, but a higher stiffness of the mesh may delay or hamper mesh-local tissue integration (Siegel, Kim et al. 2005).

Results of experimental mechanical tests have shown that diferences in structural and thermal features explain distinct mechanical properties (Afonso, Jorge et al. 2009) (Afonso, Martins et al. 2008) (Dietz, Vancaillie et al. 2003). Nevertheless, to the best of our knowledge, not much research has been published in regards to applying those properties to computational analysis of the outcome of placing a sling, not only regarding its interaction with the urethral (and vaginal) tissue, but also on its effectiveness regarding the position of the bladder neck, as performed in Study VI. A recent study published by Peng *et al.* showed that placing the sling in the mid-distal urethra provides sufficient reposicioning during valsalva maneuver with reduced force between the sling and the posterior urethral wall (Peng, Khavari et al. 2015).

The results of Study IV and the interest on studying SUI, lead us to focus on the impairment of the pelvic floor muscles, muscles and different pelvic ligaments (the PUL, the uterosacral and the cardinal ligaments, and the lateral ligaments of the rectum), but also the combined impairment of the PUL and muscles, which is often described in the case of SUI associated to vaginal chilbirth injury (Sajadi, Gill et al. 2010). In Study V we set distinct material parameters in order to model a mesh with “higher” and another with “lower” stiffness. The numerical model was able to reproduce the presence of the sling, by

reducing the α-angle and the magnitude displacement of the bladder and the urethra, and that of the bladder neck. We found that whether $Mesh_{HS}$ or $Mesh_{LS}$ are applied, the α-angle measured at valsalva was reduced to values similar to that of the existing literature for asymptomatic women (Pregazzi, Sartore et al. 2002) (Sweed and Sharara 2016). Despite the fact that both slings can reduce the α-angle and the motion of the bladder and urethra, the additional force exerted by the $Mesh_{HS}$ in the urethral wall, as it may imply higher transmission of loads to the tissue, can contribute to explain urethral erosion in the long-term (Dietz, Vancaillie et al. 2003), and this is why Reddy *et al* advised to adjust the tensioning techniques (Reddy, Williams et al. 2009). The drawback of using meshes with a lower stiffness may be related its excessive (abnormal) deformation (Jones, Feola et al. 2009) (Moalli, Papas et al. 2008) which may compromise their effectiveness and, therefore, an increase in the α-angle may be expected. The results of Study V could be enriched by a longitudinal clinical evaluation of patients with diferent types of meshes, and MRI / ultrasound measurements along with subject-specific numerical modeling for comparison.

The 3 *levator ani* subdivisions are not easy to fully differentiate in conventional multi-planar MR images, but efforts were made to define their orientation, and to approximate the direction of the muscles fibers and their line of action (Margulies, Huebner et al. 2007) (Margulies, Hsu et al. 2006). Furthermore, as pointed out by Betschart *et al.*, these two features determine the mechanical behavior of each muscle component, as well as their pennation angle, among others (Betschart, Kim et al. 2014). Organ positioning and lifting seems to be provided by the *iliococcygeus* and *pubococcygeus* muscles, while the *puborectalis* muscle is the main hiatal constrictor. This was substantiated by the findings of Betschart and collegues, with positive (and higher) angles ($33.1^{o}\pm8.8$ and $40.7^{o}\pm8.0$, for the

former two) and negative (and lower) angles (-19.0º±0.1 for the latter) relative to an axial reference axis (Betschart, Kim et al. 2014). Along the same line, Heemskerk *et al.* found the longest fibers in the *puboviscerali*s component of the *levator ani*, which explains its relaxation to allow defecation, and its shortening to close the *levator hiatus*, actions that require large muscle excursions (Heemskerk and Damon 2007).

Modeling active conscious contraction of the pelvic floor muscles may be considered of interest to understand the mechanisms of PDF. The pelvic floor muscles antero-superior movement promotes urethral closure to prevent urine leakage and also to a certain degree, organ descent. In Study III, we found muscles to move anteriorly at a maximum of nodal displacement of 5.2 mm and 6.6 mm upward, similar to that of the dynamic MR images of the same women (these showing 0.2 mm less anterior and 4.1 mm less upward displacement). One one hand, the differences can be related with the value of the baseline ("organ load") IAP assumed in the modeling process as the reference for displacement assessment. This could be lower than the real baseline pressure of the subject laying in the scanner, which afforded a more evident upward lift of the pelvic floor muscles (and organs) when compared to the ones of dynamic MRI. On the other hand, since we lacked quantitative real-time assessment on the subject´s performance while contracting the pelvic floor muscles, we cannot discard the possibility that the differences could be related to the demands of maintaning maximum contraction, which was performed in the numerical simulation (maximum activation level, $\alpha=1$), and resulted in nodal displacements in the range of what is clinically expected and meaningful for an asymptomatic woman.

Despite the abovementioned methodological issues, the numerical model developed in Study III was able to reproduce the expected pattern of muscle displacement, being higher in the posterior portion of the pelvic floor (corresponding to the anorectal region), in line with previous studies using MRI and ultrasound (Constantinou, Hvistendahl et al. 2002)

(Raizada, Bhargava et al. 2010) (Yang, Huang et al. 2009). Furthermore, the model showed that this strong antero-superior pulling that makes the anorectal angle move ventrally and cephaladly, and seems to create a higher stress field in the vaginal region where larger deformations seem to occur. This may be consistent with the vaginal higher pressure zone described by Raizada and collegues (Raizada, Bhargava et al. 2010).

Muscles are structurally anisotropic, which is necessary for generating mechanical events related to the direction of the required task. When modeled as transversely isotropic structures (Blemker and Delp 2005) (Khodaei, Mostofizadeh et al. 2013) (Martins, Pato et al. 2007) (Odegard, Donahue et al. 2008), often the direction of anisotropy (the one that provides the fiber direction) is assumed as being coincident with the fiber direction in each finite element (Gielen, Oomens et al. 2000). This concept has been applied by different authors - with distinct constitutive equations (d'Aulignac, Martins et al. 2005) (Gielen, Oomens et al. 2000) (Martins, Pato et al. 2007) (Oomens, Maenhout et al. 2003) - including when studying the pelvic floor muscles (d'Aulignac, Martins et al. 2005) (Martins, Pato et al. 2007)**.**

While some of those authors assume muscle passive response as largely attributable to the collagen in the extracellular matrix and therefore do not include muscle fiber direction in their mathematical formulations (Gielen, Oomens et al. 2000) (Oomens, Maenhout et al. 2003), others have that into consideration for numerical simulation of muscle´s active response (d'Aulignac, Martins et al. 2005) (Martins, Pato et al. 2007) (Odegard, Donahue et al. 2008) (Parente, Natal Jorge et al. 2010) (Blemker, Pinsky et al. 2005) (Oomens, Maenhout et al. 2003). This seems of relevance, since its architecture is a predictor of function (Lieber and Friden 2000), i.e., upon activation, the cross-bridging in skeletal

muscle creates a tensile stress along the muscle fiber axis (Van Donkelaar, Kretzers et al. 1999).

One approach for modeling muscle fibers is to assume that the fibers are aligned with the direction of the maximum principal stress lines (Boriek, Hwang et al. 2005) (Huiskes, Van Campen et al. 1982). That can be obtained for the pelvic floor muscles when this "bowl-like"structure is subjected to a distributed load normal to its inner surface (d'Aulignac, Martins et al. 2005), which was performed in Studies III and VI. This resulted in an adequate pattern of deformation of the finite element model, mimicking the default anatomical behavior and a globally expected orientation of the maximum principal stress lines.

To the best of our knowledge, no previous study compared the direction of the muscles fibers obtained with the maximum principal stress lines and those from DTI of the pelvic floor muscles. Comparing the first eigenvector of the stress tensor and the one from the DT tensor is inherently equivalent to comparing an approximation to the main orientation of the muscle fibers.

Performing pelvic floor DTI and obtaining good-quality images for reliable diffusion tensor estimates and 3D representation brings several technical challenges, as well detailed by Rousset *et al.* (Rousset, Delmas et al. 2012), and also explained in Study VI. In this Study, we chose to focus on the *pubovisceralis* muscle, for four reasons: first, it is easier to identify and segment; second, it is thick and therefore it is represented in the DT images by a sufficient number of voxels; third, it has smaller changes in direction than the *iliococcygeus* muscle. Finally, due to its abovementioned important role on (urinary and fecal) (in)continence, it is intensely evaluated for strength and morphologic abnormalities (Dietz, Hyland et al. 2006). The prevalence of injuries in the *pubovisceralis* is reported to be up to 36% in women having performed vaginal delivery, and can be observed as a

partial or complete loss of attachment to its pubic insetion or loss of muscle bulk (Lammers, Futterer et al. 2012).

The results of Study VI revealed lower similarity between the methods in the muscles insertions and in the anorectal area when compared to its middle portion, and the boundary conditions inherent to the modeling process were pointed out as a possible reason for that. Despite the fact that data points of fixed boundary conditions mimicking muscle insertions were set according to detailed visual inspection of the axial images, this procedure lacks histological validation, and therefore we cannot discard that it can be the source of some errors.

Different acqusition schemes and post-processing strategies have been applied to brain DTI to identify the complex anatomy of axons. The use of probabilistic (Onu 2014) tractography (which outputs connection strengths or probabilistic distribution when determining the direction for propagating fiber tracts) seems to show good results describing highly angulated fibers (Bach, Behrens et al. 2011) (O'Donnell and Westin 2011) in DT datasets with a sufficient number of diffusion gradient encoding directions (GadElkarim, Zhan et al. 2011) (e.g., 32 as in the case of our study). This could improve the results for the anorectal area, although at the cost of increased computational complexity and time, which can be explored in a near future.

Recent acquisition schemes such as high angular resolution diffusion-weighted imaging (HARDI) allow applying nonparametric approaches to compute molecular probability distribution function without assuming a particular (Gaussian) diffusion model (Tuch 2004), which can reveal further details on the distribution of fiber directions. HARDI implies acquiring high diffusion sensitization values (b-values), and this presents several drawbacks, e.g., a decrease in signal-to-noise ratio (SNR) that can only be compensated for by increasing the acquisition time. Furthermore, they are more prone to

artifacts from eddy currents, leading to geometric distortion of the DT images. Finally, the increase in the echo time (TE) required for high b-values may go far above the selected for our study (TE=40msec) according to the T2 relaxation time of skeletal muscle, which is around 35 msec at 3.0T (Froeling, Nederveen et al. 2013).

A previous study with a very high-resolution DTI acquisition in an anesthetized rat showed that a voxel size of around $1mm^3$ provides sufficient resolution and acceptable accuracy to map the direction of the muscle fibers (validated against histology) to import those to a finite element mesh (Van Donkelaar, Kretzers et al. 1999). However, acquiring female pelvic DT images with such spatial resolution to accomplish 1:1 direct integration of the tensor data is very challenging. Therefore, averaging the MPSL vectors within all the finite elements included in each voxel was the chosen methodology, as explained in the Discussion section of Study VI.

Study VI was the first approach to retrieve and compare two indirect methods for obtaining the direction of the pelvic floor muscle fibers. It should therefore be viewed in this way, as a starting point for reflection on the methodological difficulties that require additional strategies to be developed considering dedicaded pelvic floor DTI protocols and post-processing approaches.

Chapter 5

Conclusions

The work developed in this PhD Thesis provided new insights on the biomechanical behavior of the pelvic floor muscles, with a relevant contribution from MRI. With the Studies performed, we were able to further confirm MRI as bringing important inputs to the modeling process, not only regarding the geometry of the structures involved, but also providing non-invasive assessment of the dynamic maneuvers, such as contraction or valsava maneuver, that allow validating the numerical results. The models built for the purpose of these Studies showed similar displacement of the pelvic floor muscles and organs than that of the real-subject dynamic MR acquisitions, which means that the most relevant methodological options for the modeling process were adequate. Furthermore, the direction of the muscle fibers retrieved from DTI and the finite element method were compared. Despite the fact that these methods may require additional optimization and computational work, the results are indicative of a possible application of MRI for evaluating pelvic floor muscles microstructure to be included in the modeling, which has not been performed yet.

Chapter 6

Future Perspectives

The results of this dissertation emphasize that translational research should continue to further study the biomechanics of female PFD.

One of the first issues to which to give higher research priority in the future is the relation between the vertebral column and PFD. A pronounced curvature of the lumbar lordosis may change the pelvic girdle tilt and the static and dynamic positions of the soft tissues, since the bony pelvis has attachment points to the pelvic floor muscles such as the obturator fascia and the anococcygeal raphe. It is plausible to speculate that it probably changes the way that downward intra-abdominal forces are deflected/absorbed before they reach the pelvic floor, and may therefore be associated with PFD. Few clinical studies have evaluated the relation between spinal and pelvic morphometry and associated symptoms of UI and POP (Nguyen, Lind et al. 2000) (Sahinkanat, Arikan et al. 2011) but this has not yet been extensively studied through computational models of the pelvis. A research project *"Estudo biomecânico da relação do grau de lordose lombar com a disfunção do pavimento pélvico da mulher*." has already been approved by the Conselho de Administração e Comissão de Ética do Centro Hospitalar de São João - EPE (CES 255-14) for this purpose. The main goal is to analyze the influence of the lumbar spine curvature in the distribution of the IAP, since the lack of support due to an abnormal position of the pelvic floor muscles seems to be associated to a functional biomechanical deficit. We believe that this coud add relevant information for conservative physiotherapeutic approaches including postural reeducation.

Secondly, I would be interested in performing a more clinical study on the role of MR-defecography using a multi-disciplinary approach (surgery, radiology, physical medicine and rehabilitation) of defecation disorders by evaluating the effectiveness of this static and dynamic examination protocol on patient management in a university hospital, by performing "a 4-years experience" analysis.

Thirdly, the dynamic MR images used to confirm the results of the computational analysis were acquired in supine position, which does not reflect the real physiological conditions in the daily-life. Acquiring similar images in existing scanners that allow standing or upright sitting positions is a goal to materialize in the short term. For that purpose, it is our goal to establish a visit protocol to a clinical or research center equipped with such MR scanners.

Finally, it is also in our interest to establish a research cooperation to develop and test an MR-compatible pressure sensor to retrieve real-time and subject-specific measurements of the IAP, which could feed subsequent numerical simulation studies.

In a more wide view of reinforcing the work on computational modeling, the mechanic properties of the connective tissue of the fascia and its role on developing PFD should be further elaborate in the numerical simulation studies. In the same line, the mechanical properties of the pelvic floor muscles associated to different groups (e.g. women with SUI or POP), should be included in the modeling and validated against (dynamic) MRI or ultrasound studies. At last, the damage of the the pelvic floor muscles during vaginal delivery is and perhaps will continue to be one of the main focus of this research context. Perhaps future investigations could include performing MRI or ultrasound acqusitions at the last weeks of pregnancy in women with increased risk for pelvic floor muscle damage during vaginal birth, followed by modeling the delivery options and then complementing again with a real-time evaluation during birth. We believe that ethical questions may raise, but women´s health may stand to gain.

References

Afonso, J. S., R. M. Jorge, P. S. Martins, S. Soldi Mda, O. L. Alves, B. Patricio, T. Mascarenhas, M. G. Sartori and M. J. Girao (2009). "Structural and thermal properties of polypropylene mesh used in treatment of stress urinary incontinence." Acta Bioeng Biomech **11**(3): 27-33.

Afonso, J. S., P. A. Martins, M. J. Girao, R. M. Natal Jorge, A. J. Ferreira, T. Mascarenhas, A. A. Fernandes, J. Bernardes, E. C. Baracat, G. Rodrigues de Lima and B. Patricio (2008). "Mechanical properties of polypropylene mesh used in pelvic floor repair." Int Urogynecol J Pelvic Floor Dysfunct **19**(3): 375-380.

Ahmad, A. N., A. Hainsworth, A. B. Williams and A. M. Schizas (2015). "A review of functional pelvic floor imaging modalities and their effectiveness." Clin Imaging **39**(4): 559-565.

Almeida, M. B., A. A. Barra, F. Saltiel, A. L. Silva-Filho, A. M. Fonseca and E. M. Figueiredo (2016). "Urinary incontinence and other pelvic floor dysfunctions in female athletes in Brazil: A cross-sectional study." Scand J Med Sci Sports **26**(9): 1109-1116.

Andrew, B. P., K. L. Shek, V. Chantarasorn and H. P. Dietz (2013). "Enlargement of the levator hiatus in female pelvic organ prolapse: cause or effect?" Aust N Z J Obstet Gynaecol **53**(1): 74-78.

Ashton-Miller, J. A. and J. O. DeLancey (2007). "Functional anatomy of the female pelvic floor." Ann N Y Acad Sci **1101**: 266-296.

Atherton, M. J. and S. L. Stanton (2005). "The tension-free vaginal tape reviewed: an evidence-based review from inception to current status." BJOG **112**(5): 534-546.

Bach, D. R., T. E. Behrens, L. Garrido, N. Weiskopf and R. J. Dolan (2011). "Deep and superficial amygdala nuclei projections revealed in vivo by probabilistic tractography." J Neurosci **31**(2): 618-623.

Bertschinger, K. M., F. H. Hetzer, J. E. Roos, K. Treiber, B. Marincek and P. R. Hilfiker (2002). "Dynamic MR imaging of the pelvic floor performed with patient sitting in an open-magnet unit versus with patient supine in a closed-magnet unit." Radiology **223**(2): 501-508.

Betschart, C., J. Kim, J. M. Miller, J. A. Ashton-Miller and J. O. DeLancey (2014). "Comparison of muscle fiber directions between different levator ani muscle subdivisions: in vivo MRI measurements in women." Int Urogynecol J **25**(9): 1263-1268.

Blemker, S. S. and S. L. Delp (2005). "Three-dimensional representation of complex muscle architectures and geometries." Ann Biomed Eng **33**(5): 661-673.

Blemker, S. S., P. M. Pinsky and S. L. Delp (2005). "A 3D model of muscle reveals the causes of nonuniform strains in the biceps brachii." J Biomech **38**(4): 657-665.

Bo, K. and J. Sundgot-Borgen (2010). "Are former female elite athletes more likely to experience urinary incontinence later in life than non-athletes?" Scand J Med Sci Sports **20**(1): 100-104.

Boriek, A. M., W. Hwang, L. Trinh and J. R. Rodarte (2005). "Shape and tension distribution of the active canine diaphragm." Am J Physiol Regul Integr Comp Physiol **288**(4): R1021-1027.

Boyadzhyan, L., S. S. Raman and S. Raz (2008). "Role of static and dynamic MR imaging in surgical pelvic floor dysfunction." Radiographics **28**(4): 949-967.

Bozkurt, M., A. E. Yumru and L. Sahin (2014). "Pelvic floor dysfunction, and effects of pregnancy and mode of delivery on pelvic floor." Taiwan J Obstet Gynecol **53**(4): 452-458.

Brandao, A. C. and P. Ianez (2013). "MR imaging of the pelvic floor: defecography." Magn Reson Imaging Clin N Am **21**(2): 427-445.

Chamochumbi, C. C., F. R. Nunes, R. R. Guirro and E. C. Guirro (2012). "Comparison of active and passive forces of the pelvic floor muscles in women with and without stress urinary incontinence." Rev Bras Fisioter **16**(4): 314-319.

Chanda, A., V. Unnikrishnan, S. Roy and H. E. Richter (2015). "Computational Modeling of the Female Pelvic Support Structures and Organs to Understand the Mechanism of Pelvic Organ Prolapse: A Review." Applied Mechanics Reviews **67**(4).

Chen, L., J. A. Ashton-Miller and J. O. DeLancey (2009). "A 3D finite element model of anterior vaginal wall support to evaluate mechanisms underlying cystocele formation." J Biomech **42**(10): 1371-1377.

Chen, L., J. A. Ashton-Miller, Y. Hsu and J. O. DeLancey (2006). "Interaction among apical support, levator ani impairment, and anterior vaginal wall prolapse." Obstet Gynecol **108**(2): 324-332.

Colgan, N. C., M. D. Gilchrist and K. M. Curran (2010). "Applying DTI white matter orientations to finite element head models to examine diffuse TBI under high rotational accelerations." Prog Biophys Mol Biol **103**(2-3): 304-309.

Constantinou, C. E., G. Hvistendahl, A. Ryhammer, L. L. Nagel and J. C. Djurhuus (2002). "Determining the displacement of the pelvic floor and pelvic organs during voluntary contractions using magnetic resonance imaging in younger and older women." BJU Int **90**(4): 408-414.

Costantini, E., M. Lazzeri and M. Porena (2007). "Managing Complications after Midurethral Sling for Stress Urinary Incontinence. ." European Association of Urology. EAU-EBU Update Series **5**(6): 232-240.

Costantini, E., L. M. and M. Porena (2007). "Managing Complications after Midurethral Sling for Stress Urinary Incontinence." EAU-EBU Update Series,. **5**(6): 232-240.

d'Aulignac, D., J. A. Martins, E. B. Pires, T. Mascarenhas and R. M. Jorge (2005). "A shell finite element model of the pelvic floor muscles." Comput Methods Biomech Biomed Engin **8**(5): 339-347.

Da Roza, T., S. Brandao, T. Mascarenhas, R. N. Jorge and J. A. Duarte (2015). "Volume of training and the ranking level are associated with the leakage of urine in young female trampolinists." Clin J Sport Med **25**(3): 270-275.

Damon, B. M., A. K. Buck and Z. Ding (2011). "Diffusion-Tensor MRI Based Skeletal Muscle Fiber Tracking." Imaging Med **3**(6): 675-687.

DeLancey, J. O., R. Kearney, Q. Chou, S. Speights and S. Binno (2003). "The appearance of levator ani muscle abnormalities in magnetic resonance images after vaginal delivery." Obstet Gynecol **101**(1): 46-53.

DeLancey, J. O., D. M. Morgan, D. E. Fenner, R. Kearney, K. Guire, J. M. Miller, H. Hussain, W. Umek, Y. Hsu and J. A. Ashton-Miller (2007). "Comparison of levator ani muscle defects and function in women with and without pelvic organ prolapse." Obstet Gynecol **109**(2 Pt 1): 295-302.

Demaagd, G. A. and T. C. Davenport (2012). "Management of urinary incontinence." P T **37**(6): 345-361H.

Denson, L. and S. A. Shobeiri (2014). "Three-dimensional endovaginal sonography of synthetic implanted materials in the female pelvic floor." J Ultrasound Med **33**(3): 521-529.

Dietz, H. P. (2010). "Pelvic floor ultrasound: a review." Am J Obstet Gynecol **202**(4): 321-334.

Dietz, H. P., G. Hyland and J. Hay-Smith (2006). "The assessment of levator trauma: a comparison between palpation and 4D pelvic floor ultrasound." Neurourol Urodyn **25**(5): 424-427.

Dietz, H. P., C. Shek and B. Clarke (2005). "Biometry of the pubovisceral muscle and levator hiatus by three-dimensional pelvic floor ultrasound." Ultrasound Obstet Gynecol **25**(6): 580-585.

Dietz, H. P., P. Vancaillie, M. Svehla, W. Walsh, A. B. Steensma and T. G. Vancaillie (2003). "Mechanical properties of urogynecologic implant materials." Int Urogynecol J Pelvic Floor Dysfunct **14**(4): 239-243; discussion 243.

El Sayed, R. F., C. D. Alt, F. Maccioni, M. Meissnitzer, G. Masselli, L. Manganaro, V. Vinci, D. Weishaupt, Esur and E. P. F. W. Group (2016). "Magnetic resonance imaging of pelvic floor dysfunction - joint recommendations of the ESUR and ESGAR Pelvic Floor Working Group." Eur Radiol.

El Sayed, R. F., S. El Mashed, A. Farag, M. M. Morsy and M. S. Abdel Azim (2008). "Pelvic floor dysfunction: assessment with combined analysis of static and dynamic MR imaging findings." Radiology **248**(2): 518-530.

Eliasson, K., T. Larsson and E. Mattsson (2002). "Prevalence of stress incontinence in nulliparous elite trampolinists." Scand J Med Sci Sports **12**(2): 106-110.

Fozzatti, C., C. Riccetto, V. Herrmann, M. F. Brancalion, M. Raimondi, C. H. Nascif, L. R. Marques and P. P. Palma (2012). "Prevalence study of stress urinary incontinence in women who perform high-impact exercises." Int Urogynecol J **23**(12): 1687-1691.

Froeling, M., A. J. Nederveen, K. Nicolay and G. J. Strijkers (2013). "DTI of human skeletal muscle: the effects of diffusion encoding parameters, signal-to-noise ratio and T2 on tensor indices and fiber tracts." NMR Biomed **26**(11): 1339-1352.

GadElkarim, J. J., L. Zhan, S. L. Yang, A. F. Zhang, L. Altshuler, M. Lamar, O. Ajilore, P. M. Thompson and A. L. Kumar, A. (2011). "TDF-TRACT: Probabilistic tractography using the tensor distribution function." Biomedical Imaging: From Nano to Macro, 2011 IEEE International Symposium on: 812-816.

Gielen, A. W., C. W. Oomens, P. H. Bovendeerd, T. Arts and J. D. Janssen (2000). "A Finite Element Approach for Skeletal Muscle using a Distributed Moment Model of Contraction." Comput Methods Biomech Biomed Engin **3**(3): 231-244.

Gill, B. C., C. Moore and M. S. Damaser (2010). "Postpartum stress urinary incontinence: lessons from animal models." Expert Rev Obstet Gynecol **5**(5): 567-580.

Giri, S. K., J. Drumm, F. Wallis and H. Flood (2011). "Postoperative magnetic resonance imaging characterization of slings for female stress urinary incontinence." Neurourol Urodyn **30**(1): 108-112.

Gregory, W. T., R. Nardos, T. Worstell and A. Thurmond (2011). "Measuring the levator hiatus with axial MRI sequences: adjusting the angle of acquisition." Neurourol Urodyn **30**(1): 113-116.

Hecht, E. M., V. S. Lee, T. P. Tanpitukpongse, J. S. Babb, B. Taouli, S. Wong, N. Rosenblum, J. A. Kanofsky and G. L. Bennett (2008). "MRI of pelvic floor dysfunction: dynamic true fast imaging with steady-state precession versus HASTE." AJR Am J Roentgenol **191**(2): 352-358.

Heemskerk, A. M. and B. M. Damon (2007). "Diffusion Tensor MRI Assessment of Skeletal Muscle Architecture." Curr Med Imaging Rev **3**(3): 152-160.

Herschorn, S. (2004). "Female Pelvic Floor Anatomy: The Pelvic Floor, Supporting Structures, and Pelvic Organs. ." Rev Urol. **6**(S5): 2-10.

Hoyte, L., M. Jakab, S. K. Warfield, S. Shott, G. Flesh and J. R. Fielding (2004). "Levator ani thickness variations in symptomatic and asymptomatic women using magnetic resonance-based 3-dimensional color mapping." Am J Obstet Gynecol **191**(3): 856-861.

Hoyte, L., L. Schierlitz, K. Zou, G. Flesh and J. R. Fielding (2001). "Two- and 3-dimensional MRI comparison of levator ani structure, volume, and integrity in women with stress incontinence and prolapse." Am J Obstet Gynecol **185**(1): 11-19.

Huiskes, H. W., D. Van Campen and J. R. E. de Wijn (1982). "Biomechanics: Principles and Applications." Selected Proceedings of the 3rd General Meeting of the European Society of Biomechanics.

Iacobellis, F., A. Brillantino, A. Renzi, L. Monaco, N. Serra, B. Feragalli, A. Iacomino, L. Brunese and S. Cappabianca (2016). "MR Imaging in Diagnosis of Pelvic Floor Descent: Supine versus Sitting Position." Gastroenterology Research and Practice.

Jones, E. J., P. A. Bishop, A. K. Woods and J. M. Green (2008). "Cross-sectional area and muscular strength: a brief review." Sports Med **38**(12): 987-994.

Jones, K. A., A. Feola, L. Meyn, S. D. Abramowitch and P. A. Moalli (2009). "Tensile properties of commonly used prolapse meshes." Int Urogynecol J Pelvic Floor Dysfunct **20**(7): 847-853.

Kearney, R., J. M. Miller and J. O. Delancey (2006). "Interrater reliability and physical examination of the pubovisceral portion of the levator ani muscle, validity comparisons using MR imaging." Neurourol Urodyn **25**(1): 50-54.

Khodaei, H., S. Mostofizadeh, K. Brolin, H. Johansson and J. Osth (2013). "Simulation of active skeletal muscle tissue with a transversely isotropic viscohyperelastic continuum material model." Proc Inst Mech Eng H **227**(5): 571-580.

Lacima, G. and M. Espuna (2008). "[Pelvic floor disorders]." Gastroenterol Hepatol **31**(9): 587-595.

Lamblin, G., E. Delorme, M. Cosson and C. Rubod (2015). "Cystocele and functional anatomy of the pelvic floor: review and update of the various theories." Int Urogynecol J.

Lammers, K., J. J. Futterer, M. Prokop, M. E. Vierhout and K. B. Kluivers (2012). "Diagnosing pubovisceral avulsions: a systematic review of the clinical relevance of a prevalent anatomical defect." Int Urogynecol J **23**(12): 1653-1664.

Lammers, K., M. Prokop, M. E. Vierhout, K. B. Kluivers and J. J. Futterer (2013). "A pictorial overview of pubovisceral muscle avulsions on pelvic floor magnetic resonance imaging." Insights Imaging **4**(4): 431-441.

Larson, K. A., Y. Hsu, L. Chen, J. A. Ashton-Miller and J. O. DeLancey (2010). "Magnetic resonance imaging-based three-dimensional model of anterior vaginal wall position at rest and maximal strain in women with and without prolapse." Int Urogynecol J **21**(9): 1103-1109.

Law, Y. M. and J. R. Fielding (2008). "MRI of pelvic floor dysfunction: review." AJR Am J Roentgenol **191**(6 Suppl): S45-53.

Lieber, R. L. and J. Friden (2000). "Functional and clinical significance of skeletal muscle architecture." Muscle Nerve **23**(11): 1647-1666.

Loubeyre, P., M. Copercini, P. Petignat and J. B. Dubuisson (2012). "Levator ani muscle complex: anatomic findings in nulliparous patients at thin-section MR imaging with double opacification." Radiology **262**(2): 538-543.

Luber, K. M. (2004). "The definition, prevalence, and risk factors for stress urinary incontinence." Rev Urol **6 Suppl 3**: S3-9.

Macura, K. J. and R. R. Genadry (2008). "Female urinary incontinence: pathophysiology, methods of evaluation and role of MR imaging." Abdom Imaging **33**(3): 371-380.

Macura, K. J., R. R. Genadry and D. A. Bluemke (2006). "MR imaging of the female urethra and supporting ligaments in assessment of urinary incontinence: spectrum of abnormalities." Radiographics **26**(4): 1135-1149.

Macura, K. J., R. E. Thompson, D. A. Bluemke and R. Genadry (2015). "Magnetic resonance imaging in assessment of stress urinary incontinence in women: Parameters differentiating urethral hypermobility and intrinsic sphincter deficiency." World J Radiol **7**(11): 394-404.

Maglinte, D. D., F. M. Kelvin, K. Fitzgerald, D. S. Hale and J. T. Benson (1999). "Association of compartment defects in pelvic floor dysfunction." AJR Am J Roentgenol **172**(2): 439-444.

Mannella, P., G. Palla, M. Bellini and T. Simoncini (2013). "The female pelvic floor through midlife and aging." Maturitas **76**(3): 230-234.

Margulies, R. U., Y. Hsu, R. Kearney, T. Stein, W. H. Umek and J. O. DeLancey (2006). "Appearance of the levator ani muscle subdivisions in magnetic resonance images." Obstet Gynecol **107**(5): 1064-1069.

Margulies, R. U., M. Huebner and J. O. DeLancey (2007). "Origin and insertion points involved in levator ani muscle defects." Am J Obstet Gynecol **196**(3): 251 e251-255.

Martins, J. A., M. P. Pato, E. B. Pires, R. M. Jorge, M. Parente and T. Mascarenhas (2007). "Finite element studies of the deformation of the pelvic floor." Ann N Y Acad Sci **1101**: 316-334.

Moalli, P. A., S. Jones Ivy, L. A. Meyn and H. M. Zyczynski (2003). "Risk factors associated with pelvic floor disorders in women undergoing surgical repair." Obstet Gynecol **101**(5 Pt 1): 869-874.

Moalli, P. A., N. Papas, S. Menefee, M. Albo, L. Meyn and S. D. Abramowitch (2008). "Tensile Properties of Five Commonly used Mid-urethral Slings Relative to the TVT." Int Urogynecol J Pelvic Floor Dysfunct. **19**(5): 655-663.

Morgan, D. M., W. Umek, T. Stein, Y. Hsu, K. Guire and J. O. DeLancey (2007). "Interrater reliability of assessing levator ani muscle defects with magnetic resonance images." Int Urogynecol J Pelvic Floor Dysfunct **18**(7): 773-778.

Morrow, D. A., T. L. Haut Donahue, G. M. Odegard and K. R. Kaufman (2010). "Transversely isotropic tensile material properties of skeletal muscle tissue." J Mech Behav Biomed Mater **3**(1): 124-129.

Nguyen, J. K., L. R. Lind, J. Y. Choe, F. McKindsey, R. Sinow and N. N. Bhatia (2000). "Lumbosacral spine and pelvic inlet changes associated with pelvic organ prolapse." Obstet Gynecol **95**(3): 332-336.

Noakes, K. F., A. J. Pullan, I. P. Bissett and L. K. Cheng (2008). "Subject specific finite elasticity simulations of the pelvic floor." J Biomech **41**(14): 3060-3065.

Nygaard, I. E. and J. M. Shaw (2016). "Physical activity and the pelvic floor." Am J Obstet Gynecol **214**(2): 164-171.

O'Donnell, L. J. and C. F. Westin (2011). "An introduction to diffusion tensor image analysis." Neurosurg Clin N Am **22**(2): 185-196, viii.

Odegard, G. M., T. L. Donahue, D. A. Morrow and K. R. Kaufman (2008). "Constitutive modeling of skeletal muscle tissue with an explicit strain-energy function." J Biomech Eng **130**(6): 061017.

Onu, M. (2014). "Modeled and Model-free diffusion process assessment in tissues by Magnetic Resonance Imaging - a short review." Romanian Reports in Physics **66**(6): 658-671.

Oomens, C. W., M. Maenhout, C. H. van Oijen, M. R. Drost and F. P. Baaijens (2003). "Finite element modelling of contracting skeletal muscle." Philos Trans R Soc Lond B Biol Sci **358**(1437): 1453-1460.

Parente, M. P., R. M. Natal Jorge, T. Mascarenhas, A. A. Fernandes and J. A. Martins (2009a). "The influence of the material properties on the biomechanical behavior of the pelvic floor muscles during vaginal delivery." J Biomech **42**(9): 1301-1306.

Parente, M. P., R. M. Jorge, T. Mascarenhas, A. A. Fernandes and J. A. Martins (2009b). "The influence of an occipito-posterior malposition on the biomechanical behavior of the pelvic floor." Eur J Obstet Gynecol Reprod Biol **144 Suppl 1**: S166-169.

Parente, M. P., R. M. Natal Jorge, T. Mascarenhas and A. L. Silva-Filho (2010). "The influence of pelvic muscle activation during vaginal delivery." Obstet Gynecol **115**(4): 804-808.

Peng, Y., R. Khavari, N. A. Nakib, J. N. Stewart, T. B. Boone and Y. Zhang (2015). "The Single-Incision Sling to Treat Female Stress Urinary Incontinence: A Dynamic Computational Study of Outcomes and Risk Factors." J Biomech Eng **137**(9).

Perk, H., B. Oral, A. Yesildag, T. A. Serel, M. Ozsoy and T. Turgut (2002). "Magnetic resonance imaging for stress incontinence: evaluation of patients before and after surgical correction." Eur J Radiol **44**(1): 44-47.

Petros, P. E. (1998). "The pubourethral ligaments--an anatomical and histological study in the live patient." Int Urogynecol J Pelvic Floor Dysfunct **9**(3): 154-157.

Petros, P. E. and U. I. Ulmsten (1990). "An integral theory of female urinary incontinence. Experimental and clinical considerations." Acta Obstet Gynecol Scand Suppl **153**: 7-31.

Petros, P. E. and P. J. Woodman (2008). "The Integral Theory of continence." Int Urogynecol J Pelvic Floor Dysfunct **19**(1): 35-40.

Pizzoferrato, A. C., K. Nyangoh Timoh, X. Fritel, E. Zareski, G. Bader and A. Fauconnier (2014). "Dynamic Magnetic Resonance Imaging and pelvic floor disorders: how and when?" Eur J Obstet Gynecol Reprod Biol **181**: 259-266.

Poswiata, A., T. Socha and J. Opara (2014). "Prevalence of stress urinary incontinence in elite female endurance athletes." J Hum Kinet **44**: 91-96.

Pregazzi, R., A. Sartore, P. Bortoli, E. Grimaldi, L. Troiano and S. Guaschino (2002). "Perineal ultrasound evaluation of urethral angle and bladder neck mobility in women with stress urinary incontinence." BJOG **109**(7): 821-827.

Raizada, V., V. Bhargava, S. A. Jung, A. Karstens, D. Pretorius, P. Krysl and R. K. Mittal (2010). "Dynamic assessment of the vaginal high-pressure zone using high-definition manometery, 3-dimensional ultrasound, and magnetic resonance imaging of the pelvic floor muscles." Am J Obstet Gynecol **203**(2): 172 e171-178.

Raizada, V. and R. K. Mittal (2008). "Pelvic floor anatomy and applied physiology." Gastroenterol Clin North Am **37**(3): 493-509, vii.

Reddy, S. K., B. J. Williams and A. Gomelsky (2009). "Is Sling Stiffness Associated with Postoperative Voiding Dysfunction? A Comparison of Two Polypropylene Midurethral Slings." ICS Annual Meeting, San Francisco, CA. October 2, 2009.

Reiner, C. S. and D. Weishaupt (2013). "Dynamic pelvic floor imaging: MRI techniques and imaging parameters." Abdom Imaging **38**(5): 903-911.

Ren, S., B. Xie, J. Wang and Q. Rong (2015). "Three-dimensional modeling of the pelvic floor support systems of subjects with and without pelvic organ prolapse." Biomed Res Int **2015**: 845985.

Rinne, K., S. Kainulainen, S. Aukee, S. Heinonen and C. G. Nilsson (2011). "Dynamic MRI confirms support of the mid-urethra by TVT and TVT-O surgery for stress incontinence." Acta Obstet Gynecol Scand **90**(6): 629-635.

Rivaux, G., C. Rubod, B. Dedet, M. Brieu, B. Gabriel and M. Cosson (2013). "Comparative analysis of pelvic ligaments: a biomechanics study." Int Urogynecol J **24**(1): 135-139.

Rodriguez-Mias, N. L., E. Martinez-Franco, J. Aguado, E. Sanchez and L. Amat-Tardiu (2015). "Pelvic organ prolapse and stress urinary incontinence, do they share the same risk factors?" Eur J Obstet Gynecol Reprod Biol **190**: 52-57.

Rousset, P., V. Delmas, J. N. Buy, A. Rahmouni, D. Vadrot and J. F. Deux (2012). "In vivo visualization of the levator ani muscle subdivisions using MR fiber tractography with diffusion tensor imaging." J Anat **221**(3): 221-228.

Sahinkanat, T., D. C. Arikan, E. Turgut, C. Ozkurkcugil, H. Yilmaz and H. Ekerbicer (2011). "Effects of lumbar lordosis and pelvic inlet orientation on the outcome of the transobturator tape sling operation in women." Arch Gynecol Obstet **284**(1): 125-130.

Sajadi, K. P., B. C. Gill and M. S. Damaser (2010). "Neurogenic aspects of stress urinary incontinence." Curr Opin Obstet Gynecol **22**(5): 425-429.

Saleme, C. S., M. P. Parente, R. M. Natal Jorge, M. Pinotti, A. L. Silva-Filho, T. Roza, T. Mascarenhas and J. M. Tavares (2011). "An approach on determining the displacements of the pelvic floor during voluntary contraction using numerical simulation and MRI." Comput Methods Biomech Biomed Engin **14**(4): 365-370.

Sangsawang, B. and N. Sangsawang (2013). "Stress urinary incontinence in pregnant women: a review of prevalence, pathophysiology, and treatment." Int Urogynecol J **24**(6): 901-912.

Schaer, G. N., O. R. Koechli, B. Schuessler and U. Haller (1995). "Perineal ultrasound for evaluating the bladder neck in urinary stress incontinence." Obstet Gynecol **85**(2): 220-224.

Schuettoff, S., D. Beyersdorff, A. Gauruder-Burmester and R. Tunn (2006). "Visibility of the polypropylene tape after tension-free vaginal tape (TVT) procedure in women with stress urinary incontinence: comparison of introital ultrasound and magnetic resonance imaging in vitro and in vivo." Ultrasound Obstet Gynecol **27**(6): 687-692.

Shah, H. N. and G. H. Badlani (2012). "Mesh complications in female pelvic floor reconstructive surgery and their management: A systematic review." Indian J Urol **28**(2): 129-153.

Siegel, A. L., M. Kim, M. Goldstein, S. Levey and P. Ilbeigi (2005). "High incidence of vaginal mesh extrusion using the intravaginal slingplasty sling." J Urol **174**(4 Pt 1): 1308-1311.

Simeone, C., A. Moroni, A. Petteno, A. Antonelli, D. Zani, C. Orizio and S. Cosciani Cunico (2010). "Occurrence rates and predictors of lower urinary tract symptoms and incontinence in female athletes." Urologia **77**(2): 139-146.

Stothers, L. and B. Friedman (2011). "Risk factors for the development of stress urinary incontinence in women." Curr Urol Rep **12**(5): 363-369.

Sweed, M. S. and S. Sharara (2016). "Transperineal Ultrasound Evaluation of Females with Stress Urinary Incontinence." Int J Reprod Contracept Obstet Gynecol. **5**(3): 637-641.

Takaza, M., K. M. Moerman, J. Gindre, G. Lyons and C. K. Simms (2013). "The anisotropic mechanical behaviour of passive skeletal muscle tissue subjected to large tensile strain." J Mech Behav Biomed Mater **17**: 209-220.

Tarhan, S., B. Bilali Gumus, G. k. Temeltas, G. l. n. Yilmaz Ovali, S. Selim Serter and C. GÖktan (2010). "The comparison of MRI findings with severity score of incontinence after pubovaginal sling surgery." Turk J Med Sci **40**(4): 549-556.

Tasali, N., R. Cubuk, O. Sinanoglu, K. Sahin and B. Saydam (2012). "MRI in stress urinary incontinence: endovaginal MRI with an intracavitary coil and dynamic pelvic MRI." Urol J **9**(1): 397-404.

Tuch, D. S. (2004). "Q-ball imaging." Magn Reson Med **52**(6): 1358-1372.

Tumbarello, J. A., Y. Hsu, C. Lewicky-Gaupp, S. Rohrer and J. O. DeLancey (2010). "Do repetitive Valsalva maneuvers change maximum prolapse on dynamic MRI?" Int Urogynecol J **21**(10): 1247-1251.

Tunn, R., J. O. DeLancey and E. E. Quint (2001). "Visibility of pelvic organ support system structures in magnetic resonance images without an endovaginal coil." Am J Obstet Gynecol **184**(6): 1156-1163.

Vakili, B., Y. T. Zheng, H. Loesch, K. T. Echols, N. Franco and R. R. Chesson (2005). "Levator contraction strength and genital hiatus as risk factors for recurrent pelvic organ prolapse." Am J Obstet Gynecol **192**(5): 1592-1598.

Van Donkelaar, C. C., L. J. Kretzers, P. H. Bovendeerd, L. M. Lataster, K. Nicolay, J. D. Janssen and M. R. Drost (1999). "Diffusion tensor imaging in biomechanical studies of skeletal muscle function." J Anat **194 (Pt 1)**: 79-88.

van Raalte, H. and V. Egorov (2015). "Tactile Imaging Markers to Characterize Female Pelvic Floor Conditions." Open J Obstet Gynecol **5**(9): 505-515.

Verelst, M. and G. Leivseth (2007). "Force and stiffness of the pelvic floor as function of muscle length: A comparison between women with and without stress urinary incontinence." Neurourol Urodyn **26**(6): 852-857.

Walker, G. J. and P. Gunasekera (2011). "Pelvic organ prolapse and incontinence in developing countries: review of prevalence and risk factors." Int Urogynecol J **22**(2): 127-135.

Weidner, A. C., M. D. Barber, A. G. Visco, R. C. Bump and D. B. Sanders (2000). "Pelvic muscle electromyography of levator ani and external anal sphincter in nulliparous women and women with pelvic floor dysfunction." Am J Obstet Gynecol **183**(6): 1390-1399; discussion 1399-1401.

Wood, L. N. and J. T. Anger (2014). "Urinary incontinence in women." BMJ **349**: g4531.

Yang, J. M., S. H. Yang and W. C. Huang (2006). "Biometry of the pubovisceral muscle and levator hiatus in nulliparous Chinese women." Ultrasound Obstet Gynecol **28**(5): 710-716.

Yang, S. H., W. C. Huang, S. Y. Yang, E. Yang and J. M. Yang (2009). "Validation of new ultrasound parameters for quantifying pelvic floor muscle contraction." Ultrasound Obstet Gynecol **33**(4): 465-471.

Ying, T., Q. Li, L. Xu, F. Liu and B. Hu (2012). "Three-dimensional ultrasound appearance of pelvic floor in nulliparous women and pelvic organ prolapse women." Int J Med Sci **9**(10): 894-900.

Yip, C., E. Kwok, F. Sassani, R. Jackson and G. Cundiff (2014). "A biomechanical model to assess the contribution of pelvic musculature weakness to the development of stress urinary incontinence." Comput Methods Biomech Biomed Engin **17**(2): 163-176.

Zijta, F. M., M. Froeling, M. P. van der Paardt, M. M. Lakeman, S. Bipat, A. D. van Swijndregt, G. J. Strijkers, A. J. Nederveen and J. Stoker (2011). "Feasibility of diffusion tensor imaging (DTI) with fibre tractography of the normal female pelvic floor." Eur Radiol **21**(6): 1243-1249.

Zijta, F. M., M. M. Lakeman, M. Froeling, M. P. van der Paardt, C. S. Borstlap, S. Bipat, A. D. Montauban van Swijndregt, G. J. Strijkers, J. P. Roovers, A. J. Nederveen and J. Stoker (2012). "Evaluation of the female pelvic floor in pelvic organ prolapse using 3.0-Tesla diffusion tensor imaging and fibre tractography." Eur Radiol **22**(12): 2806-2813.

Appendix

1. Informed Consent

2. ICIQ-SF International Consultation on Incontinence Questionnaire - Short Form and **PFIQ-7** pelvic floor impact questionnaire - short form 7

3. Authorizations of the IRB (CES -Comissão de Ética para a Saúde) of:

Centro Hospitalar de São João-EPE - (195/12).

Centro Hospitalar of Lisboa Norte-EPE (Hospital de Sta. Maria / Faculdade de Medicina da Universidade de Lisboa) - (675/14).

DECLARAÇÃO DE CONSENTIMENTO

Considerando a "Declaração de Helsínquia" da Associação Médica Mundial
(Helsínquia 1964; Tóquio 1975; Veneza 1983; Hong Kong 1989; Somerset West 1996 e Edimburgo 2000)

Designação do Estudo (em português):

"*Aplicação da Imagiologia por Tensor de Difusão por Ressonância Magnética na análise biomecânica dos músculos do pavimento pélvico feminino.*"

Eu, abaixo-assinado, (nome completo do doente ou voluntário são) ----------
---------- , declaro não ter participado em nenhum outro projecto de investigação durante este internamento, tendo compreendido a explicação que me foi fornecida acerca do meu caso clínico e da investigação que se tenciona realizar. Foi-me ainda dada oportunidade de fazer as perguntas que julguei necessárias, e de todas obtive resposta satisfatória.
Tomei conhecimento de que, de acordo com as recomendações da Declaração de Helsínquia, a informação ou explicação que me foi prestada versou os objectivos, os métodos, os benefícios previstos, os riscos potenciais e o eventual desconforto. Além disso, foi-me afirmado que tenho o direito de recusar a todo o tempo a minha participação no estudo, sem que isso possa ter como efeito qualquer prejuízo na assistência que me é prestada.
Por isso, consinto que me seja aplicado o método, o tratamento ou o inquérito proposto pelo investigador.

Data: ____ / _____ / 201___

Assinatura da voluntária: _____

O Investigador responsável:

Nome: Fernanda Sofia Quintela da Silva Brandão

Assinatura:

ICIQ-SF (versão validada para português, Tamanini *et al.* 2004)

Código:_____ Data: ___/____/_____

Muitas pessoas perdem urina algumas vezes. Este questionário vai ajudá-la a perceber como a incontinência a incomoda. Responda às questões que se seguem, pensando em como tem passado, em média, NAS ÚLTIMAS QUATRO SEMANAS.

1. Data de Nascimento: ___/____/_____ (Dia / Mês / Ano)
2. Sexo: Feminino ____ Masculino ____

3. Com que frequência perde urina? (assinale uma resposta)

Nunca __ 0

Uma vez por semana ou menos __ 1

Duas ou três vezes por semana __ 2

Uma vez ao dia __ 3

Diversas vezes ao dia __ 4

A toda a hora __ 5

4. Qual a quantidade que pensa que perde? (assinale uma resposta)

Nenhuma __ 0

Uma pequena quantidade __ 2

Uma moderada quantidade __ 4

Uma grande quantidade __ 6

5. Em geral quanto é que a perda de urina interfere na sua vida diária? Por favor, circule um número entre = (não interfere) e 10 (interfere muito)

0 1 2 3 4 5 7 8 9 10

Não interfere Interfere muito

ICIQ Score: soma dos resultados 3 + 4 + 5 =

6. Quando perde urina?
(Por favor assinale todas as alternativas que se aplica a si)

Nunca __

Perco antes de chegar à casa-de-banho __

Perco quando tusso ou espirro __

Perco quando durmo __

Perco quando faço atividades físicas __

Perco quando terminei de urinar e estou a vestir-me __

Perco sem motivo aparente __

Perco a toda a hora __

Obrigada por ter respondido às questões

Pelvic Floor Impact Questionnaire-Short Form (PFIQ-7)

Código:_____ Data: _____

Data de Nascimento: ___/____/_____

Instructions: Some women find that bladder, bowel, or vaginal symptoms affect their activities, relationships, and feelings. For each question, check the response that best describes how much your activities, relationships, or feelings have been affected by your bladder, bowel, or vaginal symptoms or conditions **over the last 3 months.** Please make sure you mark an answer in **all 3 columns** for each question.

How do symptoms or conditions in the following usually affect your	***Bladder or urine***	***Bowel or rectum***	***Vagina or pelvis***
1. Ability to do household chores (cooking, laundry housecleaning)?	□Not at all □Somewhat □Moderately □Quite a bit	□Not at all □Somewhat □Moderately □Quite a bit	□Not at all □Somewhat □Moderately □Quite a bit
2. Ability to do physical activities such as walking, swimming, or other exercise?	□Not at all □Somewhat □Moderately □Quite a bit	□Not at all □Somewhat □Moderately □Quite a bit	□Not at all □Somewhat □Moderately □Quite a bit
3. Entertainment activities such as going to a movie or concert?	□Not at all □Somewhat □Moderately □Quite a bit	□Not at all □Somewhat □Moderately □Quite a bit	□Not at all □Somewhat □Moderately □Quite a bit
4. Ability to travel by car or bus for a distance greater than 30 minutes away from home?	□Not at all □Somewhat □Moderately □Quite a bit	□Not at all □Somewhat □Moderately □Quite a bit	□Not at all □Somewhat □Moderately □Quite a bit
5. Participating in social activities outside your home?	□Not at all □Somewhat □Moderately □Quite a bit	□Not at all □Somewhat □Moderately □Quite a bit	□Not at all □Somewhat □Moderately □Quite a bit
6. Emotional health (nervousness, depression, etc)?	□Not at all □Somewhat □Moderately □Quite a bit	□Not at all □Somewhat □Moderately □Quite a bit	□Not at all □Somewhat □Moderately □Quite a bit
7. Feeling frustrated?	□Not at all □Somewhat □Moderately □Quite a bit	□Not at all □Somewhat □Moderately □Quite a bit	□Not at all □Somewhat □Moderately □Quite a bit

195-12

Exmo. Senhor
Presidente do Conselho de Administração do
Centro Hospitalar de S. João – EPE

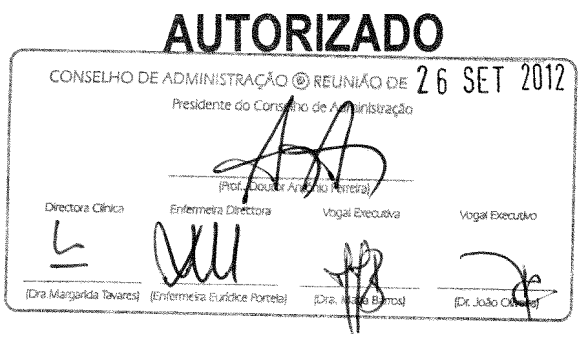

Assunto: Pedido de autorização para realização de estudo/projecto de investigação

Nome do Investigador Principal: Fernanda Sofia Quintela da Silva Brandão

Título do projecto de investigação: *"Aplicação da Imagiologia por Tensores de Difusão por Ressonância Magnética na análise biomecânica dos músculos do pavimento pélvico feminino."*

Pretendendo realizar no(s) Serviço(s) de Ginecologia e Obstetrícia, e de Radiologia do Centro Hospitalar de S. João – EPE o estudo/projecto de investigação em epígrafe, pelo que solicito a V. Exa., na qualidade de Investigador/Promotor, autorização para a sua efectivação.

Para o efeito, anexa toda a documentação referida no dossier da Comissão de Ética do Centro Hospitalar de S. João respeitante a estudos/projectos de investigação, à qual endereçou pedido de apreciação e parecer.

Com os melhores cumprimentos.

Porto, 13 / Julho / 2012

O INVESTIGADOR/PROMOTOR

Fernanda Sofia Brandão

Exma. Senhora
Mestre Fernanda Sofia Quintela S. Brandão
Centro Hospitalar de São João, E.P.E.

Lisboa, 8 de Junho de 2015

Nossa Refª. Nº 675/14

Assunto: Projecto de Investigação **"Aplicação da imagiologia por Tensor de Difusão por Ressonância Magnética na análise biomecânica dos músculos do pavimento pélvico feminino"**

Relator - *Profª. Doutora Mafalda Videira*

Pela presente informamos que o projecto citado em epígrafe obteve, na reunião realizada em 8 de Abril de 2015, parecer favorável da Comissão de Ética, após esclarecimento das objecções levantadas.

Mais se informa que o referido foi autorizado pela Sra. Directora Clínica, Dra. Margarida Lucas.

Com os melhores cumprimentos,

O Presidente da Comissão de Ética do CAML

Prof. Doutor José Pereira Miguel